Dissertation zur Erlangung des Doktorgrades der
Naturwissenschaften (Dr. rer. nat.)

an der Fakultät für Biologie
der Ludwig-Maximilians-Universität München

ATP-dependent nucleosome sliding by ISWI - molecular mechanism and regulation

Henrike Klinker

München
Juni 2014

Dissertation eingereicht am 24.06.2014

Mündliche Prüfung am 12.09.2014

1. Gutachter: Prof. Dr. Peter B. Becker

2. Gutachter: Prof. Dr. Dirk Eick

3. Gutachter: Prof. Dr. Heinrich Leonhardt

4. Gutachterin: Prof. Dr. Kirsten Jung

Eidesstattliche Erklärung

Ich versichere hiermit an Eides statt, dass die vorgelegte Dissertation von mir selbständig und ohne unerlaubte Hilfe angefertigt ist.

München, den ....

(Henrike Klinker)

Erklärung

Hiermit erkläre ich, dass die Dissertation nicht ganz oder in wesentlichen Teilen einer anderen Prüfungskommission vorgelegt worden ist und dass ich mich nicht anderweitig einer Doktorprüfung ohne Erfolg unterzogen habe.

München, den ....

(Henrike Klinker)

Table of contents

Preface 1

Summary 2

Zusammenfassung 3

1 Introduction 5

1.1 ORGANIZATION AND STRUCTURE OF CHROMATIN 5

  1.1.1 The nucleosome 5

  1.1.2 The linker histone 7

  1.1.3 Higher order chromatin structure 9

1.2 DYNAMICS AND REGULATION OF CHROMATIN 13

  1.2.1 Histone variants 14

  1.2.2 Post-translational modifications of histones 14

  1.2.3 Acetylation of histone H4 at lysine 16 16

1.3 ATP-DEPENDENT CHROMATIN REMODELING 19

  1.3.1 The ISWI-type chromatin remodeling factors 21

  1.3.2 Mechanism of ISWI-mediated nucleosome sliding 24

  1.3.3 Regulation of the ISWI enzyme 25

  1.3.4 Interplay of ISWI, H4K16ac, and the linker histone *in vivo* 26

1.4 *IN VITRO* SYSTEMS TO STUDY CHROMATIN REMODELING 28

1.5 AIMS OF THIS STUDY 29

2 Results 31

2.1 THE ATPASE DOMAIN OF ISWI IS AN AUTONOMOUS NUCLEOSOME REMODELING MACHINE 31

  Supplementary material 55

2.2 NUCLEOSOME SLIDING MECHANISMS: NEW TWISTS IN A LOOPED HISTORY 68

2.3 NO NEED FOR A POWER STROKE IN ISWI-MEDIATED NUCLEOSOME SLIDING 86

  Supplementary material 93

2.4 ISWI REMODELLING OF PHYSIOLOGICAL CHROMATIN FIBRES ACETYLATED AT LYSINE 16 OF HISTONE H4 96

  Supplementary material 109

2.5 RAPID PURIFICATION OF RECOMBINANT HISTONES 115

  Supplementary material 129

3 Discussion 131
3.1 THE MOLECULAR MECHANISM OF ISWI-MEDIATED NUCLEOSOME SLIDING 131
3.2 REGULATION OF ISWI BY THE HISTONE H4 TAIL 134
  3.2.1 The regulatory potential of H4K16ac 135
  3.2.2 Implications for the *in vivo* role of ISWI in chromatin organization 136
3.3 FUTURE GOALS 137
References 139
Declaration of contributions 154
Abbreviations 156
Curriculum Vitae 158
Acknowledgements 160

Preface

The results of the work I conducted during my PhD thesis in the laboratory of Prof. Dr. Peter B. Becker on the chromatin remodeling enzyme ISWI are published in three original research papers. A fourth manuscript reporting the establishment of a rapid histone purification method is currently under revision. The research papers and the manuscript constitute the main part of the results section of this cumulative thesis. Furthermore, the results section contains a published review article that I co-authored. It focuses on recent developments in the field of chromatin remodeling – contributed by us and others – that provided novel and exciting insights into the mechanism and regulation of nucleosome sliding. As they refer to each other, the articles are presented in a chronological order according to their publication dates to facilitate reading. My contributions to the individual manuscripts are listed at the beginning of each chapter of the results section and in a comprehensive form in the enclosed declaration of contributions (see page 154). Due to copyright issues the articles published in the journal *Nature Structural and Molecular Biology* are not included in the final, published version. Instead, the accepted manuscript after peer-review is enclosed in the format of this thesis. Each chapter of the results section contains the respective reference list. The references of the introduction and discussion are summarized and listed subsequent to the discussion section (see page 139).

List of the publications included in this thesis:

Mueller-Planitz F, **Klinker H**, Ludwigsen J, Becker PB (2013)
The ATPase domain of ISWI is an autonomous nucleosome remodeling machine.
Nature Structural & Molecular Biology 20, 82-89.

Mueller-Planitz F, **Klinker H**, Becker PB (2013)
Nucleosome sliding mechanisms: new twists in a looped history.
Nature Structural & Molecular Biology 20, 1026-1032.

Ludwigsen J, **Klinker H**, Mueller-Planitz F (2013)
No need for a power stroke in ISWI-mediated nucleosome sliding.
EMBO reports 14, 1092-1097.

Klinker H, Mueller-Planitz F, Yang R, Forné I, Liu CF, Nordenskiöld L, Becker PB (2014)
ISWI Remodelling of Physiological Chromatin Fibres Acetylated at Lysine 16 of Histone H4.
PLoS ONE 9(2), e88411.

Unpublished manuscript included in this thesis:

Klinker H, Haas C, Becker PB, Mueller-Planitz F
Rapid purification of recombinant histones

Summary

The organization of DNA into nucleosomes and higher order chromatin structures poses an obstacle to the nuclear machinery by restricting DNA access. To dynamically regulate DNA accessibility and the transition of chromatin functional states, a complex network comprising various factors and mechanisms evolved. Key players in this network are a class of conserved, ATP-dependent chromatin remodeling factors catalyzing nucleosome eviction, assembly, reconfiguration, and repositioning (“sliding”). Among the most intensively studied remodeling complexes are those containing the ISWI enzyme as catalytic core. These complexes possess nucleosome sliding activity and assist in chromatin assembly. Notably, *in vitro* the isolated ISWI enzyme displays remodeling activity, and the associated subunits have modulating functions. Besides the central ATPase domain that shares homology with helicases, ISWI harbors a DNA binding module, the HAND-SANT-SLIDE domain (HSS). For maximal activity, ISWI requires the histone H4 tail, and acetylation of the tail at lysine 16 (H4K16ac), a mark mediating chromatin decompaction, was proposed to negatively affect ISWI activity, providing a means to regulate the enzyme *in vivo*. However, the molecular mechanisms of a remodeling reaction and of the H4 tail-dependency of ISWI remain elusive.

In this study, we biochemically characterized the wild-type ISWI enzyme and various mutants to gain insights into the function of different protein domains during catalysis. Furthermore, we quantitatively analyzed the effect of H4K16ac on ISWI activity in the context of *in vitro* reconstituted, physiological chromatin fibers. Employing folded chromatin fibers instead of the commonly used isolated mononucleosomes allowed assessing potential effects of H4K16ac-induced chromatin decompaction on ISWI remodeling that would have escaped notice in previous studies. To facilitate *in vitro* studies of chromatin, we developed – based on established methods – a rapid purification protocol for bacterially expressed histones.

Unexpectedly and contrary to prominent models, we found the HSS domain of ISWI to be dispensable for nucleosome sliding. Instead, the isolated ATPase domain acted as an autonomous nucleosome remodeling machine that was stimulated by DNA and nucleosomes, was sensitive to the H4 tail, and repositioned nucleosomes. While the HSS domain enhanced sliding activity and substrate specificity, our results did not support active co-operation with the ATPase domain. In conjunction with recent findings by other groups, in our model of nucleosome sliding by ISWI the helicase-like DNA translocation activity of the ATPase domain is the driving force, whereas the HSS domain assumes regulating and optimizing functions. Moreover, we could confirm a general regulatory potential of the H4 tail for ISWI activity. However, in conflict with previous reports we did not observe a reducing, but rather a stimulating effect of H4K16ac in the context of chromatin fibers. We conclude that ISWI regulation by H4K16ac is context-dependent and simple models on the interplay of these chromatin-organizing factors *in vivo* have to be reconsidered.

Zusammenfassung

Die Organisation von DNA in Nukleosomen und höhere Chromatinstrukturen limitiert im Allgemeinen ihre Zugänglichkeit für DNA bindende Faktoren der nukleären Maschinerie. Um den Zugriff auf bestimmte DNA-Sequenzen und den Übergang zwischen Chromatinzuständen dynamisch zu regulieren, hat sich ein komplexes Netzwerk ausgebildet, das eine Vielzahl von Faktoren und Mechanismen umfasst. In diesem Netzwerk nehmen die evolutionär konservierten, ATP-abhängigen Chromatin-Remodulierungs-Faktoren („Remodeling-Faktoren“) eine Schlüsselstellung ein. Sie katalysieren sowohl den Auf- als auch Ab- und Umbau von Nukleosomen und ihre Repositionierung. Dabei zählen zu den am besten charakterisierten Remodeling-Faktoren die Komplexe, die das Enzym ISWI als katalytischen Kern enthalten. Diese Komplexe besitzen Repositionierungsaktivität und assistieren zudem bei der Chromatin-Assemblierung. Auch außerhalb von Komplexen weist das ISWI-Enzym *in vitro* Remodeling-Aktivität auf, die durch die Assoziation von weiteren Untereinheiten moduliert und gesteuert wird. Neben einer zentralen ATPase-Domäne, die wie bei allen Remodeling-Enzymen Homologie zu Helikasen aufweist, umfasst ISWI eine DNA-Bindedomäne, die sogenannte HAND-SANT-SLIDE-Domäne (HSS-Domäne). Für maximale Remodeling-Aktivität benötigt ISWI den flexiblen N-Terminus von Histon H4. Dessen Acetylierung an Lysin 16 (H4K16ac) – eine Histonmodifikation, die Chromatin-Dekondensation bewirkt – wurde wiederum eine inhibierende Wirkung auf ISWI zugeschrieben. Folglich stellt diese posttranslationale Modifikation ein potentielles Mittel zur Regulation der Aktivität von ISWI-Komplexen *in vivo* dar. Die molekularen Mechanismen, die einer Remodeling-Reaktion und der H4-Abhängigkeit von ISWI zugrunde liegen, sind jedoch noch unverstanden.

In der vorliegenden Arbeit wurden das ISWI-Enzym in voller Länge sowie unterschiedliche Mutanten biochemisch charakterisiert, um die Funktion der verschiedenen Proteindomänen zu untersuchen. Außerdem wurde der Effekt von H4K16ac auf die ISWI-Aktivität im Kontext von *in vitro* rekonstituierten, physiologischen Chromatinfasern quantitativ analysiert. Dabei ermöglichte die Verwendung von gefalteten Chromatinfasern als Remodeling-Substrat anstelle der häufig eingesetzten isolierten Mononukleosomen, potentielle Effekte der H4K16ac-induzierten Chromatin-Dekondensation auf die Remodeling-Aktivität von ISWI zu detektieren. Solche Effekte wären in früheren Analysen unentdeckt geblieben. Um die Assemblierung von Chromatin *in vitro* zu beschleunigen und zu erleichtern, haben wir, basierend auf etablierten Methoden, ein Protokoll zur schnellen Aufreinigung von bakteriell exprimierten Histonen entwickelt.

Im Gegensatz zu bisher vorherrschenden Modellen zeigten unsere Analysen, dass die HSS-Domäne von ISWI nicht in essentieller Weise zur Repositionierung von Nukleosomen beiträgt. Stattdessen stellt die isolierte ATPase-Domäne eine autonome Remodeling-

Maschine dar, die durch DNA und Nukleosomen stimuliert wird, auf den N-Terminus von H4 reagiert und Nukleosomen repositioniert. Die HSS-Domäne hingegen steigert die Repositionierungsaktivität und Substratspezifität von ISWI. Eine aktive Koordination beider Domänen jedoch scheint aufgrund unserer Ergebnisse ausgeschlossen. In Verbindung mit neuesten Erkenntnissen anderer Labore schlagen wir ein Modell der Nukleosomen-Repositionierung durch ISWI vor, in dem die den Helikasen verwandte DNA-Translokationsaktivität der ATPase-Domäne als treibende Kraft fungiert. Die HSS-Domäne erfüllt dabei regulierende und optimierende Funktionen. Darüber hinaus konnten wir ein generelles regulatorisches Potential des N-Terminus von H4 im Zusammenhang mit ISWI bestätigen. Allerdings beobachteten wir im Kontrast zu früheren Studien keinen inhibierenden, sondern eher einen stimulierenden Effekt der Acetylierung auf die ISWI-Aktivität. Daraus schließen wir, dass die Regulation von ISWI durch H4K16ac kontextabhängig ist und vereinfachte Modelle des Zusammenspiels dieser beiden Chromatin organisierenden Faktoren *in vivo* überdacht werden müssen.

1 Introduction

1.1 Organization and structure of chromatin

To accommodate eukaryotic genomes in the restricted volume of a cell nucleus, the DNA is organized into a nucleoprotein complex termed “chromatin“. The tight association with proteins not only serves to compact and protect DNA, but also to regulate all DNA-based processes by timely adjusting DNA accessibility. Different levels of DNA packaging and chromatin condensation can be distinguished and the underlying organizational principles will be discussed in the following.

1.1.1 The nucleosome

The “nucleosome” constitutes the first level of DNA compaction and the basic repeating unit of chromatin. A “nucleosome core particle” comprises ~147 base pairs (bp) of DNA tightly wrapped in about 1.65 left-handed superhelical turns around a histone octamer (Figure 1A) (Luger et al., 1997). This disc-shaped octamer consist of two copies each of the highly conserved histone proteins H2A, H2B, H3, and H4. Histones are small, basic proteins (~100–130 amino acids) and bipartite in their structure. On the one hand, they contain a structured core that includes the characteristic “histone fold” motif consisting of three

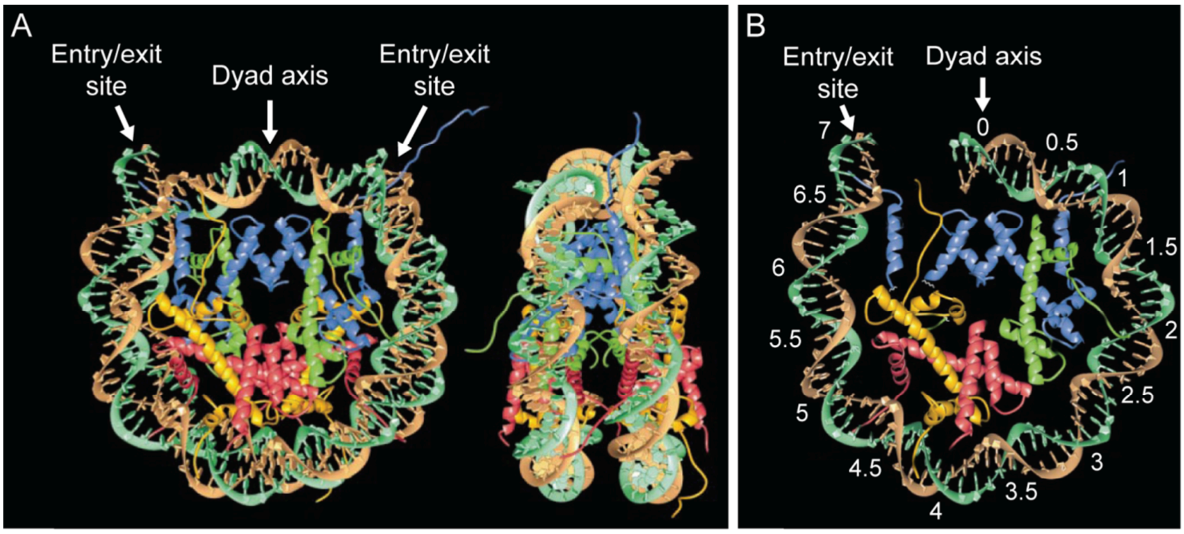

Figure 1 The nucleosome core particle. The structure of the nucleosome core particle as derived from X-ray crystallography (2.8 Å) is depicted. (**A**) Two views of the complete particle varying by 90° are shown with the dyad axis aligned vertically. The sites where the DNA enters and exits the nucleosome core particle, respectively, are indicated. The unstructured histone tails crystallized only partially. (**B**) One half of the nucleosome core particle (four histones and 73 bp of DNA) is shown. Additionally, three helices of the second H3 histone are depicted. The numbers indicate the superhelix locations (SHLs). The SHLs of the two halves of a nucleosome are distinguished by positive and negative algebraic signs, respectively. DNA backbone: brown and turquoise; H3: blue; H4: green; H2A: yellow; H2B: red (Adapted and reprinted with permission from Macmillan Publishers Ltd: Nature (Luger et al., 1997))

α-helices connected by two loops. On the other hand, histones feature an unstructured N-terminal region comprising 20–35 amino acids termed “histone tail”. H2A additionally harbors a disordered domain at its C-terminus. While the structured domains form the vast majority of protein-protein and protein-DNA contacts within a nucleosome, the flexible and exposed tails constitute important interaction surfaces (see chapters 1.1.3 and 1.2.2) (Andrews and Luger, 2011; Luger et al., 1997).

Stable wrapping of the nucleosomal DNA around the histone octamer is achieved by multiple direct interactions of the DNA and the histone proteins as well as numerous water-mediated bonds (Davey et al., 2002; Luger et al., 1997). The DNA contacts the octamer surface once per helical turn where the minor groove faces the octamer (superhelix locations (SHL) ± 0.5 to ± 6.5; Figure 1B), yielding 14 distinct sites of interaction. These interaction sites vary in strength with the strongest region of interaction located at the nucleosome dyad (Hall et al., 2009). Notably, none of the histone-DNA contacts is base-specific. Therefore, observed preferences for the assembly of certain DNA sequences into nucleosomes likely reflect sequence-dependent differences in DNA bendability (Davey et al., 2002). The nucleosomal organization of DNA generally limits its accessibility for sequence-specific binding factors due to occluded interaction epitopes. In addition, the unusual and bent DNA conformation imposed by the octamer may prevent sequence recognition (Richmond and Davey, 2003). Due to its tight wrapping around the octamer, nucleosomal DNA is largely protected from cleavage by nucleases like micrococcal nuclease or restriction enzymes (Noll and Kornberg, 1977; van Holde, 1989).

The primary structure of a chromatin fiber consists of an array of nucleosome core particles connected by stretches of free DNA called “linker DNA”. The entity of a nucleosome core particle and its flanking linker DNA is termed “nucleosome”. The mean length of the linker DNA varies not only in a species- and tissue-specific manner ranging from 7 bp in fission yeast (Lantermann et al., 2010) to ~90 bp in sea urchin sperm (Spadafora et al., 1976) but also locally within one nucleus (Valouev et al., 2011). This variability is of functional relevance for further levels of chromatin compaction as outlined in chapter 1.1.3.

Despite their pronounced stability, nucleosomes are dynamic, variable particles that can adopt different structural states (Andrews and Luger, 2011). For example, transient unwrapping of nucleosomal DNA especially at the entry/exit sites was observed, opening a window of opportunity for the interaction of chromatin factors with the DNA as well as the histone moiety (Buning and van Noort, 2010; Li et al., 2005; Miyagi et al., 2011; Poirier et al., 2008; Tims et al., 2011; Zlatanova et al., 2009). Furthermore, sequence-dependent structural plasticity of the nucleosomal DNA was reported. At SHL±2 or ±5, the nucleosome core particle can accommodate DNA stretching, allowing the organization of a variable number of base pairs (145–147 bp) on the octamer surface (Tan and Davey, 2011). Moreover, alternative nucleosome architectures deviating considerably from the canonical structure were described, including split nucleosomes, an inverted direction of the DNA supercoil, and particles comprising less than a full complement of eight histones (Andrews and Luger, 2011; Zlatanova et al., 2009). The molecular composition, abundance, and functional relevance of such nucleosomal assemblies are currently under intense investigation. The dynamic and versatile nature of nucleosomes is further elevated by the incorporation of non-canonical histone isoforms and the post-translational covalent chemical modification of histone residues as discussed in chapter 1.2.1 and 1.2.2, respectively.

1.1.2 The linker histone

In most eukaryotic cells, the majority of nucleosomes is associated with an additional small and basic protein, the "linker histone", often referred to as "histone H1" (Woodcock et al., 2006). Linker histone-bound nucleosomes are generally termed "chromatosomes". Contrary to the highly conserved core histones, linker histones of different species are more divergent in sequence. Typically, higher eukaryotes express different isoforms of linker histones in a tissue- and developmental stage-dependent manner (Izzo et al., 2008; Kowalski and Palyga, 2012). These isoforms differ in their biochemical properties, for example their nucleosome binding affinities and chromatin compaction capabilities (Catez et al., 2006; Clausell et al., 2009; Orrego et al., 2007; Sun et al., 1990; Talasz et al., 1998), and vary in their genomic distribution (e.g. (Izzo et al., 2013; Millan-Arino et al., 2014)). Until recently, *Drosophila melanogaster* was assumed to possess only one linker histone homolog called "H1". However, Pérez-Montero et al. discovered a second isoform, "dBigH1", that was abundant during early embryogenesis and was replaced by H1 in somatic cells upon cellularization (Perez-Montero et al., 2013). Therefore, in adult flies dBigH1 is only present in germline cells, whereas H1 is ubiquitously expressed in somatic cells.

Metazoan linker histones comprise three distinct structural domains. A well conserved globular core domain comprising ~80 amino acids (aa) is flanked by an intrinsically disordered N- (13–40 aa) and C-terminal (~100 aa) region, respectively (Caterino and Hayes, 2011; McBryant et al., 2010). The globular domain harbors two DNA-binding surfaces and is sufficient for nucleosome binding (Allan et al., 1980; Brown et al., 2006; Goytisolo et al., 1996). Nevertheless, the lysine-rich C-terminus contributes to nucleosome binding affinity and is essential for H1-mediated chromatin condensation and linker DNA organization (see chapter 1.1.3 and below) (Allan et al., 1986; Caterino and Hayes, 2011; Hendzel et al., 2004; Lu and Hansen, 2004; Syed et al., 2010). Recently, also a role of the N-terminal domain in determining the binding affinity of linker histones was reported *in vivo* (Oberg and Belikov, 2012; Vyas and Brown, 2012). It is well established that the linker histone associates with the nucleosome close to the DNA entry/exit site and induces a change in the trajectory of the linker DNA leading to the formation of a stem-like structure (Bednar et al., 1998; Hamiche et al., 1996). Still, despite several decades of research the precise location and orientation of the linker histone on the nucleosome has not been resolved. However, mounting evidence supports simultaneous association of the globular domain of the linker histone with DNA at the nucleosomal dyad as well as extranucleosomal DNA at the entry/exit site (Brown et al., 2006; Syed et al., 2010; Zhou et al., 2013; Zhou et al., 1998). Whether the interaction with the extranucleosomal DNA is symmetric involving both linker DNAs or asymmetric to only one linker remains controversial. In addition to the globular domain, parts of the C-terminus are engaged with the linker DNA and support formation of a stem-like structure (Caterino et al., 2011; Hamiche et al., 1996; Lu and Hansen, 2004; Syed et al., 2010). Notably, also protein-protein contacts between H1 and the histone octamer may contribute to linker histone association (Boulikas et al., 1980; Vogler et al., 2010).

A number of early *in vitro* observations suggested linker histones to be general repressors of chromatin-based processes. Linker histone association did not only limit the mobility of nucleosomes (Pennings et al., 1994) but also protected about 20 additional base pairs at the entry/exit site from cleavage by micrococcal nuclease (Simpson, 1978). Moreover, H1 presence promoted chromatin condensation (see chapter 1.1.3), and some studies reported impairment of transcription from chromatin templates (Laybourn and Kadonaga, 1991; O'Neill et al., 1995). However, others found transcription to be unaffected by the linker histone in *in vitro* systems (Sandaltzopoulos et al., 1994). Moreover, also *in vivo* studies challenged the concept of a universal repressive role of H1 as depletion of linker histones in unicellular organisms as well as knock-out of individual isoforms in higher eukaryotes yielded generally mild phenotypes and mostly specific, variable effects on transcription (Izzo et al., 2008; Woodcock et al., 2006). Although subsequent analyses revealed that the reported subtle effects in higher eukaryotes could be explained by isoform-specific compensatory up-regulation of other linker histone variants and reduction of H1 levels beneath a certain threshold had more severe effects (see chapter 1.1.3), the expected global, repressive role of H1 could not be confirmed. Thus, the concept of a more specific linker histone function emerged (Izzo et al., 2008). On a related note, experiments employing fluorescence recovery after photobleaching (FRAP) demonstrated that H1 is highly mobile *in vivo* (Catez et al., 2006), which is in line with earlier *in vitro* findings (Caron and Thomas, 1981) and draws into question the model of a static, permanently inaccessible and repressive chromatin structure in presence of H1.

Despite availability of genome-wide mapping data in different cell systems (e.g. (Braunschweig et al., 2009; Izzo et al., 2013)), knowledge regarding the *in vivo* deposition and metabolism of H1 is scarce. Potential roles of chromatin remodeling factors in the deposition of linker histones will be discussed in chapter 1.3.4. Another aspect of linker histone biology currently gaining much attention is the emerging role of H1 as recruiting factor for effector proteins acting on nucleosomes (e.g. (Kalashnikova et al., 2013b; Lu et al., 2013; McBryant et al., 2010)). Taken together, linker histones seem to fulfill various functions in the nucleus, but the underlying mechanisms are just starting to be elucidated.

1.1.3 Higher order chromatin structure

The organization of DNA into nucleosomes and chromatosomes as a first level of compaction leads to the formation of nucleosome arrays that resemble a beads-on-the-string structure, commonly referred to as “10 nm fiber”. Further compaction is achieved by folding of individual arrays into coiled fibers as observed *in vitro* and *in situ*. As these fibers were reported to harbor a diameter of approximately 30 nm under various conditions, this level of chromatin compaction is commonly referred to as “30 nm fiber” (Grigoryev and Woodcock, 2012; van Holde, 1989). Molecular determinants of 30 nm fiber formation, its topology, and recent advances in elucidating higher order chromatin organization *in vivo* are discussed in the following chapter.

Chromatin condensation *in vitro* is mainly driven by electrostatic interactions and strongly depends on the presence of cations to partially neutralize the negative charge of the DNA (Clark and Kimura, 1990; Korolev et al., 2010; Sun et al., 2005; van Holde, 1989; Widom, 1986). With increasing salt concentrations, chromatin arrays progressively compact due to intra-array interactions. At elevated ionic strength, inter-array contacts are formed, leading to reversible oligomerization (Hansen, 2002).

Early on, a key role of the flexible, positively charged N-terminal tails of histones in facilitating chromatin compaction was recognized as tail-deleted nucleosome arrays failed to fully compact (Allan et al., 1982; Fletcher and Hansen, 1995; Garcia-Ramirez et al., 1992). While the tails of all four core histones contributed to chromatin folding and oligomerization (Carruthers and Hansen, 2000; Moore and Ausio, 1997; Pepenella et al., 2013; Schwarz et al., 1996; Tse and Hansen, 1997), the H4 tail was of particular importance (Dorigo et al., 2003; Gordon et al., 2005; Robinson et al., 2008). Central to H4 tail-mediated compaction is the interaction of a basic patch of amino acids of the tail (aa 16–20) with an acidic patch formed by H2A/H2B dimers of adjacent nucleosomes (Dorigo et al., 2003; Dorigo et al., 2004; Fan et al., 2004; Luger et al., 1997; Sinha and Shogren-Knaak, 2010; Zhou et al., 2007). Thereby, the H4 tail is expected to bridge nucleosomes, promoting chromatin fiber condensation as well as inter-array association. In addition to its interaction with the acidic patch, the H4 tail was suggested to bind to linker DNA (Chodaparambil et al., 2007; Kan et al., 2009), a distinct H2B epitope (Allahverdi et al., 2011), and further low-affinity binding sites on the histones (Chodaparambil et al., 2007). Furthermore, association with the acidic patch of the same nucleosome in *cis* was described (Kan et al., 2009; Zhou et al., 2007). However, the individual significance of the different interactions for chromatin condensation remains unclear. Local chromatin context including post-translational modifications of histones (see chapter 1.2.3), H2A variants (see chapter 1.2.1), and association of non-histone proteins presumably determines which of the possible interactions is predominantly formed (Kalashnikova et al., 2013a).

In addition to the histone tails, linker histones considerably contribute to the formation of higher order chromatin structures by facilitating condensation (Hansen, 2002; McBryant et al., 2010; van Holde, 1989). Accordingly, *in vitro* chromatosome arrays reach higher degrees of compaction at a given salt concentration than nucleosome arrays (Carruthers et al., 1998; Hizume et al., 2005; Robinson et al., 2008; Routh et al., 2008; Schalch et al., 2005; Thoma et al., 1979). The H1-dependent organization of the linker DNA flanking a nucleosome into a stem-like structure and the concomitant altered trajectory of the DNA are expected to be critical for the H1-effect on chromatin condensation (see chapter 1.1.2) (Bednar et al., 1998; Hamiche et al., 1996; Meyer et al., 2011; Wu et al., 2007). However, whether linker histones simply fulfill stabilizing functions or profoundly change chromatin fiber conformation and compaction capabilities is still under debate (Bednar et al., 1998; Carruthers et al., 1998; Dorigo et al., 2004; Kruithof et al., 2009; Maresca et al., 2005; McBryant et al., 2010; Robinson and Rhodes, 2006; Routh et al., 2008; Wu et al., 2007). Observed differences in the role of linker histones for chromatin compaction may be accounted for by variations in the applied analysis techniques, linker histone variants, H1 stoichiometry, and design of chromatosome arrays including their nucleosome repeat lengths (NRL), i.e. the average length of DNA associated with one nucleosome (Routh et al., 2008). Nevertheless, accumulating evidence supports an important role of linker histones in chromatin compaction *in vivo*. Although low levels of protein could be tolerated in mice (Fan et al., 2003), a change in chromatin compaction capability upon H1 depletion was evident in oligonucleosome arrays isolated from embryonic stem cells, which is in accordance with observations in *Drosophila melanogaster* where H1 loss resulted in global chromosome decondensation (Fan et al., 2005; Lu et al., 2009; Siriaco et al., 2009). Strikingly, in both systems H1 depletion was accompanied by a decrease in NRL (Fan et al., 2003; Lu et al., 2009; Siriaco et al., 2009). This compensatory mechanism was also observed *in vitro* in chromatin reconstitution systems (Blank and Becker, 1995; Rodriguez-Campos et al., 1989; Stein and Bina, 1984; Tremethick and Frommer, 1992) and was speculated to help restore proper chromatin compaction as well as charge homeostasis in absence of the linker histone (Woodcock et al., 2006). In line with this hypothesis, linker histone overexpression resulted in increased NRL (Gunjan et al., 1999), and a general correlation between linker histone abundance and NRL was reported in a number of cell types (Woodcock et al., 2006).

The impact of the NRL on the formation of chromatin higher order structures is a field of current research (Grigoryev, 2012; Perisic et al., 2010; Szerlong and Hansen, 2011; Wong et al., 2007; Wu et al., 2007). Careful *in vitro* analyses by the Rhodes laboratory employing regularly spaced arrays harboring a variety of linker lengths differing in multiples of 10 bp (177–237 bp) showed that chromatin fiber dimensions depended on the NRL (Robinson et al., 2006). Chromatosome arrays with a NRL of 217–237 bp displayed a higher fiber diameter and nucleosome density (number of nucleosomes per 11 nm) than arrays with shorter NRL. In the absence of linker histones, however, arrays with a very short NRL of 167 bp formed more condensed and ordered structures than arrays with a NRL of 197 bp (Routh et al., 2008). This finding was further confirmed by Correll et al. reporting a negative correlation of NRL and fiber compaction for nucleosome arrays lacking linker histones (Correll et al., 2012). Moreover, this study demonstrated that slight deviation of linker DNA length from the 10*n* bp increments typically found *in vivo* (Widom, 1992) and widely applied in *in vitro* studies did not affect the compaction capabilities of chromatosome or nucleosome fibers harboring long linkers. Contrary, nucleosome arrays with short NRLs (165–177 bp) were sensitive to these variations. Therefore, nucleosome packaging and chromatin compaction in densely spaced fibers apparently depends – at least in the absence of linker histones – on the inter-nucleosomal rotational setting. Collectively, these results indicate a fundamental contribution of the NRL to chromatin condensation. However, *in vivo* a plethora of architectural proteins in addition to linker histones, for example HP1, PRC1, or Sir3, act in concert to shape the higher order structure of chromatin, potentially overriding some of the fiber`s intrinsic dynamics (Luger and Hansen, 2005; McBryant et al., 2006).

Despite its recognition as fundamental building block of chromatin higher order structures, the topology of the 30 nm fiber remains controversial. Different structural models were proposed and the most prominent ones can be divided into two classes: the “two-start” and the “one-start” helical models (Figure 2) (Grigoryev and Woodcock, 2012; Wu et al., 2007). According to the two-start models, the nucleosomes of one array are arranged in two stacks forming a double-helical structure. Consecutive nucleosomes are connected in a zigzag manner by essentially straight running linker DNA (Figure 2A) (Dorigo et al., 2004; Schalch et al., 2005; Thoma et al., 1979; Woodcock et al., 1984; Worcel et al., 1981). Contrary, the one-start models propose the formation of a solenoid structure with consecutive nucleosomes following a helical path. In contrast to the two-start model, the linker DNA is bent into the

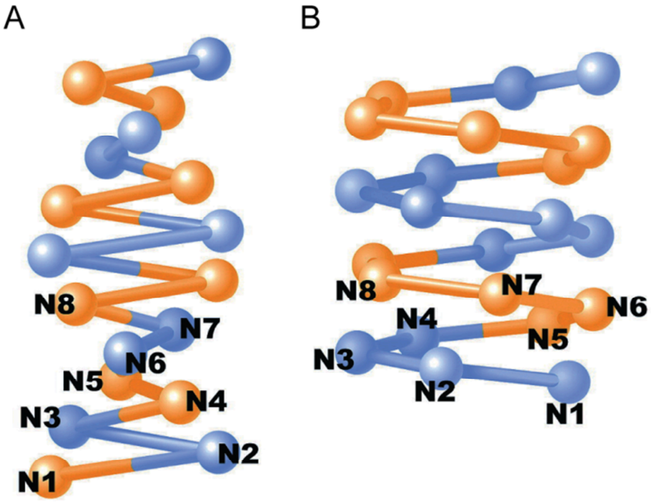

Figure 2: Models of the 30 nm fiber. Schematic depictions of the two-start (**A**) and the one-start (**B**) topological model of the 30 nm chromatin fiber are shown. Nucleosome core particles (N) are represented by spheres, the linker DNA by sticks. The first eight nucleosome core particles are numbered according to their position along the DNA. For reasons of clarity, consecutive pairs of neighboring nucleosomes in (A) and consecutive helical gyres in (B), respectively, are indicated in blue and orange. (Reprinted from (Maeshima et al., 2010) with permission from Elsevier)

inside of the fiber (Figure 2B) (Daban and Bermudez, 1998; Finch and Klug, 1976; Robinson et al., 2006). Notably, recent modeling and experimental data suggest that – at least *in vitro* – even chromatin fibers with unified NRL are not uniformly organized but indeed show conformational heterogeneity (Diesinger and Heermann, 2009; Grigoryev et al., 2009; Schlick et al., 2012; Schlick and Perisic, 2009). Therefore, long-held concepts of a universal chromatin fiber conformation on the 30 nm fiber level have to be reconsidered.

Until recently, the prevalent model of nuclear chromatin organization postulated a hierarchical, ordered folding of 30 nm fibers into higher order structures ultimately giving rise to the highly condensed mitotic chromosomes (Figure 3A). However, this view was lately called into question. While the debate over the topology of the 30 nm fiber *in vitro* continues, *in vivo* its mere existence was challenged. Attempts to visualize distinct 30 nm fibers *in vivo* using various EM techniques as well as a combination of electron spectroscopic imaging and tomography largely failed (Fussner et al., 2011; Fussner et al., 2012; Horowitz-Scherer and

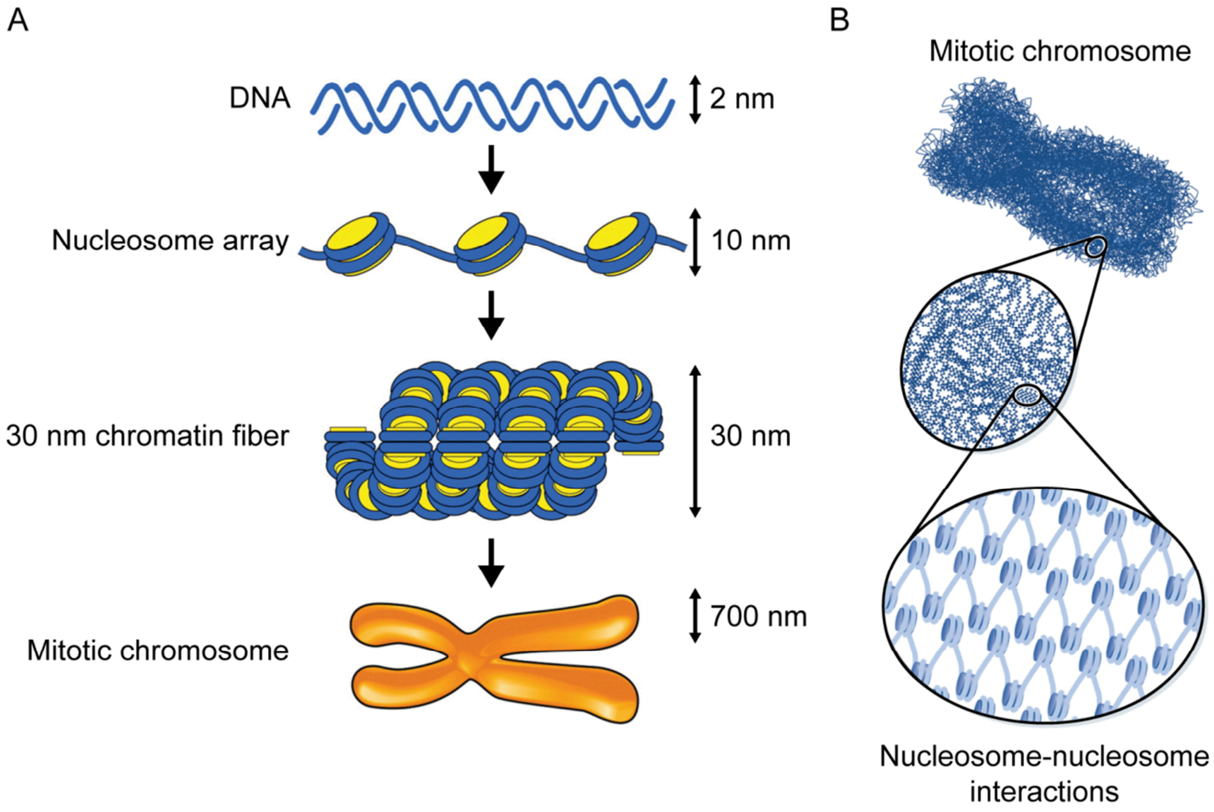

Figure 3: Models of chromatin higher order structure formation *in vivo*. (**A**) The different levels of DNA compaction according to the traditional text-book view are depicted schematically. (Adapted from (Maeshima et al., 2010) and reprinted with permission from Elsevier) (**B**) The emerging concept of a fractal nature of chromatin organization is illustrated. Interactions form between nucleosomes of different fibers and between distant nucleosomes of one fiber by folding back. No regular structures beyond 10 nm fibers can be observed, but structural features appearing similar to each other at many magnifications result. (Adapted from (Hansen, 2012) and reprinted with permission from John Wiley and Sons)

Woodcock, 2006; Maeshima et al., 2010). Only in specialized, transcriptionally mostly inactive cell types structures resembling the 30 nm fiber found *in vitro* were observed (Woodcock, 1994). Moreover, the Maeshima laboratory recently provided compelling evidence for a lack of regular chromatin structures beyond 10 nm fibers in human interphase and mitotic chromosomes applying small angle X-ray scattering (SAXS) (Joti et al., 2012; Nishino et al., 2012). These observations prompted the concept of a fractal nature of chromatin organization *in vivo* (Hansen, 2012). In this model, nucleosomes interact and interdigitate extensively with distant nucleosomes or nucleosomes of distinct fibers, forming irregular, highly dynamic structures that display similar features at different magnifications (Figure 3B) (Hansen, 2012; Maeshima et al., 2010). Array oligomerization at high chromatin concentrations and elevated salt conditions was suggested to be the *in vitro* correlate of these structures (Hansen, 2012). Although local, transient, and tissue-specific formation of 30 nm fiber structures cannot be excluded *in vivo*, the majority of chromatin fibers seems to adopt alternative structures, dominated by contacts between non-neighboring nucleosomes. However, the molecular determinants driving nucleosome interactions and chromatin compaction in the proposed fractal structures *in vivo* are expected to be the same that were identified to be responsible for chromatin condensation *in vitro* (Fussner et al., 2011; Hansen, 2012). Therefore, *in vitro* reconstitution and biochemical analysis of chromatin fibers remain important tools to elucidate basic mechanisms of chromatin organization as well as dynamics.

1.2 Dynamics and regulation of chromatin

The chromatin organization of DNA constitutes a considerable obstacle to the nuclear machineries involved in processes like transcription, replication, and DNA repair that need to gain access to DNA in a coordinated manner. DNA binding sites are largely occluded from their cognate interaction factors when packaged into nucleosomes, and compaction of nucleosomal arrays into higher order structures is expected to further impede DNA accessibility. However, to allow cells to adapt their transcriptional programs in response to outside stimuli, to ensure proper progression through the cell cycle, and to regulate DNA repair processes DNA accessibility and thus chromatin structure, nucleosome positioning and stability need to be highly dynamic and tightly regulated (Luger et al., 2012). Strategies evolved to allow and reinforce dynamic transitions between chromatin states will be outlined in the following with an emphasis on the role of the histones that are much more than mere scaffolds for DNA wrapping. It should be noted that besides the histone-based mechanisms described here also DNA methylation, association of non-coding RNAs, and the binding of architectural proteins are involved in regulating chromatin-related processes and delineating functional genomic domains (Bergmann and Spector, 2014; McBryant et al., 2006; Smith and

Meissner, 2013). Chromatin remodeling enzymes as key players in chromatin dynamics and nucleosome positioning will be discussed in chapter 1.3.

1.2.1 Histone variants

An important means to site-specifically modulate nucleosome stability, structure, and chromatin condensation is the deposition of non-allelic core histone variants. Numerous of these variants – especially of H3 and H2A – that differ in their primary sequence from the canonical histones and display distinct expression patterns have been and still continue to be discovered (Szenker et al., 2014). Many are evolutionarily conserved, underlining their non-redundant functions (Talbert and Henikoff, 2010). In contrast to the canonical histones, variants are incorporated into nucleosomes in a DNA synthesis-independent manner at specific genomic sites through mechanisms that are still under investigation (Szenker et al., 2014). Consequently, particular functional states of chromatin are commonly marked by enrichment of specific histone variants (Henikoff et al., 2004).

Variant incorporation confers distinct biochemical properties to nucleosomes by creating unique interaction epitopes. These may affect intra-nucleosomal protein-protein or DNA-protein contacts, thereby influencing nucleosome stability and structure (Kurumizaka et al., 2013; Luger et al., 2012). On the other hand, variants provide specific interaction surfaces for the recruitment of effector proteins and factors of the nuclear signaling machinery as well as for inter-nucleosomal contacts (Bönisch and Hake, 2012; Szenker et al., 2014). Thereby, histone variants importantly contribute to chromatin higher order structure formation. Some H2A variants, for instance, harbor altered amino acid sequences that lead to changes in the composition of the acidic patch formed by H2A and H2B (see chapter 1.1.3) (Bönisch and Hake, 2012). These changes were found to correlate with altered chromatin condensation capabilities of nucleosome arrays *in vitro*, highlighting the relevance of the acidic patch in higher order structure formation. Taken together, histone variant incorporation – including linker histone isoforms (see chapter 1.1.2) – provides a major mechanism to locally fine-tune DNA accessibility through modulation of nucleosome and chromatin structure.

1.2.2 Post-translational modifications of histones

Post-translational modifications (PTMs) of histones – including the linker histones –, so-called “histone marks”, add an additional level of complexity to nucleosome diversity and chromatin dynamics. Multiple different modifications on numerous histone residues were identified. These modifications include well known types like acetylation, methylation, or ubiquitylation of lysine and phosphorylation of serine or threonine as well as less characterized marks, for example crotonylation or succinylation of lysine and methylation of glutamate (Du et al., 2011; Kouzarides, 2007; Tan et al., 2011; Tessarz et al., 2014). Still, novel sites as well as types of modifications continue to be discovered at a rapid pace.

Initially, the lysine-rich and exposed histone tails were considered to be the major sites of post-translational modifications. However, recently also histone modifications located in the structured domains of the histones have come into focus (Tropberger and Schneider, 2013).

The post-translational modification of histones is a dynamic, reversible process involving the interplay of dedicated enzymes that install or remove the marks, respectively (Bannister and Kouzarides, 2011; Kouzarides, 2007). These enzymes are frequently part of large complexes that may combine various catalytic activities acting together to achieve desired outcomes (Bannister and Kouzarides, 2011). For example, the NuRD chromatin remodeling complex (see chapter 1.3) contains histone deacetylases in addition to the remodeling enzyme Mi-2. Both enzymatic activities presumably act in concert to establish transcriptionally repressed chromatin states (Clapier and Cairns, 2009). Some modifying enzymes, like the methyltransferases Set1 and 2, were furthermore found to travel with RNA polymerase II, catalyzing histone modifications concomitant with transcription (Sims et al., 2004).

In vivo, the enrichment of particular histone marks strongly correlates with chromatin functional states – like active transcription or silenced genes – and *cis*-regulatory elements including enhancers and promoters (Bannister and Kouzarides, 2011). While, for example, trimethylation of H3 at lysine 4 marks active promoters, trimethylation of the same histone at lysine 36 is enriched over gene bodies of actively transcribed genes (Hon et al., 2009). Despite the noted remarkable correlations, the significance and functional relevance of individual histone PTMs for the establishment and maintenance of chromatin states is still under debate. Nevertheless, numerous *in vitro* and *in vivo* studies addressed the impact of histone PTMs on nucleosome and chromatin dynamics. The derived mechanisms will be discussed in the following.

Analogous to histone variants, PTMs can affect the stability and dynamics of nucleosomes by modifying intra-nucleosomal interactions. Acetylation of H3 at lysine 56 residing in the structured region of the histone, for example, destabilizes DNA wrapping close to the entry/exit site, facilitating transcription factor binding *in vitro* and presumably also *in vivo* (Tropberger and Schneider, 2013). Moreover, a key feature of histone marks is the formation or occlusion of specific binding epitopes for the interaction with chromatin factors. Multiple protein domains were identified that recognize histone PTMs and are shared by chromatin-associated proteins of diverse function like modifying enzymes themselves, chromatin remodeling factors, or architectural proteins. Bromodomains, for example, preferentially bind to acetylated lysine residues within histones, whereas chromodomains typically interact with methylated histone tails, often in a site-specific manner (Patel and Wang, 2013; Yun et al., 2011). Frequently, chromatin factors possess several different histone recognition domains, potentially allowing differential read-out of complex histone modification patterns occurring on the same or neighboring nucleosomes. How and to what extent combinatorial histone marks influence the binding of chromatin factors *in vivo* is currently under intense investigation

(Rando, 2012; Ruthenburg et al., 2007). Notably, accumulating evidence suggests that certain histone modifications primarily function as allosteric regulators of interacting effector proteins rather than targeting signals (Rando, 2012).

A further important mechanism of histone modification-regulated chromatin dynamics is the direct impact of some marks on chromatin structure by modulating inter-nucleosomal interactions. However, only a limited number of modifications was shown to be capable of influencing chromatin compaction *in vitro*. Among them is the acetylation of histone H4 at lysine 16, as discussed in detail in the next section.

1.2.3 Acetylation of histone H4 at lysine 16

Histone acetylation marks in general are highly abundant (Jung et al., 2013; Phanstiel et al., 2008; Smith et al., 2003) and typically display rapid turnover in comparison to other histone PTMs like methylation (Barth and Imhof, 2010; Evertts et al., 2013; Zheng et al., 2013). Histone acetylation is catalyzed by specific, conserved enzymes, the histone acetyltransferases (HATs), often possessing a rather broad substrate specificity including non-histone targets (Bannister and Kouzarides, 2011; Shahbazian and Grunstein, 2007; Yang and Seto, 2008). These enzymes transfer an acetyl group from acetyl coenzyme A to the ε-amino group of lysines (Figure 4). The reverse reaction, acetyl group removal, is catalyzed by histone deacetylases (HDACs).

Several lines of evidence led to the widely accepted notion that histone acetylation provides a crucial mechanism for the regulation of gene expression (Eberharter and Becker, 2002). HATs were recognized as transcriptional activators or co-activators, whereas HDACs were found to be involved in gene repression (Roth et al., 2001; Struhl, 1998). Consistently, early on an association of histone acetylation with sites of active transcription and open, more permissive chromatin structures was observed (Hebbes et al., 1994; Mizzen and Allis, 1998; Turner, 1991). Moreover, transcription from chromatin templates *in vitro* was markedly enhanced in presence of hyperacetylated histones (Allfrey et al., 1964; Protacio et al., 2000; Wolffe and Hayes, 1999). Mechanistically, weakened electrostatic interactions between

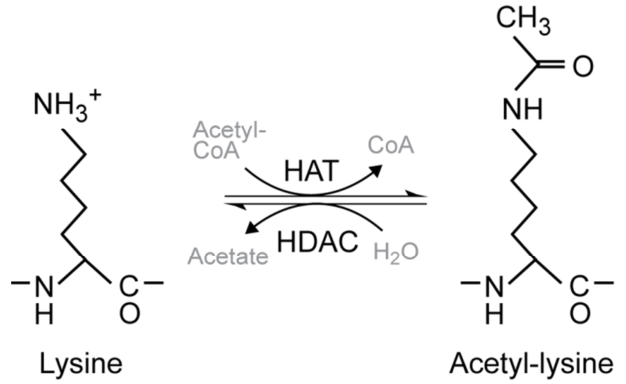

Figure 4: Lysine acetylation. Lysine acetylation in the context of histones is catalyzed by histone acetyltransferases (HAT) transferring an acetyl group from coenzyme A (CoA) to lysine. Histone deacetylases (HDACs) can reverse the acetylation.

acetylated histones and DNA resulting in increased DNA accessibility were proposed to be important, as acetylation neutralizes the positive charge of lysine (Figure 4) (Calestagne-Morelli and Ausio, 2006). This assumption was fuelled by *in vitro* findings demonstrating markedly reduced chromatin compaction and oligomerization properties of hyperacetylated chromatin fibers (Garcia-Ramirez et al., 1995; Tse et al., 1998). However, the individual contributions of the tails and specific sites initially remained unclear.

In a pioneering study, Peterson and co-workers could demonstrate a critical role of the acetylation of lysine 16 of H4 (H4K16ac) in chromatin condensation *in vitro* by incorporating engineered, site-specifically acetylated histone H4 (see chapter 1.4) into short nucleosome arrays (12 nucleosomes, NRL: 177 bp) (Shogren-Knaak et al., 2006). As lysine 16 is part of the basic patch that had previously been shown to be crucially involved in chromatin condensation (see chapter 1.1.3), modification of this residue seemed to be a likely mechanism for regulating inter-nucleosomal contacts. Indeed, the arrays carrying H4K16ac displayed reduced folding and oligomerization capabilities in comparison to unmodified controls (Shogren-Knaak et al., 2006). Consistently, the Rhodes laboratory reported comparable results employing long nucleosome as well as chromatosome arrays (61 nucleosomes, NRL: 202 bp) (Robinson et al., 2008). Enzymatic acetylation of just about 30% of the H4 tails led to dramatically reduced fiber compaction, notably also in presence of the linker histone variant H5. Moreover, subsequent systematic analyses of the folding capabilities of the short nucleosome arrays already employed by Shogren-Knaak et al. (see above) by the Nordenskiöld laboratory demonstrated that triple-acetylation of the other three lysine residues within the H4 tail did not affect chromatin compaction to a comparable degree, underlining the unique role of H4K16ac (Allahverdi et al., 2011). Furthermore, whereas triple-mutation of lysines 5, 8, and 12 to glutamine, which mimicks acetylated lysine, affected chromatin compaction in a similar manner as triple-acetylation of these residues, lysine 16 mutation had a much weaker effect than H4K16ac, confirming earlier observations of the Rhodes` laboratory (Robinson et al., 2008). Therefore, the mechanism of H4K16ac-driven chromatin decompaction cannot be solely explained by electrostatic effects. Conversely, specific inter-nucleosomal contacts seem to be altered by the acetylation (Allahverdi et al., 2011). It is conceivable that H4K16ac specifically interferes with the interaction between the basic patch of the H4 tail and the acidic patch of adjacent nucleosomes. However, also other mechanisms were proposed (Allahverdi et al., 2011) (see also chapter 1.1.3). Notably, in contrast to intra-fiber folding fiber oligomerization was found to be governed by electrostatic mechanisms. Lysine to glutamine mutations disrupted inter-fiber contacts to the same extent as the respective acetylations (Allahverdi et al., 2011). In summary, *in vitro* analyses strongly suggest a unique regulatory potential of H4K16ac for fiber compaction through disrupting specific inter-nucleosomal interactions.

Consistent with the chromatin decompaction properties of H4K16ac evidenced *in vitro*, in *Drosophila melanogaster* the mark was found enriched in open, accessible regions of the genome including sites of active transcription and replication origins (Bell et al., 2010; Gelbart et al., 2009; Schwaiger et al., 2009). Remarkably, the mark is globally enriched on the X chromosome of male flies, where it covers gene bodies (Gelbart et al., 2009). This enrichment is accompanied by a chromosome-wide two-fold up-regulation of gene expression and a more permissive chromatin structure, as evidenced by enhanced nuclease accessibility and visible chromatin decondensation in the context of polytene chromosomes (Bell et al., 2010; Conrad and Akhtar, 2011; Offermann, 1936). Increased transcription from the single male X chromosome serves to compensate the lack of a second X chromosome as present in females and is mediated by the specific targeting of the dosage compensation complex (DCC) (Conrad and Akhtar, 2011). This complex contains the acetyltransferase MOF which is the major HAT for lysine 16 of H4 (H4K16) in flies. Notably, MOF activity is essential for proper dosage compensation and therefore viability of male flies (Akhtar and Becker, 2000; Hilfiker et al., 1997). Moreover, in cell-free *Drosophila* extracts H4K16 acetylation by MOF is accompanied by elevated transcription from a reconstituted chromatin template, and targeting of MOF to a reporter construct in yeast cells results in strong acetylation activity-dependent reporter expression (Akhtar and Becker, 2000). Therefore, it is widely accepted that X chromosomal H4K16ac enrichment is a key principle in dosage compensation in *Drosophila* to induce a permissive chromatin structure and facilitate transcription, although details of the underlying mechanisms remain elusive (Conrad and Akhtar, 2011). However, genome-wide mapping studies of H4K16ac in cell systems of other organisms do not unequivocally support a universal, critical role of H4K16ac in facilitating gene activation. For example, in budding and fission yeast, human HEK293, or neural progenitor cells a clear correlation between enrichment of H4K16ac and gene activity is largely lacking (Horikoshi et al., 2013; Kurdistani et al., 2004; Liu et al., 2005; Taylor et al., 2013; Wiren et al., 2005). Notably, in contrast to localization of H4K16ac over gene bodies as observed on the X chromosome of male flies, in other cell systems the mark was found enriched in promoter regions. Additionally, studies on the function of H4K16ac in transcription yielded conflicting results. Whereas some described a positive role of the modification by for instance promoting the release of paused RNA polymerase II (Pol II) (Kapoor-Vazirani et al., 2011; Zippo et al., 2009), others reported an inhibitory effect on Pol II passage and therefore gene expression (Heise et al., 2012). Besides transcription, acetylation of H4K16 was implicated to affect processes like DNA repair and gene silencing (Vaquero et al., 2007; Zhou and Grummt, 2005). Altered levels of the acetylation mark are frequently found in human cancers, but the significance of this event in cell transformation is currently unknown (Leroy et al., 2013; Vaquero et al., 2007). Taken together, the *in vivo* roles of H4K16ac are more complex, diverse, and context-dependent than might have been expected from *in vitro* observations, and gaining a comprehensive understanding of H4K16ac function in various cellular environments remains an important goal.

Notably, the mechanisms of H4K16ac-mediated regulation of chromatin processes are most likely not solely imparted by its chromatin decompaction capabilities. Also more indirect mechanisms including H4K16ac-specific recruitment of effector proteins may be involved (Shahbazian and Grunstein, 2007). A potential role for H4K16ac in factor targeting was, for example, indicated by the recent observation that at the level of nucleosomes the mark specifically enhances binding affinity of BPTF, the human homolog of Nurf301, a subunit of the NURF chromatin remodeling complex (see chapter 1.3.1), when it co-occurs with trimethylation of lysine 4 of histone H3 on the same nucleosome (Ruthenburg et al., 2011). BPTF engages the methylation via a so-called “PHD finger” domain, whereas the acetylation is recognized by the adjacent bromodomain. This bivalent interaction was suggested to be of relevance for targeting NURF in vertebrates. Moreover, H4K16ac can also block binding sites on the H4 tail. In budding yeast, the SIR complex mediates gene silencing, and its subunit Sir3 binds unmodified H4 tails with higher affinity than those acetylated at lysine 16, a mechanism involved in proper establishment of repressive chromatin structures (Oppikofer et al., 2013). It is furthermore conceivable that H4K16ac, by altering intra- or inter-nucleosomal contacts, opens up otherwise occluded interaction surfaces. Finally, a role for H4K16ac in regulating the activity of the chromatin remodeling enzyme ISWI and its complexes was proposed. As discussed in detail in chapters 1.3.3 and 1.3.4, the acetylation was reported to inhibit the remodeling factors, a mechanism that bears important implications for the establishment of higher order chromatin structures.

1.3 ATP-dependent chromatin remodeling

Central players in the dynamic regulation of chromatin-based processes are the chromatin remodeling enzymes (also referred to as “nucleosome remodeling enzymes”). Coupled to ATP hydrolysis, these highly abundant and conserved enzymes are capable of altering the interactions between nucleosomal DNA and the histone octamer (Becker and Workman, 2013; Clapier and Cairns, 2009). This activity translates into a variety of biological outcomes, including nucleosome repositioning (termed “sliding” hereafter), eviction as well as assembly, and exchange of histone variants (Figure 5). Thus, chromatin remodeling enzymes are fundamentally involved in determining local DNA access and nucleosome dynamics as well as in establishing and maintaining higher order chromatin structures. Virtually all chromatin-based processes require chromatin remodeling activities for proper regulation and progression. Consistently, mutation and mis-regulation of chromatin remodeling enzymes is a common feature in cancer and other diseases (Berdasco and Esteller, 2013; Narlikar et al., 2013).

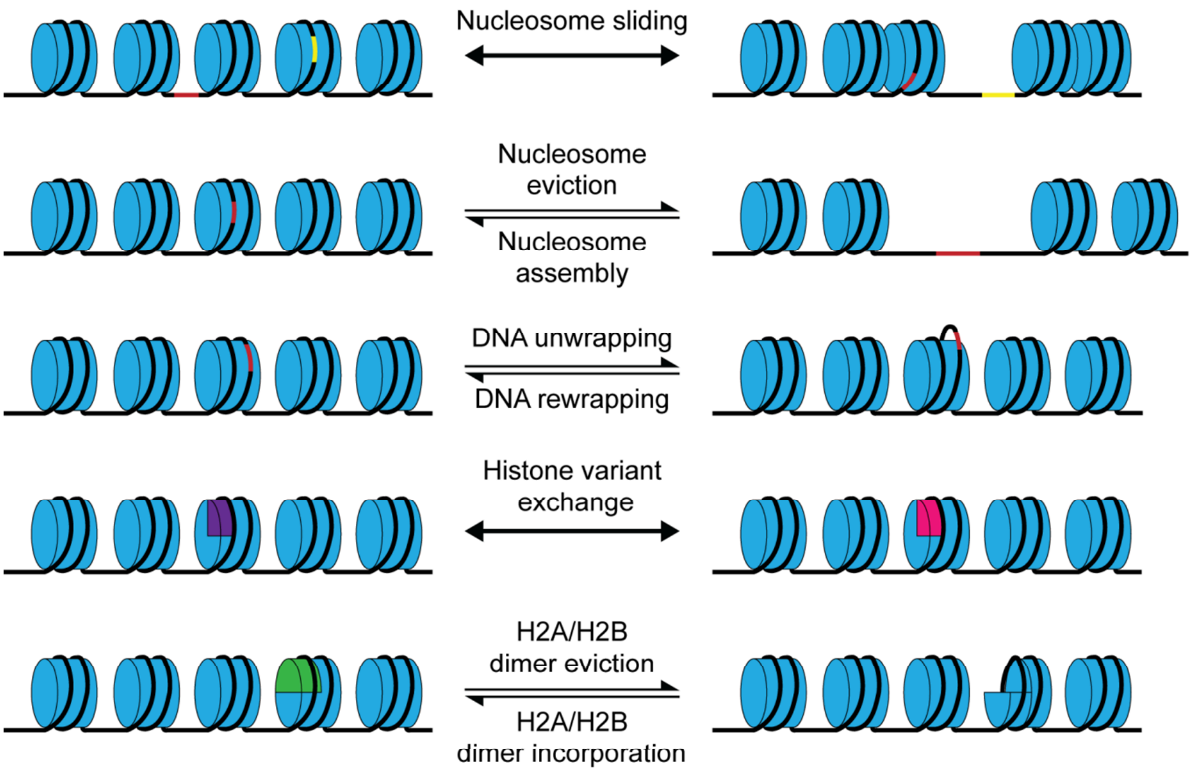

Figure 5: Activities of chromatin remodeling factors. Chromatin remodeling factors catalyze a range of different reactions. Histone octamers are depicted in blue, DNA in black. Red and yellow colored DNA patches illustrate how specific DNA sites get occluded by nucleosomes or are rendered accessible upon remodeling. Histone variants that get exchanged are marked in pink or violet, respectively. An H2A/H2B dimer evicted or incorporated with the assistance of chromatin remodeling factors is highlighted in green.

As illustrated in the enclosed review article (see Figure 1 of chapter 2.2), all chromatin remodeling enzymes belong to the Snf2 family of proteins and share a homologous, DNA helicase-like ATPase domain (Flaus et al., 2006). According to the sequence similarities of their ATPase domains, the remodeling enzymes are further grouped into subfamilies. Notably, members of a subfamily typically display homology also outside the ATPase domain and are characterized by the presence of certain domain motifs, many of which are implicated in protein-protein or DNA-protein interactions. Among them are domains whose homologs were identified as histone PTM recognition motifs, like chromo- or bromodomains (see chapters 1.2.2 and 1.2.3).

In vivo, the vast majority of chromatin remodeling enzymes resides in multimeric complexes (referred to as “remodeling factors” hereafter) (Clapier and Cairns, 2009; Gangaraju and Bartholomew, 2007b). The associated subunits are mostly non-catalytic but critically involved in targeting and regulating the enzymatic activity and determining the biological outcome of remodeling reactions. Frequently, the same enzyme is found as part of different complexes in a tissue- and developmental stage-dependent manner (Clapier and Cairns, 2009). The remodeling factors of the ISWI subfamily constitute an instructive example for these features as discussed in the next chapter.

1.3.1 The ISWI-type chromatin remodeling factors

Chromatin remodeling factors harboring enzymes belonging to the ISWI subfamily (termed “ISWI complexes” hereafter) were initially identified in *Drosophila melanogaster* and turned out to be conserved among eukaryotes. Whereas most eukaryotes, including budding yeast and humans, contain several different ISWI homologs, flies express only one ISWI enzyme that assembles into a number of different complexes (Figure 6A; see below) (Emelyanov et al., 2012; Yadon and Tsukiyama, 2011).

All ISWI-type enzymes share a conserved domain structure (Figure 6B). The N-terminal region is poorly characterized and its properties are just starting to be elucidated (see

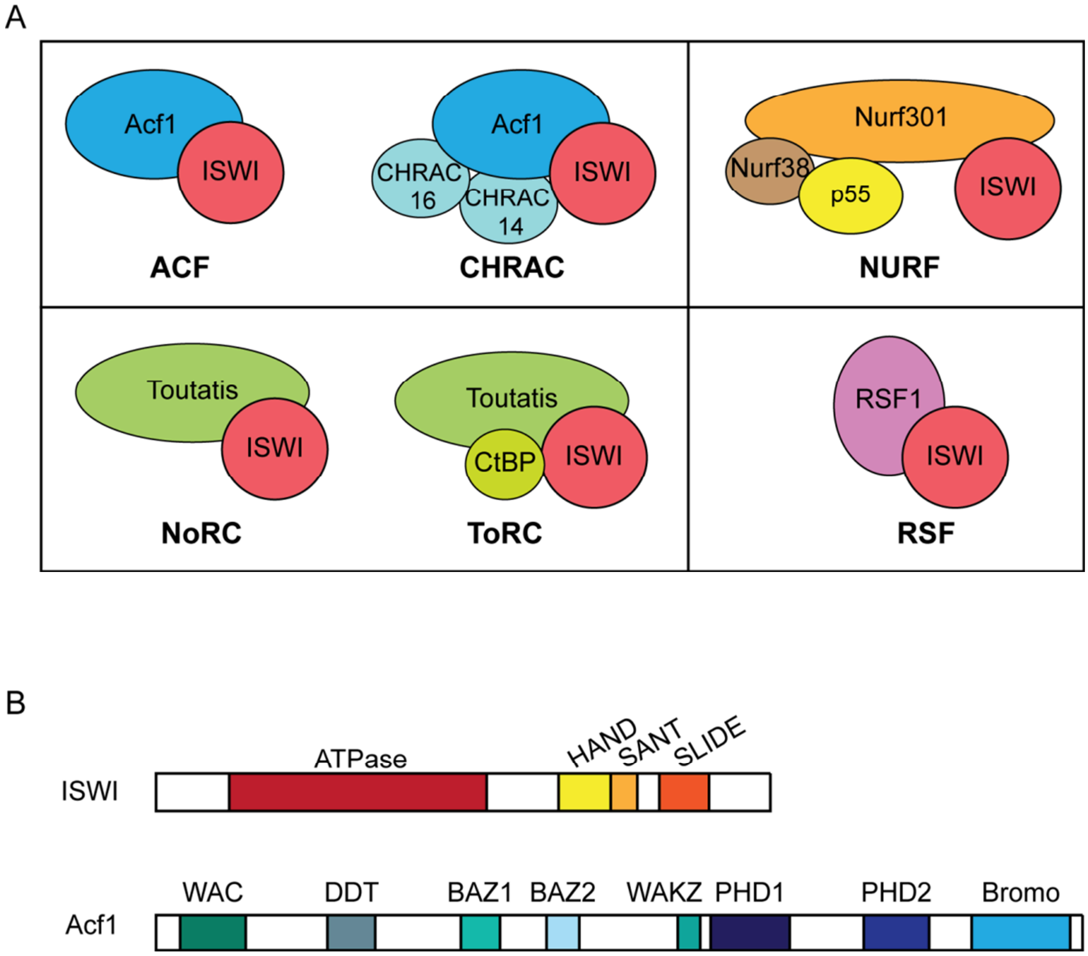
A
Acf1
ISWI
ACF
Acf1
CHRAC 16
CHRAC 14
ISWI
CHRAC
Nurf301
Nurf38
p55
ISWI
NURF
Toutatis
ISWI
NoRC
Toutatis
CtBP
ISWI
ToRC
RSF1
ISWI
RSF
B
ISWI
ATPase
HAND
SANT
SLIDE
Acf1
WAC
DDT
BAZ1
BAZ2
WAKZ
PHD1
PHD2
Bromo

Figure 6: The ISWI complexes of *Drosophila melanogaster*. (**A**) The subunit compositions of all ISWI-containing complexes identified in *Drosophila* to date are depicted. The names of the complexes are highlighted in bold. (**B**) Acf1 and ISWI contain several protein domains that are shown schematically. (Domain structure of Acf1 according to (Eberharter et al., 2004))

chapters 2.1, 2.2, and 3.2). Notably, it contains conserved motifs of so far unknown function. The ATPase domain consists of two lobes comprising a succession of sequence motifs typically found in helicase-like enzymes (Dürr et al., 2006). C-terminal to the ATPase domain and connected by a presumably unstructured hinge, a structural module comprising three motifs, HAND, SANT, and SLIDE (HSS), was identified (Grüne et al., 2003). This module was described to be importantly involved in DNA and nucleosome recognition. The HAND domain was characterized by crystallization, consists of four helices, and does neither share sequence nor structural similarity to other protein domains. Contrary, the SANT domain of ISWI was assigned based on sequence similarity to canonical SANT domains that were implicated to mediate chromatin interactions (Aasland et al., 1996). The sequence of the SLIDE domain, short for "SANT-like ISWI domain", is related to SANT domains, but harbors insertions. The crystal structure of the isolated HSS domain confirmed relatedness of the SANT and SLIDE domain with canonical SANT domains (Grüne et al., 2003). The SANT-SLIDE modules of ISWI and the related chromatin remodeling enzyme Chd1 harbor a basic as well as an acidic surface (Grüne et al., 2003; Ryan et al., 2011; Sharma et al., 2011; Yamada et al., 2011). The basic surface mediates DNA interactions, whereas the acidic surface was suggested to be involved in contacting the histone octamer.

The ATPase activity of enzymes of the ISWI subfamily is stimulated by DNA and even more so by nucleosomes (Corona et al., 1999; Grüne et al., 2003). How the specificity for the nucleosome is mediated is still unclear, and information on the interactions between the histone octamer and ISWI are scarce, although the orientation of productively bound ISWI on the nucleosome has been mapped. As detailed and illustrated in the enclosed publications (see chapters 2.1 and 2.2), ISWI engages the nucleosome with its ATPase domain located at SHL2, whereas the HSS domain interacts with extranucleosomal DNA at the entry/exit site. Notably, localization of the ATPase domain at SHL2 is a common feature of chromatin remodeling enzymes. The mechanistic implications of the reported enzyme orientation on the nucleosomal substrate are discussed in the next chapter (1.3.2).

In *Drosophila*, ISWI was found to reside in at least six different remodeling complexes (Figure 6A) (Emelyanov et al., 2012; Yadon and Tsukiyama, 2011). To date, the most intensively studied and characterized ones are the ACF (ATP-utilizing chromatin assembly and remodeling factor), CHRAC (chromatin accessibility complex), and NURF (nucleosome remodeling factor) complexes. ACF and CHRAC share a common non-catalytic subunit, the Acf1 protein. Acf1 contains several conserved sequence motifs, including two PHD fingers and a bromodomain (Figure 6B). The PHD fingers were suggested to interact with the histone octamer, thereby enhancing nucleosome sliding efficiency, but molecular details of this mechanism remain unknown (Eberharter et al., 2004). In addition to Acf1, CHRAC harbors two small proteins, termed CHRAC 14 and 16 according to their molecular weights, that both comprise a histone fold motif and can bind to DNA (Corona et al., 2000; Poot et al., 2000). Association of CHRAC 14 and 16 with ISWI and Acf1 enhances nucleosome sliding (Hartlepp et al., 2005; Kukimoto et al., 2004). The underlying mechanism, however, is not fully understood. The NURF complex contains three subunits in addition to ISWI (Tsukiyama and Wu, 1995). Analogous to Acf1, Nurf301, the largest subunit of NURF, harbors PHD fingers and a bromodomain (Xiao et al., 2001). Notably, one of the PHD fingers of BPTF, the human homolog of Nurf301, was shown to specifically interact with histone H3 trimethylated at K4, thereby stabilizing NURF at its genomic target sites (Wysocka et al., 2006). As already mentioned in chapter 1.2.3, additional engagement of the bromodomain with an H4 tail acetylated at K16 further strengthened nucleosome binding of BPTF (Ruthenburg et al., 2011).

All ISWI complexes analyzed so far catalyze the repositioning of nucleosomes along DNA in *cis* without nucleosome disruption (Hamiche et al., 1999; Längst et al., 1999). This reaction is termed “nucleosome sliding”, and mechanistic details are discussed in the next chapter (1.3.2). The sliding activity is inherent to the ISWI enzyme, but the associated subunits are important modulators of the reaction (see chapter 2.2). They not only enhance the efficiency of nucleosome sliding but also determine the outcome of a remodeling reaction (Eberharter et al., 2001; Hamiche et al., 1999; Hartlepp et al., 2005; Ito et al., 1999). For instance, in *in vitro* studies the Acf1-containing complexes ACF and CHRAC introduced a regular spacing of characteristic NRL into nucleosome arrays, whereas NURF apparently randomly repositioned nucleosomes and did not confer regularity (Ito et al., 1997; Varga-Weisz et al., 1997). The isolated ISWI enzyme was found to introduce regularity and a compact spacing of nucleosomes (Corona et al., 1999). Moreover, employing isolated, single nucleosomes positioned on a short linear DNA fragment (mononucleosomes) as substrates for sliding, ACF and CHRAC were shown to center the nucleosome. Contrary, the ISWI enzyme moved the nucleosomes to positions close to the DNA ends (Eberharter et al., 2001; Längst et al., 1999). In summary, accessory subunits possess remarkable regulatory potential in the context of ISWI-catalyzed remodeling reactions. However, the underlying mechanisms are still under investigation.

Besides nucleosome sliding, ISWI complexes, including *Drosophila* ISWI, ACF, CHRAC, and ToRC, facilitate chromatin assembly *in vitro* in conjunction with the histone chaperone NAP1 (Corona et al., 1999; Emelyanov et al., 2012; Ito et al., 1997; Varga-Weisz et al., 1997). ACF and ISWI were shown to catalyze the conversion of a histone-DNA intermediate formed by histones deposited onto DNA by NAP1 into canonical nucleosomes (Torigoe et al., 2011). Notably, ISWI and ACF were reported to assemble not only nucleosomes but also chromatosomes (Lusser et al., 2005). This activity distinguished them from the related remodeling factor Chd1 that possessed nucleosome assembly activity but failed to incorporate linker histones. On a related note, ISWI and ACF were capable of catalyzing chromatosome repositioning in the context of chromatin fibers *in vitro*, whereas Chd1 sliding activity was blocked by the linker histone (Maier et al., 2008). The molecular details of a chromatosome sliding reaction are, however, unknown. It is, for example, not clear whether H1 stays closely associated with the nucleosome throughout the sliding process or is temporarily displaced. In accordance with their ability to “handle” the linker histone *in vitro*, some ISWI complexes were implicated to be involved in H1 metabolism *in vivo*, as further detailed below (see chapter 1.3.4).

The *in vivo* functions of ISWI complexes seem to be manifold, and they were found to play a role in various chromatin-based processes, including transcription repression as well as activation, chromatin assembly and higher order structure formation, DNA repair and replication (Bouazoune and Brehm, 2006; Clapier and Cairns, 2009). However, unambiguously assigning cellular functions to the individual complexes often remains difficult as *in vivo* approaches, for example knock-out or overexpression studies, suffer from difficulties in discriminating direct from secondary effects. Nevertheless, in *Drosophila* Acf1-containing complexes are commonly associated with the establishment of repressive chromatin structures in embryos and undifferentiated cells (Chioda et al., 2010; Fyodorov et al., 2004). NURF, on the other hand, was found to regulate transcription by interacting with several transcription factors and to be involved in chromatin higher order structure formation (see chapter 1.3.4) (Badenhorst et al., 2002; Hochheimer et al., 2002; Kwon et al., 2008; Xiao et al., 2001). ToRC contains the transcriptional corepressor CtBP and functions in gene repression (Emelyanov et al., 2012). Finally, RSF was suggested to be involved in the formation of silent chromatin (Hanai et al., 2008).

1.3.2 Mechanism of ISWI-mediated nucleosome sliding

Elucidating the molecular details of a nucleosome sliding reaction catalyzed by chromatin remodeling factors has been a major goal ever since the discovery of this activity. As already mentioned, not only ISWI enzymes but also most other chromatin remodeling enzymes characterized so far are capable of repositioning nucleosomes along DNA without disrupting the histone octamer (Clapier and Cairns, 2009). Moreover, recent evidence suggests that chromatin remodeling enzymes indeed share a basic sliding mechanism that is tunable to achieve variable outputs (Narlikar et al., 2013). Thereby, the helicase-like DNA translocation activity of the ATPase domain engaging the nucleosome at SHL2 is expected to be of key importance. This notion is further explicated in the enclosed review article (chapter 2.2; see also chapter 3.1).

At the outset of the studies compiled in this thesis, different models of the sliding reaction catalyzed by ISWI were controversially discussed (Bowman, 2010; Gangaraju and Bartholomew, 2007b). These models are shortly summarized in the introductory sections of the research articles presented in chapters 2.1 and 2.3 and outlined in more detail in the review article constituting chapter 2.2. Most importantly, the prevalent model predicted the

HSS domain of ISWI and its association with extranucleosomal DNA to be critical for nucleosome sliding. ATP hydrolysis-dependent conformational changes between the ATPase and HSS domain were suggested to result in a kind of “power stroke” that pushed extranucleosomal DNA into the nucleosome. However, results from studies on the related chromatin remodeling enzyme Chd1 indicated that the SANT-SLIDE domain was dispensable for catalysis of a basic sliding reaction (Hauk et al., 2010; McKnight et al., 2011). Therefore, deciphering the basal molecular mechanism of nucleosome sliding, determining the role of the HSS domain for ISWI activity, and clarifying the degree of conservation of the sliding mechanism remained major goals.

1.3.3 Regulation of the ISWI enzyme

Besides the molecular details of the sliding mechanism of ISWI, also strategies to target and regulate ISWI complexes are currently under investigation. Whereas in *Drosophila* targeting of NURF includes its association with transcription factors and ToRC is localized via its CtBP subunit, recruiting strategies for Acf1-containing complexes are poorly understood (Clapier and Cairns, 2009; Emelyanov et al., 2012). As already mentioned above, histone PTMs are implicated in recruiting ISWI complexes or fine-tuning their interaction with nucleosomes (see chapters 1.2.3 and 1.3.1). Potential roles of histone PTMs in regulating the catalytic activity of the complexes will be outlined below.

In vitro studies offered some insights into possible mechanisms for the regulation of ISWI activity by features of the nucleosome that may impact substrate choice also *in vivo*. The ATPase and sliding activity of ISWI and its complexes in various species – as probed so far – are sensitive to the length of the linker DNA flanking a nucleosome, showing a positive correlation (Dang et al., 2006; Gangaraju and Bartholomew, 2007a; He et al., 2006; Kagalwala et al., 2004; Stockdale et al., 2006; Whitehouse et al., 2003; Yang et al., 2006; Zofall et al., 2004). Linker length discrimination was suggested to be fundamental for the nucleosome spacing ability reported for some ISWI complexes (see chapter 1.3.1). However, mechanistic details are still under debate. Based on experiments employing mononucleosomes of varying linker lengths as remodeling substrates for Snf2H, a human homolog of ISWI, and the human ACF complex, Narlikar and co-workers proposed a length discrimination at the kinetic level (Yang et al., 2006). Thereby, up to a certain threshold, linker length is sensed by the remodeling factor and regulates its sliding activity. Within a nucleosome array, this mechanism would eventually result in equalized linker lengths and therefore regular spacing. An alternative model put forward the idea of a “protein ruler” to explain the spacing activity of remodeling factors. According to this mechanism, the factors interact with two neighboring nucleosomes in an array and adjust their distance (Yamada et al., 2011). Thereby, the domains interacting with extranucleosomal DNA are expected to act as “rulers”, determining the distance between nucleosomes. In any case, the requirement for a certain length of free linker DNA for proper nucleosome binding and sliding activity may critically contribute to regulating the activity of ISWI complexes *in vivo* (see chapter 2.2).

Early on, a dependency of the activity of ISWI complexes on the histone H4 N-terminal tail was described. Sliding of nucleosomes depleted of the tail was dramatically reduced (Clapier et al., 2001; Dang et al., 2006; Eberharter et al., 2001; Hamiche et al., 2001). Intriguingly, the epitope of H4 mediating the stimulation was mapped to aa $R_{17}H_{18}R_{19}$ within the basic patch of the tail (see chapter 1.1.3) (Clapier et al., 2002; Fazzio et al., 2005; Hamiche et al., 2001). As outlined in detail in the introduction of the research article presented in chapter 2.4, acetylation of lysine 16 of H4 was reported to inhibit ISWI as well as ACF activity *in vitro* at the level of mononucleosomes or tail peptides (Clapier et al., 2002; Corona et al., 2002; Ferreira et al., 2007; Shogren-Knaak et al., 2006). Therefore, the site-specific acetylation was proposed to be involved in regulating ISWI complexes *in vivo* by rendering nucleosomes refractory of sliding by ISWI. However, the observed effects of the acetylation on ISWI activity were mostly moderate, and it remained unclear which step of the sliding reaction was affected. Moreover, at the level of nucleosome arrays conflicting data were obtained (Nightingale et al., 2007). Given the outstanding role of the basic patch of the H4 tail and H4K16ac for chromatin fiber condensation (see chapters 1.1.3 and 1.2.3), investigating the impact of H4K16ac on ISWI activity in the context of folded chromatin arrays is expected to reflect the *in vivo* situation more accurately and to be more revealing than studying effects at the level of mononucleosomes.

A further nucleosomal feature that may contribute to the regulation of ISWI activity is the association of linker histones. As outlined above (see chapter 1.3.1), H1 does not abolish but reduces the sliding activity of ACF and ISWI *in vitro*, although a quantitative measure of the effect is not yet available (Maier et al., 2008).

The *in vivo* relevance of the reported regulatory potential of H4 tail modifications and linker histone incorporation on the nucleosome sliding activity of ISWI complexes remains to be determined. However, observations in flies indeed support an interplay of H4K16ac, the linker histone, and ISWI complexes in the establishment and maintenance of higher order chromatin structures. This notion is topic of the following chapter. Further regulatory mechanisms and molecular details of the principles described above that are just starting to be elucidated are discussed in the enclosed review article (chapter 2.2).

1.3.4 Interplay of ISWI, H4K16ac, and the linker histone *in vivo*

The main aspects of the interplay of ISWI complexes, H4K16ac, and the linker histone as suggested by *in vivo* observations in *Drosophila melanogaster* are summarized in the introduction of the research article presented in chapter 2.4. Here, the respective observations are briefly discussed, and some more background information is provided.

Depletion of ISWI in flies is accompanied by larval lethality and a striking decondensation of the dosage-compensated male X chromosome in polytene chromosome spreads (Deuring et al., 2000). Later analyses demonstrated that the DCC is necessary and sufficient to cause the decondensation phenotype in ISWI mutants (Corona et al., 2002). In conjunction with experiments revealing genetic interactions between ISWI and MOF, this notion prompted the hypothesis that the enrichment of H4K16ac on the male X chromosome (see chapter 1.2.3) is responsible for its sensitivity to reduced ISWI activity. Of note, depletion of Nurf301, the largest subunit of the NURF complex (see chapter 1.3.1), had the same phenotypic consequences on the male X chromosome (Badenhorst et al., 2002). Contrary, loss of Acf1 did not lead to aberrant chromosome structures (Fyodorov et al., 2004). Therefore, NURF seems to be the ISWI complex mainly responsible for regulating the structure of the X chromosome. Mechanistically, ISWI activity was proposed to promote chromatin compaction, thereby counteracting the decompacting effect of H4K16ac (see chapter 1.2.3) in the wild-type situation. Moreover, inherently reduced activity of ISWI on nucleosomes carrying H4K16ac as evidenced *in vitro* (see chapter 1.3.3) was hypothesized to further explain the sensitivity of the male X chromosome to ISWI loss.

A limitation of the initial experiments employing ISWI null flies was the presence of residual, active ISWI due to maternal contribution. To further reduce ISWI activity, a dominant negative mutant of the enzyme was expressed, resulting in global decondensation of all chromosomes (Corona et al., 2007). This observation underlines a general role of ISWI complexes in the establishment and maintenance of higher order chromatin structures also beyond the male X chromosome. Notably, as H4K16ac is not restricted to the X chromosome (see chapter 1.2.3) the modification may play a role in mediating these global effects on chromatin condensation as well. Unexpectedly, the decondensation was accompanied by dramatic loss of H1 from the chromosomes, although the total protein level of the linker histone appeared unaffected. Independent knock-down studies demonstrated that loss of H1 led to chromatin decompaction (see chapter 1.1.3) (Lu et al., 2009; Siriaco et al., 2009), suggesting that indeed altered linker histone incorporation was the main reason for the disrupted higher order chromatin structures observed in ISWI-depleted flies. As the average NRL was unaffected by ISWI loss (Corona et al., 2007), whereas it was shortened upon H1 depletion (Lu et al., 2009; Siriaco et al., 2009), it was suggested that ISWI mediates H1 retention in chromatin outside replication (see chapter 1.1.3). However, how ISWI complexes mechanistically contribute to H1 metabolism and homeostasis and how this activity is connected to H4K16ac remain open questions.

Taken together, knock-down experiments indicated a role of ISWI complexes in the formation of higher order chromatin structures. Apparently, a complex interplay between the chromatin remodeling factors, H4K16ac, and the linker histone is responsible for proper chromatin condensation, but mechanistic details are poorly understood.

1.4 *In vitro* systems to study chromatin remodeling

To investigate chromatin remodeling reactions *in vitro* in a quantitative manner, it is crucial to employ homogenous, well-defined chromatin substrates that for example allow monitoring changes in nucleosome position or DNA accessibility. *In vitro* reconstituted mono-, oligo-, or polynucleosomes (nucleosome arrays) are commonly used for these purposes. In principle, every DNA sequence can assemble into nucleosomes (see chapter 1.1.1). Nevertheless, an intrinsic preference of the histone octamer for certain DNA sequences was demonstrated originating in base composition-dependent differences in DNA bendability (Struhl and Segal, 2013). DNA sequences that preferentially assemble into and reproducibly position nucleosomes *in vitro* are termed “nucleosome positioning sequences” (Lowary and Widom, 1998). The currently most widely employed sequence, the so-called “Widom 601 nucleosome positioning sequence”, was identified in an unbiased screen of synthetic sequences (Lowary and Widom, 1998). It is characterized by extraordinarily high affinity to the histone octamer and gives rise to homogenously positioned nucleosome in *in vitro* chromatin assembly reactions. In the context of short linear DNA fragments, the Widom 601 nucleosome positioning sequence can be used to reconstitute mononucleosomes with homogenous positioning. Tandem arrays of the sequence are used to assemble regular, fully saturated nucleosome arrays of defined and variable NRL (see chapter 2.4) (Dorigo et al., 2003; Lusser and Kadonaga, 2004).

Histones for the reconstitution of nucleosome arrays can be obtained from either native sources or by recombinant protein expression and purification (Lusser and Kadonaga, 2004). Whereas purification of native histones yields a mix of various variants and post-translationally modified histones, recombinant histones expressed in bacteria harbor a defined sequence and are unmodified. Canonical histones from different organisms, histone variants as well as mutants can be produced in bacteria. However, the current standard protocol for histone purification from bacteria is laborious and time-consuming (see chapter 2.4) (Luger et al., 1999). Histone preparation may therefore become the limiting step in chromatin studies requiring large quantities of histone octamers, rendering simplification of current methods a desirable goal.

Over the past decade, different methods were developed to site-specifically introduce histone PTMs or modified amino acids mimicking modified residues into recombinant histones to create so-called “designer histones” (Allahverdi et al., 2011; Chatterjee and Muir, 2010; Li et al., 2011; Robinson et al., 2008). Whereas enzymatic modification reactions suffer from insufficient efficiencies, specificities, and yields, chemical methods, including those based on peptide ligation (see chapter 2.4), and the generation of bacteria capable of incorporating engineered amino acids proved to be highly successful. Thus, it became possible to investigate the specific properties of individual histone PTMs or their combinations. In conjunction with the aforementioned DNA fragments carrying repeats of a nucleosome positioning sequence, nucleosome arrays of defined NRL and modification status can be reconstituted *in vitro*. Moreover, also linker histones can be incorporated into these arrays to yield chromatosome arrays (Huynh et al., 2005). As these arrays were shown to compact in a salt-dependent manner very similar to chromatin fibers isolated from native sources (Huynh et al., 2005), they constitute a valuable tool for studying chromatin folding and stability. Furthermore, they serve as *in vivo*-like substrates for chromatin enzymes, including remodeling factors, in biochemical assays.

Taken together, folded chromatin fibers assembled from recombinant, purified components allow to model different physiological chromatin states by incorporation of designer histones carrying certain histone PTMs, histone variants, or architectural proteins. Employing these fibers as substrates for chromatin remodeling enzymes, the influence of various chromatin features on the activity of the enzymes can be monitored.

1.5 Aims of this study

As outlined above, ISWI complexes are essential, conserved chromatin factors implicated in a plethora of nuclear processes. However, the mechanism of nucleosome sliding by ISWI, how the energy derived from ATP hydrolysis is translated into the repositioning of nucleosomes, and how this activity is targeted and regulated is still not fully understood. The major goal of this study was to gain insights into the molecular details of the catalytic activity of ISWI using quantitative biochemical methods. Notably, we aimed at analyzing ISWI activity in an *in vivo*-like context by employing synthetic, folded chromatin fibers instead of the commonly used mononucleosomes as remodeling substrates whenever applicable.

To elucidate the specific roles of the HSS and the ATPase domain of ISWI during catalysis and their mechanism of co-operation – a long-standing question in the field –, we characterized mutants of the *Drosophila* ISWI enzyme in a range of *in vitro* assays. The results of these analyses are presented in the research articles contained in chapters 2.1 and 2.3. The implications of our findings for the sliding mechanism are discussed therein and set into a broader context in the review article of chapter 2.2.

Furthermore, we explored the regulatory potential of the H4 tail for ISWI remodeling in a quantitative manner employing nucleosome arrays (see chapter 2.1). H4K16ac was reported to inhibit ISWI activity at the level of mononucleosomes, but the effect of this mark in a more physiological chromatin context where the H4 tail is engaged in inter-nucleosomal interactions remained controversial. Therefore, we assessed the influence of H4K16ac on ISWI at the level of chromatin fibers in the absence and presence of linker histone H1. These analyses are detailed in chapter 2.4.

The synthetic chromatin substrates employed in the various remodeling assays were reconstituted *in vitro* from purified components. To facilitate our as well as future studies, we developed, based on established protocols, a simplified, rapid purification method for bacterially expressed histones that considerably shortens the required preparation times (see chapter 2.5).

2. Results

2.1 The ATPase domain of ISWI is an autonomous nucleosome remodeling machine

Felix Mueller-Planitz, Henrike Klinker, Johanna Ludwigsen and Peter B. Becker

Adolf Butenandt Institute and Center for Integrated Protein Science Munich,
Ludwig-Maximilians-Universität München, Munich, Germany

Published in *Nature Structural and Molecular Biology,* 20, 82-89 (2013);
doi: 10.1038/nsmb.2457

Important note: As the published version of the paper cannot be included into this thesis for copyright reasons, the final, accepted version of the article as submitted to *Nature Structural and Molecular Biology* is presented in the following instead. The published paper can be downloaded from http://www.nature.com/nsmb/journal/v20/n1/full/nsmb.2457.html.

Declaration of contributions to "The ATPase domain of ISWI is an autonomous nucleosome remodeling machine"

This study was conceived by F. Mueller-Planitz. I contributed the mono- and polynucleosome-sliding experiments (Figure 5a, c) and the restriction enzyme accessibility experiment shown in Figure 5d. Furthermore, I performed all the restriction enzyme accessibility experiments employing wt-H4 arrays and some of the experiments employing g-H4 arrays that are summarized in Figure 6 and Figure S7. I prepared Figure 5 and the corresponding figure legend and materials and methods sections. Together with J. Ludwigsen, I prepared Figure 6 including figure legend and the respective materials and methods sections. I assisted in developing and revising the manuscript that was mostly written by F. Mueller-Planitz and P.B. Becker and edited it at all stages of the publication process.

Abstract

ISWI slides nucleosomes along DNA, enabling the structural changes of chromatin that underlie a regulated use of eukaryotic genomes. Prominent mechanistic models imply cooperation of the ATPase domain of ISWI with a C-terminal DNA-binding function residing in the HAND-SANT-SLIDE (HSS) domain. Contrary to these models, we show by quantitative biochemical means that all fundamental aspects of nucleosome remodeling are contained within the compact ATPase module of *Drosophila* ISWI. This domain can independently associate with DNA and nucleosomes, which in turn activate ATP turnover by inducing a conformational change in the enzyme, and it can autonomously reposition nucleosomes. The role of the HSS domain is to increase the affinity and specificity for nucleosomes. Nucleosome remodeling enzymes may thus have evolved directly from ancestral helicase-type motors, and peripheral domains have furnished regulatory capabilities that bias the remodeling reaction towards different structural outcomes.

Introduction

The chromatin organization endows eukaryotic genomes with stability and regulates gene expression. DNA within chromatin is spooled around histone proteins forming nucleosomes. Arrays of nucleosomes are further folded to accommodate the genome in the nuclear volume. Tight packaging inevitably leads to occlusion of DNA sequences that can no longer be accessed by regulatory proteins. However, chromatin has to be dynamic in order to permit cells to respond to environmental or developmental challenges. Crucial to a dynamic and regulated use of the genome are the actions of ATP-consuming nucleosome remodeling enzymes[1,2].

Nucleosome remodeling enzymes use the energy from ATP hydrolysis to weaken or disrupt histone-DNA contacts in the otherwise extremely stable nucleosome particle. They thereby catalyze histone exchange, partial or complete nucleosome disassembly, formation of new, or repositioning of existing nucleosomes. The precise outcome of a remodeling reaction is frequently determined by regulatory subunits that associate with the ATPase[2-5].

The ATPase domains of all nucleosome remodeling complexes are conserved and distantly related to superfamily 2 (SF2) DNA helicases. Based on similarity of their ATPase domain sequences, all known or presumed nucleosome remodeling enzymes constitute 24 subfamilies[4,6]. Despite this complexity, it is becoming clear that at least the remodeling enzymes studied to date are related in structure and mechanism. Deciphering the fundamental mechanism of a basic ‘remodeling’ reaction remains an important goal[2-5].

Most insight into the mechanism of nucleosome remodeling has been obtained studying representatives of three subfamilies of remodelers: ISWI, Snf2 and Chd1. They all slide nucleosomes along DNA, and although differences have been noted[7,8], they share a strategic interaction site on the nucleosome. Their ATPase 'motor' domain engages the nucleosomal DNA about two helical turns off the nucleosomal dyad at superhelix location 2 (SHL2)[9-11]. This site is characterized by structural variability of the histone-DNA interactions. It can accommodate a gain or loss of one base pair (bp), a feature that could be exploited during the remodeling reaction[12-14]. Furthermore, the histone H4 N-terminus, which is mechanistically involved in remodeling reactions catalyzed by ISWI and Chd1, emanates from the nucleosome core around SHL2[15-19]. At SHL2, the ATPase domain is thought to translocate on DNA in accord with its helicase ancestry[9,20,21]. The ATPase domain thereby may force additional DNA into the nucleosome, change the twist in the DNA, or otherwise perturb histone-DNA contacts[2,4,22].

In several cases it was observed that successful remodeling required accessory domains in addition to the ATPase. These domains are thought to be crucial for remodeling by providing the appropriate mechanical or topological context. For ISWI-type enzymes, such a domain resides in the C-terminus. It harbors a DNA-binding module in form of the HSS domain (Fig. 1a, top). Deletion of the HSS domain markedly reduced the ability of *Drosophila* ISWI to associate with and remodel nucleosomes[23]. Subsequent crosslinking and cryo-EM studies with the ISWI orthologs in yeast revealed interactions of the HSS domain with DNA flanking the nucleosome, so called linker or extranucleosomal DNA[24,25]. Deletion of this DNA not only diminished the binding affinity but also ATP turnover and the remodeling capacity of ISWI[26,27].

These results collectively support models in which the nucleosomal contacts made by the ISWI ATPase and HSS modules delimit a topological domain of nucleosomal DNA. Conceivably, a conformational change between the ATPase and the HSS modules, mediated via a 'hinge' that connects the two, may destabilize the DNA-histone contacts in this domain and pull linker DNA into the nucleosome[16,18]. The excess DNA would initially bulge out from the histone surface. Eventually it may escape on the other side of the nucleosome, reforming the canonical nucleosome structure at a different position on DNA.

This model predicts that the HSS domain plays an integral role during the remodeling reaction. Underscoring its importance, deletion of a related domain in Chd1 strongly reduced the overall remodeling efficiency[28]. Curiously, a different study concluded that deletion of the DNA binding module in the C-terminus of Chd1 does not completely abolish the nucleosome sliding activity. Rather, the C-terminus was suggested to affect the directionality of the process[11]. Thus, the DNA binding domain may not be essential for the remodeling process as such. It might rather determine the overall outcome of the remodeling reaction, either the direction of nucleosome sliding[11] or the positioning of the substrate nucleosome in the context of nucleosome spacing[28]. This conclusion is not readily compatible with the 'hinge' model discussed above, which was mainly derived from studies on ISWI-type enzymes. Do these studies reveal a fundamental difference between ISWI- and Chd1-type remodelers with respect to their utilization of binding domains for linker DNA? How can ATP hydrolysis-driven conformational changes be productive in the absence of the main linker DNA binding domain?

We set out to address these issues in the context of *Drosophila* ISWI. Our quantitative analysis reveals two conformations of the ATPase domain, which drastically differ in their catalytic competency. Nucleic acids induce a change of the conformation, thereby activating the enzyme. Furthermore, we show that the ATPase domain has an innate ability to bind nucleosomes, to functionally interact with the H4 N-terminus, and to remodel nucleosomes. Accessory domains in chromatin remodelers may thus have evolved to regulate an autonomous basic remodeling module. Our data place firm limits on mechanistic models of nucleosome remodeling and favor models in which the ATPase domain performs the fundamental steps involved in remodeling, such as breaking histone-DNA contacts and moving nucleosomes, whereas the HSS domain fulfills auxiliary duties, such as increasing the affinity and specificity for nucleosomes.

Results

The ATPase domain of ISWI adopts two different conformations in solution

The ATPase activity of ISWI is activated by free and nucleosomal DNA[23,29]. To dissect this effect in a quantitative manner, we obtained highly purified enzyme preparations using an optimized purification protocol that included affinity, ion exchange and size exclusion chromatography. Further purification did not affect the results.

We first measured ATP turnover by unliganded ISWI and determined the reaction velocities for varying ATP concentrations. Whereas enzymes typically show a simple saturation behavior with increasing substrate concentrations, ISWI featured a more complex, biphasic response. After an initial rise of the reaction velocity with increasing ATP concentrations, the curve entered a second phase and continued to rise until at least 50 mM of ATP (Fig. 1a).

The two phases of the curve indicated that different enzyme populations existed with strongly differing Michaelis ($K_{M,obs}$) values. We hypothesized that these populations may correspond to ISWI molecules in different conformations. Kinetic and thermodynamic modeling confirmed that this scenario could indeed account for the data (Suppl. Fig. 1).

However, the biphasic ATPase response could also be due to a number of trivial reasons. Most importantly, we ruled out that a contaminating ATPase was responsible for one of the two phases by analyzing a point mutant in the Walker B motif of the ISWI ATPase domain (E257Q), which prevents ATP hydrolysis. Although this mutant was expressed at similar levels and prepared in the same way as the wild-type, we could not detect any ATP

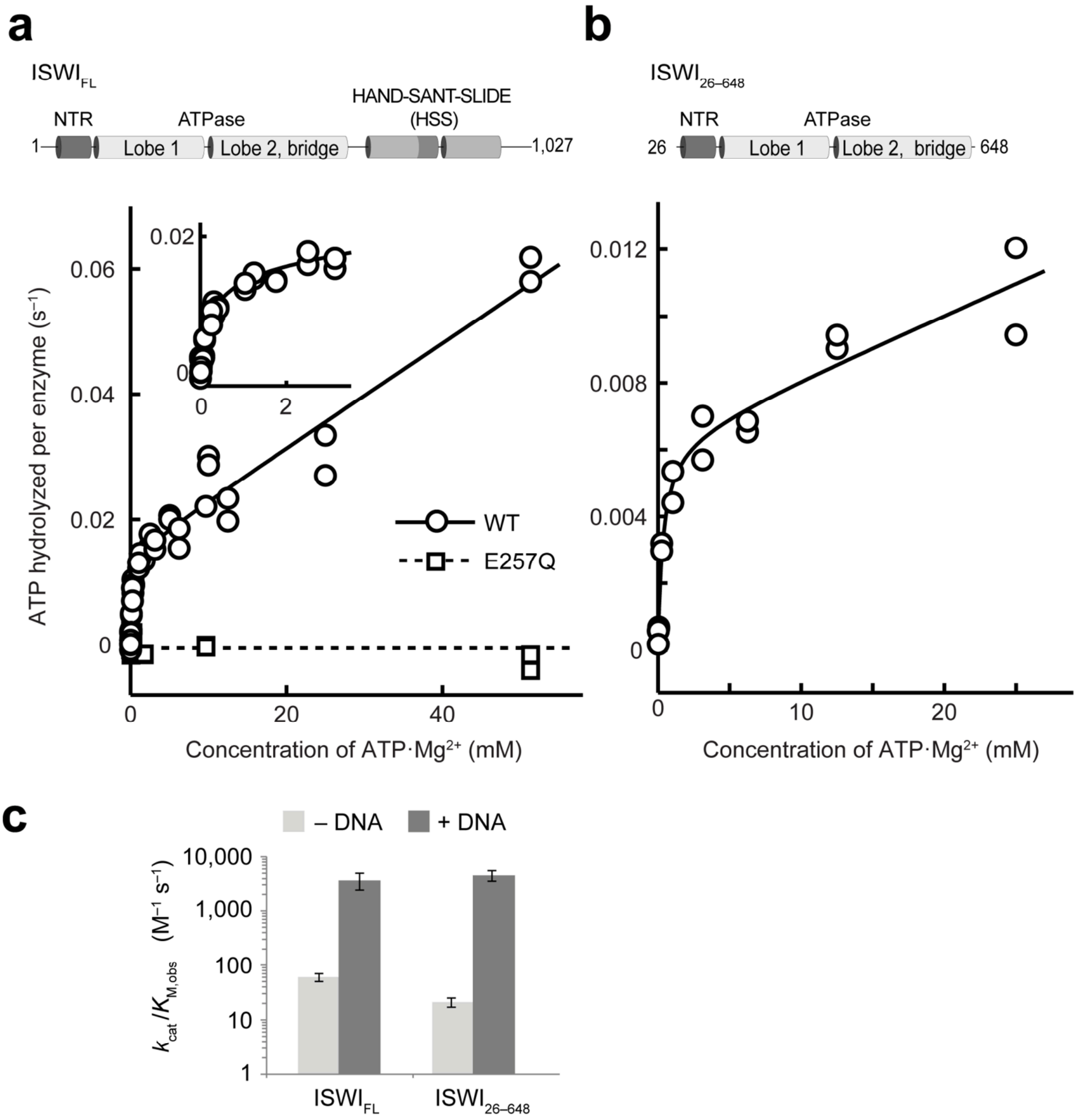

Figure 1: Steady-state ATP hydrolysis. The ATP concentration dependence of ATP turnover by DNA-free ISWI$_{FL}$ (**a**) and ISWI$_{26–648}$ (**b**; both 4 µM) was biphasic. The first phase was completed with sub-millimolar concentrations of ATP (a, inset). Steady-state ATPase parameters extracted from fits (lines) are listed in Table 1. Domain schematics for ISWI$_{FL}$ and ISWI$_{26–648}$ are shown on top. In addition to wild-type (WT), an ATPase deficient mutant (E257Q) was used as a negative control in a. (**c**) Saturating concentrations of a 39-bp long DNA duplex strongly stimulated ATP hydrolysis of ISWI$_{FL}$ and ISWI$_{26–648}$ (80 to 400 nM). The assays were performed with 100 mM Mg^{2+}; similar results were obtained in a buffer containing lower Mg^{2+} concentrations or varying enzyme concentrations (Suppl. Table 1; Suppl. Fig. 2a,b and data not shown).

hydrolysis for this mutant (Fig. 1a). In the Supplementary Information, we discuss and rule out additional scenarios, such as enzyme dimerization and contamination with DNA, which could in principle explain the unusual shape of the curve (Suppl. Note; Suppl. Fig. 2a,b).

According to prominent models of ISWI function, the HSS and ATPase domains intimately cooperate during nucleosome remodeling[2-4,24,30]. In this scenario one might expect that the

HSS domain directly influences ATP hydrolysis. We tested this hypothesis by truncating ISWI in a poorly conserved region that separates the ATPase domain from the HSS domain (Fig. 1b, top). Our construct spanned a conserved N-terminal region (NTR; Suppl. Fig. 3), both ATPase lobes, and the ‘bridge’ at the C-terminal end, which is conserved between ISWI and Chd1 remodelers and docks against both ATPase lobes[31,32]. In most experiments, we used a construct that lacked non-conserved amino acids at the N-terminus, spanning amino acids 26–648 (ISWI$_{26–648}$). We repeated a number of experiments with ISWI$_{1–697}$, which also included lesser-conserved regions on both termini.

Similar to full-length ISWI (ISWI$_{FL}$), the ATP concentration dependencies of unliganded ISWI$_{26–648}$ and ISWI$_{1–697}$ were biphasic, suggesting that the two conformations involve the ATPase domain (Fig. 1b and data not shown). Surprisingly, steady-state ATPase parameters ($k_{cat}/K_{M,obs}$, $k_{cat,obs}$, and $K_{M,obs}$) differed by less than three-fold between the three enzymes (Table 1 and data not shown). This similarity attested to the integrity of the two truncated proteins and showed that the C-terminus did not substantially influence ATP hydrolysis, at least when no DNA ligand was bound.

DNA ligands strongly influence the ATP hydrolysis mechanism

To test how DNA binding affected the catalytic parameters, we repeated the analyses in the presence of a 39-bp long DNA duplex. Varying the length of the DNA from 19 to ~3000 bp did not considerably affect the $k_{cat,obs}$ (see below and data not shown). In contrast to the ligand-free enzyme, DNA-bound ISWI$_{FL}$ exhibited standard Michaelis-Menten-type kinetics (data not shown). Furthermore, DNA strongly stimulated $k_{cat}/K_{M,obs}$ (61-fold; Fig. 1c; Table 1).

Like stimulation by DNA, stimulation by chromatin abolished the biphasic response to the ATP concentration (data not shown). Relative to DNA, chromatin binding increased the affinity for nucleotides six-fold (Suppl. Fig. 4). In addition, $k_{cat,obs}$ increased four- to 14-fold

Table 1: Steady-state ATPase parameters^{a}

		ISWI$_{FL}$			ISWI$_{26–648}$		
		$k_{cat}/K_{M,obs}$ (M^{-1} s^{-1})	$k_{cat,\ obs}$ (s^{-1})	$K_{M,\ obs}$ (mM)	$k_{cat}/K_{M,obs}$ (M^{-1} s^{-1})	$k_{cat,\ obs}$ (s^{-1})	$K_{M,\ obs}$ (mM)
– DNA	**Phase 1**	60 ± 10	0.014 ± 0.004	0.24 ± 0.03	21 ± 3*	0.007 ± 0.002	0.36 ± 0.02*
	Phase 2	N.a.	>0.046	>50	N.a.	>0.02	>25
+ DNA		3,700 ± 900*	0.51 ± 0.09	0.15 ± 0.05	4,100 ± 900*	1.0 ± 0.1	0.25 ± 0.01

^{a}: Values were measured in reaction buffer containing 100 mM Mg^{2+}. Where indicated (asterisk), errors are min and max values of two independent measurements. Otherwise, errors are standard deviations of at least three independent measurements. DNA reactions contained saturating concentrations of a 39-bp DNA duplex. N.a.: Not applicable.

depending on the enzyme concentration (Suppl. Fig. 2c; Suppl. Table 1; note that we employed here lower Mg^{2+} concentrations to prevent aggregation of chromatin). This dependence of $k_{\mathrm{cat,obs}}$ on the enzyme concentration is consistent with binding of two functionally interacting ISWI molecules per nucleosome as previously suggested (Suppl. Fig. 2d,e)[33].

DNA binding to the ATPase domain activates ATP hydrolysis

Nucleic acids typically directly bind to the ATPase domain of SF2 helicases [34,35]. Using the $\mathrm{ISWI}_{26\text{–}648}$ construct, we confirmed in a double-filter binding assay that the ATPase domain of ISWI indeed harbors a DNA binding site (Suppl. Fig. 5). Consistent with its DNA binding function[23-25,36], the HSS domain increased the DNA affinity 20-fold.

DNA could, in principle, activate ATP hydrolysis by binding to either of the two binding sites or to both. Whereas nucleic acids often directly bind and stimulate the ATPase activity of SF2 helicases[34,35], we previously suggested that it was DNA binding to the HSS domain that conferred most DNA stimulation[23]. However, at that time we did not account for the reduced DNA affinity when the HSS domain is missing. To differentiate between the two sites and to probe their involvement in regulation of ATP turnover, we titrated DNA to the ISWI constructs that lacked the HSS domain and measured ATP turnover. DNA was a potent activator of ATP hydrolysis of $\mathrm{ISWI}_{26\text{–}648}$ and $\mathrm{ISWI}_{1\text{–}697}$ (Fig. 1c and data not shown). Overall, their ATPase parameters were strikingly similar to those of $\mathrm{ISWI}_{\mathrm{FL}}$, indicating that DNA binding at the ATPase domain, not the HSS domain, drives the stimulation (Table 1).

DNA binding affects the conformation of the ATPase domain

To test if DNA binding activated ATP turnover by triggering a conformational change in the ATPase domain as seen for evolutionary related proteins[37], we turned to limited proteolysis experiments. Consistent with a structural change, limited digestion with trypsin led to a different cleavage pattern and a substantially faster cleavage of $\mathrm{ISWI}_{26\text{–}648}$ in the presence of DNA (Fig. 2a). A different protease (GluC) and partial trypsin digests of $\mathrm{ISWI}_{\mathrm{FL}}$ yielded analogous results (data not shown).

Additional proteolysis experiments firmly ruled out that the different cleavage pattern was simply due to occlusion of the predominant cleavage sites by DNA. From a comparison of the electrophoretic mobility of proteolytic fragments obtained with trypsin, which cleaves at lysines and arginines, and LysC, which is specific for lysine, we concluded that the major tryptic digestion product of the DNA-free enzyme arose from a cut next to a lysine (Suppl. Fig. 6). Importantly, DNA binding did not affect the digestion kinetics of LysC, providing strong evidence against occlusion (Fig. 2b). If accessibility of the lysine remained the same, then arginine residues must become more exposed with DNA to explain the trypsin results.

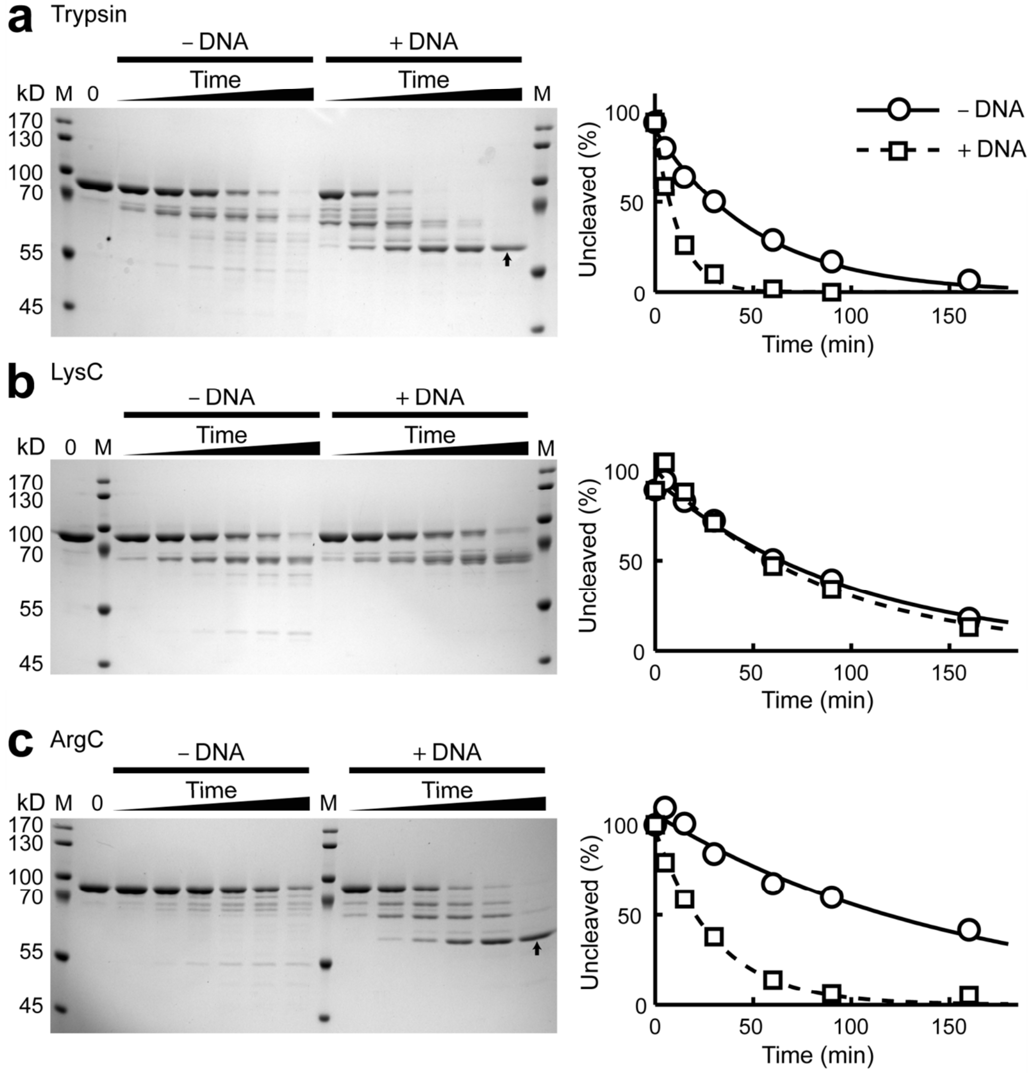

Figure 2: Limited proteolysis revealed a DNA-induced conformational change within the ATPase domain of ISWI. (**a–c**) DNA-free and DNA-bound ISWI$_{26\text{–}648}$ was digested with the indicated proteases for 5, 15, 30, 60, 90 and 160 min. Left panels: SDS-PAGE gels. Undigested protein served as the zero time point (0). M: molecular weight marker. Right panels: Quantification of the gel bands. The data were fit by a single exponential function (lines). Addition of 39-bp long DNA duplexes (10 µM) led to a different banding pattern and 4.4-fold and 5.1-fold faster digestion rates by trypsin and ArgC, respectively, without affecting LysC digests. Arrows (a, c) indicate a protease-stable fragment only seen in the presence of DNA.

We confirmed this prediction with the arginine-specific protease ArgC. ArgC produced a similar cleavage pattern as trypsin in presence of DNA and experienced a similar rate enhancement by DNA (Fig. 2a,c). In summary, the proteolysis experiments showed that the enzyme conformation changed upon DNA binding. We suggest that these conformations are related to the conformations detected independently by the ATP hydrolysis results above.

We noted that a ~60 kDa fragment accumulated in trypsin and ArgC digests when DNA was present (Fig. 2a,c, arrows), suggesting that DNA binding led to a well-folded, protease-resistant structure. N-terminal Edman sequencing and LC-MS-MS analysis of this fragment mapped the cleavage sites to accessory sequences outside of the ATPase core (Arg91 and Arg93 in the NTR, and Arg589 at the C-terminus; Suppl. Fig. 3). These accessory regions therefore took part in regulatory conformational changes induced by DNA binding (see Discussion).

The ATPase and HSS domains contribute to nucleosome recognition

Our data showed that the ISWI ATPase domain independently reacted to DNA association. We asked next if the ATPase domain alone could specifically recognize an entire nucleosome, if the HSS domain increased this specificity, and to what extent stimulation of ATP hydrolysis by nucleosomes required the HSS domain.

We started by titrating nucleosomal arrays to $\text{ISWI}_{26\text{–}648}$ and ISWI_{FL} under subsaturating ATP conditions, measuring the $k_{\text{cat}}/K_{\text{M,obs}}$ (Fig. 3a,b). Effects of nucleosomes on the affinity of ATP (discussed above) should be detectable under these conditions whereas they are masked with saturating ATP. Much to our surprise, saturating concentrations of nucleosomal arrays stimulated $\text{ISWI}_{26\text{–}648}$ much more strongly than DNA (17-fold). The level of stimulation and even the absolute hydrolysis rates were comparable between $\text{ISWI}_{26\text{–}648}$ and ISWI_{FL} (Fig. 3b; Suppl. Table 1). These results indicated that ISWI_{FL} and $\text{ISWI}_{26\text{–}648}$ could form the same important contacts to the nucleosome that mediated the stimulation.

We probed next if these contacts were to linker DNA by deleting the linker altogether, using nucleosome core particles (NCPs). NCPs stimulated hydrolysis of $\text{ISWI}_{26\text{–}648}$ just as well as arrays. Also the apparent affinity of arrays and NCPs remained unaffected (Fig. 3a). Remarkably, even ISWI_{FL} did not react to deletion of the linker (Fig. 3b). These results ruled out that the contact responsible for ATPase stimulation was between the HSS domain and linker DNA.

When ATP and DNA ligand are subsaturating, the specificity with which ISWI discriminates between different DNA ligands can be determined (ref. 38 and mathematical derivation not shown). $\text{ISWI}_{26\text{–}648}$ possessed a moderate ability to distinguish between naked and nucleosomal DNA (six-fold for both NCPs and arrays). In contrast, ISWI_{FL} strongly discriminated between naked and nucleosomal DNA (>60-fold for both NCPs and arrays; Fig. 3c). This result indicated that the HSS domain formed important contacts to the NCP, which increased the specificity for nucleosomes. Due to tight binding, we could only extract lower limits for the specificity of ISWI_{FL}. For the same reason, we could not test if HSS-linker interactions provided additional specificity. In addition to specificity, the HSS domain markedly improved the apparent affinity for nucleosomes, as ISWI_{FL} saturated with much lower concentrations of nucleosomes than $\text{ISWI}_{26\text{–}648}$ (≤25 nM vs. >0.5 µM, respectively; Fig. 3a and data not shown).

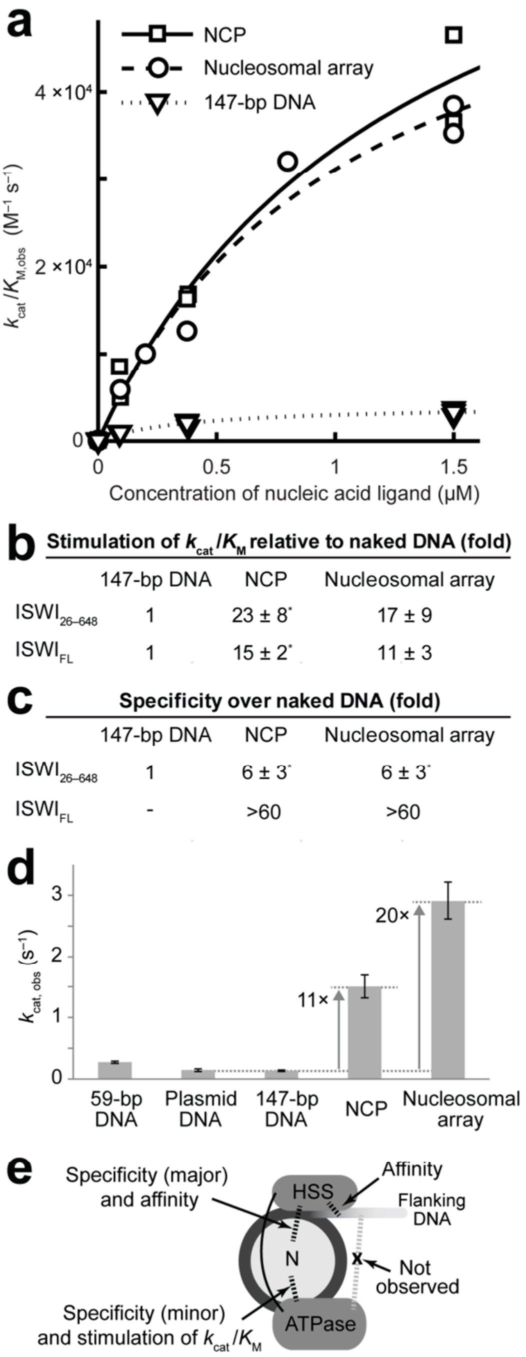

b **Stimulation of k_{cat}/K_M relative to naked DNA (fold)**

	147-bp DNA	NCP	Nucleosomal array
$ISWI_{26–648}$	1	23 ± 8*	17 ± 9
$ISWI_{FL}$	1	15 ± 2*	11 ± 3

c **Specificity over naked DNA (fold)**

	147-bp DNA	NCP	Nucleosomal array
$ISWI_{26–648}$	1	6 ± 3*	6 ± 3*
$ISWI_{FL}$	-	>60	>60

Figure 3: Interactions between domains of ISWI and the nucleosome and their importance for catalysis and substrate specificity. (**a**) NCPs and nucleosomal arrays markedly stimulated $k_{cat}/K_{M,obs}$ for ATP hydrolysis of $ISWI_{26–648}$ (80 nM). Data were fit to a simple binding isotherm (lines). Results of two or more independent experiments are superimposed. (**b**) Stimulation of $k_{cat}/K_{M,obs}$ by NCPs and arrays relative to DNA. $k_{cat}/K_{M,obs}$ values for saturating concentrations of NCPs and arrays were normalized by corresponding values for 147-bp long DNA (Suppl. Table 1). Where indicated (asterisk), errors are min and max values of two independent measurements. Otherwise, errors are standard deviations (n = 3). (**c**) Discrimination between nucleosomal and naked DNA. $k_{cat}/K_{M,obs}$ values at subsaturating NCP and array concentrations were normalized by corresponding values for DNA-stimulated $ISWI_{26–648}$. Errors as in b. (**d**) The $k_{cat,obs}$ of $ISWI_{FL}$ was strongly stimulated by saturating NCPs and arrays (200 nM enzyme; 0.5 mM ATP). Errors represent 95% confidence intervals of fits to a binding isotherm. (**e**) Summary of functional interactions (dotted lines) between ISWI and the nucleosome.

We confirmed that the HSS-linker DNA interaction is negligible for ATPase activation also under saturating ATP conditions (Fig. 3d). NCPs stimulated the $k_{cat,obs}$ 11-fold relative to naked DNA, whereas nucleosomal arrays stimulated $k_{cat,obs}$ at most ~two-fold better than NCPs. Interestingly, $ISWI_{26–648}$ apparently lost its ability to discriminate free DNA from NCPs or arrays with saturating ATP as all these ligands gave indistinguishable stimulation at similar concentrations (data not shown). This result suggested that the relatively poor discriminatory power that $ISWI_{26–648}$ possessed at subsaturating ATP concentrations was further reduced when the enzyme was saturated with nucleotides, resulting in enzyme that did not profit from the nucleosomal activation at SHL2 (see below) but that instead sampled DNA elsewhere on the surface of the nucleosome (Suppl. Note). Figure 3e summarizes ISWI-nucleosome interactions and their functions uncovered in this section.

The ATPase domain senses the histone H4 N-terminal tail

Stimulation of ATP turnover by nucleosomes has been shown to require the histone H4 N-terminal tail[17,19]. The location of the H4 tail near the interaction site of the ATPase domain at SHL2 would be consistent with a direct effect of the H4 tail on the ATPase domain. Structural similarity of the SANT domain with histone tail binding proteins on the other hand would rather point to the HSS domain as the sensor of the H4 tail[23,39]. Employing $\text{ISWI}_{26–648}$, we directly tested whether the HSS domain is required to detect the H4 tail.

In a previous publication, we showed that ATP turnover was faster when ISWI_{FL} was presented with a synthetic H4 tail peptide in addition to DNA[40]. Surprisingly, $\text{ISWI}_{26–648}$ was similarly sensitive to the presence of the peptide (Fig. 4). Based on these results, we suggest that the HSS domain is not necessary for the recognition of the H4 tail, a conclusion that is further corroborated below.

The ATPase domain is sufficient to remodel nucleosomes

Our results so far argued that many important functionalities of ISWI are built into its ATPase module. We were curious if these functionalities sufficed to also remodel nucleosomes, which would be consistent with recent evidence obtained for Chd1[11,31], or if additional conformational changes between the HSS and ATPase were required for remodeling as previously suggested[2,3,24,30].

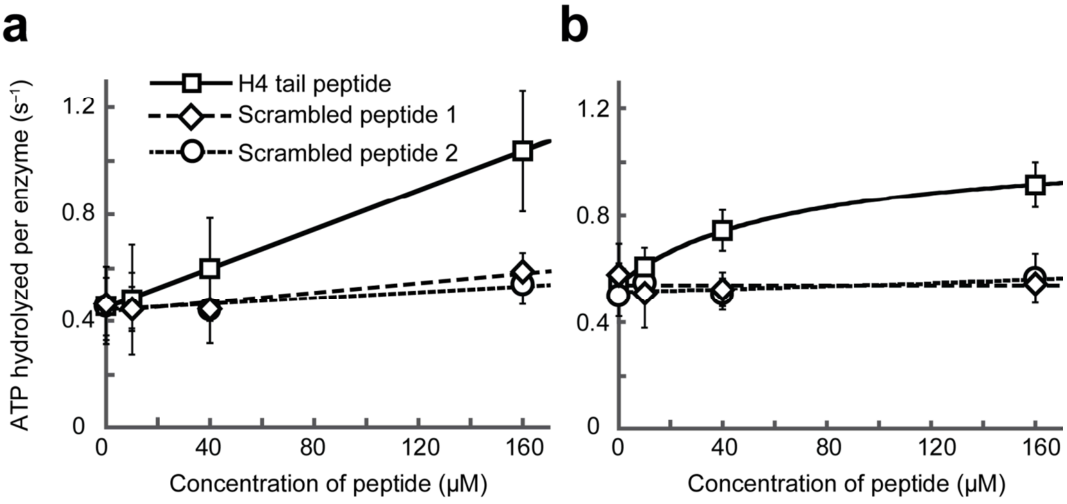

Figure 4: An N- terminal peptide of histone H4 activated ATP turnover of ISWI_{FL} (**a**) and $\text{ISWI}_{26–648}$ (**b**; both 0.5 µM) in the presence of DNA (1.2 mg/mL salmon sperm DNA) and saturating ATP concentrations (1 mM). Two peptides with a scrambled amino acid sequence served as specificity controls. Error bars display standard deviations (n=4).

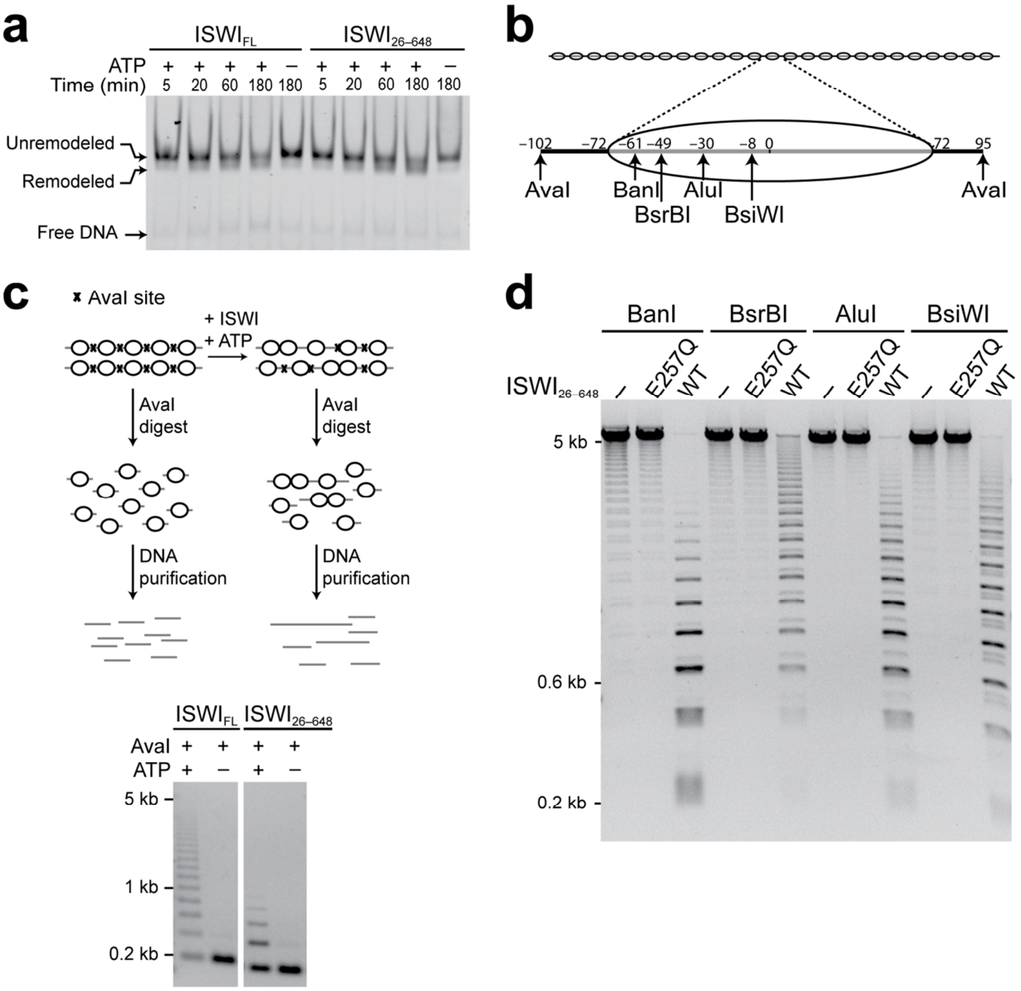
a
ISWI_FL
ISWI_26–648
ATP + + + + – + + + + –
Time (min) 5 20 60 180 180 5 20 60 180 180
Unremodeled
Remodeled
Free DNA
b
–102
–72
–61
–49
–30
–8
0
72
95
AvaI
BanI
BsrBI
AluI
BsiWI
AvaI
c
AvaI site
+ ISWI
+ ATP
AvaI digest
AvaI digest
DNA purification
DNA purification
ISWI_FL
ISWI_26–648
AvaI + + + +
ATP + – + –
5 kb
1 kb
0.2 kb
d
BanI
BsrBI
AluI
BsiWI
ISWI_26–648
/ E257Q WT / E257Q WT / E257Q WT / E257Q WT
5 kb
0.6 kb
0.2 kb

Figure 5: The HSS domain is not required for repositioning mononucleosomes or nucleosomes within arrays. (**a**) Mononucleosome sliding assay. Mononucleosomes, centrally positioned on a 197-bp Widom-601 DNA, were incubated for the indicated time with ATP and ISWI and analyzed by native PAGE. Quench DNA migrated more slowly and was cut off for clarity. Control reactions (–) were depleted of ATP with apyrase prior to addition of ISWI. (**b**) Schematic depiction of the 25-mer nucleosomal arrays used in c,d. Each nucleosome protected the indicated restriction enzyme sites, whereas the linker DNA contained an exposed AvaI site (magnification). Numbers specify base pairs relative to the pseudodyad axis (0). (**c**) Polynucleosome sliding assay. Top: schematic depiction of the assay. Bottom: nucleosomal arrays were incubated with ISWI and ATP as indicated. Control reactions were depleted of ATP as above (–). (**d**) Restriction enzyme accessibility assays. Nucleosomal arrays were incubated with ATP, the indicated restriction enzymes and wild-type (WT) or mutant $\text{ISWI}_{26\text{–}648}$ (E257Q). DNA was then deproteinized and resolved by gel electrophoresis. Samples incubated without enzyme (–) served as controls.

We analyzed nucleosome remodeling in three different ways. First, we probed if $\text{ISWI}_{26\text{–}648}$ could reposition the histone octamer in mononucleosomes, an activity that is well documented for ISWI_{FL}[41]. Differently positioned nucleosomes can be visualized through their different mobility in native gels. Surprisingly, the reaction products generated by $\text{ISWI}_{26\text{–}648}$ in this assay resembled very much those of ISWI_{FL} (Fig. 5a).

Second, we tested nucleosome repositioning in the context of 25-mer nucleosomal arrays, a more physiological substrate (Fig. 5b). Each linker DNA contained an exposed AvaI restriction site. As expected, AvaI fully digested unremodeled arrays to mononucleosomes. After remodeling by ISWI$_{26–648}$, in contrast, AvaI could not fully digest the arrays, indicating occlusion of a fraction of AvaI sites by nucleosomes (Fig. 5c). Protection of these sites by binding of ISWI was ruled out by experiments that lacked ATP and by exhaustive AvaI digests.

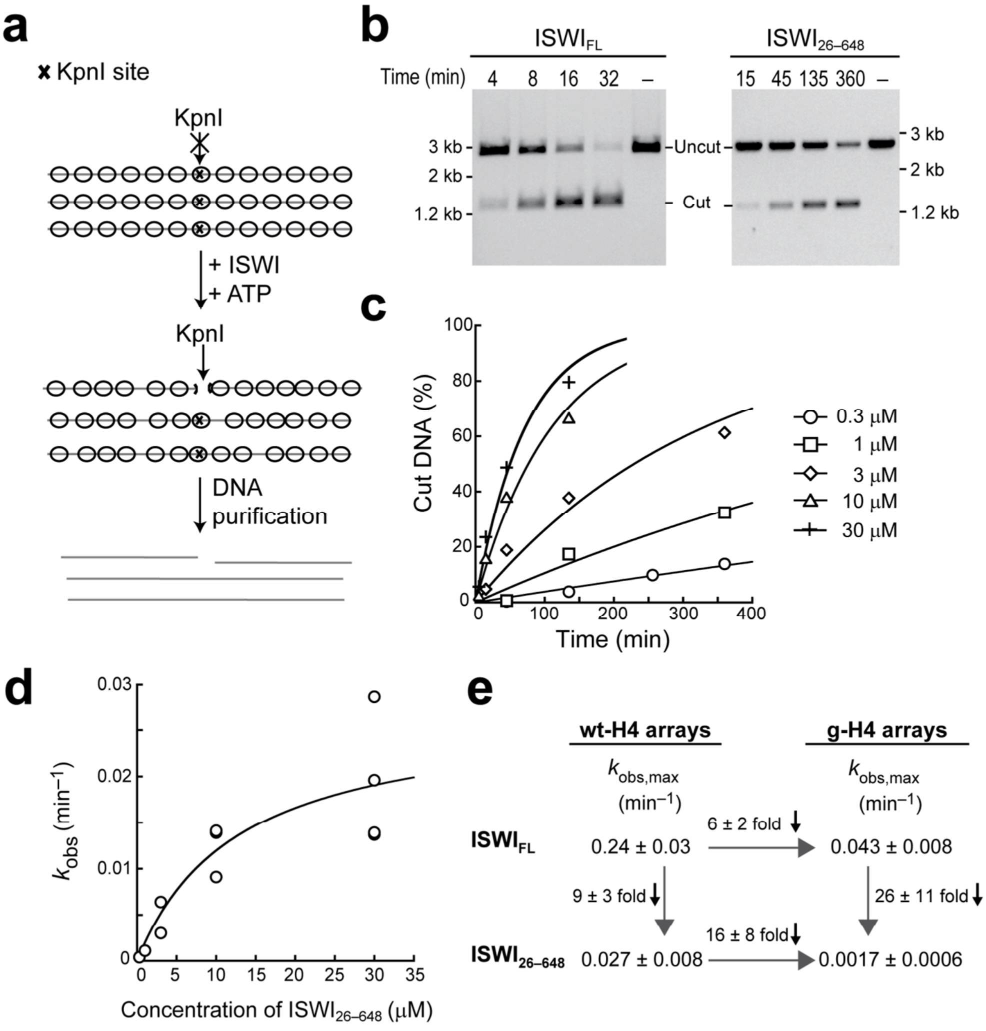

Figure 6: Remodeling by ISWI$_{26–648}$ is only moderately slower than remodeling by ISWI$_{FL}$, and it is sensitive to H4 tail deletion. (**a**) Schematic depiction of the remodeling assay. The central nucleosome in a 13-mer nucleosomal array occluded a unique KpnI site. (**b**) Exemplary time courses for remodeling by ISWI$_{FL}$ and ISWI$_{26–648}$ (both 3 µM). In control reactions (–), the quench solution was added together with ATP. (**c**) Time courses were collected for varying ISWI$_{26–648}$ concentrations, and the data fit to a single exponential function to extract the rate constant k_{obs} (line). (**d**) The maximal velocity with which ISWI$_{26–648}$ remodeled nucleosomes ($k_{obs,max}$) was obtained by extrapolating to saturating enzyme concentrations (lines). Data points were from several independent experiments. (**e**) Effects of HSS and H4-tail deletion on the maximal remodeling velocities $k_{obs,max}$. Values for $k_{obs,max}$ for ISWI$_{FL}$ and ISWI$_{26–648}$ were obtained as above at saturating ATP concentrations (Suppl. Fig. 7). Errors are standard errors of the fit.

The third assay probed accessibility of restriction sites that were protected by nucleosomes in the array before remodeling[42]. Accessibility of four restriction enzyme sites, distributed over an entire gyre of nucleosomal DNA, dramatically changed upon incubation with $\mathrm{ISWI}_{26\text{-}648}$ in an ATP hydrolysis-dependent manner (Fig. 5d).

To quantify the effect of the deletion of the HSS domain on remodeling, we adapted an assay originally developed by the Peterson lab[43]. We generated nucleosomal arrays in which the central nucleosome protected a unique restriction site before remodeling (KpnI; Fig. 6a). By following the accessibility of the KpnI site, we collected time courses for increasing ISWI concentrations at saturating ATP and plotted the observed remodeling rate constants over the enzyme concentration to obtain the maximal reaction velocity (Fig. 6b–d, Suppl. Fig. 7). Comparison of the maximal velocities showed that $\mathrm{ISWI}_{\mathrm{FL}}$ remodeled arrays approximately an order of magnitude faster than $\mathrm{ISWI}_{26\text{–}648}$ (Fig. 6e). As shown above, $\mathrm{ISWI}_{\mathrm{FL}}$ also hydrolyzed ATP an order of magnitude faster than $\mathrm{ISWI}_{26\text{–}648}$ under similar conditions due to improved binding specificity. Thus, per ATP hydrolyzed, the efficiency of remodeling was similar for both enzymes.

Deletion of the histone H4 tail was shown to impair remodeling by $\mathrm{ISWI}_{\mathrm{FL}}$[15-19]. Remodeling by $\mathrm{ISWI}_{26\text{–}648}$ should be similarly affected if, as we suggested above, the ATPase domain directly recognized the H4 tail. By monitoring remodeling of nucleosomal arrays that lacked the H4 N-terminal tail (g-H4), we found that $\mathrm{ISWI}_{26\text{–}648}$ was at least as sensitive towards deletion of the H4 tail as $\mathrm{ISWI}_{\mathrm{FL}}$, confirming our previous conclusion (16-fold; Fig. 6e).

Discussion

Our major conclusion is that – contrary to widespread belief – all fundamental aspects of nucleosome remodeling catalysis are contained within the compact ATPase domain of ISWI. The ATPase module alone was able to recognize the DNA and histone moiety of substrate nucleosomes. Substrate binding triggered a conformational change within the ATPase domain along with an increased affinity for ATP. The ATPase module alone was able to remodel nucleosomes. In conjunction with recent related observations for the Chd1 remodeler[11] these findings suggest that nucleosome remodeling could have evolved from helicase-type motors without further requirements for accessory domains[44].

Mechanistic implications for nucleosome remodeling

Several current models ascribe critical functions to the HSS domain during remodeling. The HSS domain was suggested to bind and release DNA and drag it into the nucleosome upon cues from the ATPase domain, to form channels for nucleosomal DNA, or to stabilize high energy structures, such as DNA bulging off the histone surface[2-4,16,24,30]. Remarkably, we found that ISWI lacking its HSS domain still remodeled nucleosomes, albeit the reaction proceeded an order of magnitude more slowly. This defect, however, was accounted for by a proportionally decreased ATP turnover. We therefore conclude that the HSS domain is not an integral component of the motor core of ISWI.

Whereas passive, secondary roles of the HSS during remodeling are fully consistent with our results (see below), our ATPase data do not favor models that postulate active coordination, i.e. transduction of energy, between the ATPase and the HSS domains. Steady-state ATP hydrolysis parameters ($k_{cat}/K_{M,obs}$) of ligand-free, DNA- and nucleosome-bound ISWI remained largely unaffected when the HSS was deleted. Strikingly, also the characteristic biphasic ATP concentration dependence of hydrolysis was preserved when the HSS domain was missing. It remains possible, though, that energy is transduced only after the rate-limiting step of ATP hydrolysis because steady-state measurements are blind to that regime.

The autonomy of the ATPase domain does not appear to be a specialty of ISWI because Chd1 derivatives that lack their C-terminal DNA-binding domain can still slide nucleosomes[11,31]. This commonality adds to the growing list of shared functional properties of ISWI and Chd1 remodelers (ref. 28 and references therein). In fact, substantial parts of both enzymes are also structurally related. Chd1 harbors a SANT-SLIDE domain in place of the HSS domain of ISWI[28], and both enzymes contain the ‘bridge’ motif adjacent to the conserved ATPase domain[31,32]. Although the N-terminal parts of both enzymes lack any apparent homology, they nevertheless may perform similar functions (see below).

How does ISWI remodel nucleosomes without the involvement of the HSS domain? Previous studies placed the ATPase region of several remodelers close to SHL2 of the nucleosome, whereas the HSS domain of ISWI bound to the linker DNA[9-11,18,24,25,45]. As ISWI$_{26–648}$ discriminates between nucleosomes and DNA and is sensitive to the H4 tail, at least a fraction of ISWI$_{26–648}$ can productively bind at SHL2 (Fig. 7a, step I).

Strong histone-DNA contacts are present around SHL2[46,47]. Weakening the strongest contacts is expected to be rate limiting for remodeling. This could occur by exploiting binding energy of the remodeler towards the nucleosome[48] or when the ATPase domain tries to translocate on DNA while interacting with histones, e.g. at the H4 tail. The ensuing strain in form of excess DNA or change in the twist of the DNA could locally destabilize histone-DNA interactions (II)[12,13,22]. The ATPase domain may even be strong enough to pump more DNA towards the dyad than the nucleosomal surface can accommodate, causing it to detach and bulge out[2,16,18,30,49]. The latter model is difficult to envision for remodeling by the truncated ISWI enzyme due to lack of domains that help forming and stabilizing the bulge.

Once key contacts between histones and DNA are weakened, alternative sets of histone-DNA contacts might become energetically more preferable leading to a repositioning of the histones relative to DNA (III). DNA-histone contacts may adjust concertedly, or -perhaps

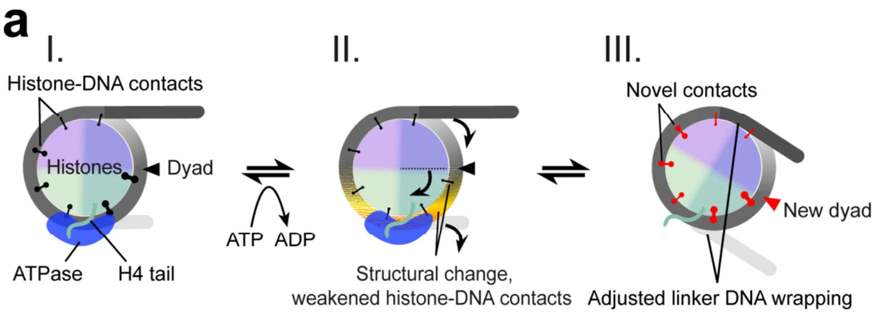

b

ATPase: basic remodeling motor	HSS: modulator of remodeling
- Autonomously hydrolyzes ATP	- Increases affinity
- Is activated by nucleosome binding	- Increases specificity for nucleosomes
- Recognizes the H4 tail	- Associates with accessory subunits*
- Weakens histone-DNA contacts	- Increases processivity†
- Slides nucleosomes	- Implicated in spacing, directionality & nucleosome positioning*

Figure 7: Model for the mechanism of nucleosome remodeling. (**a**) Suggested remodeling mechanism. The HSS domain was omitted from the model as it was evidently not required for the basic mechanism. Histones and DNA form multiple contacts with varying strengths (black clamps; shown only for the top gyre of DNA). The ATPase domain attaches to histones, for example the H4 N-terminus (I). Upon ATP hydrolysis, the ATPase domain translocates DNA relative to the histones, thereby distorting the nucleosome structure and disrupting DNA-histone interactions in the vicinity of SHL2 (II). With the strongest histone-DNA contacts destabilized, the histones rearrange relative to DNA to optimize interactions, forming a novel set of contacts and thus a repositioned nucleosome (red clamps; III). (**b**) Division of labor between the ATPase and HSS domains. Asterisks indicate prior work, a dagger anticipated function.

more likely- only locally such that the strain propagates in multiple steps around the nucleosome[4,22].

Accessory domains may have evolved to optimize catalysis and modulate the outcome of the reaction, explaining their diversity among remodeling machines (Fig. 7b)[2,4]. Consistent with previous findings[23], we showed that the HSS domain increased the affinity towards DNA, a feature that is expected to enhance processivity[16,50,51]. In agreement with crosslinking results[24], we obtained evidence for direct contacts between the HSS domain and the nucleosome core particle. This interaction was a major source for specificity towards the nucleosome. As such, the HSS domain improves productive association of the ATPase domain at SHL2, which in turn enhances remodeling. The HSS domain could also optimize catalysis by weakening the DNA-histone interactions at the edge of the nucleosome[11,16]. Through interactions with additional subunits and the linker DNA[23-25,36,52], the HSS may assist sensing the length of the linker or a preferred DNA sequence, and therefore bias the remodeling reaction towards specific outcomes such as nucleosome spacing or positioning[11,24,25,27,28].

Conformational changes within the ATPase domain

How do the conformational changes within the ATPase domain relate to previously reported structural changes in related enzymes? The catalytic domain of the distant relative *Sulfolobus* Sso1653 was crystallized with and without bound DNA[35]. The two structures only showed minor differences well inside the ATPase core, and therefore are unlikely to account for the increased exposure of peripheral arginines upon DNA binding. In conflict with the crystallographic data but in better agreement with our results, a FRET study using the same *Sulfolobus* protein concluded that DNA binding leads to a major structural rearrangement between the two ATPase lobes[37].

Additional crystallographic evidence supports a high degree of flexibility between the two ATPase lobes. The ATPase lobes of relatives of ISWI crystallized in a multitude of very different orientations[31,35,53,54]. Conformational changes between the two ATPase lobes may be functionally important for these enzymes, e.g. for translocation on DNA or regulation of enzyme activity[5,44]. Conceivably, multiple orientations of ISWI's ATPase lobes coexist in solution, accounting for the different enzyme species detected by our ATPase experiments[32]. DNA may preferentially stabilize a subset of these states, thereby aligning the composite catalytic site formed at the cleft between both lobes[5]. As motifs of both ATPase lobes are thought to contact ATP[35], a proper alignment of the lobes might increase the affinity for ATP, explaining our biochemical data.

The increased exposure of peripheral arginines upon DNA binding also suggests that these regions undergo structural changes. Trypsin cleaved DNA-bound ISWI adjacent to a conserved acidic motif in the NTR (Suppl. Fig. 3). Despite lack of sequence similarity, the NTR of Chd1 also contains a highly acidic motif, which was suggested to act as a pseudo-substrate and compete with DNA for binding to lobe 2. In excellent agreement with our proteolytic results, the authors proposed that DNA binding would force a structural rearrangement in Chd1 in which the NTR undocks from lobe 2[31]. The NTRs of both enzymes may therefore fulfill similar roles and gate the entrance to the nucleic acid binding site.

On the C-terminal side, trypsin cut the polypeptide chain within the 'brace' motif of lobe 2[4]. The brace is in close contact with lobe 1 and is directly followed by a stretch of amino acids that folds back to form a 'bridge' between both ATPase lobes[31,32]. We suggest that the brace or bridge may hold the ATPase lobes in a configuration that is not fully competent for ATP hydrolysis and that binding of nucleic acids relieves this inhibition. These results reinforce the notion that the ATPase domain represents an autonomous remodeling engine, which is optimized and modulated by the evolution of accessory domains and subunits.

Materials and Methods

Enzyme expression and purification

pPROEX-HTb-based expression plasmids with genes encoding *Drosophila* ISWI$_{FL}$, ISWI$_{FL}$ E257Q, ISWI$_{26–648}$ and ISWI$_{1–697}$ were kindly provided by C. Mueller (EMBL, Heidelberg, Germany). All genes were fused N-terminally to a 6xHis-TEV tag. The E257Q mutation was introduced into ISWI$_{26–648}$ by QuickChange mutagenesis. Expression and purification was performed as described[32]. The 6xHis-TEV tag was cleaved off by TEV protease for ISWI$_{FL}$ and ISWI$_{1–697}$. For ISWI$_{26–648}$, experiments were carried out in the presence of the tag. ATPase parameters of ISWI$_{26–648}$ with and without tag were quantitatively the same (data not shown).

Enzyme assays and enzyme ligands

Unless otherwise stated, reactions were performed at 28˚C in a buffer containing 25 mM Hepes-KOH pH 7.6, 100 mM potassium acetate, 1.5 mM magnesium acetate, 0.1 mM EDTA, 10% glycerol, 10 mM β-mercaptoethanol. As indicated, some ATPase assays were performed in a buffer with an increased buffering capacity (250 mM Hepes-KOH pH 7.6) and excess Mg^{2+} ions (100 mM magnesium acetate) to prevent high concentrations of ATP from substantially altering the pH and the concentration of free, unchelated Mg^{2+} ions. Both buffers yielded comparable ATPase parameters (Table 1, Suppl. Table 1). Remodeling was followed in 25 mM Hepes-KOH pH 7.6, 50 mM NaCl, 1 mM MgCl, 0.1 mM EDTA, 10% glycerol and 1 mM DTT at 26°C. All remodeling reactions contained an ATP regenerating system consisting of phosphoenolpyruvate (3–6 mM) and a pyruvate kinase-lactate dehydrogenase mixture (15.5 u/mL; Sigma). Nucleotides were always added as stoichiometric complexes with Mg^{2+}. ADP and AMPPNP were purified before use[55]. ATP was purified if used at concentrations exceeding 3 mM or if no ATP regenerating system was used.

Oligopeptides and DNA oligonucleotides were purchased HPLC purified (Peptide Specialty Laboratories and Biomers, respectively; Suppl. Table 2). Short DNA duplexes were created by annealing. The 147-bp DNA used for NCP reconstitution was purified from SmaI digests of a plasmid harboring derivatives of the Widom-601 sequence with terminal SmaI sites. 197-bp DNA was generated by AvaI digests of a pUC derivative containing 25 repeats of the Widom-601 sequence (kindly provided by D. Rhodes, NTU, Singapore). During nucleosome assembly, it is expected that the 147-bp and 197-bp DNA form 0-N-2 and 29-N-23 nucleosomes, respectively[14,56]. DNA used for 13-mer nucleosomal arrays was gene synthesized (Genscript). It contained 197-bp repeats of Widom- 601 derivatives with a KpnI site at bp –32 relative to the dyad axis of the central nucleosome.

Mono- and polynucleosomes were reconstituted with recombinant *Drosophila* histones by salt gradient dialysis as described[57,58]. g-H4 arrays lacked the 19 N-terminal amino acids of histone H4. Nucleosomal arrays were purified by Mg^{2+} precipitation (25-mer arrays, 3.5 mM; 13-mer wt-H4 arrays, 5 mM; 13-mer g-H4 arrays, 8.5 mM)[42,58]. 13-mer arrays were subsequently dialyzed into 10 mM Tris pH 7.7, 0.1 mM EDTA pH 8, 1 mM DTT. Mononucleosomes used in the TLC ATPase assay were purified over a glycerol gradient (10% to 30%) and buffer exchanged into reaction buffer by ultrafiltration. The concentration of nucleosomal DNA was determined by measuring its DNA content by UV absorbance at 260 nm. The indicated concentrations of nucleosomal arrays refer to the concentration of individual nucleosomes. Unless otherwise noted, nucleosomes with wt-H4 were used.

Steady-state ATP hydrolysis assays

Two different ATPase assays were employed. A thin layer chromatography (TLC) based assay was used to follow hydrolysis of γ-[^{32}P]ATP in reactions that required the use of subsaturating ATP concentrations (Fig. 3a–c, Suppl. Fig. 4). All other ATPase data were collected by a coupled ATP hydrolysis assay in 384 well plates as described[32]. For the TLC assay, reactions were initiated by addition of trace amounts of γ-[^{32}P]ATP supplemented with purified, non-radioactive ATP. Three time points (in addition to a “zero” time point from a reaction that lacked enzyme) were collected by stopping the reaction with three volumes of 2 mM EDTA, 0.3 M NaH_2PO_4, 1 M LiCl. Control experiments showed that ISWI was fully quenched on time-scales that were much faster than the experiments required. Reactions were spotted on PEI cellulose F (Merck) and developed in 0.3 M NaH_2PO_4, 1 M LiCl. After autoradiography, signals were quantified, and a line was fit through the data points of each time course. $k_{cat}/K_{M,obs}$ values were obtained from the slopes by normalizing for the enzyme concentration. When the enzyme and ATP concentrations were varied four- and five-fold, respectively, measured rates deviated less than two-fold.

Partial proteolysis assays

If not specified otherwise, $ISWI_{26–648}$ (2.5 µM) was partially proteolyzed with trypsin (20 nM; Promega), LysC (38 nM; Roche) or ArgC (21 nM; Roche). The reaction was stopped by addition of two volumes of SDS sample buffer and immediate incubation at 95°C for 10 min. Samples were separated by SDS-PAGE (12%) and stained by Coomassie Blue.

Double-filter DNA binding assay

39-bp DNA was 5’ labeled with γ-[^{32}P]ATP by polynucleotide kinase. Trace amounts of labeled DNA were incubated for 10 minutes with varying ISWI concentrations. The mixture was then applied on a membrane sandwich composed of a protein binding (Protran-BA85, Whatman) and a DNA binding membrane (Hybond-N+, Amersham) as described[59].

Nucleosome sliding assays

Mononucleosome sliding: Centrally positioned mononucleosomes (197-bp DNA; 160 nM) were incubated with ATP (0.5 mM), ISWI_{FL} (30 nM) or $\text{ISWI}_{26\text{–}648}$ (300 nM). Time points were quenched by apyrase (2.5 u/µL) and excess linearized plasmid DNA (0.4 mg/mL). Native PAGE (4.5%) was performed with 0.2 µg mononucleosomal DNA.

Polynucleosome sliding: 25-mer regular nucleosomal arrays (30 nM) were incubated with ATP (100 µM), and ISWI_{FL} (10 nM) or $\text{ISWI}_{26\text{–}648}$ (300 nM). Remodeling was quenched after 6 h with apyrase (2.5 u/µL). The arrays were then digested with AvaI (1.2 u/µL) for 3 h at 26°C. Samples were deproteinized and analyzed as described below. Exhaustive digests with high concentrations of AvaI overnight gave analogous results.

Restriction enzyme accessibility assay

25-mer nucleosomal arrays (100 nM) were incubated for 1 h with wild-type or E257Q mutant $\text{ISWI}_{26\text{–}648}$ (both 5 µM), ATP (50 µM), and the indicated restriction enzymes (AluI, 0.5 u/µL; BsrBI, 0.5 u/µL; BsiWI, 1 u/µL; BanI, 2 u/µL). The reactions were stopped with EDTA (20–40 mM) and SDS (0.4%). Samples were deproteinized, and DNA was ethanol precipitated, resolved by agarose gel-electrophoresis and visualized by ethidium bromide staining.

To quantitate remodeling, 13-mer arrays (20 or 100 nM) were incubated with ISWI_{FL} or $\text{ISWI}_{26\text{–}648}$, respectively, ATP (1 mM), and KpnI (2 u/µL). Reactions were quenched and analyzed as above. Negligible accessibility (<5 %) was seen when the reaction was simultaneously initiated and quenched or when ISWI was omitted. Controls showed that the ATP regenerating system was not depleted throughout the assay. k_{obs} for remodeling was obtained by fitting the time courses to a single exponential function (Eq. 1). The maximal remodeling velocities ($k_{\text{obs,max}}$) were obtained by fitting the data to standard or inverse binding isotherms (Eq. 2).

$$y = 100 * (1 - e^{-k_{\text{obs}} * t}) \tag{1}$$

$$y = k_{\text{obs,max}} - (amp * \frac{[E]}{K_{1/2} + [E]}) \tag{2}$$

Observed remodeling rates were proportionally faster for $\text{ISWI}_{26\text{–}648}$ (but not ISWI_{FL}) when the KpnI concentration was raised from 2 to 5 u/µL. This rate enhancement was independent of the $\text{ISWI}_{26\text{–}648}$ concentration between 0.3 and 30 µM. Reported rates, including the maximal remodeling rate constant $k_{\text{obs,max}}$, are therefore lower estimates for $\text{ISWI}_{26\text{–}648}$. The reported deleterious effect of the HSS deletion on remodeling is consequently an upper estimate.

Kinetic and thermodynamic modelling and data fitting

Modelling was performed in Mathematica (Wolfram Research). Data were fit with Matlab (The Mathworks) or KaleidaGraph (Synergy Software). The biphasic ATPase data were fit to Equation 3 (Fig. 1a,b). As saturation with ATP was not achieved, the second phase was represented only by the linear term *m**[ATP]. *m* possesses a complex dependence on the rate and equilibrium constants in the reaction scheme (Suppl. Fig. 1a) and was not interpreted further.

$$v = k_{cat,obs}^{Phase\ 1} * [\mathrm{ATP}]/\left(K_{M,obs}^{Phase\ 1} + [\mathrm{ATP}]\right) + m * [\mathrm{ATP}] \qquad (3)$$

Acknowledgements

We are grateful to C. Müller (European Molecular Biology Laboratory, Heidelberg, Germany) and D. Rhodes (Nanyang Technological University, Singapore) for the donation of plasmids, and to the following departmental colleagues for materials: N. Hepp for 13-mer nucleosomal arrays, C. Boenisch for 197-bp 601 DNA, V. K. Maier and C. Regnard for recombinant histone octamers. We thank R. Mentele for the Edman digest, I. Forné for performing the LC-MS-MS experiment and Z. Ökten for comments on the manuscript. HK acknowledges support by the Elite Network of Bavaria. This work was supported by grants of the Deutsche Forschungsgemeinschaft to PBB (SFB 594 TP A6 and Be 1140/6-1).

References

1. Hargreaves, D.C. & Crabtree, G.R. ATP-dependent chromatin remodeling: genetics, genomics and mechanisms. *Cell Res* 21, 396-420 (2011).
2. Clapier, C.R. & Cairns, B.R. The biology of chromatin remodeling complexes. *Annu Rev Biochem* 78, 273-304 (2009).
3. Hota, S.K. & Bartholomew, B. Diversity of operation in ATP-dependent chromatin remodelers. *Biochim Biophys Acta* 1809, 476-87 (2011).
4. Flaus, A. & Owen-Hughes, T. Mechanisms for ATP-dependent chromatin remodelling: the means to the end. *FEBS J* 278, 3579-95 (2011).
5. Hauk, G. & Bowman, G.D. Structural insights into regulation and action of SWI2/SNF2 ATPases. *Curr Opin Struct Biol* 21, 719-27 (2011).
6. Flaus, A., Martin, D.M., Barton, G.J. & Owen-Hughes, T. Identification of multiple distinct Snf2 subfamilies with conserved structural motifs. *Nucleic Acids Res* 34, 2887-905 (2006).
7. Dechassa, M.L. et al. Disparity in the DNA translocase domains of SWI/SNF and ISW2. *Nucleic Acids Res* (2012).
8. Fan, H.Y., Trotter, K.W., Archer, T.K. & Kingston, R.E. Swapping function of two chromatin remodeling complexes. *Mol Cell* 17, 805-15 (2005).
9. Saha, A., Wittmeyer, J. & Cairns, B.R. Chromatin remodeling through directional DNA translocation from an internal nucleosomal site. *Nat Struct Mol Biol* 12, 747-55 (2005).
10. Zofall, M., Persinger, J., Kassabov, S.R. & Bartholomew, B. Chromatin remodeling by ISW2 and SWI/SNF requires DNA translocation inside the nucleosome. *Nat Struct Mol Biol* 13, 339-46 (2006).
11. McKnight, J.N., Jenkins, K.R., Nodelman, I.M., Escobar, T. & Bowman, G.D. Extranucleosomal DNA binding directs nucleosome sliding by Chd1. *Mol Cell Biol* 31, 4746-59 (2011).
12. Richmond, T.J. & Davey, C.A. The structure of DNA in the nucleosome core. *Nature* 423, 145-50 (2003).
13. Suto, R.K. et al. Crystal structures of nucleosome core particles in complex with minor groove DNA-binding ligands. *J Mol Biol* 326, 371-80 (2003).
14. Makde, R.D., England, J.R., Yennawar, H.P. & Tan, S. Structure of RCC1 chromatin factor bound to the nucleosome core particle. *Nature* 467, 562-6 (2010).
15. Ferreira, H., Flaus, A. & Owen-Hughes, T. Histone modifications influence the action of Snf2 family remodelling enzymes by different mechanisms. *J Mol Biol* 374, 563-79 (2007).
16. Gangaraju, V.K., Prasad, P., Srour, A., Kagalwala, M.N. & Bartholomew, B. Conformational changes associated with template commitment in ATP-dependent chromatin remodeling by ISW2. *Mol Cell* 35, 58-69 (2009).
17. Clapier, C.R., Langst, G., Corona, D.F., Becker, P.B. & Nightingale, K.P. Critical role for the histone H4 N terminus in nucleosome remodeling by ISWI. *Mol Cell Biol* 21, 875-83 (2001).
18. Dang, W., Kagalwala, M.N. & Bartholomew, B. Regulation of ISW2 by concerted action of histone H4 tail and extranucleosomal DNA. *Mol Cell Biol* 26, 7388-96 (2006).
19. Hamiche, A., Kang, J.G., Dennis, C., Xiao, H. & Wu, C. Histone tails modulate nucleosome mobility and regulate ATP-dependent nucleosome sliding by NURF. *Proc Natl Acad Sci U S A* 98, 14316-21 (2001).
20. Whitehouse, I., Stockdale, C., Flaus, A., Szczelkun, M.D. & Owen-Hughes, T. Evidence for DNA translocation by the ISWI chromatin-remodeling enzyme. *Mol Cell Biol* 23, 1935-45 (2003).
21. Zhang, Y. et al. DNA translocation and loop formation mechanism of chromatin remodeling by SWI/SNF and RSC. *Mol Cell* 24, 559-68 (2006).
22. Bowman, G.D. Mechanisms of ATP-dependent nucleosome sliding. *Curr Opin Struct Biol* 20, 73-81 (2010).

23. Grune, T. et al. Crystal structure and functional analysis of a nucleosome recognition module of the remodeling factor ISWI. *Mol Cell* 12, 449-60 (2003).
24. Dang, W. & Bartholomew, B. Domain architecture of the catalytic subunit in the ISW2-nucleosome complex. *Mol Cell Biol* 27, 8306-17 (2007).
25. Yamada, K. et al. Structure and mechanism of the chromatin remodelling factor ISW1a. *Nature* 472, 448-53 (2011).
26. Gangaraju, V.K. & Bartholomew, B. Dependency of ISW1a chromatin remodeling on extranucleosomal DNA. *Mol Cell Biol* 27, 3217-25 (2007).
27. Yang, J.G., Madrid, T.S., Sevastopoulos, E. & Narlikar, G.J. The chromatin-remodeling enzyme ACF is an ATP-dependent DNA length sensor that regulates nucleosome spacing. *Nat Struct Mol Biol* 13, 1078-83 (2006).
28. Ryan, D.P., Sundaramoorthy, R., Martin, D., Singh, V. & Owen-Hughes, T. The DNA-binding domain of the Chd1 chromatin-remodelling enzyme contains SANT and SLIDE domains. *EMBO J* 30, 2596-609 (2011).
29. Corona, D.F. et al. ISWI is an ATP-dependent nucleosome remodeling factor. *Mol Cell* 3, 239-45 (1999).
30. Cairns, B.R. Chromatin remodeling: insights and intrigue from single-molecule studies. *Nat Struct Mol Biol* 14, 989-96 (2007).
31. Hauk, G., McKnight, J.N., Nodelman, I.M. & Bowman, G.D. The chromodomains of the Chd1 chromatin remodeler regulate DNA access to the ATPase motor. *Mol Cell* 39, 711-23 (2010).
32. Forne, I., Ludwigsen, J., Imhof, A., Becker, P.B. & Mueller-Planitz, F. Probing the conformation of the ISWI ATPase domain with genetically encoded photoreactive crosslinkers and mass spectrometry. *Mol Cell Proteomics* 11, M111 012088 (2012).
33. Racki, L.R. et al. The chromatin remodeller ACF acts as a dimeric motor to space nucleosomes. *Nature* 462, 1016-21 (2009).
34. Singleton, M.R., Dillingham, M.S. & Wigley, D.B. Structure and mechanism of helicases and nucleic acid translocases. *Annu Rev Biochem* 76, 23-50 (2007).
35. Durr, H., Korner, C., Muller, M., Hickmann, V. & Hopfner, K.P. X-ray structures of the Sulfolobus solfataricus SWI2/SNF2 ATPase core and its complex with DNA. *Cell* 121, 363-73 (2005).
36. Sharma, A., Jenkins, K.R., Heroux, A. & Bowman, G.D. Crystal Structure of the Chromodomain Helicase DNA-binding Protein 1 (Chd1) DNA-binding Domain in Complex with DNA. *J Biol Chem* 286, 42099-104 (2011).
37. Lewis, R., Durr, H., Hopfner, K.P. & Michaelis, J. Conformational changes of a Swi2/Snf2 ATPase during its mechano-chemical cycle. *Nucleic Acids Res* 36, 1881-90 (2008).
38. Fersht, A. *Structure and Mechanism in Protein Science: A Guide to Enzyme Catalysis and Protein Folding*, (W.H. Freeman, 1999).
39. Boyer, L.A., Latek, R.R. & Peterson, C.L. The SANT domain: a unique histone-tail-binding module? *Nat Rev Mol Cell Biol* 5, 158-63 (2004).
40. Clapier, C.R., Nightingale, K.P. & Becker, P.B. A critical epitope for substrate recognition by the nucleosome remodeling ATPase ISWI. *Nucleic Acids Res* 30, 649-55 (2002).
41. Langst, G., Bonte, E.J., Corona, D.F. & Becker, P.B. Nucleosome movement by CHRAC and ISWI without disruption or trans-displacement of the histone octamer. *Cell* 97, 843-52 (1999).
42. Maier, V.K., Chioda, M., Rhodes, D. & Becker, P.B. ACF catalyses chromatosome movements in chromatin fibres. *EMBO J* 27, 817-26 (2008).
43. Logie, C. & Peterson, C.L. Catalytic activity of the yeast SWI/SNF complex on reconstituted nucleosome arrays. *EMBO J* 16, 6772-82 (1997).
44. Durr, H., Flaus, A., Owen-Hughes, T. & Hopfner, K.P. Snf2 family ATPases and DExx box helicases: differences and unifying concepts from high-resolution crystal structures. *Nucleic Acids Res* 34, 4160-7 (2006).

45. Kagalwala, M.N., Glaus, B.J., Dang, W., Zofall, M. & Bartholomew, B. Topography of the ISW2-nucleosome complex: insights into nucleosome spacing and chromatin remodeling. *EMBO J* 23, 2092-104 (2004).
46. Hall, M.A. et al. High-resolution dynamic mapping of histone-DNA interactions in a nucleosome. *Nat Struct Mol Biol* 16, 124-9 (2009).
47. Mihardja, S., Spakowitz, A.J., Zhang, Y. & Bustamante, C. Effect of force on mononucleosomal dynamics. *Proc Natl Acad Sci U S A* 103, 15871-6 (2006).
48. Lorch, Y., Maier-Davis, B. & Kornberg, R.D. Mechanism of chromatin remodeling. *Proc Natl Acad Sci U S A* 107, 3458-62 (2010).
49. Strohner, R. et al. A 'loop recapture' mechanism for ACF-dependent nucleosome remodeling. *Nat Struct Mol Biol* 12, 683-90 (2005).
50. Blosser, T.R., Yang, J.G., Stone, M.D., Narlikar, G.J. & Zhuang, X. Dynamics of nucleosome remodelling by individual ACF complexes. *Nature* 462, 1022-7 (2009).
51. Fyodorov, D.V. & Kadonaga, J.T. Dynamics of ATP-dependent chromatin assembly by ACF. *Nature* 418, 897-900 (2002).
52. Eberharter, A., Vetter, I., Ferreira, R. & Becker, P.B. ACF1 improves the effectiveness of nucleosome mobilization by ISWI through PHD-histone contacts. *EMBO J* 23, 4029-39 (2004).
53. Thoma, N.H. et al. Structure of the SWI2/SNF2 chromatin-remodeling domain of eukaryotic Rad54. *Nat Struct Mol Biol* 12, 350-6 (2005).
54. Caruthers, J.M., Johnson, E.R. & McKay, D.B. Crystal structure of yeast initiation factor 4A, a DEAD-box RNA helicase. *Proc Natl Acad Sci U S A* 97, 13080-5 (2000).
55. Horst, M., Oppliger, W., Feifel, B., Schatz, G. & Glick, B.S. The mitochondrial protein import motor: dissociation of mitochondrial hsp70 from its membrane anchor requires ATP binding rather than ATP hydrolysis. *Protein Sci* **5**, 759-67 (1996).
56. Vasudevan, D., Chua, E.Y. & Davey, C.A. Crystal structures of nucleosome core particles containing the '601' strong positioning sequence. *J Mol Biol* 403, 1-10 (2010).
57. Dyer, P.N. et al. Reconstitution of nucleosome core particles from recombinant histones and DNA. *Methods Enzymol* 375, 23-44 (2004).
58. Huynh, V.A., Robinson, P.J. & Rhodes, D. A method for the in vitro reconstitution of a defined "30 nm" chromatin fibre containing stoichiometric amounts of the linker histone. *J Mol Biol* 345, 957-68 (2005).
59. Wong, I. & Lohman, T.M. A double-filter method for nitrocellulose-filter binding: application to protein-nucleic acid interactions. *Proc Natl Acad Sci U S A* 90, 5428-32 (1993).

Supplementary material

“The ATPase domain of ISWI is an autonomous nucleosome remodeling machine”

Mueller-Planitz et al., NSMB, 2013

Supplementary Note

Additional scenarios explaining a biphasic ATP concentration dependence of ATP hydrolysis

1) *"ISWI is mostly dimerized in solution under assay conditions and each subunit has a different K_M for ATP."*

   This possibility is ruled out by the observation that DNA-free ISWI is in a monomeric state in solution as measured by multiple angle light scattering by us (data not shown) and by analytical ultracentrifugation by others[2].

2) *"A small fraction of ISWI is dimerized in solution under assay conditions, and the monomer and the dimer have different K_M values for ATP."*

   One would expect that more dimer forms with increasing enzyme concentrations and that the observed reaction velocity would consequently change as well. This expectation is not consistent with experimental results (**Suppl. Fig. 2a,b**).

3) *"ISWI preparations contain contaminating DNA. DNA-free and the DNA-bound ISWI have a different K_M for ATP."*

   Treatment with nucleases and extensive purification of $ISWI_{FL}$ using five consecutive chromatography steps (including size exclusion chromatography in 2 M salt) did not abolish the biphasic behavior seen in Figure 1a. Moreover, we did not observe changes of the biphasic shape upon a jump in the ionic strength of the buffer (from 1.5 mM to 100 mM Mg^{2+}), which should drastically weaken protein-DNA interactions (data not shown). Finally, $ISWI_{1–697}$ and $ISWI_{26–648}$ also exhibited a biphasic response to the ATP concentration (**Fig. 1b** and data not shown) although they intrinsically bound DNA with much weaker affinity than $ISWI_{FL}$ (**Suppl. Fig. 5**).

4) *"Proteolysis fragments of ISWI are present, and they have a different K_M for ATP."*

   The extensive purification discussed above argued against this possibility. Moreover, constructs lacking the entire C-terminus ($ISWI_{1–697}$ and $ISWI_{26–648}$) still showed the biphasic response to variation of the ATP concentration, making it unlikely that the same contaminants were present in all enzyme preparations (**Fig. 1b** and data not shown).

5) *"ISWI possesses a second, allosteric binding site for ATP."*

   Neither structural nor biochemical evidence exists for ISWI or related enzymes to support a second, allosteric binding site.

6) *"A fraction of ISWI is misfolded and therefore nearly inactive".*

   Active site titration experiments with 39-bp long DNA duplexes refuted the possibility that a majority of $ISWI_{26–648}$ was misfolded to the extent that DNA could not bind and stimulate ATP hydrolysis (data not shown). Our active site titration experiments were, however, not sensitive enough to detect a minor fraction of misfolded protein. If this minor fraction were responsible for one or the other catalytic phase of the biphasic ATPase curve, its specific ATPase activity would however be considerable as the following consideration shows. In the biphasic ATPase curve, the first phase contributed 0.014 s^{-1} and the second phase >0.046 s^{-1} to the amplitude (**Table 1**). If, for example, 10% misfolded, nearly inactive protein were present, its specific activity would be 0.14 s^{-1} (= 10 × 0.014 s^{-1}) or >0.46 s^{-1} (= 10 × 0.046 s^{-1}). These values approach the DNA-stimulated $k_{\mathrm{cat,obs}}$ of 0.51s $^{-1}$. The hypothetical misfolded fraction can therefore not be considered “nearly inactive”.

Why can ISWI$_{26–648}$ not distinguish nucleosomes from free DNA in presence of saturating ATP?

The $k_{\mathrm{cat}}/K_{\mathrm{M,obs}}$ of ISWI$_{26–648}$ was markedly (17- to 23-fold) stimulated by NCPs and nucleosomal arrays relative to DNA (**Fig. 3a,b**) whereas the $k_{\mathrm{cat,obs}}$ apparently was not (data not shown). Two scenarios could explain these observations. The first scenario is discussed in the main text. In this scenario, ISWI$_{26–648}$ would recognize the DNA component of the nucleosome, leading to DNA-like stimulation, but most enzyme molecules - at steady-state - would not find the proper site at SHL2. Support for this scenario came from the observation that ISWI$_{26–648}$ could only poorly discriminate between free DNA and nucleosomes even under subsaturating ATP concentrations. ISWI$_{\mathrm{FL}}$, on the other hand, was much less prone to unproductive binding because the HSS domain strongly increased the specificity for nucleosomes (**Fig. 3c**).

The second scenario, in contrast, posits that all ISWI$_{26–648}$ molecules bind productively at SHL2 of the nucleosome. Lack of stimulation of $k_{\mathrm{cat,obs}}$ therefore cannot be explained by unproductive binding elsewhere on nucleosomal DNA in this model. If true, $K_{\mathrm{M,obs}}$ for ISWI$_{26–648}$ would have to decrease by 17- to 23-fold, such that $k_{\mathrm{cat,obs}}$ devided by $K_{\mathrm{M,obs}}$ would yield a value that is 17- to 23-fold larger relative to DNA. Evidence against this scenario came from steady-state ATPase parameters of ISWI$_{\mathrm{FL}}$. The $K_{\mathrm{M,obs}}$ of ISWI$_{\mathrm{FL}}$ was only modestly decreased (two- to three-fold; **Suppl. Table 1**). Given the high similarity of the ATPase parameters of ISWI$_{\mathrm{FL}}$ and ISWI$_{26–648}$, the second scenario seemed unlikely.

Supplementary Tables

Supplementary Table 1: ATPase parameters of $ISWI_{FL}$ and $ISWI_{26–648}$ [a]

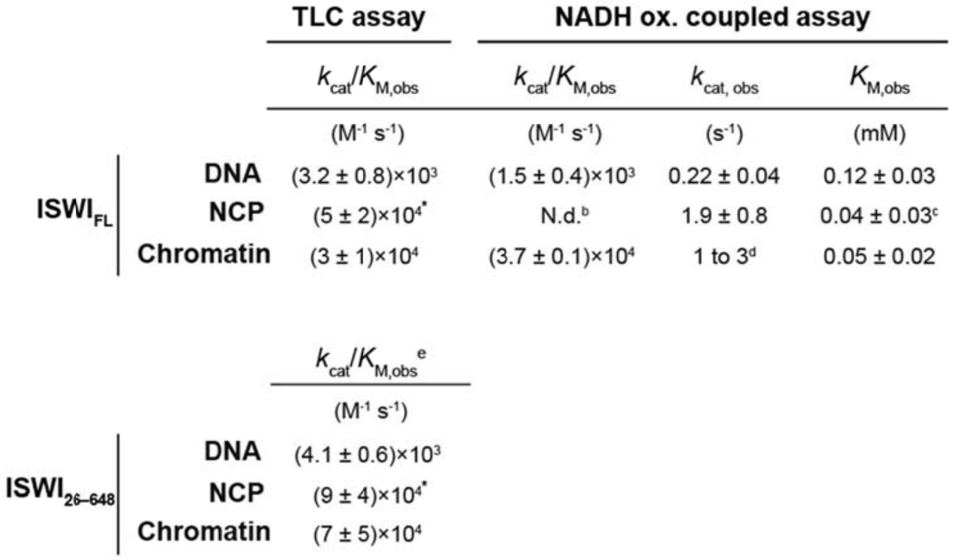

		TLC assay	NADH ox. coupled assay		
		$k_{cat}/K_{M,obs}$	$k_{cat}/K_{M,obs}$	$k_{cat, obs}$	$K_{M,obs}$
		(M^{-1} s^{-1})	(M^{-1} s^{-1})	(s^{-1})	(mM)
$ISWI_{FL}$	**DNA**	$(3.2 \pm 0.8) \times 10^3$	$(1.5 \pm 0.4) \times 10^3$	0.22 ± 0.04	0.12 ± 0.03
	NCP	$(5 \pm 2) \times 10^{4*}$	N.d.[b]	1.9 ± 0.8	0.04 ± 0.03[c]
	Chromatin	$(3 \pm 1) \times 10^4$	$(3.7 \pm 0.1) \times 10^4$	1 to 3[d]	0.05 ± 0.02

		$k_{cat}/K_{M,obs}$ [e]
		(M^{-1} s^{-1})
$ISWI_{26–648}$	**DNA**	$(4.1 \pm 0.6) \times 10^3$
	NCP	$(9 \pm 4) \times 10^{4*}$
	Chromatin	$(7 \pm 5) \times 10^4$

[a]: Compared to Table 1 in the main text, a reaction buffer containing a lower Mg^{2+} concentration (1.5 mM) was used to prevent aggregation of chromatin. All reported values were obtained with saturating ligand concentrations. DNA reactions contained a 39-bp DNA duplex (NADH oxidation coupled assay) or 147-bp DNA (TLC assay), NCP reactions nucleosome core particles assembled on the 147-bp Widom-601 sequence, and chromatin reactions 25-mer nucleosomal arrays (TLC assay) or polynucleosomes assembled on plasmid DNA (NADH assay). Where indicated (asterisk), errors are min and max values of two independent measurements. Otherwise, errors are standard deviations of at least three independent measurements.

[b]: N.d.: Not determined.

[c]: Value calculated from $k_{cat,obs}$ and $k_{cat}/K_{M,obs}$.

[d]: Values varied with the enzyme concentration (**Suppl. Fig. 2c**).

[e]: All values measured by the TLC ATPase assay.

Supplementary Table 2: (a) Oligonucleotides[a]; (b) oligopeptides used in the study[b]

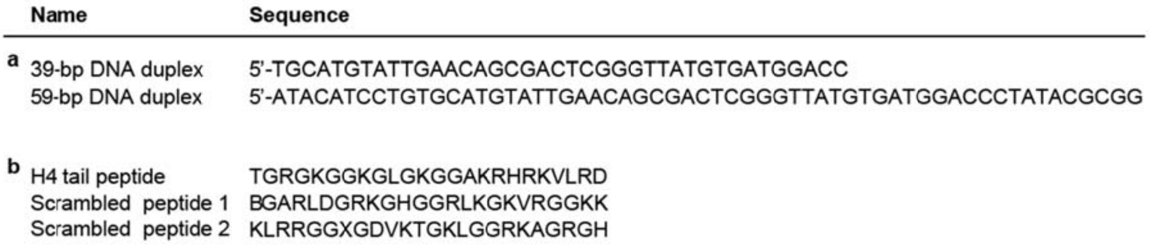

	Name	Sequence
a	39-bp DNA duplex	5'-TGCATGTATTGAACAGCGACTCGGGTTATGTGATGGACC
	59-bp DNA duplex	5'-ATACATCCTGTGCATGTATTGAACAGCGACTCGGGTTATGTGATGGACCCTATACGCGG
b	H4 tail peptide	TGRGKGGKGLGKGGAKRHRKVLRD
	Scrambled peptide 1	BGARLDGRKGHGGRLKGKVRGGKK
	Scrambled peptide 2	KLRRGGXGDVKTGKLGGRKAGRGH

[a]: Sequences of only one of the two strands per DNA duplex are shown.

[b]: X indicates an acetylated lysine residue. B stands for the unnatural amino acid *p*-benzoyl-*p*-phenylalanine, which connects to the neighbouring amino acids via a regular peptide bond.

Supplementary Figures

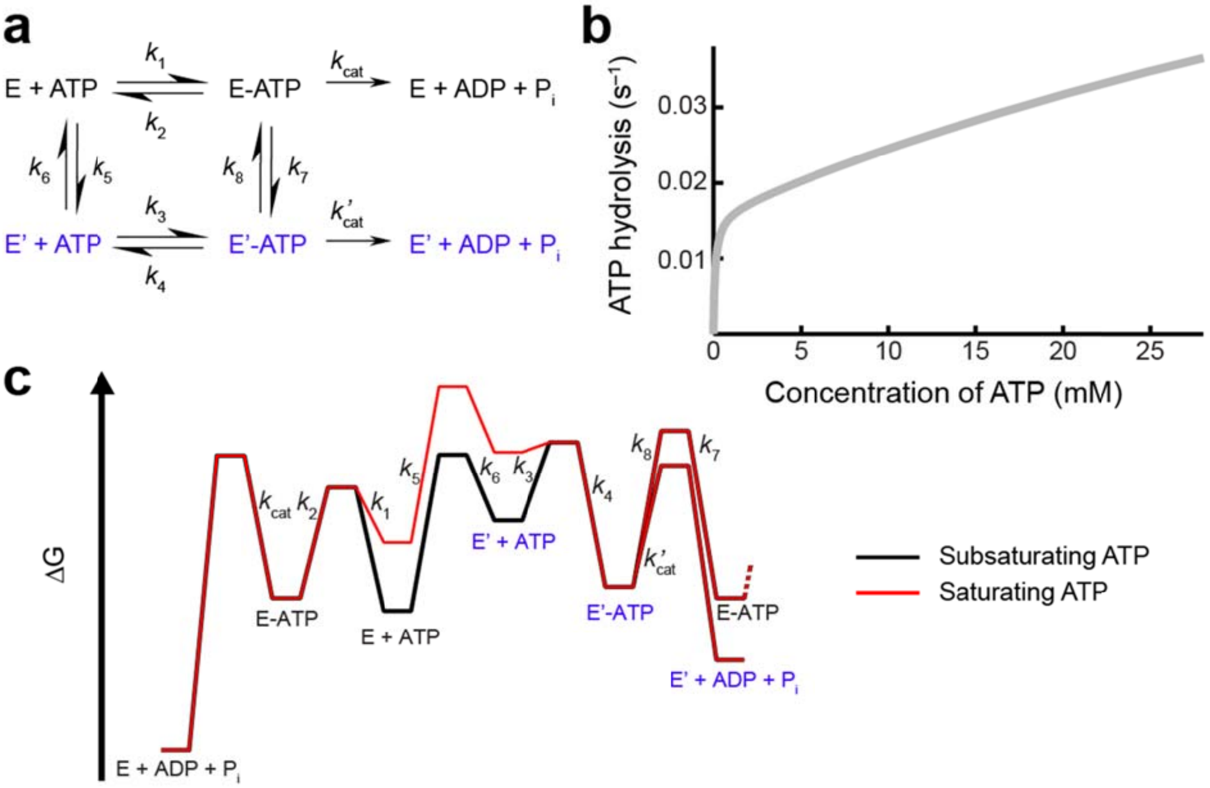
a
E + ATP
k1
k2
E-ATP
kcat
E + ADP + Pi
k6
k5
k8
k7
E' + ATP
k3
k4
E'-ATP
k'cat
E' + ADP + Pi
b
ATP hydrolysis (s-1)
0.03
0.02
0.01
0
5
10
15
20
25
Concentration of ATP (mM)
c
ΔG
kcat
k2
k1
k5
k6
k3
k4
k8
k7
k'cat
E-ATP
E + ATP
E' + ATP
E'-ATP
E-ATP
E' + ADP + Pi
E + ADP + Pi
Subsaturating ATP
Saturating ATP

Supplementary Figure 1: The presence of two ISWI conformations can result in a biphasic ATP concentration dependence of ATP hydrolysis. (**a**) A simple reaction scheme in which the enzyme exists in two conformations, E and E', each being able to bind and hydrolyze ATP with different rate constants. (**b**) Modeling of the scheme in **a** showed that a biphasic ATP concentration dependence closely resembling the data shown in Figure 1a could be obtained ($k_{cat} = 0.015\ s^{-1}$, $k'_{cat} = 1\ s^{-1}$, $k_1 = 10^5\ M^{-1}\ s^{-1}$, $k_2 = 10\ s^{-1}$, $k_3 = 10^9\ M^{-1}\ s^{-1}$, $k_4 = 10^{-2}\ s^{-1}$, $k_5 = 10^{-3}\ s^{-1}$, $k_6 = 10^5\ s^{-1}$, $k_7 = 10^{-4}\ s^{-1}$, $k_8 = 10^{-3}\ s^{-1}$). Shown is an example in which both enzyme conformations had strongly different affinities for ATP. Note that many solutions resulted in biphasic behavior, not all of which required different ATP affinities (to produce a biphasic ATP concentration dependence, the ATP affinities of E and E' may or may not be similar to each other, E and E' may or may not have similar ATP turnover rates - k_{cat} or k'_{cat} may even become zero -, the ATP binding rate constants k_1 and k_3 may or may not assume similar values and the equilibration between E <=> E' and E-ATP <=> E'-ATP may or may not be similarly fast). Solutions that produce biphasic curves, however, required the four species E, E', E-ATP and E'-ATP to be present and to interconvert (mathematical derivation not shown). All solutions that produced a biphasic ATP response exhibited an ATP-concentration dependent change in the flux through the reaction scheme, i.e., different intermediates were populated due to a change in the rate limiting step (illustrated exemplary in the next panel). (**c**) Free energy profiles using the rate constants from the previous panel. With subsaturating concentrations of ATP (black line), E + ATP is the ground state of the reaction. E and ATP react to E-ATP, and ISWI then hydrolyzes ATP via k_{cat}. With saturating concentrations of ATP (red line), E + ATP quickly reacts to E-ATP. Since k_{cat} is too slow to hydrolyze all ATP immediately, some of the E-ATP reacts via k_7 to E'-ATP from where ATP is quickly hydrolyzed via k'_{cat}.

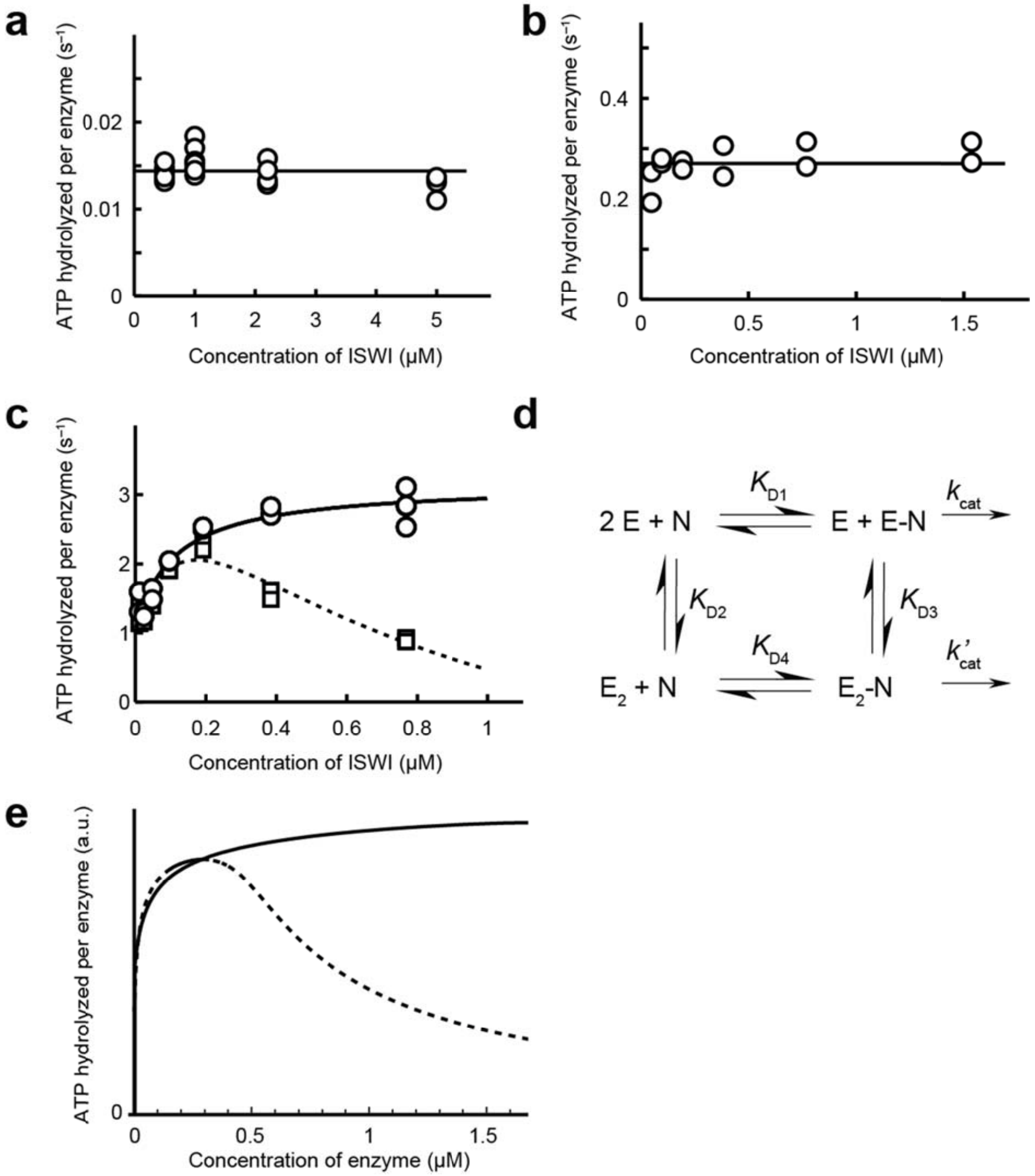

Supplementary Figure 2: Enzyme concentration dependence of ATP hydrolysis by ISWI$_{FL}$. (**a**) ATP hydrolysis by ligand-free ISWI$_{FL}$ was independent of the enzyme concentration between 0.5 and 5 μM. The biphasic ATP concentration dependence (**Fig. 1a**) therefore could not be caused by possible multimerization of ISWI. The assay was performed with 7 mM ATP in 100 mM Mg^{2+}. (**b**) ATP hydrolysis of DNA-bound ISWI$_{FL}$ remained constant between 0.05 to 1.5 μM enzyme, demonstrating that the ATPase signal was independent of possible enzyme multimerization. The assay was performed with saturating concentrations of 59-bp DNA and 3 mM ATP in 1.5 mM free Mg^{2+}. (**c**) The chromatin-stimulated reaction showed a pronounced dependence on the ISWI$_{FL}$ concentration. Two concentrations of chromatinized plasmid DNA were used (dashed line: 0.02 mg/mL, solid line: 0.1

mg/mL, referring to the DNA content). Increasing ATPase rates between 0 and 0.2 µM $ISWI_{FL}$ were consistent with enzyme dimerization on nucleosomes and subsequent enzyme activation[2]. The decreasing activity observed for the lower chromatin concentration above 0.2 µM $ISWI_{FL}$ was well explained by out-titration of available ISWI binding sites on chromatin. The data were collected with 3 mM ATP and 1.5 mM free Mg^{2+}. (**d**) Simple reaction scheme to explain the data shown in **c**. A single enzyme (E) bound to a nucleosome (N) hydrolyzes ATP with a different rate constant (k_{cat}) than an enzyme dimer (k'_{cat}). (**e**) *In silico* modeling of the reaction scheme in **d** recapitulated the features of the curves in **c**. Simulations were run for two nucleosome concentrations (0.2 µM, dashed line; 1 µM, solid line) with $K_{D1} = 10^{-1}$ µM, $K_{D2} = 10$ µM, $K_{D3} = 10^{-2}$ µM, $K_{D4} = 10^{-4}$ µM and $k'_{cat} = 4\ k_{cat}$.

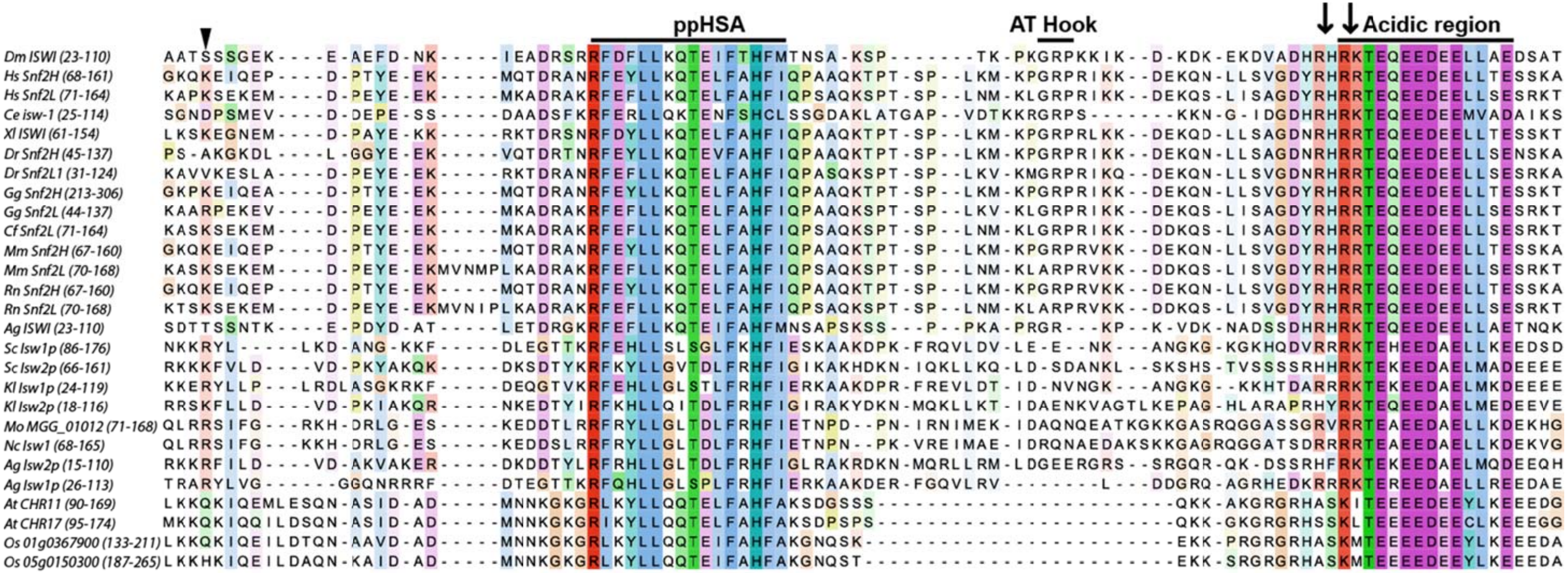
ppHSA
AT Hook
Acidic region
Dm ISWI (23-110) AATSSSGEK----E-AEFD-NK-----IEADRSRRFDFLLKQTEIFTHFMTNSA-KSP--------TK-PKGRPKKIK--D-KDK-EKDVADHRHRKTEQEEDEELLAEDSAT
Hs Snf2H (68-161) GKQKEIQEP----D-PTYE-EK-----MQTDRANRFEYLLKQTELFAHFIQPAAQKTPT-SP--LKM-KPGRPRIKK--DEKQN-LLSVGDYRHRRTEQEEDEELLTESSKA
Hs Snf2L (71-164) KAPKSEKEM----D-PEYE-EK-----MKADRAKRFEFLLKQTELFAHFIQPSAQKSPT-SP--LNM-KLGRPRIKK--DEKQS-LISAGDYRHRRTEQEEDEELLSESRKT
Ce isw-1 (25-114) SGNDPSMEV----D-DEPE-SS-----DAADSFKRFERLLQKTENFSHCLSSGDAKLATGAP--VDTKKRGRPS--------KKN-G-IDGDHRHRKTEQEEDEEMVADAIKS
Xl ISWI (61-154) LKSKEGNEM----D-PAYE-KK-----RKTDRSNRFDYLLKQTELFAHFIQPAAQKTPT-SP--LKM-KPGRPRLKK--DEKQD-LLSAGDNRHRRTEQEEDEELLTESSKT
Dr Snf2H (45-137) PS-AKGKDL----L-GGYE-EK-----VQTDRTNRFEYLLKQTEVFAHFIQPAAQKTPT-SP--LKM-KPGRPRIKK--DEKQN-LLSAGDNRHRRTEQEEDEELLSENSKA
Dr Snf2L1 (31-124) KAVVKESLA----D-PEYE-EK-----RKTDRANRFEFLLKQTELFAHFIQPASQKSPT-SP--LKV-KMGRPRIKQ--DEKQN-LLSVGDNRHRRTEQEEDEELLSESRKA
Gg Snf2H (213-306) GKPKEIQEA----D-PTYE-EK-----MQTDRANRFEYLLKQTELFAHFIQPAAQKTPT-SP--LKM-KPGRPRIKK--DEKQN-LLSVGDYRHRRTEQEEDEELLTESSKT
Gg Snf2L (44-137) KAARPEKEV----D-PEYE-EK-----MKADRAKRFEFLLKQTELFAHFIQPAAQKSPT-SP--LKV-KLGRPRIKK--DEKQS-LISAGDYRHRRTEQEEDEELLSESRKT
Cf Snf2L (71-164) KASKSEKEM----D-PEYE-EK-----MKADRAKRFEFLLKQTELFAHFIQPSAQKSPT-SP--LNM-KLGRPRIKK--DDKQS-LISAGDYRHRRTEQEEDEELLSESRKT
Mm Snf2H (67-160) GKQKEIQEP----D-PTYE-EK-----MQTDRANRFEYLLKQTELFAHFIQPAAQKTPT-SP--LKM-KPGRPRVKK--DEKQN-LLSVGDYRHRRTEQEEDEELLTESSKA
Mm Snf2L (70-168) KASKSEKEM----D-PEYE-EKMVNMPLKADRAKRFEFLLKQTELFAHFIQPSAQKSPT-SP--LNM-KLARPRVKK--DDKQS-LISVGDYRHRRTEQEEDEELLSESRKT
Rn Snf2H (67-160) GKQKEIQEP----D-PTYE-EK-----MQTDRANRFEYLLKQTELFAHFIQPAAQKTPT-SP--LKM-KPGRPRVKK--DEKQN-LLSVGDYRHRRTEQEEDEELLTESSKA
Rn Snf2L (70-168) KTSKSEKEM----D-PEYE-EKMVNIPLKADRAKRFEFLLKQTELFAHFIQPSAQKSPT-SP--LNM-KLARPRVKK--DDKQS-LISVGDYRHRRTEQEEDEELLSESRKT
Ag ISWI (23-110) SDTTSSNTK----E-PDYD-AT-----LETDRGKRFEFLLKQTEIFAHFMNSAPSKSS---P--PKA-PRGR---KP--K-VDK-NADSSDHRHRKTEQEEDEELLAETNQK
Sc Isw1p (86-176) NKKRYL-----LKD-ANG-KKF-----DLEGTTKRFEHLLSLSGLFKHFIESKAAKDPK-FRQVLDV-LE-E--NK---ANGKG-KGKHQDVRRRKTEHEEDAELLKEEDSD
Sc Isw2p (66-161) RKKKFVLD----VD-PKYAKQK-----DKSDTYKRFKYLLGVTDLFRHFIGIKAKHDKN-IQKLLKQ-LD-SDANKL--SKSHS-TVSSSSRHHRKTEKEEDAELMADEEEE
Kl Isw1p (24-119) KKERYLLP---LRDLASGKRKF-----DEQGTVKRFEHLLGLSTLFRHFIERKAAKDPR-FREVLDT-ID-NVNGK---ANGKG--KKHTDARRRKTEKEEDAELMKDEEEE
Kl Isw2p (18-116) RRSKFLLD----VD-PKIAKQR-----NKEDTYIRFKHLLQITDLFRHFIGIRAKYDKN-MQKLLKT-IDAENKVAGTLKEPAG-HLARAPRHYRKTEQEEDAELMEDEEVE
Mo MGG_01012 (71-168) QLRRSIFG---RKH-DRLG-ES-----KEDDTLRRFRYLLGLTDLFRHFIETNPD--PN-IRNIMEK-IDAQNQEATKGKKGASRQGGASSGRVRRTEAEEDAELLKDEKHG
Nc Isw1 (68-165) QLRRSIFG---KKH-DRLG-ES-----KEDDSLRRFRYLLGLTDLFRHFIETNPN--PK-VREIMAE-IDRQNAEDAKSKKGAGRQGGATSDRRRRTEAEEDAELLKDEKVG
Ag Isw2p (15-110) RKKRFILD----VD-AKVAKER-----DKDDTYLRFRHLLGLTDLFRHFIGLRAKRDKN-MQRLLRM-LDGEERGRS--SRGQR-QK-DSSRHFRKTEKEEDAELMQDEEQH
Ag Isw1p (26-113) TRARYLVG------GGQNRRRF-----DTEGTTKRFQHLLGLSPLFRHFIERKAAKDER-FGQVLRV--------L---DDGRQ-AGRHEDKRRRKTEREEDAELLREEDAE
At CHR11 (90-169) LKKQKIQEMLESQN-ASID-AD-----MNNKGKGRLKYLLQQTELFAHFAKSDGSSS-------------------------QKK-AKGRGRHASKITEEEEDEEYLKEEEDG
At CHR17 (95-174) MKKQKIQQILDSQN-ASID-AD-----MNNKGKGRIKYLLQQTELFAHFAKSDPSPS-------------------------QKK-GKGRGRHSSKLTEEEEDEECLKEEEGG
Os 01g0367900 (133-211) LKKQKIQEILDTQN-AAVD-AD-----MNNKGKGRLKYLLQQTEIFAHFAKGNQSK--------------------------EKK-PRGRGRHASKMTEEEEDEEYLKEEEDA
Os 05g0150300 (187-265) LKKHKIQEILDAQN-KAID-AD-----MNNKGKGRLKYLLQQTEIFAHFAKGNQST--------------------------EKK-SRGRGRHASKMTEEEEDEEYLKEEEDA

Supplementary Figure 3: Alignment of the N-terminal region of ISWI homologs from various organisms. Two highly conserved motifs exist: an acidic motif and the ppHSA motif, named so because it shares homology with the region after the post-HSA domain found in other family of remodelers (data not shown)[1]. The alignment is cut off at the C-terminal side before 'motif Q' of Snf2-type ATPases begins[3]. An AT hook ('GRP') has been previously described[4], but it is comparatively poorly conserved. The arrowhead points to the first amino acid included in $\text{ISWI}_{26–648}$. Arrows indicate tryptic cleavage sites obtained specifically in the DNA-bound conformation (**Fig. 3a**). *Dm: Drosophila melanogaster, Hs: Homo sapiens, Ce: Caenorhabditis elegans, Xl: Xenopus laevis, Dr: Danio rerio, Gg: Gallus gallus, Cf: Canis familiaris, Mm: Mus musculus, Rn: Rattus norvegicus, Ag: Anopheles gambiae, Sc: Saccharomyces cerevisiae, Kl: Kluyveromyces lactis, Mo: Magnaporthe oryzae, Nc: Neurospora crassa, Ag: Ashbya gossypii, At: Arabidopsis thaliana, Os: Oryza sativa.* Amino acid numbers are given in parenthesis. The color intensity is indicative of the level of conservation. The alignment was performed with T-Coffee (www.ebi.ac.uk/Tools/msa/tcoffee/), and the figure was prepared with Jalview 2.7 (www.jalview.org/).

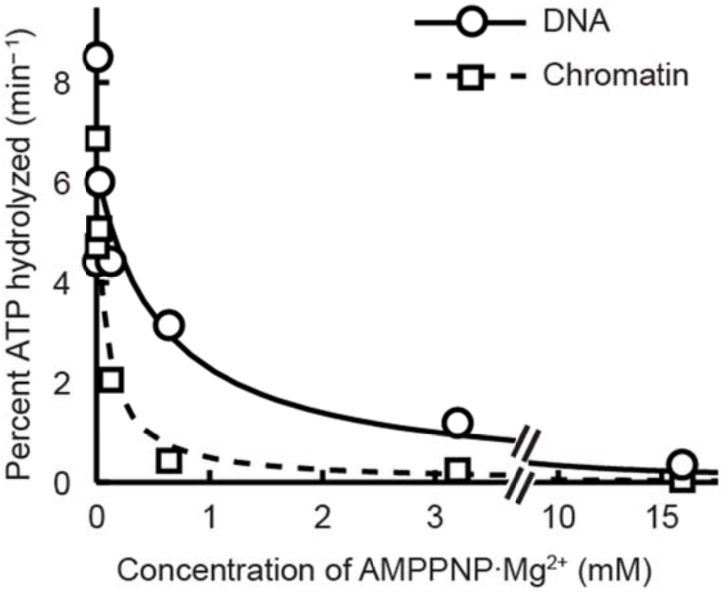

Supplementary Figure 4: The nucleotide affinity increased six-fold if ISWI was bound to chromatin instead of DNA. The affinity of the non-hydrolyzable ATP analog AMPPNP was measured in a competition experiment using ATP hydrolysis as readout. Saturating concentrations of 39-bp duplex DNA (20 µM) or chromatinized plasmid DNA (0.08 mg/mL) were incubated with ISWI_{FL} (80 nM or 10 nM, respectively) and varying concentrations of AMPPNP. The reaction was initiated with 1 µM ATP. The data were fit to a binding isotherm and yielded K_i values of 570 µM (solid line) and 90 µM (dashed line). The affinity for ADP was similarly increased (data not shown). The ~six-fold effect on the K_i was larger than the ~two-fold effect on $K_{\text{M,obs}}$ (**Suppl. Table 1**). This discrepancy indicated that the $K_{\text{M,obs}}$ values did not directly reflect the affinity for ATP.

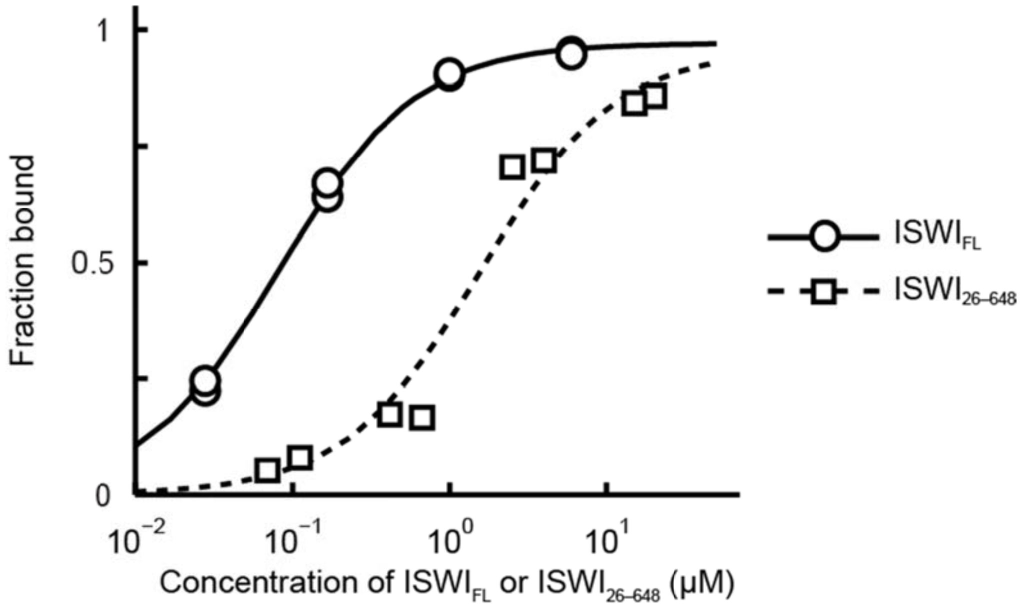

Supplementary Figure 5: Deletion of the HSS domain led to a decreased DNA affinity but did not abolish DNA binding. Binding of trace amounts of duplex DNA to ISWI$_{FL}$ or ISWI$_{26-648}$ was followed in a double-filter DNA binding assay[5]. Lines are fits of the data to a simple binding isotherm yielding K_D = 0.08 μM (solid line) and K_D = 1.6 μM (dashed line).

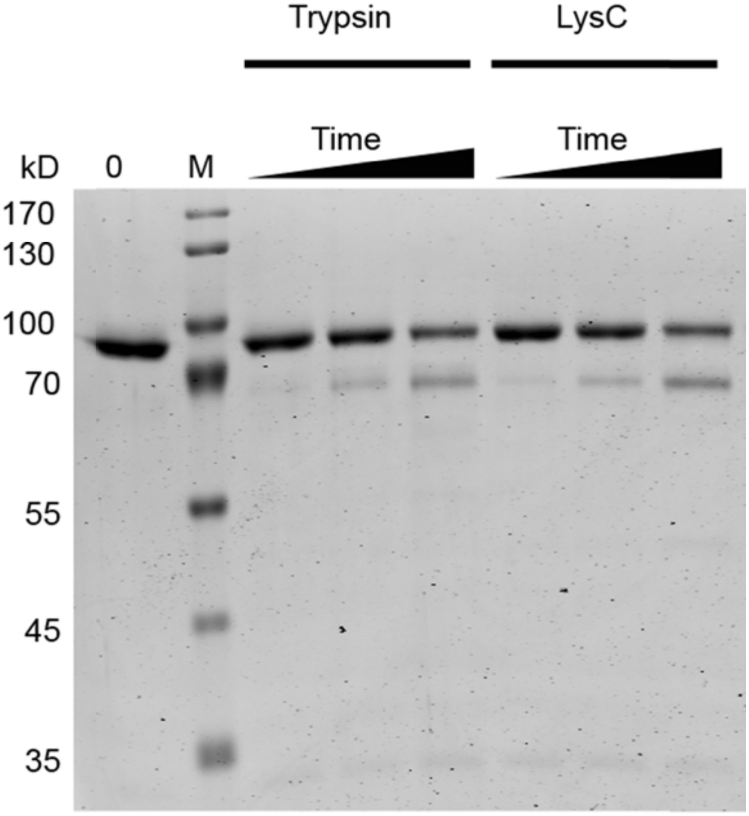

Supplementary Figure 6: Trypsin and LysC cleaved the same residues in DNA-free ISWI$_{26–648}$. Proteolytic fragments of ISWI$_{26–648}$ generated by trypsin and LysC (20 nM and 17 nM, respectively) after 5, 15 and 60 min were separated by SDS-PAGE and stained with Coomassie Blue. The identical mobility of the predominant cleavage products suggested that trypsin cleaved DNA-free ISWI$_{26–648}$ next to a lysine, not an arginine residue. 0: Undigested sample. M: Molecular weight marker.

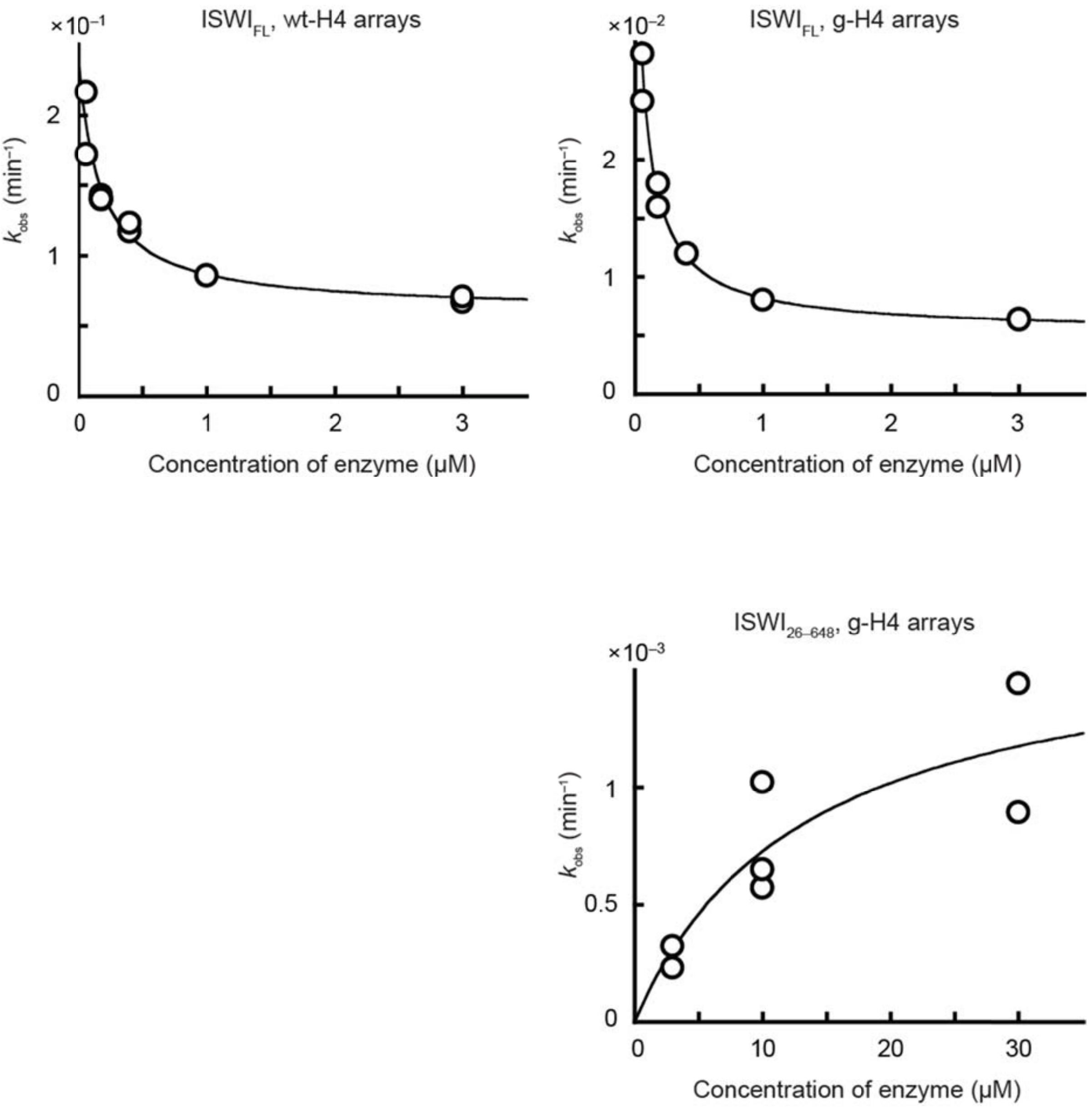

Supplementary Figure 7: Determination of the maximal remodeling velocities of ISWI$_{FL}$ and ISWI$_{26-648}$ on wt-H4 and g-H4 arrays. As described by others, the remodeling activities *decreased* with increasing enzyme concentration for ISWI$_{FL}$ (http://www.epigenesys.eu/; Protocol PROT24). To obtain the maximal remodeling velocities ($k_{obs,max}$) for ISWI$_{FL}$, we corrected for this decrease by fitting the data to inverse binding isotherms (see Methods), extrapolating back to (low) enzyme concentrations where this effect was not present. $k_{obs,max}$ for ISWI$_{26-648}$ remodeling of g-H4 arrays was determined as before (**Fig. 6d**). Data points within each graph were from multiple independent experiments.

Supplementary References

1. Szerlong, H. et al. The HSA domain binds nuclear actin-related proteins to regulate chromatin-remodeling ATPases. *Nat Struct Mol Biol* **15**, 469-76 (2008).
2. Racki, L.R. et al. The chromatin remodeller ACF acts as a dimeric motor to space nucleosomes. *Nature* **462**, 1016-21 (2009).
3. Flaus, A., Martin, D.M., Barton, G.J. & Owen-Hughes, T. Identification of multiple distinct Snf2 subfamilies with conserved structural motifs. *Nucleic Acids Res* **34**, 2887-905 (2006).
4. Aravind, L. & Landsman, D. AT-hook motifs identified in a wide variety of DNA-binding proteins. *Nucleic Acids Res* **26**, 4413-21 (1998).
5. Wong, I. & Lohman, T.M. A double-filter method for nitrocellulose-filter binding: application to protein-nucleic acid interactions. *Proc Natl Acad Sci U S A* **90**, 5428-32 (1993).

2.2 Nucleosome sliding mechanisms: new twists in a looped history

Felix Mueller-Planitz, Henrike Klinker and Peter B. Becker

Adolf Butenandt Institute and Center for Integrated Protein Science Munich,
Ludwig-Maximilians-Universität, Munich, Germany

Published in *Nature Structural and Molecular Biology,* 20, 1026-1032 (2013);
doi: 10.1038/nsmb.2648

Important note: As the published version of the review cannot be included into this thesis for copyright reasons, the final, accepted version of the article as submitted to *Nature Structural and Molecular Biology* is presented in the following instead. The published review can be downloaded from http://www.nature.com/nsmb/journal/v20/n9/full/nsmb.2648.html.

Declaration of contributions to "Nucleosome sliding mechanisms: new twists in a looped history"

This review was conceived and developed by F. Mueller-Planitz, P.B. Becker and me. I designed and prepared Figures 1, 3, 4, and 5 and all figure legends. I assisted in finalizing the text, edited and helped revising the manuscript. In addition, I wrote drafts for the short summaries of the key references.

Abstract

Nucleosomes, the basic organizational units of chromatin, package and regulate eukaryotic genomes. ATP-dependent nucleosome remodeling factors endow chromatin with structural flexibility by promoting assembly or disruption of nucleosomes and the exchange of histone variants. Furthermore most remodeling factors induce nucleosome movements, through sliding of histone octamers on DNA. We summarize recent progress towards unraveling the basic nucleosome sliding mechanism and the interplay of the remodelers' DNA translocase with accessory domains. Such domains optimize and regulate the basic sliding reaction and exploit sliding to achieve diverse structural effects, such as positioning or eviction of nucleosomes, or their regular spacing in chromatin.

Introduction

The packaging of eukaryotic genomes as chromatin evolved by accommodating the conflicting demands of storing, organizing and protecting the genetic information and at the same time making sure that it could be accessed as needed. The organization of DNA in complex with histones in the form of nucleosomes provided a successful solution to the problem. Nucleosomes are found in all eukaryotes and histones are among the most highly conserved proteins. A nucleosome organizes about 146 bp of DNA, which winds in approximately 1.7 turns around a histone octamer consisting of two of each of the histones H2A, H2B, H3 and H4 (ref. 1). Although DNA is a relatively stiff molecule, it tightly bends around the octamer thanks to a multitude of interactions between DNA and histones[2].

Nucleosomes are remarkably stable at physiological temperatures and block access to the underlying DNA. Nature solved this conundrum by evolving nucleosome remodeling ATPases that can mobilize nucleosomes, such that previously nucleosomal DNA now becomes accessible.

Comparison of the amino acid sequences of the ATPase domains of nucleosome remodeling enzymes reveals their evolutionary relationship to DNA/RNA helicases (Fig. 1). Within the SF2 superfamily of helicase-like enzymes, remodeling enzymes form the Snf2 family, which can be further subdivided into 24 subfamilies[3]. Typically, nucleosome remodeling ATPases form a variety of complexes (referred to as nucleosome remodeling factors) with several other proteins. The ubiquitous presence of nucleosome remodeling factors suggests that chromatin is a dynamic entity, characterized by constant changes in the position or composition of nucleosomes.

Remodeling factors catalyze seemingly disparate reactions. Some partially or completely disassemble nucleosomes. Others assemble them *de novo*, or exchange histones for histone variants. Most remodeling factors can move nucleosomes along DNA in a process termed nucleosome sliding[4].

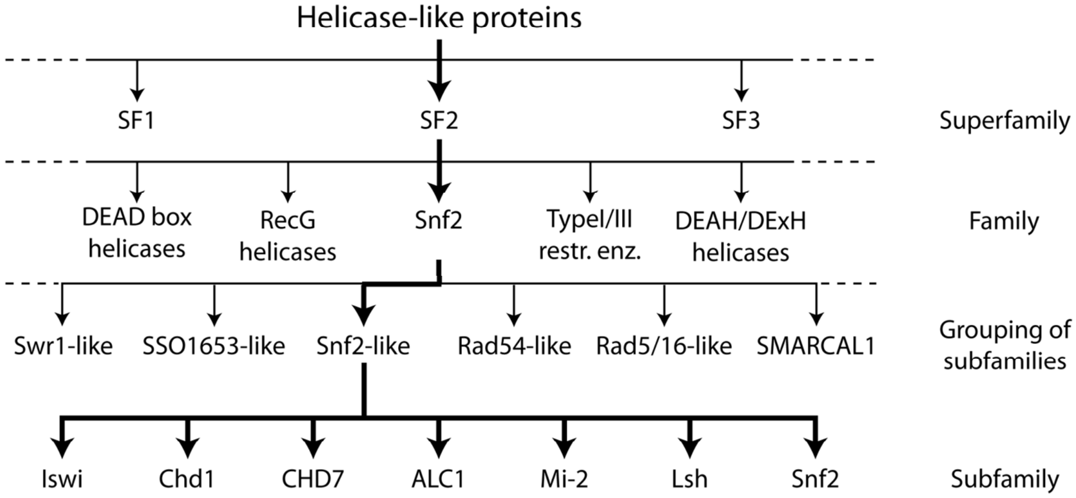
Helicase-like proteins
SF1
SF2
SF3
Superfamily
DEAD box helicases
RecG helicases
Snf2
TypeI/III restr. enz.
DEAH/DExH helicases
Family
Swr1-like
SSO1653-like
Snf2-like
Rad54-like
Rad5/16-like
SMARCAL1
Grouping of subfamilies
Iswi
Chd1
CHD7
ALC1
Mi-2
Lsh
Snf2
Subfamily

Figure 1: Schematic family tree illustrating the classification of nucleosome remodeling ATPases of the Snf2 family according to their relatedness at the sequence level. The hierarchical path from the superfamily of helicases to the subfamilies of remodelers discussed in this review is highlighted in bold. Adapted from reference 3.

Analysis of the sliding activity of remodelers *in vitro* revealed qualitative and quantitative differences. SWI/SNF and related remodelers, for instance, can push the histone octamer beyond one end of a short piece of DNA, transfer histone octamers or create unusual dinucleosomal species *in vitro*, properties that for example ISWI remodelers normally lack[5-8]. Although the outcome of remodeling by different factors can be diverse, the underlying mechanism often seems to be rooted in the sliding activity[9,10]. We will therefore focus on latest progress to unravel the mechanism and physiological outcomes of nucleosome sliding.

Physiological outcomes of nucleosome sliding

Mobilization of nucleosomes allows optimizing positions with respect to their neighbors (Fig. 2a). Removal of some remodeling factors in yeast leads to suboptimal packaging of the chromatin fiber and the spurious transcription of non-coding, often antisense RNA[11-15]. Optimal nucleosome density and appropriate spacing of nucleosomes also assures the integrity of the newly synthesized chromatin fiber in the wake of replication.

The chromatin fiber is occasionally punctuated by nucleosome-depleted regions (NDRs) due to the presence of stiff DNA sequences that resist the bending over the histone octamer surface, or due to bound proteins at regulatory elements, such as active promoters[16]. Nucleosome arrays are often positioned ‘in register’ with respect to the NDR (Fig. 2b). This kind of nucleosome phasing depends on the action of nucleosome remodeling factors and in all likelihood their capability to slide nucleosomes[17-20].

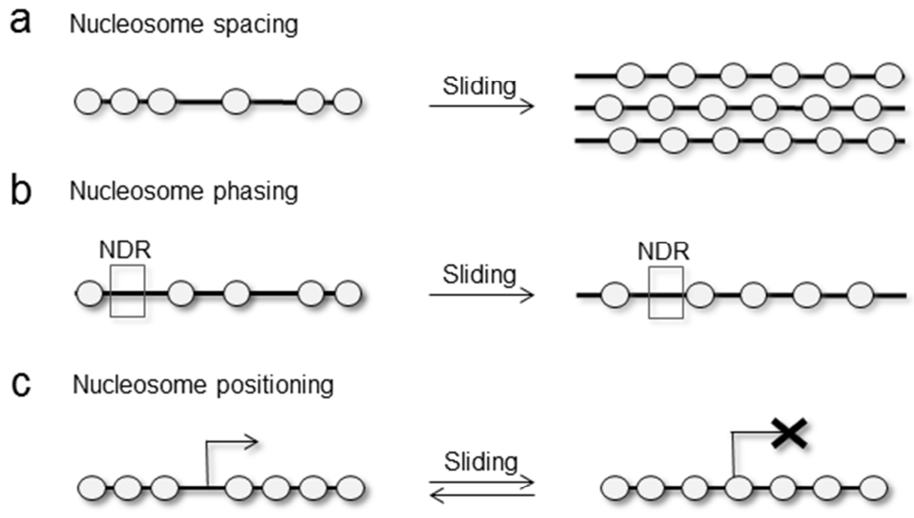

Figure 2: The different physiological outcomes of nucleosome sliding. (**a**) Nucleosome remodeling enzymes can introduce and maintain a regular spacing of nucleosomes. (**b**) The phasing of nucleosomal arrays with respect to a nucleosome-depleted region (NDR), a prominent feature of promoters, depends on nucleosome remodeling enzymes. (**c**) Nucleosome sliding activity regulates the accessibility of DNA sequences by positioning individual nucleosomes.

Besides these global effects of nucleosome sliding, there are also examples where the targeted repositioning of individual nucleosomes by dedicated remodelers renders regulatory sequences accessible or, conversely, occludes them (Fig. 2c)[21]. For example, the yeast remodeling complex RSC is widely involved in keeping promoters nucleosome-free[17,22]. By contrast, the yeast Isw2 complex shifts nucleosomes on promoter sequences to hinder transcription initiation[23-25].

Mechanistic concepts in nucleosome sliding

During nucleosome sliding, the histone octamer moves along DNA without dissociating from it. To achieve this, numerous contacts between DNA and histones must be broken and reformed in a highly coordinated manner making the catalytic process of sliding a formidable challenge. How can remodeling enzymes facilitate this process? Nucleosome remodeling enzymes are able to bind the DNA and histone moiety of a nucleosome. Once these contacts are established, a remodeling enzyme could conceivably cycle through a succession of conformational changes that are triggered by the binding of ATP, hydrolysis and dissociation of the hydrolysis products, thereby disrupting DNA-histone contacts. Some early models assumed that such action might detach DNA at the nucleosomal entry site from the histone surface and replace it by linker DNA, effectively 'looping out' a segment of DNA on the nucleosome (Fig. 3a). Such a DNA loop could be propagated around the histone octamer with little additional energy expenditure. Once it emerges on the other side, the nucleosome

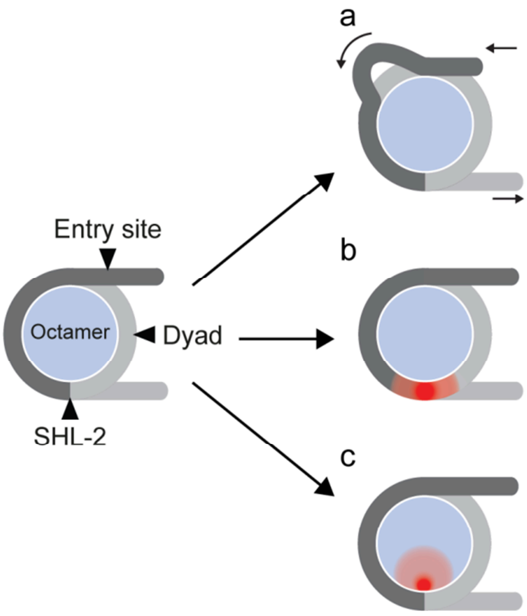

Figure 3: Nucleosome sliding mechanisms. (**a**) In the loop propagation model the action of the remodeling enzyme leads to the local detachment of DNA from the octamer surface at the entry site. This allows the formation of contacts between the octamer and the flanking DNA leading to the formation of a DNA loop. The loop propagates around the octamer resulting in the repositioning of the nucleosome. (**b**) The translocation activity of the nucleosome remodeling enzyme at SHL-2 leads to local DNA distortions that can propagate around the nucleosome. (**c**) Perturbations of the DNA-histone contacts introduced by the action of the nucleosome remodeling enzyme cause structural changes within the octamer that may result in its reorientation. Dark grey: DNA flanking the entry site and nucleosomal DNA between entry site and SHL-2. Light grey: DNA between SHL-2 and the DNA exit site, including the flanking DNA. Red: Perturbation introduced by the nucleosome remodeling enzyme. The arrows indicate movement of DNA relative to the histone octamer.

has moved. A number of early observations were used to support this model, though direct evidence for the presence of a loop and its functional relevance was lacking[26-36].

A critical step forward in our understanding of the sliding mechanism were observations made in several labs demonstrating that nucleosome remodeling ATPases are able to translocate on DNA like helicases. Indeed, they track along one strand of the DNA double helix in a 3’ to 5’ direction[35,37,38]. Unlike bona fide helicases, however, remodeling factors do not separate the DNA strands during translocation. Remarkably, remodeling ATPases do not start to translocate from the DNA that flanks the nucleosome, thereby peeling off nucleosomal DNA from the edge. Instead, their binding site appears to be well within the nucleosome, two helical turns off the dyad axis at superhelical position -2 (SHL-2)[38-42].

Rather than picturing an enzyme that moves on DNA like a train on railroad tracks, we imagine that the remodeler is anchored on the nucleosome and ratchets DNA over the histone surface. This will inevitably lead to local DNA distortions[43] and thus disruption of important histone-DNA interactions (Fig. 3b). Structural studies suggest that nucleosomes may locally accommodate a variable number of base pairs[44,45]. Such a twist defect could be propagated from one DNA segment to the next until it escapes the nucleosome.

In addition, structural changes of the histones may contribute to dissipating the strain that is imposed by the remodeler onto the nucleosome (Fig. 3c). For example, we expect that side chains that are directly involved in histone DNA interactions reorient, but detailed structural information is missing. Conceivably, the octamer could also undergo more substantial structural changes during remodeling. Indeed, the nucleosome has considerable structural plasticity at its disposal, which may play an important role during remodeling[46]. The general models for nucleosome sliding discussed above should not be considered mutually exclusive as DNA loop formation, twist changes and conformational rearrangements of the octamer may all accompany remodeling.

Mechanistic studies of remodeling ATPases are complicated by the fact that these highly specialized enzymes integrate several functions. The basic sliding reaction is enhanced and tuned by accessory domains and subunits, which assure substrate specificity and affinity and optimize kinetic parameters. Other modules may serve to regulate the remodeling activity and to harness the sliding of target nucleosomes in the context of physiological tasks, such as restoring the integrity of the chromatin fiber by regular spacing of nucleosomes. Below we review recent progress in dissecting the remodeling reaction into basic mechanism, enhancement, regulation and physiological outcome. Most insight has been derived from studying just a handful of enzymes within the Snf2-like grouping of subfamilies, in particular ISWI- and CHD-type enzymes. Nevertheless, some general concepts have emerged.

The Snf2 ATPase domain: an autonomous remodeling engine

Given the structural complexity of remodeling ATPases, what are the minimal requirements to catalyze nucleosome sliding? We and others found by studying the ISWI remodeling enzyme from *Drosophila melanogaster* that all fundamental aspects of nucleosome remodeling are contained within the central, compact ATPase module[47,48]. This domain can independently hydrolyze ATP, and its ATPase activity can be stimulated by DNA- and nucleosomes to the same extent as the full-length enzyme. Furthermore, it can recognize the flexible N-terminal domain of histone H4[47], a well-documented feature of ISWI enzymes[49]. Notably, it can autonomously reposition nucleosomes. The conclusion that the ATPase domain alone can carry out the basic mechanism of nucleosome sliding is consistent with reports on CHD enzymes[50-52] . The observation that an isolated ATPase module contained everything needed for nucleosome remodeling was surprising, as earlier studies had suggested that an accessory DNA binding domain was crucially required[53-55].

How does the basic remodeling mechanism work? The ATPase domains of all studied nucleosome remodelers interact with the nucleosome at SHL-2, although reportedly with

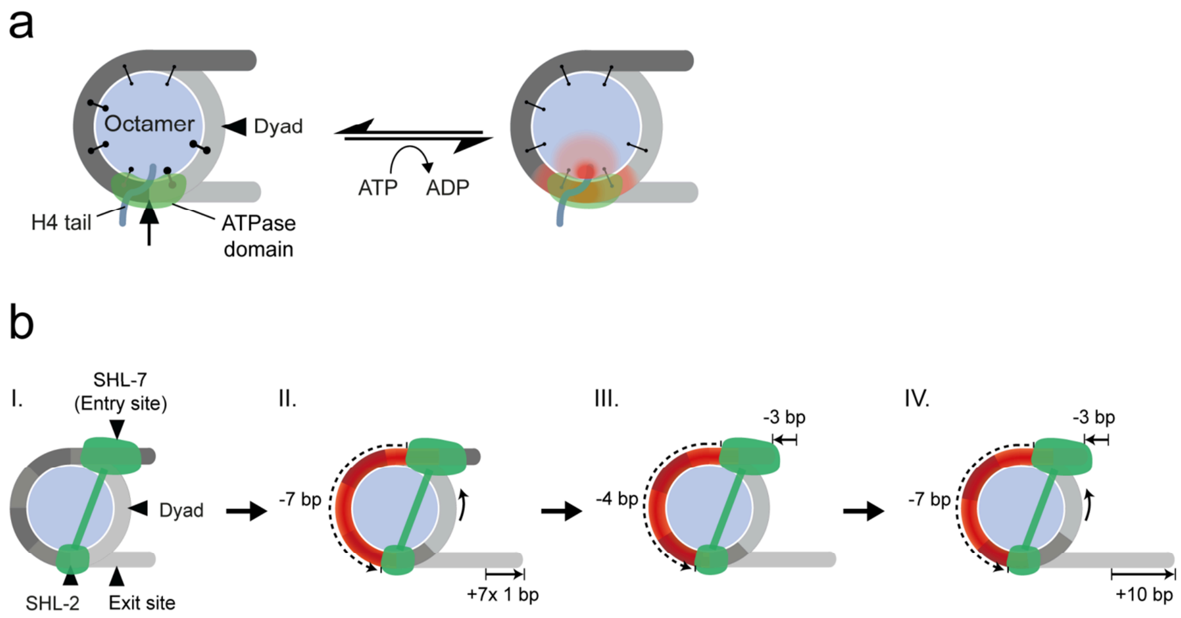

Figure 4: Recent insights into nucleosome sliding by remodeling factors of the ISWI subfamily. (**a**) Suggested mechanism of sliding by the ISWI ATPase module. An ISWI deletion mutant that comprises just the enzyme`s ATPase domain can productively engage the nucleosome at SHL-2 where it recognizes the H4 tail. Its translocase activity perturbs DNA-histone contacts in an ATP-hydrolysis dependent manner leading to nucleosome sliding. Weakening of key contacts in the proximity of SHL-2 may suffice to introduce profound structural changes in the nucleosome and allow a rearrangement of the octamer (adapted from ref. 47). SHL-2 is marked by an arrow. DNA-histone contacts and their varying strengths[57] are indicated by clamps. (**b**) Model for nucleosome sliding by remodeling factors of the ISWI subfamily according to Deindl et al. (2013). The remodeler interacts with the nucleosome at SHL-2 and at the entry site reaching out onto flanking DNA as indicated in green (I.). The translocase activity at SHL-2 leads to the consecutive exit of seven base pairs, creating a strain in the nucleosomal DNA between the remodeler contact sites (indicated in red) (II.). The strain is partly released by three base pairs entering the nucleosome at the entry site (III.), but re-established by the subsequent exit of three base pairs at the exit site (IV.).

notable differences[56]. This strategic site is marked by the emergence of the H4 tail and is adjacent to the strongest histone-DNA interactions on the nucleosome at the dyad[29,57]. The structural changes imposed by an ATPase domain that attempts to translocate DNA relative to the octamer towards the dyad may have profound energetic consequences. If the strongest histone-DNA contacts were weakened, the nucleosome could be destabilized enough so that histones spontaneously rearrange (Fig. 4a)[29,47]. Consistent with the model, the crystallographic structures reveal that nucleosomes can accommodate structural variability at SHL-2 (ref. 45). Furthermore, the earliest structural changes detectable in the nucleosome during remodeling are located around the dyad, though the exact nature of the changes has yet to be resolved[58].

In conclusion, the nucleosome sliding activity of remodeling enzymes appears to have evolved directly from ancestral helicase-type motors. Targeting the nucleosome, helicase-like

DNA translocation and the ensuing destabilization of the nucleosome may have been all that was required for a rudimentary remodeling reaction.

Remodeling single base pairs at a time

A recent study provided unprecedented detail and resolution of nucleosome sliding catalyzed by yeast ISWI complexes[59]. Single molecule FRET experiments allowed monitoring the shifting of DNA relative to the histone octamer and yielded two remarkable results. The authors found that base pairs (bp) exit the nucleosome one by one (Fig. 4b). This observation suggested that the translocation activity of the ATPase domain pumps single base pairs at a time over the surface of the nucleosome just as its helicase relatives do[60], and that the ATPase pumps DNA not fast or vigorously enough to build up DNA loops downstream of the site of translocation. The propagation of DNA as single base pairs is in agreement with the ‘twist diffusion’ model (Fig. 3b). However, earlier studies showed that nicks or single stranded gaps in the DNA between the translocase and exit site do not abrogate remodeling[28,34,35,38-40]. Apparently, the strain has multiple ways to dissipate, e.g. via rearrangement of the histone core (Fig. 3c) or – at least for nicked substrates – possibly by bulging out DNA. Local changes in DNA twist may therefore be one consequence of remodeling rather than its driving force.

The other remarkable result was that the emergence of DNA at the ‘exit’ site is uncoupled from the entry of DNA at the other end. Notably, the ISWI complexes extrude 7 bp from the nucleosome before one can observe 3 bp of DNA entering the realm of the nucleosome from the ‘entry’ site. After these initial DNA distortions, 3 bp exit before another three enter, leaving the nucleosome with a chronic lack of several base pairs at any given time.

The initial seven base pairs must originate from the DNA in between the ‘entry’ site at superhelical location -7 (SHL-7) and the translocase site (SHL-2; Fig. 4b). Assuming that the histone octamer does not profoundly change its structure, the DNA in this region would have to drastically stretch and underwind. The nucleosome’s ability to accept twist defects in each DNA segment certainly assists this mechanism. Nevertheless, the sheer magnitude of the strain raises the question if other mechanisms participate. For example, the octamer structure itself could adapt or the DNA may take an altered path on the histone surface[61-63]. These structural perturbations could conceivably provide an explanation for changes detected by DNA footprinting assays in this region early during the reaction[64]. The sequential nature of remodeling[58,59] argues against models that postulate a “concerted” histone reorientation[29], and the chronically overstretched DNA provides strong evidence against DNA loops also upstream of the site of translocation, between SHL-7 and -2.

These data suggest that the ATPase domain of ISWI, in particular its translocase activity, is the major driving force for remodeling. Given the strong conservation of the ATPase domain

(Fig. 1), this conclusion may apply also to other subfamilies. Nevertheless, remodeling factors contain prominent auxiliary domains, some of which clearly optimize catalysis and fulfill specialized functions.

Room for improvement: tweaks to optimize catalysis

Enzymes of the ISWI- and CHD1-type share C-terminal DNA binding modules (DBDs) comprising SANT and SLIDE domains[53,65]. The DBD is able to bind to DNA at the nucleosomal entry site and in the adjacent linker[66,67]. Without this module, ISWI has poor affinity for the nucleosome and can only poorly distinguish nucleosomes from naked DNA. The evolution of a DBD simultaneously solved these issues by increasing affinity and specificity[47,53]. Presumably as a direct consequence of the enhanced affinity, processivity of remodeling is also increased by the domain[58].

Anchoring the remodeler to the nucleosome with modules such as the SANT-SLIDE module also increases the likelihood that the translocase domain productively engages the nucleosome at SHL-2 (ref. 47). Anchoring modules can thereby help to couple ATP hydrolysis to sliding, increasing the energy efficiency of remodeling[68,69]. They do not have to fulfill highly specialized functions, though. The SANT-SLIDE domain of Chd1, for instance, can be substituted by generic DBDs that recognize special consensus sequences in the linker DNA[52]. Even streptavidin-biotin linkages that tether the ATPase domain to the nucleosome suffice[10].

To what extent the ATPase domain actively coordinates with auxiliary domains to improve catalysis is unclear. For example, it has been suggested that the ATPase cycle triggers a power stroke between the DBD and ATPase domain of ISWI to pull in 3 bp of flanking DNA[58,59]. Alternatively, the flanking DNA may simply passively ratchet into the nucleosome as soon as the tension created by the DNA translocase becomes too large and the DBD loses its grip on the DNA, a mechanism that does not require a precisely timed power stroke between the DBD and ATPase domain. The plethora of auxiliary domains and subunits present in remodeling factors suggests the existence of numerous other routes to optimize catalysis.

Regulating the remodeling engine

The succession of steps throughout the catalytic cycle is tightly regulated in molecular machines. Every step triggers the next. The regulatory framework that allows the enzyme to proceed through catalysis in such a controlled manner must be exposed to understand the overall mechanism. Binding of nucleic acid substrate, for example, elicits a conformational change within the ATPase domain, which in turn activates ATP hydrolysis[47,70]. ISWI and

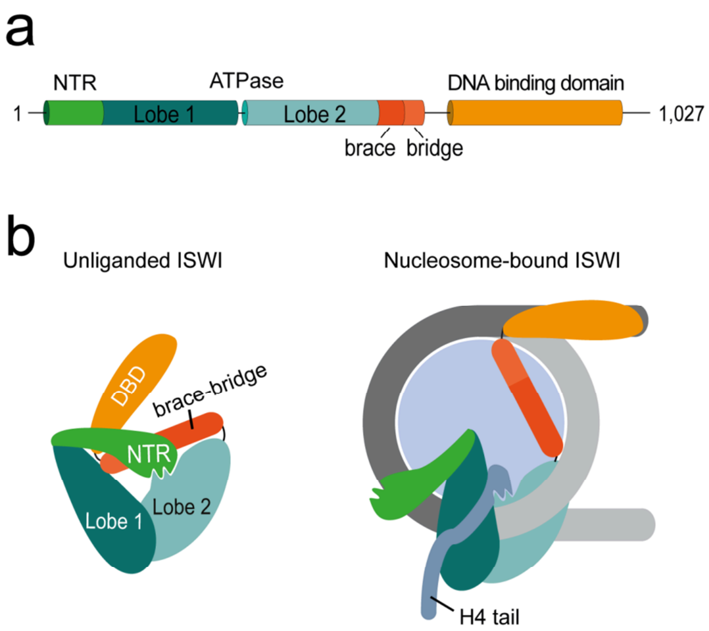

Figure 5: Model for the regulation of the activity of ISWI-type remodeling enzymes. (**a**) Schematic depiction of the ISWI domain structure. (**b**) Scheme of unliganded (left) and nucleosome-bound (right) ISWI according to current models. In the unliganded state, the NTR contacts the ATPase domain. This contact includes the AutoN motif, an H4-tail basic-patch mimic in the NTR, which interacts with a binding site in the ATPase domain. The brace-bridge region makes contacts with both ATPase lobes. These interactions stabilize the two lobes in a state incompatible with ATP hydrolysis. Binding of the ATPase domain to nucleosomal DNA and the H4 tail releases the NTR. The brace-bridge is released when the DBD engages flanking DNA. This allows the ATPase lobes to adopt a more compact conformation that is competent for ATP hydrolysis and proper coupling of ATP hydrolysis to nucleosome sliding.

CHD1 contain a number of regulatory structures at their N- and C-termini that mediate this and other structural transitions.

Among these regulatory structures are two peptide motifs immediately C-terminal to the ATPase domain of ISWI and CHD1, the ‘brace’ and ‘bridge’ (a.k.a. ‘NegC’; Fig. 5a). By contacting the two ATPase lobes, they are thought to restrict the conformational flexibility of the two lobes against each other and hold them splayed apart in a catalytically inactive conformation in the absence of nucleic acids[51,71]. Conformational changes in the brace upon DNA binding correlate with strong activation of ATP hydrolysis[47]. Consistent with a negative regulatory role, it was found that the deletion of the bridge activated nucleosome sliding[48]. Together these studies suggest that nucleic acid binding counteracts the auto-inhibition provided by these motifs and allows the two ATPase lobes to contact each other to form a catalytically competent state (Fig. 5b).

The N-termini (NTRs) of ISWI and CHD enzymes contain further regulatory structures (Fig. 5). Although the NTRs of ISWI and CHD1 are not related at the sequence level, recent observations suggest that they carry out similar duties. Both may be part of a sensor for the histone H4 tail of the nucleosome. They also have been implicated in ‘gating’ the binding site for DNA that resides in the ATPase domain. Just like the C-terminus, the N-terminus of ISWI and CHD1 therefore rearranges its conformation before the enzymes can properly dock onto the nucleosomes[48,51]. Intriguingly, Clapier and Cairns found that the N-terminus of ISWI contains a short peptide motif, 'AutoN', whose sequence resembles the 'basic patch' of histone H4, an important motif required by ISWI remodelers for optimal catalysis[72,73]. According to their recent model, the interaction of AutoN with the ATPase domain is inhibitory until the H4 epitope on the nucleosomal substrate successfully competes for ATPase interaction (Fig. 5b). Together, the N- and C-termini of ISWI and CHD1 remodelers provide specificity for the nucleosome and prevent ATP hydrolysis in the absence of a proper substrate. Their conformational changes are part of a regulatory network that ensures the timed and controlled succession of steps through the reaction cycle. It remains to be seen if similar networks are at work in other remodeling factors.

Auxiliary domains direct the outcome of nucleosome sliding

As discussed above, nucleosome sliding may have very different effects on chromatin. Although the ATPase domains of different remodelers differ from each other in fine detail and in ways that may affect catalytic parameters[56,74], the presence of auxiliary domains with very different features – and associated subunits contributing such domains – can have major impact on the final outcome of sliding[75-78]. In addition, the prevalent presence of domains that recognize ('read') histone modifications suggests that the substrate recognition may be sensitive to modifications[4,79].

An instructive example how auxiliary domains directly influence the outcome of a basic remodeling reaction is the SANT-SLIDE DBD of ISWI- and CHD-type remodelers. Replacement of the DBD of Chd1 with domains that recognize specific DNA sequences led to sliding of nucleosomes towards and onto the binding site[10,52], a feature that wild-type remodelers may indeed exploit to position nucleosomes. By the same logic, association of subunits that are able to recognize specific DNA elements will affect substrate selection and may contribute to positioning[80-83]. Interaction of the remodeler with a certain length of linker DNA may limit the extent and direction of nucleosome sliding and thus provide a way to adjust the length of the linker DNA between neighboring nucleosomes promoting their even spacing[41,54,67,84-87].

By binding to the DNA adjacent to the nucleosome, the SANT-SLIDE modules anchor the remodeler to the nucleosome[66]. The module however may not fit between two nucleosomes if the linker DNA is too short. Consequently, short spacing of nucleosomes could hinder interaction of CHD and ISWI remodelers with chromatin. This is apparently the case in the yeasts *S. cerevisiae* and *S. pombe*, which feature only 18 bp or 7 bp of average linker DNA length, respectively[88]. Only upon disruption of the nucleosome array through transcription, longer stretches of free DNA arise. The remodelers seize the opportunity to bind and then help reinstall the integrity of the fiber by nucleosome spacing[88]. A global state of chromatin disruption can be experimentally induced by depletion of nucleosomes *in vivo*. Under those critical conditions, the yeast Isw2 complex was found to be particularly involved in moving nucleosomes in what appeared to be an effort to optimize the packaging of the DNA[89].

By developing domains that interact with DNA flanking the nucleosome, ISWI and CHD remodelers also may have evolved a way to guard against damaging nucleosome collisions[10]. SWI/SNF–type remodelers on the other hand do not tightly interact with linker DNA. These remodelers are able to move histone octamers into the territory of the adjacent nucleosome, effectively ‘peeling off’ DNA of the nucleosome neighbor and releasing an H2A-H2B dimer[90]. The removal of H2A-H2B dimers in promoter nucleosomes may render transcription factor binding sites accessible and thus constitutes a step towards the activation of certain genes[91]. An extreme scenario poses that a remodeler may use a histone octamer as a wedge to unravel a neighboring nucleosome entirely[9,90,92,93]. Some cases of histone and nucleosome eviction can therefore be explained by extension of the nucleosome sliding mechanisms. The presence of accessory subunits or collaborating factors, like histone chaperones, will regulate the precise outcome of such reactions.

The possibilities to implement additional regulatory levels that profoundly affect the final outcome of remodeling are manifold. For example, ISWI dimerizes when it binds to nucleosomes. Dimerization improves catalysis and allows the sliding reaction to change directions in the middle of a processive run[94,95]. CHD1 on the other hand appears to slide nucleosomes as a monomer[96]. Association with additional, non-catalytic subunits can confer or increase processivity[59]. Since remodeling occurs on nucleosomal arrays, it is possible that some remodeling complexes may recognize features of neighboring nucleosomes and that their physiological substrates are dinucleosomes[67].

Concluding remarks

Nucleosome remodeling enzymes evolved from helicase-like ancestors by harnessing a basic DNA translocation reaction to disrupt histone-DNA interactions. This activity is inherent to the remodeler`s ATPase domains and is the basic mechanism underlying nucleosome remodeling. Accessory DNA and histone binding domains have been added to optimize nucleosome recognition and the processivity, directionality and efficiency of sliding. Some of these domains acquired regulatory roles as competitive or allosteric auto-inhibitors in the absence of the correct substrate. Sequence or length preferences for binding to linker DNA helped determine whether nucleosome sliding leads to positioning of individual nucleosomes, to regular spacing of nucleosome arrays or to eviction of histones or nucleosomes.

The sliding mechanism is likely to take full advantage of the structural flexibility built into nucleosomes. Remodeling intermediates in which the DNA is detached from the surface of the histones may accumulate under certain circumstances. Other intermediates may have altered DNA twist or octamer structure. We are looking forward to a comprehensive tracking of these nucleosome remodeling intermediates. Distinguishing structural intermediates that are indispensable for the remodeling process from those that arise purely as a consequence of remodeling remains a challenge and requires a combination of quantitative functional and structural assays.

Detailed quantitative dissections of the remodeling mechanisms are so far only available for select remodelers. The future will tell to what extent the mechanisms are shared. High-resolution single molecule measurements on a variety of remodeling complexes will be particularly revealing in this respect.

Short summaries of key references

(Patel et al., 2013):
Chd1 acquired SWI/SNF-like properties when its DBD was substituted for streptavidin and the remodeler was targeted to nucleosomes via a biotin tag on histones. This result suggested that binding of the remodeler to linker DNA constrains nucleosome mobility and alters the specificity of the reaction.

(Mueller-Planitz et al., 2013):
This quantitative study showed that the ATPase domain of ISWI is an autonomous, rudimentary nucleosome remodeling machine. It can recognize and remodel nucleosomes und its ATPase is properly regulated by the nucleosomal substrate.

(Hota et al., 2013):
This paper showed that interactions of Isw2 with extranucleosomal DNA promote nucleosome mobilization. The authors resolved several unconcerted structural changes within the nucleosome well before the nucleosome was shifted to a new DNA location.

(Deindl et al., 2013):
Single molecule FRET experiments revealed the succession of events during nucleosome sliding by ISWI remodelers in unprecedented detail: the remodelers extruded several bp of DNA in single bp increments from the nucleosome before adjacent DNA entered from the opposite end.

(Clapier and Cairns, 2012):
This study identified two auto-inhibitory modules in the N- and C-terminus of ISWI that regulate the enzyme. These inhibitory structures are released when the remodeler interacts with the histone H4 tail and extranucleosomal DNA.

(Hauk et al., 2010):

This work presented the crystal structure of Chd1 comprising its NTR and ATPase domain and provided evidence that the NTR regulates the enzyme`s ATPase activity by occluding its binding site for nucleic acids.

(McKnight et al., 2011):

Sequence-specific DBDs of unrelated proteins could substitute for the DBD of Chd1 suggesting that the DBD and ATPase domains can function as independent modules. Notably, the chimeric remodeler now shifted nucleosomes towards and onto the corresponding DNA consensus site.

References:

1. Luger, K., Mader, A.W., Richmond, R.K., Sargent, D.F. & Richmond, T.J. Crystal structure of the nucleosome core particle at 2.8 A resolution. *Nature* 389, 251-60 (1997).
2. Davey, C.A., Sargent, D.F., Luger, K., Maeder, A.W. & Richmond, T.J. Solvent mediated interactions in the structure of the nucleosome core particle at 1.9 a resolution. *J Mol Biol* 319, 1097-113 (2002).
3. Flaus, A., Martin, D.M., Barton, G.J. & Owen-Hughes, T. Identification of multiple distinct Snf2 subfamilies with conserved structural motifs. *Nucleic Acids Res* 34, 2887-905 (2006).
4. Clapier, C.R. & Cairns, B.R. The biology of chromatin remodeling complexes. *Annu Rev Biochem* 78, 273-304 (2009).
5. Lorch, Y., Zhang, M. & Kornberg, R.D. Histone octamer transfer by a chromatin-remodeling complex. *Cell* 96, 389-92 (1999).
6. Bouazoune, K., Miranda, T.B., Jones, P.A. & Kingston, R.E. Analysis of individual remodeled nucleosomes reveals decreased histone-DNA contacts created by hSWI/SNF. *Nucleic Acids Res* 37, 5279-94 (2009).
7. Ulyanova, N.P. & Schnitzler, G.R. Human SWI/SNF generates abundant, structurally altered dinucleosomes on polynucleosomal templates. *Mol Cell Biol* 25, 11156-70 (2005).
8. Bruno, M. et al. Histone H2A/H2B dimer exchange by ATP-dependent chromatin remodeling activities. *Mol Cell* 12, 1599-606 (2003).
9. Boeger, H., Griesenbeck, J. & Kornberg, R.D. Nucleosome retention and the stochastic nature of promoter chromatin remodeling for transcription. *Cell* 133, 716-26 (2008).
10. Patel, A. et al. Decoupling nucleosome recognition from DNA binding dramatically alters the properties of the Chd1 chromatin remodeler. *Nucleic Acids Res* 41, 1637-48 (2013).
11. Hennig, B.P., Bendrin, K., Zhou, Y. & Fischer, T. Chd1 chromatin remodelers maintain nucleosome organization and repress cryptic transcription. *EMBO Rep* (2012).
12. Yadon, A.N. et al. Chromatin remodeling around nucleosome-free regions leads to repression of noncoding RNA transcription. *Mol Cell Biol* 30, 5110-22 (2010).
13. Shim, Y.S. et al. Hrp3 controls nucleosome positioning to suppress non-coding transcription in eu- and heterochromatin. *EMBO J* 31, 4375-87 (2012).
14. Tirosh, I., Sigal, N. & Barkai, N. Widespread remodeling of mid-coding sequence nucleosomes by Isw1. *Genome Biol* 11, R49 (2010).

15. Cheung, V. et al. Chromatin- and transcription-related factors repress transcription from within coding regions throughout the Saccharomyces cerevisiae genome. *PLoS Biol* 6, e277 (2008).
16. Struhl, K. & Segal, E. Determinants of nucleosome positioning. *Nat Struct Mol Biol* 20, 267-73 (2013).
17. Wippo, C.J. et al. The RSC chromatin remodelling enzyme has a unique role in directing the accurate positioning of nucleosomes. *EMBO J* 30, 1277-88 (2011).
18. Zhang, Z. et al. A packing mechanism for nucleosome organization reconstituted across a eukaryotic genome. *Science* 332, 977-80 (2011).
19. Gkikopoulos, T. et al. A role for Snf2-related nucleosome-spacing enzymes in genome-wide nucleosome organization. *Science* 333, 1758-60 (2011).
20. Pointner, J. et al. CHD1 remodelers regulate nucleosome spacing in vitro and align nucleosomal arrays over gene coding regions in S. pombe. *EMBO J* (2012).
21. Korber, P. & Becker, P.B. Nucleosome dynamics and epigenetic stability. *Essays Biochem* 48, 63-74 (2010).
22. Badis, G. et al. A library of yeast transcription factor motifs reveals a widespread function for Rsc3 in targeting nucleosome exclusion at promoters. *Mol Cell* 32, 878-87 (2008).
23. Fazzio, T.G. & Tsukiyama, T. Chromatin remodeling in vivo: evidence for a nucleosome sliding mechanism. *Mol Cell* 12, 1333-40 (2003).
24. Whitehouse, I. & Tsukiyama, T. Antagonistic forces that position nucleosomes in vivo. *Nat Struct Mol Biol* 13, 633-40 (2006).
25. Whitehouse, I., Rando, O.J., Delrow, J. & Tsukiyama, T. Chromatin remodelling at promoters suppresses antisense transcription. *Nature* 450, 1031-5 (2007).
26. Liu, N., Peterson, C.L. & Hayes, J.J. SWI/SNF- and RSC-catalyzed nucleosome mobilization requires internal DNA loop translocation within nucleosomes. *Mol Cell Biol* 31, 4165-75 (2011).
27. Strohner, R. et al. A 'loop recapture' mechanism for ACF-dependent nucleosome remodeling. *Nat Struct Mol Biol* 12, 683-90 (2005).
28. Langst, G. & Becker, P.B. ISWI induces nucleosome sliding on nicked DNA. *Mol Cell* 8, 1085-92 (2001).
29. Bowman, G.D. Mechanisms of ATP-dependent nucleosome sliding. *Curr Opin Struct Biol* 20, 73-81 (2010).
30. Zhang, Y. et al. DNA translocation and loop formation mechanism of chromatin remodeling by SWI/SNF and RSC. *Mol Cell* 24, 559-68 (2006).
31. Lia, G. et al. Direct observation of DNA distortion by the RSC complex. *Mol Cell* 21, 417-25 (2006).
32. Aoyagi, S. & Hayes, J.J. hSWI/SNF-catalyzed nucleosome sliding does not occur solely via a twist-diffusion mechanism. *Mol Cell Biol* 22, 7484-90 (2002).
33. Aoyagi, S., Wade, P.A. & Hayes, J.J. Nucleosome sliding induced by the xMi-2 complex does not occur exclusively via a simple twist-diffusion mechanism. *J Biol Chem* 278, 30562-8 (2003).
34. Lorch, Y., Davis, B. & Kornberg, R.D. Chromatin remodeling by DNA bending, not twisting. *Proc Natl Acad Sci U S A* 102, 1329-32 (2005).
35. Saha, A., Wittmeyer, J. & Cairns, B.R. Chromatin remodeling by RSC involves ATP-dependent DNA translocation. *Genes Dev* 16, 2120-34 (2002).
36. Fan, H.Y., He, X., Kingston, R.E. & Narlikar, G.J. Distinct strategies to make nucleosomal DNA accessible. *Mol Cell* 11, 1311-22 (2003).
37. Whitehouse, I., Stockdale, C., Flaus, A., Szczelkun, M.D. & Owen-Hughes, T. Evidence for DNA translocation by the ISWI chromatin-remodeling enzyme. *Mol Cell Biol* 23, 1935-45 (2003).
38. Zofall, M., Persinger, J., Kassabov, S.R. & Bartholomew, B. Chromatin remodeling by ISW2 and SWI/SNF requires DNA translocation inside the nucleosome. *Nat Struct Mol Biol* 13, 339-46 (2006).
39. Saha, A., Wittmeyer, J. & Cairns, B.R. Chromatin remodeling through directional DNA translocation from an internal nucleosomal site. *Nat Struct Mol Biol* 12, 747-55 (2005).

40. Schwanbeck, R., Xiao, H. & Wu, C. Spatial contacts and nucleosome step movements induced by the NURF chromatin remodeling complex. *J Biol Chem* 279, 39933-41 (2004).
41. Dang, W., Kagalwala, M.N. & Bartholomew, B. Regulation of ISW2 by concerted action of histone H4 tail and extranucleosomal DNA. *Mol Cell Biol* 26, 7388-96 (2006).
42. Dechassa, M.L. et al. Architecture of the SWI/SNF-nucleosome complex. *Mol Cell Biol* 28, 6010-21 (2008).
43. Havas, K. et al. Generation of superhelical torsion by ATP-dependent chromatin remodeling activities. *Cell* 103, 1133-42 (2000).
44. Richmond, T.J. & Davey, C.A. The structure of DNA in the nucleosome core. *Nature* 423, 145-50 (2003).
45. Tan, S. & Davey, C.A. Nucleosome structural studies. *Curr Opin Struct Biol* 21, 128-36 (2011).
46. Luger, K., Dechassa, M.L. & Tremethick, D.J. New insights into nucleosome and chromatin structure: an ordered state or a disordered affair? *Nat Rev Mol Cell Biol* 13, 436-47 (2012).
47. Mueller-Planitz, F., Klinker, H., Ludwigsen, J. & Becker, P.B. The ATPase domain of ISWI is an autonomous nucleosome remodeling machine. *Nat Struct Mol Biol* 20, 82-9 (2013).
48. Clapier, C.R. & Cairns, B.R. Regulation of ISWI involves inhibitory modules antagonized by nucleosomal epitopes. *Nature* (2012).
49. Clapier, C.R., Langst, G., Corona, D.F., Becker, P.B. & Nightingale, K.P. Critical role for the histone H4 N terminus in nucleosome remodeling by ISWI. *Mol Cell Biol* 21, 875-83 (2001).
50. Bouazoune, K. & Kingston, R.E. Chromatin remodeling by the CHD7 protein is impaired by mutations that cause human developmental disorders. *Proc Natl Acad Sci U S A* 109, 19238-43 (2012).
51. Hauk, G., McKnight, J.N., Nodelman, I.M. & Bowman, G.D. The chromodomains of the Chd1 chromatin remodeler regulate DNA access to the ATPase motor. *Mol Cell* 39, 711-23 (2010).
52. McKnight, J.N., Jenkins, K.R., Nodelman, I.M., Escobar, T. & Bowman, G.D. Extranucleosomal DNA binding directs nucleosome sliding by Chd1. *Mol Cell Biol* 31, 4746-59 (2011).
53. Grune, T. et al. Crystal structure and functional analysis of a nucleosome recognition module of the remodeling factor ISWI. *Mol Cell* 12, 449-60 (2003).
54. Ryan, D.P., Sundaramoorthy, R., Martin, D., Singh, V. & Owen-Hughes, T. The DNA-binding domain of the Chd1 chromatin-remodelling enzyme contains SANT and SLIDE domains. *EMBO J* 30, 2596-609 (2011).
55. Pinskaya, M., Nair, A., Clynes, D., Morillon, A. & Mellor, J. Nucleosome remodeling and transcriptional repression are distinct functions of Isw1 in Saccharomyces cerevisiae. *Mol Cell Biol* 29, 2419-30 (2009).
56. Dechassa, M.L. et al. Disparity in the DNA translocase domains of SWI/SNF and ISW2. *Nucleic Acids Res* (2012).
57. Hall, M.A. et al. High-resolution dynamic mapping of histone-DNA interactions in a nucleosome. *Nat Struct Mol Biol* 16, 124-9 (2009).
58. Hota, S.K. et al. Nucleosome mobilization by ISW2 requires the concerted action of the ATPase and SLIDE domains. *Nat Struct Mol Biol* (2013).
59. Deindl, S. et al. ISWI Remodelers Slide Nucleosomes with Coordinated Multi-Base-Pair Entry Steps and Single-Base-Pair Exit Steps. *Cell* 152, 442-52 (2013).
60. Ha, T., Kozlov, A.G. & Lohman, T.M. Single-molecule views of protein movement on single-stranded DNA. *Annu Rev Biophys* 41, 295-319 (2012).
61. Lorch, Y., Maier-Davis, B. & Kornberg, R.D. Mechanism of chromatin remodeling. *Proc Natl Acad Sci U S A* 107, 3458-62 (2010).
62. Chaban, Y. et al. Structure of a RSC-nucleosome complex and insights into chromatin remodeling. *Nat Struct Mol Biol* 15, 1272-7 (2008).

63. Bohm, V. et al. Nucleosome accessibility governed by the dimer/tetramer interface. *Nucleic Acids Res* 39, 3093-102 (2011).
64. Gangaraju, V.K., Prasad, P., Srour, A., Kagalwala, M.N. & Bartholomew, B. Conformational changes associated with template commitment in ATP-dependent chromatin remodeling by ISW2. *Mol Cell* 35, 58-69 (2009).
65. Ryan, D.P. & Owen-Hughes, T. Snf2-family proteins: chromatin remodellers for any occasion. *Curr Opin Chem Biol* 15, 649-56 (2011).
66. Dang, W. & Bartholomew, B. Domain architecture of the catalytic subunit in the ISW2-nucleosome complex. *Mol Cell Biol* 27, 8306-17 (2007).
67. Yamada, K. et al. Structure and mechanism of the chromatin remodelling factor ISW1a. *Nature* 472, 448-53 (2011).
68. Sen, P. et al. The SnAC domain of SWI/SNF is a histone anchor required for remodeling. *Mol Cell Biol* 33, 360-70 (2013).
69. Patel, A., McKnight, J.N., Genzor, P. & Bowman, G.D. Identification of Residues in Chromodomain Helicase DNA-Binding Protein 1 (Chd1) Required for Coupling ATP Hydrolysis to Nucleosome Sliding. *J Biol Chem* 286, 43984-93 (2011).
70. Lewis, R., Durr, H., Hopfner, K.P. & Michaelis, J. Conformational changes of a Swi2/Snf2 ATPase during its mechano-chemical cycle. *Nucleic Acids Res* 36, 1881-90 (2008).
71. Forne, I., Ludwigsen, J., Imhof, A., Becker, P.B. & Mueller-Planitz, F. Probing the conformation of the ISWI ATPase domain with genetically encoded photoreactive crosslinkers and mass spectrometry. *Mol Cell Proteomics* 11, M111 012088 (2012).
72. Clapier, C.R., Nightingale, K.P. & Becker, P.B. A critical epitope for substrate recognition by the nucleosome remodeling ATPase ISWI. *Nucleic Acids Res* 30, 649-55 (2002).
73. Hamiche, A., Kang, J.G., Dennis, C., Xiao, H. & Wu, C. Histone tails modulate nucleosome mobility and regulate ATP-dependent nucleosome sliding by NURF. *Proc Natl Acad Sci U S A* 98, 14316-21 (2001).
74. Fan, H.Y., Trotter, K.W., Archer, T.K. & Kingston, R.E. Swapping function of two chromatin remodeling complexes. *Mol Cell* 17, 805-15 (2005).
75. Eberharter, A. et al. Acf1, the largest subunit of CHRAC, regulates ISWI-induced nucleosome remodelling. *EMBO J* 20, 3781-8 (2001).
76. Eberharter, A., Vetter, I., Ferreira, R. & Becker, P.B. ACF1 improves the effectiveness of nucleosome mobilization by ISWI through PHD-histone contacts. *EMBO J* 23, 4029-39 (2004).
77. Watson, A.A. et al. The PHD and Chromo Domains Regulate the ATPase Activity of the Human Chromatin Remodeler CHD4. *J Mol Biol* (2012).
78. He, X., Fan, H.Y., Narlikar, G.J. & Kingston, R.E. Human ACF1 alters the remodeling strategy of SNF2h. *J Biol Chem* 281, 28636-47 (2006).
79. Hargreaves, D.C. & Crabtree, G.R. ATP-dependent chromatin remodeling: genetics, genomics and mechanisms. *Cell Res* 21, 396-420 (2011).
80. Sims, H.I., Lane, J.M., Ulyanova, N.P. & Schnitzler, G.R. Human SWI/SNF drives sequence-directed repositioning of nucleosomes on C-myc promoter DNA minicircles. *Biochemistry* 46, 11377-88 (2007).
81. Rippe, K. et al. DNA sequence- and conformation-directed positioning of nucleosomes by chromatin-remodeling complexes. *Proc Natl Acad Sci U S A* 104, 15635-40 (2007).
82. van Vugt, J.J. et al. Multiple aspects of ATP-dependent nucleosome translocation by RSC and Mi-2 are directed by the underlying DNA sequence. *PLoS One* 4, e6345 (2009).
83. Floer, M. et al. A RSC/nucleosome complex determines chromatin architecture and facilitates activator binding. *Cell* 141, 407-18 (2010).
84. Yang, J.G., Madrid, T.S., Sevastopoulos, E. & Narlikar, G.J. The chromatin-remodeling enzyme ACF is an ATP-dependent DNA length sensor that regulates nucleosome spacing. *Nat Struct Mol Biol* 13, 1078-83 (2006).

85. Gangaraju, V.K. & Bartholomew, B. Dependency of ISW1a chromatin remodeling on extranucleosomal DNA. *Mol Cell Biol* 27, 3217-25 (2007).
86. Kagalwala, M.N., Glaus, B.J., Dang, W., Zofall, M. & Bartholomew, B. Topography of the ISW2-nucleosome complex: insights into nucleosome spacing and chromatin remodeling. *EMBO J* 23, 2092-104 (2004).
87. Stockdale, C., Flaus, A., Ferreira, H. & Owen-Hughes, T. Analysis of nucleosome repositioning by yeast ISWI and Chd1 chromatin remodeling complexes. *J Biol Chem* 281, 16279-88 (2006).
88. Zentner, G.E., Tsukiyama, T. & Henikoff, S. ISWI and CHD Chromatin Remodelers Bind Promoters but Act in Gene Bodies. *PLoS Genet* 9, e1003317 (2013).
89. Gossett, A.J. & Lieb, J.D. In vivo effects of histone H3 depletion on nucleosome occupancy and position in Saccharomyces cerevisiae. *PLoS Genet* 8, e1002771 (2012).
90. Dechassa, M.L. et al. SWI/SNF has intrinsic nucleosome disassembly activity that is dependent on adjacent nucleosomes. *Mol Cell* 38, 590-602 (2010).
91. Ballare, C. et al. Nucleosome-driven transcription factor binding and gene regulation. *Mol Cell* 49, 67-79 (2013).
92. Engeholm, M. et al. Nucleosomes can invade DNA territories occupied by their neighbors. *Nat Struct Mol Biol* 16, 151-8 (2009).
93. Lorch, Y., Griesenbeck, J., Boeger, H., Maier-Davis, B. & Kornberg, R.D. Selective removal of promoter nucleosomes by the RSC chromatin-remodeling complex. *Nat Struct Mol Biol* 18, 881-5 (2011).
94. Racki, L.R. et al. The chromatin remodeller ACF acts as a dimeric motor to space nucleosomes. *Nature* 462, 1016-21 (2009).
95. Blosser, T.R., Yang, J.G., Stone, M.D., Narlikar, G.J. & Zhuang, X. Dynamics of nucleosome remodelling by individual ACF complexes. *Nature* 462, 1022-7 (2009).
96. Lusser, A., Urwin, D.L. & Kadonaga, J.T. Distinct activities of CHD1 and ACF in ATP-dependent chromatin assembly. *Nat Struct Mol Biol* 12, 160-6 (2005).

2.3 No need for a power stroke in ISWI-mediated nucleosome sliding

Johanna Ludwigsen[1], Henrike Klinker[1,2] and Felix Mueller-Planitz[1]

[1]Adolf Butenandt Institute and [2]Center for Integrated Protein Science Munich,
Ludwig-Maximilians-Universität, Munich, Germany

Published in *EMBO reports,* 14, 1092-1097 (2013);
doi: 10.1038/embor.2013.160

Declaration of contributions to “No need for a power stroke in ISWI-mediated nucleosome sliding”

This study was conceived by J. Ludwigsen and F. Mueller-Planitz. I performed the nucleosome sliding experiment shown in Figure 4, edited and helped revising the manuscript.

EMBO reports

TRANSPARENT PROCESS

scientific report

No need for a power stroke in ISWI-mediated nucleosome sliding

Johanna Ludwigsen[1], *Henrike Klinker*[1,2] *& Felix Mueller-Planitz*[1+]
[1]Adolf-Butenandt-Institute, Ludwig-Maximilians-Universität and [2]Center for Integrated Protein Science Munich, Munich, Germany

Nucleosome remodelling enzymes of the ISWI family reposition nucleosomes in eukaryotes. ISWI contains an ATPase and a HAND-SANT-SLIDE (HSS) domain. Conformational changes between these domains have been proposed to be critical for nucleosome repositioning by pulling flanking DNA into the nucleosome. We inserted flexible linkers at strategic sites in ISWI to disrupt this putative power stroke and assess its functional importance by quantitative biochemical assays. Notably, the flexible linkers did not disrupt catalysis. Instead of engaging in a power stroke, the HSS module might therefore assist DNA to ratchet into the nucleosome. Our results clarify the roles had by the domains and suggest that the HSS domain evolved to optimize a rudimentary remodelling engine.

Keywords: ISWI; chromatin remodelling; nucleosome sliding
EMBO *reports* (2013) **14,** 1092–1097. doi:10.1038/embor.2013.160

INTRODUCTION

Nucleosomes are the basic packaging units of chromatin in eukaryotes. By binding tightly to ~146 bp of DNA, they act as physical barriers for the cellular machinery that needs to access the underlying DNA, for example, during transcription, DNA replication and DNA repair. The cell must precisely control the genomic location of nucleosomes to allow for a regulated use of the genetic material in response to different environmental and developmental stimuli.

Mobilizing the nucleosomes is a challenge for the cell as they are inherently stable particles. Dozens of DNA-histone contacts must be broken to rearrange nucleosomes. The cell thus employs dedicated enzymes, so called ATP-dependent nucleosome remodelling factors, to shift the position of nucleosomes along DNA [1]. Remodelling factors of the ISWI and several other families can move nucleosomes along DNA in a process that is termed nucleosome sliding. Elucidating the molecular mechanisms of remodelling enzymes remains a pressing goal.

Early mechanistic clues came from the observation that all remodelling factors contain ATPase engines that are evolutionary related to DNA helicases [2]. Indeed, many remodellers can translocate on DNA much like helicases do [3–5]. However, unlike helicases, they do not separate the DNA strands. Remarkably, the ATPase domains of several remodellers localize to DNA well within the nucleosome, two helical turns away from the nucleosomal dyad, suggesting that helicase-like translocation of DNA takes place inside the nucleosome [5–9].

DNA translocation within the nucleosome begs the question how DNA enters the nucleosome in the first place. For remodelling by ISWI enzymes, it has been proposed that a conformational change mechanically pulls flanking DNA into the nucleosome [10–13]. The energy required for this conformational change would come from hydrolysis of ATP. A step that uses chemical energy to perform mechanical work is often called a power stroke, a terminology that we adopt herein. The carboxy-terminal DNA-binding domain (DBD) of ISWI, which comprises the HAND, SANT and SLIDE (HSS) domains, would be intimately involved in such a power stroke, as it binds to the DNA that flanks the nucleosome [14]. Notably, recent models propose that the power stroke takes place only after the first 7 bp of DNA have been extruded already from the nucleosome's exit site through the translocase activity of the ATPase domain. The size of the proposed power stroke has been measured to be ≤3 bp [11].

Other data appear to be in conflict but can be reconciled with the power stroke model. We and others have shown that ISWI can remodel nucleosomes even if the HSS module is missing [15,16]. Similarly, the C-terminal DBD of Chd1, composed of a related SANT-SLIDE module [17], is also not required for remodelling [18,19]. Nevertheless, the remodelling activity of ISWI decreases an order of magnitude on deletion or mutation of the HSS module [10,15]. This drop in activity could potentially be attributed to a missing power stroke in the deletion mutants.

Other scenarios, however, can also explain the drop in activity incurred by deletion of the HSS module without invoking a power stroke. As the HSS domain is the nucleosome recognition module [15,20], the ATPase domain lacks sufficient specificity to dock productively to its binding site on the nucleosome. Lack of specificity can result in lower observed ATPase and remodelling activity. This problem becomes especially apparent with saturating concentrations of ATP [15]. In addition, the

---

[1]Adolf-Butenandt-Institute, Ludwig-Maximilians-Universität, Schillerstrasse 44, 80336 Munich, Germany
[2]Center for Integrated Protein Science Munich, Ludwig-Maximilians-Universität, Munich, Germany
[+]Corresponding author. Tel: +089 2180 75 431; Fax: +089 2180 75 425;
E-mail: felix.mueller-planitz@med.uni-muenchen.de

Received 23 July 2013; revised 4 September 2013; accepted 16 September 2013;
published online 11 October 2013

©2013 EUROPEAN MOLECULAR BIOLOGY ORGANIZATION

removal of the HSS module might allow a polypeptide motif at the C-terminal end of the ATPase domain known as 'bridge' or 'NegC' to inhibit the enzyme by holding the ATPase domain in a catalytically less active conformation [15,16].

Here we explore whether a power stroke operating between the ATPase and HSS module constitutes an important part of the catalytic strategy of *Drosophila* ISWI. As rigidity in the force-transducing regions of the protein is necessary during a power stroke, one can test the functional relevance of the putative power stroke by artificially increasing the flexibility of these enzyme regions [21,22]. To this end, we inserted glycine-serine rich linkers at several strategic locations in the protein. These linkers act like random coils with a high degree of flexibility [23,24]. Surprisingly, ISWI enzymes with these artificial, flexible hinges showed no defect in ATPase, restriction enzyme accessibility-based remodelling and nucleosome sliding assays. These results strongly argue against the power stroke model. We instead conclude that the HSS module assumes a more passive role during catalysis in that it mainly increases the time the ATPase engine can productively engage with the proper binding site on the nucleosome. With regards to how DNA enters the nucleosome, we propose that DNA ratchets into the nucleosome once the tension that builds up by extruding base pairs (bp) from the exit site becomes too large.

RESULTS

To probe for the importance of the putative ATP-dependent power stroke, we inserted glycine- and serine-rich flexible linkers [23,24] into regions of ISWI that could conceivably transmit the force. The 'brace' and 'bridge' at the C-terminal end of the ATPase domain could be such elements, because they intimately contact both ATPase lobes and thus could directly react to the ATPase cycle [2,15,16,19,25]. The connection between the ATPase and HSS modules is another prime candidate, as the force generated by the ATPase domain must reach the HSS module. Force transmitted from the HAND-SANT to the SLIDE domain would have to go through the connecting spacer helix, as no tertiary contacts between SANT and SLIDE exist [20]. We chose altogether four insertion points (Fig 1A). Linker lengths varied between 10 and 20 amino acids. When fully extended, these linkers can reach ~4–8 nm, a significant range considering the size of the proposed power stroke (≤3 bp, equivalent to ≤1 nm; [11]). All ISWI preparations (Fig 1B) were monodisperse as judged by size exclusion chromatography (supplementary Fig S1 online). The monodispersity attests to the overall structural integrity of the enzymes.

The HSS domain has been proposed to communicate to the ATPase domain and modulate its ATP hydrolysis. Mutations in the SLIDE domain, for instance, can allosterically affect ATP hydrolysis [10]. Moreover, nucleosomes no longer stimulate ATP hydrolysis better than naked DNA when the HSS domain is removed with saturating, although not with sub-saturating, concentrations of ATP [15]. We therefore tested if the ISWI derivatives that have a more flexible link between the ATPase and C-terminal domains could efficiently hydrolyse ATP. We used saturating ATP concentrations to measure ATP turnover, and in fact throughout this study, as defects in the function of the HSS domain become maximally apparent under these conditions [15].

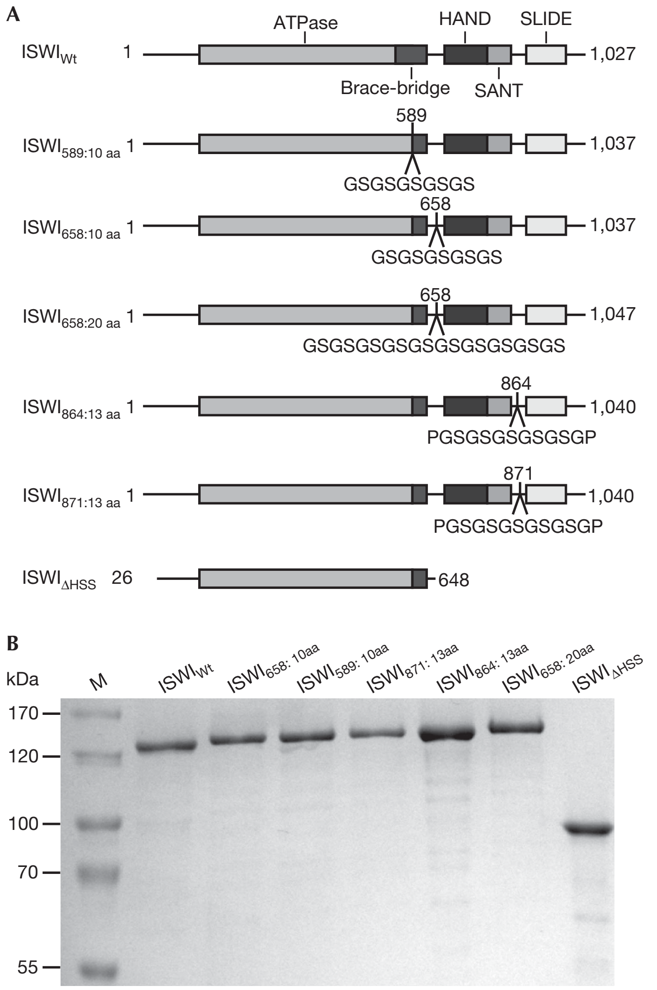

Fig 1 | ISWI derivatives used in this study. (**A**) Schematic representation of ISWI derivatives. Glycine-rich inserts were introduced behind the indicated amino-acid positions. Numbers in subscript refer to the insertion position and the size of the insert. ISWI$_{\Delta HSS}$ spans the amino acids 26–648 and lacks the C-terminal HSS domains. (**B**) Coomassie-stained SDS–PAGE gel showing the purified ISWI derivatives from A. aa, amino acid; HSS, HAND, SANT and SLIDE; SDS–PAGE, SDS–polyacrylamide gel electrophoresis; WT, wild type.

DNA-stimulated ATPase rates of all mutants were indistinguishable from wild-type ISWI (ISWI$_{Wt}$), deviating no more than 1.3-fold (Fig 2). All mutants, just as the wild type, hydrolysed ATP an order of magnitude faster when bound to nucleosomes than to DNA. Importantly, absolute rates for the nucleosome stimulated reaction varied by no more than 1.8-fold between ISWI$_{Wt}$ and all its derivatives. As ATPase rates were largely unaffected, we conclude that the artificial flexible joints did not disrupt the putative communication between the domains and suggest that force transduction is not necessary for efficient ATP hydrolysis. In addition, we conclude that all mutants were properly folded and recognized DNA and nucleosomes like their wild-type counterpart. Indeed, similar concentrations of DNA and nucleosomes saturated the wild type and insertion mutants. For comparison, an order of magnitude higher concentrations

©2013 EUROPEAN MOLECULAR BIOLOGY ORGANIZATION

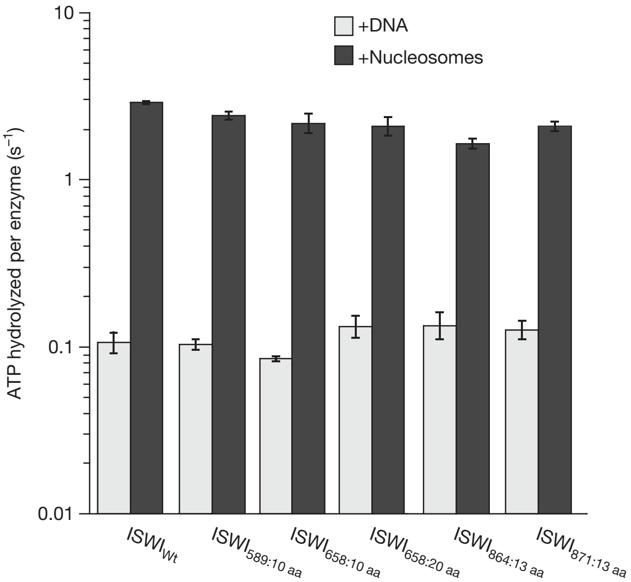

Fig 2 | Insertion of flexible polypeptide linkers does not disrupt DNA- and nucleosome-stimulated ATP hydrolysis. ATPase rates were measured in the presence of saturating concentrations of ATP, DNA or nucleosomes. Errors are s.d. for ISWI$_{Wt}$ ($n=3$) and minimal and maximal values of two independent measurements for all other enzyme derivatives. ATPase rates in the absence of DNA were $<0.02\,s^{-1}$ under otherwise identical conditions (data not shown). ISWI$_{Wt}$, wild-type ISWI.

had to be used to saturate ISWI that completely lacked the HSS domain (ISWI$_{\Delta HSS}$; [15] and data not shown).

The ATPase results do not favour but also do not rule out the power stroke hypothesis. For example, even though the insertion mutants efficiently hydrolysed ATP, a power stroke might be necessary to couple hydrolysis to remodelling. To test this scenario, we performed remodelling assays.

Remodelling leads to exposure of nucleosomal DNA to solvent and can be detected with restriction endonucleases that cut the exposed DNA. We used a quantitative assay that monitors exposure of a unique KpnI site that is occluded by the central nucleosome in a 13-mer nucleosomal array [15]. Rate constants for remodelling (k_{obs}) were determined by measuring exposure of the KpnI site over time and fitting the data to single exponential functions (Fig 3A). Several remodeller concentrations were used to control for possible differences in binding affinities between the ISWI derivatives and the known property of full-length ISWI to inhibit its own catalysis at higher concentrations (Fig 3B) [15].

Unexpectedly, none of the ISWI derivatives containing flexible linkers showed remodelling defects. Used at the same concentration, they all exposed the KpnI site as efficiently as ISWI$_{Wt}$, with k_{obs} differing by no more than a factor of 1.3. For comparison, ISWI$_{\Delta HSS}$ exposed nucleosomal DNA an order of magnitude more slowly (Fig 3C), confirming previous results [15].

As exposed nucleosomal DNA might be an early intermediate during nucleosome sliding, it was important to test if formation of these intermediates was successfully coupled to nucleosome sliding. We monitored sliding in the context of nucleosomal arrays. Each linker DNA contained an exposed AvaI restriction site that became protected upon sliding (Fig 4A) [15].

Surprisingly, but in accordance with the results shown above, all insertion mutants were able to slide nucleosomes over the AvaI sites (Fig 4B). In fact, time courses showed that ISWI$_{Wt}$ and all insertion mutants moved nucleosomes with similar efficiency. As shown before [15], also ISWI$_{\Delta HSS}$ relocated nucleosomes, although higher concentrations and longer incubation times were necessary.

DISCUSSION AND CONCLUSIONS

According to recent mechanistic models, the ATPase engine of ISWI is bound to DNA well within the nucleosome and starts the remodelling process by translocating single bp of DNA in the direction of the exit side of the nucleosome. ATP hydrolysis is required for the transport of each bp. Only after the initial 7 bp of DNA have exited the nucleosome will fresh DNA enter from the opposite side of the nucleosome [10,11]. How DNA enters the nucleosome is unclear.

Prominent models favor a power stroke as a mechanism for how DNA enters the nucleosome [10–13]. At this stage of remodelling, hydrolysis of ATP does not fuel transport of DNA according to these models. Instead, ATP hydrolysis would be coupled to a conformational change between the HSS and ATPase modules. This conformational change exerts force onto the HSS domain and the DNA at the entry site bound by it. Three bp thereby enter the nucleosome (Fig 5A). Subsequently, the ATPase engine resumes transporting single bp toward the exit site [10,11].

In striking opposition to predictions derived from the power stroke model, none of the glycine-rich flexible insertions caused any detectable catalytic defects. Apparently, ISWI can tolerate considerable flexibility between individual domains. Notably, the Bowman lab came to very similar conclusions in a recent study that focused on the related remodelling enzyme Chd1 [26]. We note that inherent flexibility in the remodellers might allow the DBD and ATPase domain of one enzyme molecule to simultaneously contact two neighbouring nucleosomes, a situation that has recently been suggested to be important for remodelling by ISWI enzymes [27].

We were particularly surprised that the 10–20 amino acid long insertions on either side of the brace–bridge polypeptide did not hamper catalysis, as this polypeptide makes intimate contacts with the ATPase domain and was proposed to regulate the enzyme [15,16,19,25]. Depending on whether or not the structure of the brace and bridge is disrupted by the insertions, we can either conclude that this region might be of lesser importance for remodelling than previously hypothesized [16] or that build-up of force is not necessary for proper function of the brace–bridge polypeptide.

If not by a power stroke, how else can flanking DNA enter the nucleosome? We propose that the HSS and ATPase domains work independently of each other with no need for direct coordination during catalysis (Fig 5B). The HSS domain is an important recognition module for the nucleosome [15,20] and is expected to anchor the enzyme to the nucleosome. Anchoring increases the chance for the ATPase engine to productively engage the nucleosome and start with the translocation of DNA. After the first seven translocation steps, the structure of the nucleosome becomes highly strained, particularly around the DNA delimited by the ATPase and HSS module, such that translocation stalls.

©2013 EUROPEAN MOLECULAR BIOLOGY ORGANIZATION

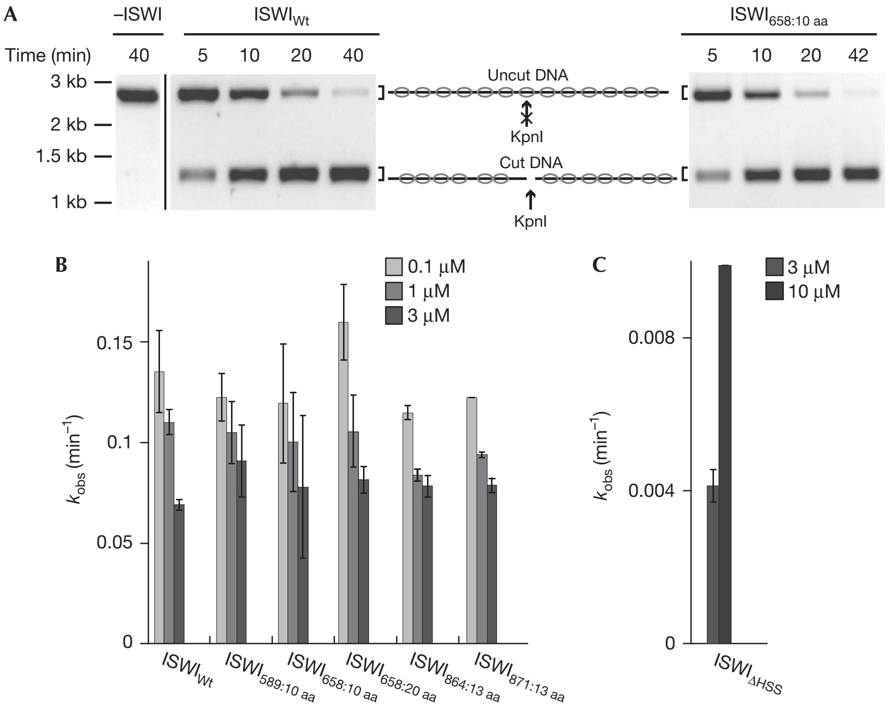

Fig 3 | Insertion of flexible polypeptide linkers does not disrupt nucleosome remodelling. (**A**) Remodelling activity was probed by following the accessibility of a unique, central KpnI restriction site in a 13-mer nucleosomal array (see schematic). Exemplary time courses for remodelling by ISWI$_{Wt}$ and ISWI$_{658:10\ aa}$ (both 3 µM). In mock-treated samples (– ISWI), the KpnI site was not accessible. The original unspliced gel picture containing the mock-treated sample and the ISWI$_{Wt}$ time-course is provided as supplementary Fig S2 online. (**B**,**C**) The observed rate constants for remodelling, k_{obs}, were determined for ISWI derivatives at the indicated concentrations by fitting time courses as in **A** to single exponential functions. Errors are s.d. for ISWI$_{589:10\ aa}$ and ISWI$_{658:10\ aa}$ ($n=4$ for 0.1 µM and 1 µM; $n=3$ for 3 µM) and 1 µM ISWI$_{Wt}$ ($n=3$). In all other instances, minimal and maximal values of two independent measurements are shown. aa, amino acid; ISWI$_{Wt}$, wild-type ISWI; kb, kilobases.

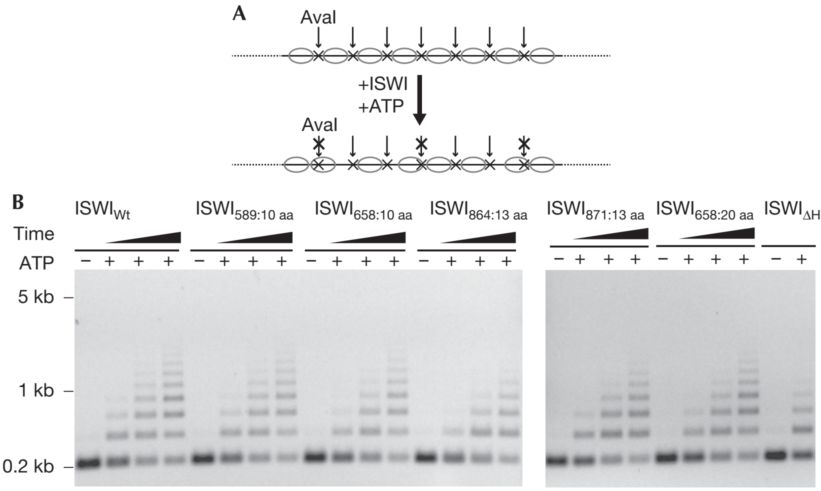

Fig 4 | Insertion of flexible polypeptide linkers does not compromise nucleosome sliding. (**A**) Schematic depiction of the nucleosome sliding assay. 25-mer nucleosomal arrays containing exposed AvaI restriction sites in the linker DNA were used to follow nucleosome sliding. Accessibility to AvaI (arrows) changes upon remodelling. Nucleosomes (ovals) and AvaI sites (x) are indicated. (**B**) ISWI$_{Wt}$ and the insertion mutants were incubated with nucleosomal arrays for 3, 13 and 48 min, whereas ISWI$_{\Delta HSS}$ was incubated for 6 h. Control reactions (–) were depleted of ATP with apyrase before addition of ISWI and incubated for 6 h (ISWI$_{\Delta HSS}$) or 48 min (all other enzymes). ISWI$_{Wt}$, wild-type ISWI.

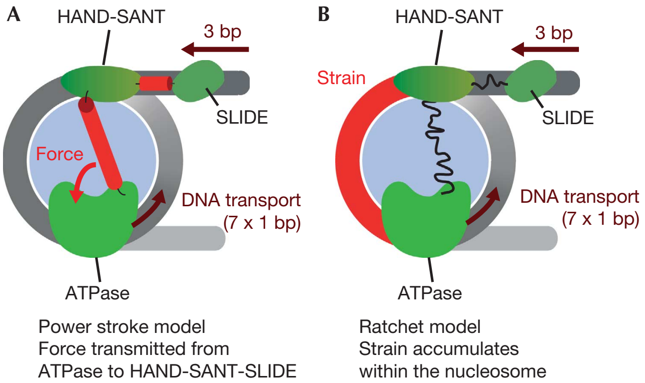

Fig 5 | Models for nucleosome remodelling by ISWI. (**A**) Power stroke model. First, the ATPase engine of ISWI translocates 7 bp of DNA. The ATPase and HSS domains then undergo a power stroke that exerts force on the HSS domains. The power stroke pulls 3 bp of flanking DNA into the nucleosome. Hypothetical force-transducing elements are coloured red. (**B**) Ratchet model. As in **A**, the ATPase engine translocates 7 bp. This translocation strains the structure of the nucleosome, in particular the DNA delimitated by the ATPase and HSS domains (red). When the strain on the nucleosome structure becomes too large, 3 bp of DNA ratchet into the nucleosome. No direct coordination between the HSS and ATPase domain is required for this mechanism and flexible linkage between individual domains (curved lines) does not affect remodelling. Histones are light blue; DNA is grey.

Eventually, the HSS domain loses its grip on the DNA flanking the nucleosome, allowing 3 bp to ratchet in.

Although not part of a power stroke, the HSS module clearly evolved to carry out important functions that collectively optimize remodelling by an order of magnitude [10,15]. Besides established functions such as anchoring the remodeller to the nucleosome and increasing the processivity [10,15], we hypothesize that the HSS module improves catalysis by changing the structure of the nucleosome around the DNA entry site, perhaps by locally separating the DNA from the histone surface [13,28]. Other remodelling subfamilies that do not interact with flanking DNA and therefore cannot engage in a power stroke in the first place might in fact use a similar mechanism [29], pointing to an unified remodelling strategy shared between several remodeller subfamilies.

METHODS

Protein expression and purification. pPROEX-HTb-based expression plasmids with genes encoding *Drosophila melanogaster* ISWI$_{\mathrm{Wt}}$ and ISWI$_{\Delta\mathrm{HSS}}$ were kindly provided by C. Müller (EMBL, Heidelberg, Germany). All genes were fused amino-terminally to a His$_6$-TEV tag. Flexible linkers were introduced into ISWI$_{\mathrm{Wt}}$ by polymerase incomplete primer extension at the appropriate positions [30]. All ISWI derivatives were fully sequenced. Expression and purification were performed as described [25]. The His$_6$-TEV tag was cleaved off by TEV protease for all ISWI constructs except for ISWI$_{\Delta\mathrm{HSS}}$. Catalytic parameters of ISWI$_{\Delta\mathrm{HSS}}$ are unaffected by the presence of the tag [15].

Enzyme assays and enzyme ligands. All assays were performed in 25 mM HEPES-KOH, pH 7.6, 50 mM NaCl, 1 mM MgCl$_2$, 0.1 mM EDTA, 10% glycerol, 0.2 g/l BSA and 1 mM DTT at 26 °C in the presence of an ATP-regenerating system as described [15]. Nucleosomes were reconstituted with recombinant *Drosophila melanogaster* histones by salt-gradient dialysis [31]. The concentration of nucleosomal DNA was determined by measuring its UV absorption at 260 nm. For nucleosomal arrays, concentrations refer to the concentration of individual nucleosomes.

ATP hydrolysis assays. ATP hydrolysis was monitored using an NADH-coupled assay as described [25]. Saturating concentrations of ATP-Mg^{2+} (1 mM), linearized plasmid DNA (pT7blue derivative; 0.2 mg/ml) and nucleosomes reconstituted on the same plasmid DNA (0.1 mg/ml) were used. Saturation was controlled in all cases by titration of the ligand at least over a 16-fold range.

Nucleosome remodelling assay. Remodelling activity was probed as previously described [15] by incubating 13-mer nucleosomal arrays (100 nM) with ISWI derivatives at the indicated concentrations, ATP-Mg^{2+} (1 mM) and KpnI (2 U/μl). Reactions were quenched with SDS (0.4%) and EDTA (20 mM) before the samples were deproteinized and analysed as described [15].

Nucleosome sliding assay. Nucleosome sliding was performed as described [15] by incubation of 25-mer nucleosomal arrays (30 nM) with ATP-Mg^{2+} (0.2 mM) and the respective ISWI derivative (ISWI$_{\Delta\mathrm{HSS}}$: 300 nM; all other enzymes: 5 nM). After quenching the reaction with apyrase (2.5 U/μl), arrays were digested with AvaI (1.1 U/μl) at 26 °C for 3–3.5 h. The AvaI digest was terminated with EDTA (40 mM) and SDS (0.4%) before the samples were deproteinized and analysed as described [15].

Supplementary information is available at EMBO *reports* online (http://www.emboreports.org).

ACKNOWLEDGEMENTS

We are grateful to Nadine Harrer for collecting preliminary data, Katharina Braunger and Franziska Henze for help with protein purification, Nicola Hepp for preparation of 13-mer nucleosomal DNA and Gregory D. Bowman and Peter B. Becker for discussions and comments. J.L. thanks the Ernst Schering foundation for granting a predoctoral fellowship. H.K. was supported by a grant of the 'Center for Integrated Protein Science Munich' available to Peter B. Becker. This research was supported by the Deutsche Forschungsgemeinschaft by grant MU3613/1-1 available to F.M.-P.

Author contributions: J.L. and H.K. performed all experiments, interpreted the results and contributed to the manuscript. F.M.-P. conceived the study, interpreted the results and wrote the manuscript.

CONFLICT OF INTEREST

The authors declare that they have no conflict of interest.

REFERENCES

1. Clapier CR, Cairns BR (2009) The biology of chromatin remodeling complexes. *Annu Rev Biochem* **78:** 273–304
2. Flaus A, Martin DM, Barton GJ, Owen-Hughes T (2006) Identification of multiple distinct Snf2 subfamilies with conserved structural motifs. *Nucleic Acids Res* **34:** 2887–2905
3. Saha A, Wittmeyer J, Cairns BR (2002) Chromatin remodeling by RSC involves ATP-dependent DNA translocation. *Genes Dev* **16:** 2120–2134
4. Whitehouse I, Stockdale C, Flaus A, Szczelkun MD, Owen-Hughes T (2003) Evidence for DNA translocation by the ISWI chromatin-remodeling enzyme. *Mol Cell Biol* **23:** 1935–1945
5. Zofall M, Persinger J, Kassabov SR, Bartholomew B (2006) Chromatin remodeling by ISW2 and SWI/SNF requires DNA translocation inside the nucleosome. *Nat Struct Mol Biol* **13:** 339–346
6. Saha A, Wittmeyer J, Cairns BR (2005) Chromatin remodeling through directional DNA translocation from an internal nucleosomal site. *Nat Struct Mol Biol* **12:** 747–755

©2013 EUROPEAN MOLECULAR BIOLOGY ORGANIZATION

7. Schwanbeck R, Xiao H, Wu C (2004) Spatial contacts and nucleosome step movements induced by the NURF chromatin remodeling complex. *J Biol Chem* **279:** 39933–39941
8. Dang W, Kagalwala MN, Bartholomew B (2006) Regulation of ISW2 by concerted action of histone H4 tail and extranucleosomal DNA. *Mol Cell Biol* **26:** 7388–7396
9. Dechassa ML, Zhang B, Horowitz-Scherer R, Persinger J, Woodcock CL, Peterson CL, Bartholomew B (2008) Architecture of the SWI/SNF-nucleosome complex. *Mol Cell Biol* **28:** 6010–6021
10. Hota SK, Bhardwaj SK, Deindl S, Lin YC, Zhuang X, Bartholomew B (2013) Nucleosome mobilization by ISW2 requires the concerted action of the ATPase and SLIDE domains. *Nat Struct Mol Biol* **20:** 222–229
11. Deindl S, Hwang WL, Hota SK, Blosser TR, Prasad P, Bartholomew B, Zhuang X (2013) ISWI remodelers slide nucleosomes with coordinated multi-base-pair entry steps and single-base-pair exit steps. *Cell* **152:** 442–452
12. Langst G, Becker PB (2001) ISWI induces nucleosome sliding on nicked DNA. *Mol Cell* **8:** 1085–1092
13. Strohner R, Wachsmuth M, Dachauer K, Mazurkiewicz J, Hochstatter J, Rippe K, Langst G (2005) A 'loop recapture' mechanism for ACF-dependent nucleosome remodeling. *Nat Struct Mol Biol* **12:** 683–690
14. Dang W, Bartholomew B (2007) Domain architecture of the catalytic subunit in the ISW2-nucleosome complex. *Mol Cell Biol* **27:** 8306–8317
15. Mueller-Planitz F, Klinker H, Ludwigsen J, Becker PB (2013) The ATPase domain of ISWI is an autonomous nucleosome remodeling machine. *Nat Struct Mol Biol* **20:** 82–89
16. Clapier CR, Cairns BR (2012) Regulation of ISWI involves inhibitory modules antagonized by nucleosomal epitopes. *Nature* **492:** 280–284
17. Ryan DP, Sundaramoorthy R, Martin D, Singh V, Owen-Hughes T (2011) The DNA-binding domain of the Chd1 chromatin-remodelling enzyme contains SANT and SLIDE domains. *EMBO J* **30:** 2596–2609
18. McKnight JN, Jenkins KR, Nodelman IM, Escobar T, Bowman GD (2011) Extranucleosomal DNA binding directs nucleosome sliding by Chd1. *Mol Cell Biol* **31:** 4746–4759
19. Hauk G, McKnight JN, Nodelman IM, Bowman GD (2010) The chromodomains of the Chd1 chromatin remodeler regulate DNA access to the ATPase motor. *Mol Cell* **39:** 711–723
20. Grune T, Brzeski J, Eberharter A, Clapier CR, Corona DF, Becker PB, Muller CW (2003) Crystal structure and functional analysis of a nucleosome recognition module of the remodeling factor ISWI. *Mol Cell* **12:** 449–460
21. Yildiz A, Tomishige M, Gennerich A, Vale RD (2008) Intramolecular strain coordinates kinesin stepping behavior along microtubules. *Cell* **134:** 1030–1041
22. Hackney DD, Stock MF, Moore J, Patterson RA (2003) Modulation of kinesin half-site ADP release and kinetic processivity by a spacer between the head groups. *Biochemistry* **42:** 12011–12018
23. Evers TH, van Dongen EM, Faesen AC, Meijer EW, Merkx M (2006) Quantitative understanding of the energy transfer between fluorescent proteins connected via flexible peptide linkers. *Biochemistry* **45:** 13183–13192
24. Sahoo H, Roccatano D, Zacharias M, Nau WM (2006) Distance distributions of short polypeptides recovered by fluorescence resonance energy transfer in the 10 A domain. *J Am Chem Soc* **128:** 8118–8119
25. Forne I, Ludwigsen J, Imhof A, Becker PB, Mueller-Planitz F (2012) Probing the conformation of the ISWI ATPase domain with genetically encoded photoreactive crosslinkers and mass spectrometry. *Mol Cell Proteomics* **11:** M111 012088
26. Nodelman IM, Bowman GD (2013) Nucleosome sliding by Chd1 does not require rigid coupling between DNA-binding and ATPase domains. *EMBO Rep* **14:** 1098–1103
27. Yamada K, Frouws TD, Angst B, Fitzgerald DJ, DeLuca C, Schimmele K, Sargent DF, Richmond TJ (2011) Structure and mechanism of the chromatin remodelling factor ISW1a. *Nature* **472:** 448–453
28. Gangaraju VK, Prasad P, Srour A, Kagalwala MN, Bartholomew B (2009) Conformational changes associated with template commitment in ATP-dependent chromatin remodeling by ISW2. *Mol Cell* **35:** 58–69
29. Lorch Y, Maier-Davis B, Kornberg RD (2010) Mechanism of chromatin remodeling. *Proc Natl Acad Sci USA* **107:** 3458–3462
30. Klock HE, Lesley SA (2009) The polymerase incomplete primer extension (PIPE) method applied to high-throughput cloning and site-directed mutagenesis. *Methods Mol Biol* **498:** 91–103
31. Dyer PN, Edayathumangalam RS, White CL, Bao Y, Chakravarthy S, Muthurajan UM, Luger K (2004) Reconstitution of nucleosome core particles from recombinant histones and DNA. *Methods Enzymol* **375:** 23–44

©2013 EUROPEAN MOLECULAR BIOLOGY ORGANIZATION

Supplementary material

“No need for a power stroke in ISWI-mediated nucleosome sliding”

Ludwigsen et al., EMBO reports, 2013

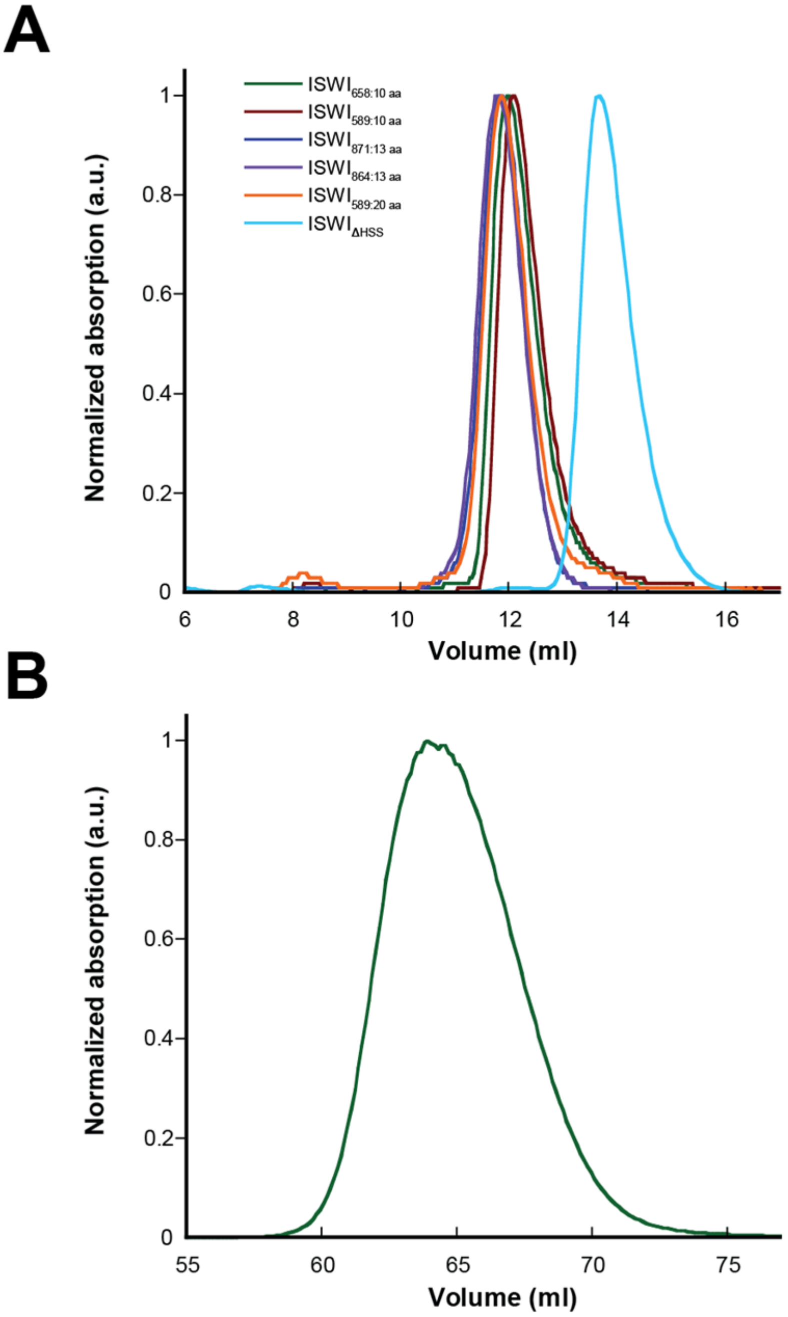

Supplementary Figure 1: Proteins of this study analyzed by size exclusion chromatography (SEC). All proteins were purified by metal affinity and ion exchange chromatography prior to SEC (see Methods). (**A**) ISWI mutants (1 to 1.6 mg of insertion mutants and 3.4 mg of ISWI$_{\Delta HSS}$) were separated over a Superdex 200 10/300 GL column (GE Healthcare). UV absorption was measured at 280 nm except for ISWI$_{\Delta HSS}$ (254 nm) to prevent saturation of the UV detector. (**B**) ISWI$_{Wt}$ (7 mg) was separated over a HiLoad 16/600 Superdex 200 column (GE Healthcare). Absorption was measured at 280 nm. The mobile phase contained 50 mM Hepes-KOH pH 7.6, 0.2 mM EDTA, 200 mM potassium acetate and 1 mM dithiothreitol for all insertion mutants and ISWI$_{Wt,}$ and 25 mM Hepes-KOH pH 7.6, 1.5 mM magnesium acetate, 0.1 mM EDTA, 100 mM potassium chloride, 10% glycerol and 10 mM beta-mercaptoethanol for ISWI$_{\Delta HSS}$.

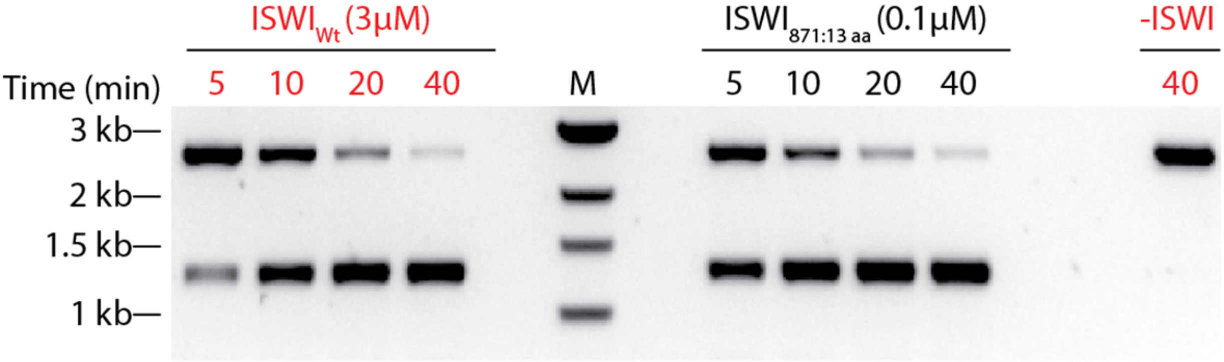
ISWI$_{Wt}$ (3µM)
ISWI$_{871:13\ aa}$ (0.1µM)
-ISWI
Time (min)
5
10
20
40
M
5
10
20
40
40
3 kb—
2 kb—
1.5 kb—
1 kb—

Supplementary Figure 2: Original agarose gel used to generate Figure 3A. Remodeling time courses were obtained for ISWI$_{Wt}$ and ISWI$_{871:13\ aa}$ as explained in Figure 3. Mock-treated sample (-ISWI) served as a control. Red labeled lanes are shown in Figure 3A. M: molecular weight marker; kb: kilobases.

2.4 ISWI Remodelling of Physiological Chromatin Fibres Acetylated at Lysine 16 of Histone H4

Henrike Klinker[1,2], Felix Mueller-Planitz[1], Renliang Yang[3], Ignasi Forné[2,4], Chuan-Fa Liu[3], Lars Nordenskiöld[3], Peter B. Becker[1,2]

[1]Department of Molecular Biology and [4]Protein Analysis Unit, Adolf Butenandt Institute, Ludwig-Maximilians-Universität München, Munich, Germany; [2]Center for Integrated Protein Science Munich, Munich, Germany; [3]School of Biological Sciences, Nanyang Technological University, Singapore

Published in *PLoS ONE* (2014), 9(2): e88411;
doi: 10.1371/journal.pone.0088411

Declaration of contributions to "ISWI Remodelling of Physiological Chromatin Fibres Acetylated at Lysine 16 of Histone H4"

This study was conceived by P.B. Becker and me. I performed all experiments except for the mass spectrometry analysis that was done by I. Forné (Figure S1C, D). He also wrote the corresponding materials and methods section and revised the figure legend. The acetylated and unmodified histones H4 were provided by R. Yang, C.-F. Liu, and L. Nordenskiöld. I conceived and wrote the first draft of the manuscript and developed the final version together with P.B. Becker and F. Mueller-Planitz. I prepared all figures and figure legends.

ISWI Remodelling of Physiological Chromatin Fibres Acetylated at Lysine 16 of Histone H4

Henrike Klinker[1,2], Felix Mueller-Planitz[1], Renliang Yang[3], Ignasi Forné[2,4], Chuan-Fa Liu[3], Lars Nordenskiöld[3], Peter B. Becker[1,2]*

1 Department of Molecular Biology, Adolf Butenandt Institut, Ludwig-Maximilians-Universität München, Munich, Germany, **2** Center for Integrated Protein Science Munich, Munich, Germany, **3** School of Biological Sciences, Nanyang Technological University, Singapore, Singapore, **4** Protein Analysis Unit, Adolf Butenandt Institut, Ludwig-Maximilians-Universität München, Munich, Germany

Abstract

ISWI is the catalytic subunit of several ATP-dependent chromatin remodelling factors that catalyse the sliding of nucleosomes along DNA and thereby endow chromatin with structural flexibility. Full activity of ISWI requires residues of a basic patch of amino acids in the N-terminal 'tail' of histone H4. Previous studies employing oligopeptides and mononucleosomes suggested that acetylation of the H4 tail at lysine 16 (H4K16) within the basic patch may inhibit the activity of ISWI. On the other hand, the acetylation of H4K16 is known to decompact chromatin fibres. Conceivably, decompaction may enhance the accessibility of nucleosomal DNA and the H4 tail for ISWI interactions. Such an effect can only be evaluated at the level of nucleosome arrays. We probed the influence of H4K16 acetylation on the ATPase and nucleosome sliding activity of *Drosophila* ISWI in the context of defined, *in vitro* reconstituted chromatin fibres with physiological nucleosome spacing and linker histone content. Contrary to widespread expectations, the acetylation did not inhibit ISWI activity, but rather stimulated ISWI remodelling under certain conditions. Therefore, the effect of H4K16 acetylation on ISWI remodelling depends on the precise nature of the substrate.

Citation: Klinker H, Mueller-Planitz F, Yang R, Forné I, Liu C-F, et al. (2014) ISWI Remodelling of Physiological Chromatin Fibres Acetylated at Lysine 16 of Histone H4. PLoS ONE 9(2): e88411. doi:10.1371/journal.pone.0088411

Editor: Yamini Dalal, National Cancer Institute, United States of America

Received November 28, 2013; **Accepted** January 4, 2014; **Published** February 6, 2014

Copyright: © 2014 Klinker et al. This is an open-access article distributed under the terms of the Creative Commons Attribution License, which permits unrestricted use, distribution, and reproduction in any medium, provided the original author and source are credited.

Funding: This work was supported by grants of the Deutsche Forschungsgemeinschaft to PBB (SFB 594 TPA6 and the Gottfried Wilhelm Leibniz Programme BE 1140/6), the Center for Integrated Protein Science, Munich, and the Singapore Agency for Science Technology and Research (A*STAR) through Biomedical Research Council (BMRC) grants to LN (10/1/22/19/666) and CFL (08/1/22/19/588). HK acknowledges support by the Elite Network of Bavaria. The funders had no role in study design, data collection and analysis, decision to publish, or preparation of the manuscript.

Competing Interests: The authors have declared that no competing interests exist.

* E-mail: pbecker@med.uni-muenchen.de

Introduction

The nucleosomal organisation of genomic DNA constitutes a barrier to DNA binding factors. Therefore, nucleosome positions have to be tightly, yet dynamically controlled to enable the interaction of regulators of replication and transcription programmes with their cognate DNA binding sites. Of key importance in these processes are chromatin remodelling factors, a conserved class of enzymes that utilize the energy from ATP hydrolysis to reposition, evict, and assemble nucleosomes [1,2]. ISWI, a prominent member of this class of 'remodelling' ATPases, is the catalytic subunit of several different chromatin remodelling complexes [3,4]. All ISWI complexes investigated to date mobilize nucleosomes by repositioning histone octamers along DNA in a process termed 'nucleosome sliding' [5,6]. Furthermore, some of them, such as the ACF-type complexes that consist minimally of the non-catalytic subunit Acf1 in addition to ISWI, assist nucleosome assembly and introduce a regular spacing into nucleosome arrays *in vitro* [7–12]. *In vivo*, ISWI complexes are involved in multiple essential nuclear processes, such as transcription regulation, DNA repair, and the maintenance of chromatin higher order structure [13,14]. Still, how ISWI complexes are targeted and regulated and how their biochemical properties are translated into various biological outcomes remains largely elusive.

Since the ATPase ISWI is able to slide nucleosomes *in vitro* in absence of associated complex subunits, it serves as valuable model for mechanistic analyses. ISWI engages the nucleosome via its ATPase domain about two helical turns off the nucleosomal dyad [15–18]. At this site, the N-terminal tail domain of histone H4 (referred to as 'H4 tail' hereafter) emanates [19]. Notably, full activation of ISWI requires a basic patch of the H4 tail (amino acids 16–20), more specifically the residues $R_{17}H_{18}R_{19}$ [16,20–24].

Besides regulating ISWI activity, the H4 tail is critically involved in the folding of chromatin fibres. It strongly promotes fibre condensation, mainly by interacting with an acidic patch formed by histones H2A and H2B of nearby nucleosomes [25]. Notably, deletion of the tail as well as its acetylation causes considerable decompaction of chromatin at the level of intra- as well as inter-fibre interactions *in vitro* [26–29]. Especially acetylation of lysine 16 (H4K16ac) dramatically reduces the compaction capability of chromatin arrays even in presence of linker histones that have a strong chromatin condensation effect [30–33]. This *in vitro* finding is in accordance with *in vivo* data that found the H4K16ac mark to be enriched in open and accessible chromatin regions [34–36].

Given the importance of the H4 tail for ISWI activity, it is conceivable that posttranslational modifications, especially of residues within the basic patch, may modulate ISWI catalysis. Indeed, several observations suggest that H4 tail acetylation – in particular on lysine 16 – inhibits the activity of ISWI complexes. For example, ISW2, an ACF-related complex in *S. cerevisiae*, showed reduced activity if the H4 tail of substrate mononucleosomes was acetylated on all four lysines [37]. Although the inhibitory effect of the tetra-acetylation on the ATPase activity of ISW2 was minor (1.1-fold), acetylated mononucleosomes were repositioned 1.4-fold more slowly than unmodified ones. In a different study, site-specific acetylation of lysines 12 or 16 reduced the ATPase activity of *Drosophila* ISWI to approximately 65% when H4 tail peptides were used along with DNA to mimic nucleosome stimulation [23]. Peptide competition assays further confirmed inhibition of ISWI activity by these acetylation marks [38]. Moreover, H4K16ac markedly reduced *Drosophila* ACF-catalysed mononucleosome sliding by a factor of 2.7 [30]. Notably, contrary to the inhibitory effect of H4 tail acetylation observed in the context of mononucleosomes and tail peptides, hyperacetylation of chromatin fibres permitted faster remodelling by *Drosophila* ACF-type complexes and ISWI [39]. This might reflect better accessibility of the nucleosome and H4 tail in the acetylated, unfolded fibres.

Also studies in physiological settings hint at a complex interplay of H4K16ac and ISWI activity. Male *Drosophila* larvae lacking ISWI expression show striking decondensation of the X chromosome in spreads of polytene chromosomes [38,40]. The male X chromosome is characterized by H4K16ac enrichment due to the activity of the dosage compensation machinery [36]. This activity was found to be necessary and sufficient for the X chromosome decompaction observed upon ISWI loss. Thus, it was proposed that ISWI complexes are involved in chromatin compaction by counteracting the decondensing effect of H4K16ac. In this model, reduced activity of ISWI on H4K16ac-carrying nucleosomes, as suggested by *in vitro* data, leads to an inherently more open structure of the male X chromosome.

However, the situation is more complex. Complete ISWI depletion is accompanied by striking loss of linker histone H1 from chromatin along with global chromatin decondensation [41]. This finding is in line with *in vitro* experiments showing that *Drosophila* ISWI and ACF can assist H1 incorporation into chromatin arrays [42] and slide H1-associated nucleosomes, although with reduced efficiency [43]. An ISWI complex may therefore contribute to H1 homeostasis in chromosomes. Nevertheless, the mechanism – direct or indirect – through which ISWI promotes chromatin condensation *in vivo* and the contributions of H4K16ac as well as H1 in this process remain unclear. Yet, investigating the interplay of these factors in cells is complicated and hampered by indirect effects. *In vitro* experiments on the other hand thus far mostly involved non-physiological substrates, like mononucleosomes or H4 tail peptides.

Here, in appreciation of the particular influence of H4K16ac on chromatin fibre folding, we investigated the effect of the modification on the remodelling activities of *Drosophila* ISWI and ACF in the context of fully defined, *in vitro* reconstituted chromatin arrays [44]. These arrays consisted of 25 nucleosomes that were either bound or unbound by linker histone and reflected the physiological chromatin substrate in several respects. They featured a nucleosomal repeat length of 197 bp, which is typically found in *D. melanogaster* [45]. H4K16ac was demonstrated earlier to enhance linker DNA accessibility [46] and to decrease salt-dependent compaction of similar arrays with different nucleosome spacing [30–32], whereas the linker histone strongly promoted condensation [31,47]. The abundance of H1 in the nuclei of *Drosophila* cells suggests that the majority of nucleosomes is associated with the linker histone, forming so-called chromatosomes [48]. Therefore, chromatosome arrays are expected to resemble the physiological chromatin fibre even more accurately than nucleosome arrays. Employing the reconstituted nucleosome and chromatosome arrays as remodelling substrates, we found that in contrast to widespread expectations the homogenous acetylation of H4 on lysine 16 does not negatively affect ISWI and ACF activity.

Results

Reconstitution of nucleosome arrays carrying H4K16ac

To investigate the influence of H4K16ac on ISWI catalysis, we reconstituted 25-mer nucleosome arrays carrying either unmodified or site-specifically acetylated H4 from recombinant histones *in vitro*. The acetylated H4 was generated using a semi-synthetic approach employing native chemical ligation as illustrated in Figure S1A [32]. This method introduces a lysine analogue (K$_S$) at position 20 of histone H4 (H4K$_S$20). K$_S$ is identical to lysine except for a thioether in its side chain (Figure S1A, B). Previous studies found H4K$_S$20-carrying nucleosome arrays to behave similar to unmodified arrays in salt-dependent compaction [49]. Furthermore, remodelling by hACF was undisturbed in presence of trimethylated H4K$_S$20 [50]. Tandem mass spectrometry confirmed quantitative acetylation of the semi-synthetic histone on lysine 16 (Figure S1C, D).

We assembled the acetylated H4 into histone octamers and reconstituted regularly spaced nucleosome arrays applying a method first described by the Rhodes lab [44]. To yield a regular spacing of nucleosomes, we assembled the arrays by salt gradient dialysis on a linear DNA fragment comprising 25 repeats of a 197 bp derivative of the Widom-601 nucleosome positioning sequence (Figure 1A) [51,52]. To prevent oversaturation of the arrays with histones during assembly, short DNA fragments were present during the reconstitution. These DNA fragments did not

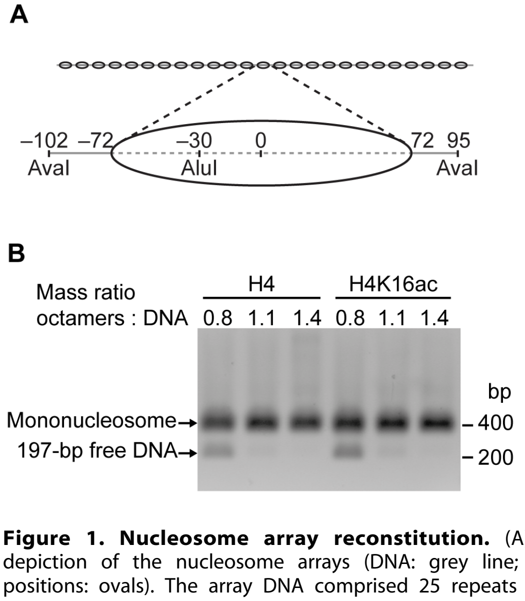

Figure 1. Nucleosome array reconstitution. (A) Schematic depiction of the nucleosome arrays (DNA: grey line; nucleosome positions: ovals). The array DNA comprised 25 repeats of a 197 bp fragment (magnification) harbouring the Widom-601 nucleosome positioning sequence (dashed line). Numbers indicate positions of restriction enzyme sites and nucleosome boundaries with respect to the nucleosomal dyad axis (0). (B) AvaI digests of purified nucleosome arrays reconstituted with increasing amounts of unmodified (H4) or acetylated (H4K16ac) octamers. The reactions were loaded onto a native agarose gel and DNA visualized by ethidium bromide stain. (bp: base pairs).

doi:10.1371/journal.pone.0088411.g001

harbour nucleosome positioning sequences and served as low affinity competitors that bound excess histones.

Through titrations, we determined how much of the octamers was needed to saturate the DNA template. After assembly, the nucleosome arrays were purified by $MgCl_2$ precipitation, which removed histone-bearing and free competitor DNA fragments [53]. Saturation was controlled on native agarose gels (Figure S2B), and histone stoichiometry was assessed on Coomassie-stained SDS gels (Figure S2A). We independently confirmed saturation by digesting the arrays with the restriction enzyme AvaI that cuts in the linker DNA between Widom-601 repeats (Figure 1). On native gels, mononucleosomes migrated more slowly than the corresponding free DNA, and disappearance of the 197 bp DNA band with increasing histone octamer concentrations indicated full occupancy of the Widom-601 sites with nucleosomes. In a complementary approach, arrays were digested with AluI. In contrast to AvaI, the AluI site is located within the Widom-601 sequence and was occluded upon nucleosome formation (Figure 1A). None of the AluI sites were cleaved when the arrays were saturated with octamers (Figure S2C). All quality controls indicated that comparable amounts of acetylated and unmodified histone octamers were required to reach saturation (Figures 1B; S2B, C). We subjected each array preparation to the described quality controls to assure full nucleosome occupancy.

H4K16ac does not influence ISWI ATPase activity

Previous studies suggested that acetylation of H4K16 on mononucleosomes or H4 tail peptides in conjunction with DNA reduces ISWI and ACF activity [23,30,37,38,54]. Our aim was to test whether H4K16ac influences ISWI activity also in the context of nucleosome arrays, a more physiological substrate. Therefore, we saturated ISWI with unmodified or acetylated nucleosome arrays and measured ATP turnover at steady-state (Figure 2A). We controlled for saturation of ISWI with arrays by titrating the nucleosomal substrate (Figure S3). Surprisingly, ATP turnover increased by the same amount with both array types. Thus, at the level of nucleosome arrays H4K16ac did not influence ISWI ATPase activity.

On the basis of previous studies, we also tested the stimulation of the ATPase activity of DNA-bound ISWI by H4 tail peptides [23,52,54]. Notably, also in this assay H4K16ac did not affect ATP turnover by ISWI (Figure 2B). Acetylated H4 peptides stimulated only marginally (1.2-fold) worse than unmodified ones, as can be estimated from the slopes of the curves. This 1.2-fold effect is slightly smaller than the previously documented one of ~1.5-fold in similar experiments [23,54] and well within the error of our assay. We conclude that, contrary to common interpretations of published data, the acetylation of H4K16 does not significantly influence the ATPase activity of ISWI under our assay conditions.

H4K16ac does not inhibit remodelling by ISWI and ACF

H4K16ac may influence ISWI remodelling activity even though ATP hydrolysis remained unaffected. Using the 25-mer nucleosome arrays as substrates, we followed the remodelling activity of ISWI by monitoring accessibility of the AluI restriction site [43,52]. This site was protected from cleavage by a positioned nucleosome at the outset of the reaction (Figure 1A), but was rendered accessible upon remodelling. Therefore, the array DNA got fragmented over time. To be able to directly compare remodelling of unmodified and acetylated arrays in the same reaction, we differentially labelled both array types with a unique fluorescent tag at one DNA end. Figure 3A illustrates the set-up of the remodelling assay.

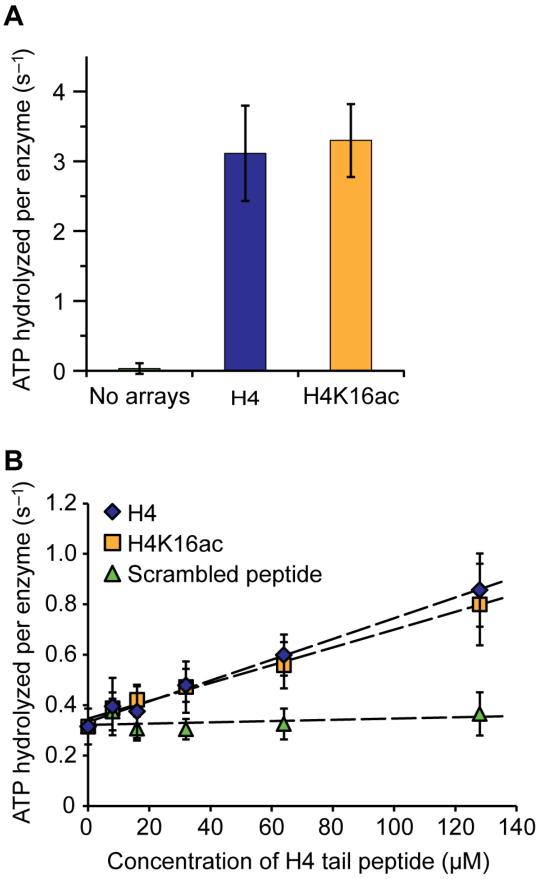

Figure 2. ISWI ATPase activity is not influenced by H4K16ac. (A) Steady-state ATPase assay. ATPase activity of ISWI (100 nM) was stimulated with saturating concentrations of nucleosome arrays (600 nM) carrying unmodified (H4) or acetylated H4 (H4K16ac). ATP hydrolysis rates in presence of saturating concentrations of ATP (1 mM) were determined. Control reactions did not contain nucleosome arrays. Error bars represent standard deviations (No arrays: n = 4; H4 and H4K16ac: n = 5). (B) ISWI (350 nM) was stimulated with DNA (1.2 mg/ml salmon sperm DNA) and increasing concentrations of an unmodified or H4K16ac-carrying histone H4 N-terminal peptide (H4 tail peptide). ATP hydrolysis rates were determined as above at 1 mM ATP. A peptide with scrambled amino acid sequence of the H4 tail harbouring an acetylated lysine residue served as control. Data were fit to lines to extract slopes (dashed lines; H4: $4.1*10^3$ s^{-1} M^{-1}; H4K16ac: $3.5*10^3$ s^{-1} M^{-1}). Error bars display standard deviations (n = 3–4).
doi:10.1371/journal.pone.0088411.g002

To discriminate the influence of the acetylation on different steps of ISWI catalysis, we performed the assay under two conditions. First, we saturated the arrays with ISWI by adding an excess of enzyme at high concentrations (Figure 3B). In this experimental setting, remodelling velocity is expected to depend only on catalytic steps after substrate binding, as all ISWI binding sites on the arrays were occupied regardless of affinity (Figure 3B top panel). Under these conditions, H4K16ac-carrying arrays were remodelled with the same velocity as unmodified arrays (Figure 3B middle and bottom panel). Thus, we conclude that the acetylation did not affect catalytic steps subsequent to nucleosome binding.

Yet, it remained possible that H4K16ac changed the affinity of ISWI for the nucleosomes. To investigate this possibility, we added ISWI in substoichiometric concentrations to the nucleosome arrays. Under these conditions, ISWI distributed among the

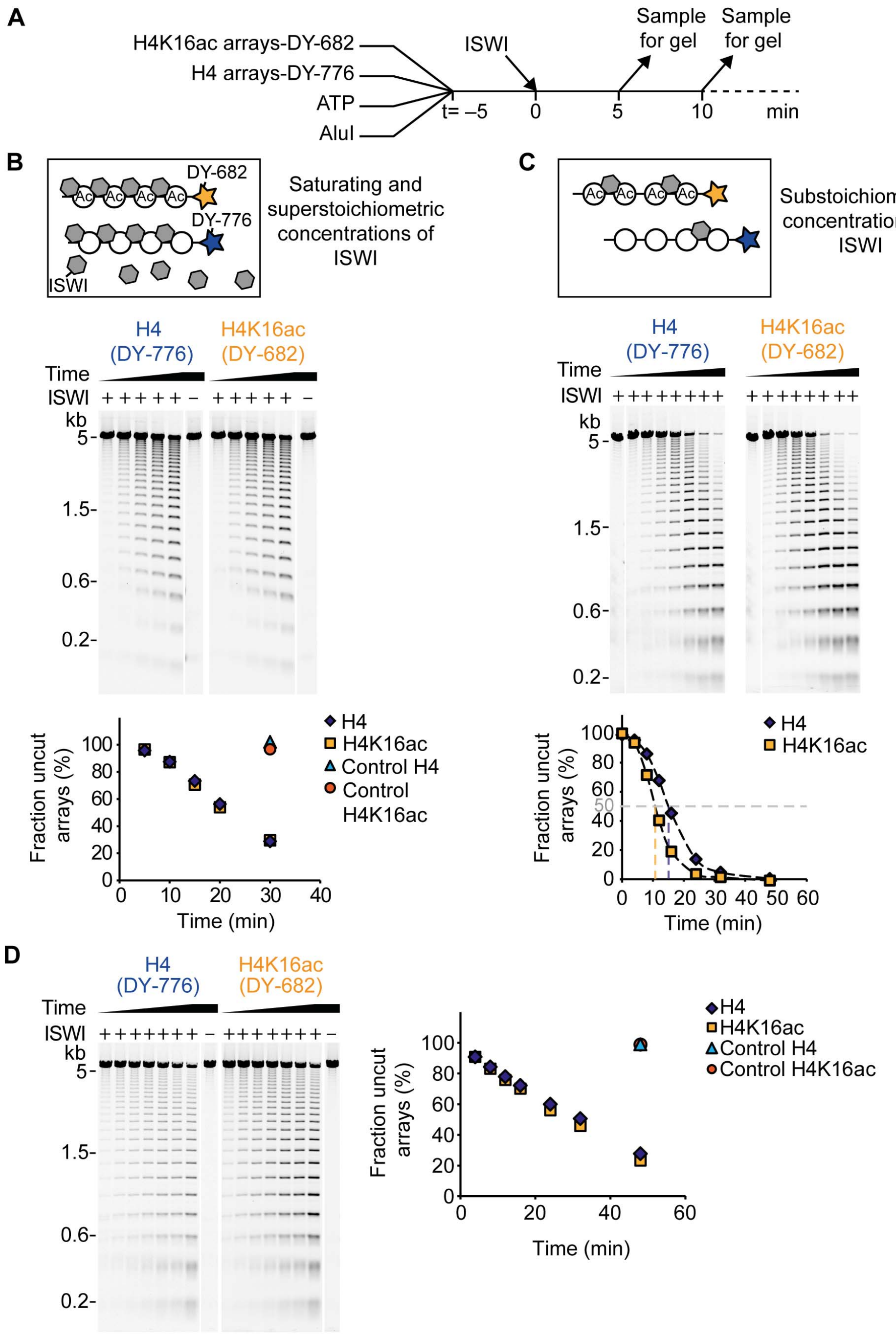

Figure 3. ISWI and ACF remodelling activity is not inhibited by H4K16ac. (A) Scheme of the remodelling assay. Acetylated (H4K16ac) and unmodified (H4) arrays were labelled at one DNA end with the fluorescent dyes DY-682 and DY-776, respectively. Remodelling reactions contained both array types along with ATP, AluI and the remodeller. Samples of the reaction were taken at different time points (t) and the DNA fragments were analysed on an agarose gel. (B) Top: Schematic depiction of the reaction conditions of the remodelling assay. (Ac: acetylated arrays). Middle: Exemplary result of a remodelling time course with ISWI (500 nM). Nucleosome concentration was 25 nM per array type and ATP concentration was 1 µM. All samples were run on the same agarose gel and the two fluorescent labels were visualized separately by scanning the gel at the respective wave lengths. Lanes were rearranged for presentation purposes. Control reactions did not contain ISWI (–). Bottom: Quantification of remodelling progress. Based on the fluorescent signal intensity the fraction of uncut array DNA was determined for each gel lane and plotted against the remodelling time. (C) Remodelling assay as in B, but with ISWI and nucleosome concentrations of 5 nM and 100 nM, respectively. ATP concentration was 200 µM. In the plot shown in the bottom panel, the remodelling times needed to reach 50% cut array DNA were interpolated by connecting the data points by smooth lines (Excel; Microsoft). (D) Exemplary result of a remodelling time course with ACF. Reaction conditions were as in C. (kb: kilobases).

doi:10.1371/journal.pone.0088411.g003

unmodified and acetylated arrays according to its affinity (Figure 3C top panel). In this setting, acetylated arrays were remodelled modestly faster than unmodified ones (Figure 3C middle and bottom panel). To quantify the difference, we interpolated the time needed to cut 50% of the arrays (dashed lines in Figure 3C bottom panel; H4: 15 min; H4K16ac: 11 min). These values differed by a factor of 1.4. Several independent repetitions of the experiment with varying enzyme and array concentrations confirmed these results (data not shown). As long as ISWI was substoichiometric to nucleosomes, unmodified arrays were reproducibly remodelled 1.3–1.7-fold more slowly than acetylated arrays (1.5-fold on average). Since we already showed that ISWI remodelling subsequent to substrate binding was unaffected by H4K16ac (Figure 3B), the difference in remodelling velocity observed here hints at a preferred binding of ISWI to acetylated arrays. Our results contrast previous studies reporting reduced remodelling activity of ACF-type complexes in presence of H4K16ac at the level of mononucleosomes [30,37], but reiterate observations of enhanced remodelling activity on hyperacetylated nucleosome arrays [39].

To test whether the discrepancy between our and published data was due to working with the isolated ISWI enzyme as opposed to the ACF complex, we repeated the remodelling assay with ACF. To capture possible effects of the acetylation on binding affinity as well as later catalytic steps, we employed substoichiometric concentrations of ACF. We found ACF to remodel H4K16ac-carrying and unmodified arrays with comparable velocities (Figure 3D). Thus, we reason that neither ACF binding affinity nor further steps of the remodelling mechanism were influenced by the acetylation.

In principle, the discrepancy between our and published findings could be accounted for by differences in the design of the employed remodelling assays. In the remodelling assay used here, accessibility of AluI sites could be caused by different remodelling events. The sites could, for example, be exposed by sliding a nucleosome away from its original position, by nucleosome eviction, or by transient changes in the canonical nucleosome structure. Previous studies reporting reduced remodelling of ISWI and its complexes in presence of H4K16ac exclusively looked at sliding events [30,37]. Therefore, we next performed sliding assays.

To follow nucleosome sliding, remodelling-dependent changes in the accessibility of the AvaI sites located in the linker DNA between nucleosomes (Figure 1A) were monitored [52,55]. Protection of the initially exposed AvaI sites was indicative of nucleosome sliding (Figure 4A). We found that ISWI repositioned acetylated nucleosomes slightly faster than unmodified ones, as evidenced by the accumulation of longer DNA fragments at earlier time points (Figure 4B). At equilibrium, the DNA patterns were comparable for both array types (Figure 4B, time points 27 and 82 min). Contrary to ISWI, ACF repositioned unmodified and acetylated nucleosomes with equal velocity (Figure 4C). These observations closely reiterate the results we obtained with the remodelling assay under similar conditions (Figure 3C, D).

Taken together, the acetylation neither inhibited ISWI nor ACF remodelling at the level of nucleosome arrays. Rather, ISWI showed a modest preference for remodelling H4K16ac-carrying arrays.

Reconstitution of chromatosome arrays carrying H4K16ac

To investigate the effect of H4K16ac on the activity of ISWI on a substrate that resembles the *in vivo* situation even better than nucleosome arrays, we assembled arrays containing linker histone H1, so-called chromatosome arrays [44]. H1 was titrated to determine the ratio of H1 to nucleosomes needed in the reconstitution reactions to saturate the arrays. Saturation with H1 was tested by two complementary approaches. First, arrays were digested with AvaI into monomers. On native gels, monochromatosomes showed altered mobility in comparison to mononucleosomes, and disappearance of the mononucleosome band indicated quantitative formation of chromatosomes (Figure 5A for H4K16ac-carrying chromatosome arrays; data for unmodified arrays not shown).

Second, we controlled the relative stoichiometry of linker histone incorporation on Coomassie-stained SDS gels (Figure 5B). Increasing the H1 amounts up to a molar ratio of approximately four H1 per nucleosome in the reconstitution reactions led to a corresponding increase in H1 incorporation. At this point, a plateau in linker histone incorporation was reached, indicating saturation of primary binding sites in agreement with the results obtained in the AvaI digests (Figure 5A). Despite the buffering effect of competitor DNA, addition of H1 beyond the saturation plateau led to aggregation and loss of material during assembly (data not shown) [44].

Similar H1 amounts saturated unmodified and H4K16ac-carrying arrays (Figure 5B). Yet, unmodified chromatosome arrays tended to aggregate at lower H1 input amounts than acetylated ones (data not shown). The described quality controls were performed for every chromatosome array preparation to ensure saturation.

H1 inhibits ISWI activity irrespective of H4K16ac

We first probed the effect of H1 on the steady-state ATP hydrolysis of ISWI. Under saturating array concentrations, the presence of H1 reduced ISWI ATP turnover by a factor of two and acetylation did not cause additional effects (Figure 6A).

We next tested ISWI remodelling activity on chromatosome arrays. In contrast to the remodelling assay described in Figure 3, we performed the assay with unlabelled arrays and set up separate reactions for each array type. H1 incorporation markedly reduced remodelling velocity of ISWI, confirming published results (Figure 6B, C) [43]. However, we hesitated to quantify the effect of the linker histone on ISWI remodelling because the reduction in AluI accessibility on chromatosomes might in part be caused by remodelling-independent, inherent properties of the arrays. H1 is expected to occlude about 20 bp of the 50 bp long linker DNA [56]. This reduces the probability to expose an AluI site simply due to restricted sliding possibilities.

Nevertheless, we could use the assay to quantitatively compare the remodelling activity of ISWI on chromatosome arrays harbouring unmodified and acetylated H4. H4K16ac seemed to counteract the inhibitory effect of H1 as indicated by faster remodelling of acetylated arrays (Figure 6B, C). This observation was reproducible for different array preparations when comparing ISWI activity on pairs of arrays reconstituted with the same ratio of H1 to nucleosomes in the assembly reactions (data not shown).

However, control experiments showed that remodelling was markedly dependent on the H1 to nucleosome ratio present in the reconstitution reactions. Although all arrays were saturated with H1 according to our quality controls, they were remodelled with different velocity (Figure 6D). Increasing the amount of H1 in the array assembly reactions by as little as 10% reduced the remodelling velocity considerably. Accordingly, using slightly more H1 in the reconstitution reactions of acetylated in comparison to unmodified arrays resulted in equal ISWI remodelling activity on both array types (Figure 6D). Therefore, we cannot exclude that the observed faster remodelling of

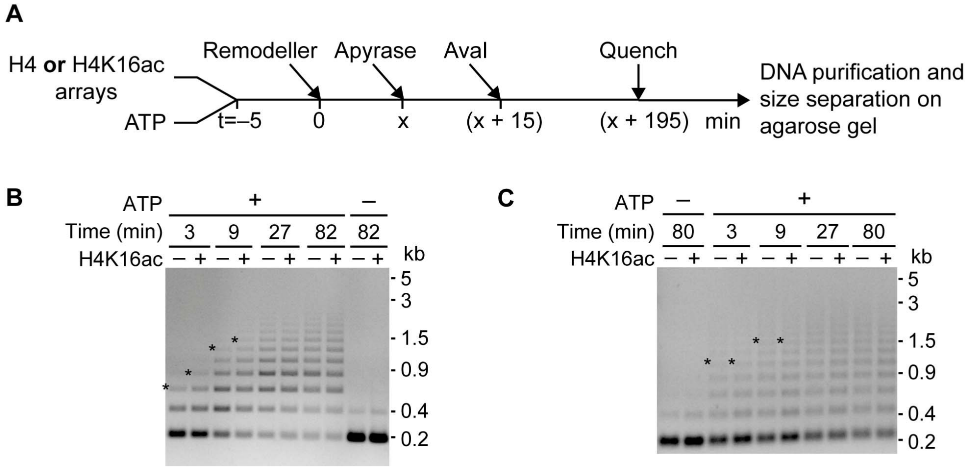

Figure 4. Sliding activity of ISWI and ACF is not reduced by H4K16ac. (A) Schematic depiction of the sliding assay. Each reaction contained either unmodified (H4) or acetylated (H4K16ac) arrays (30 nM) along with ATP (125 μM) and was started by addition of the remodeller (5 nM). At different time points (x) samples were taken, remodelling was quenched by ATP depletion with apyrase, and AvaI was added. AvaI activity was quenched with EDTA (40 mM) and SDS (0.4%) before purifying the DNA fragments and size-separating them on an agarose gel. (B) and (C) ISWI and ACF sliding time courses, respectively. The asterisks mark the slowest migrating still well visible DNA band in the respective gel lanes. In control reactions ATP was depleted before remodeller addition (– ATP). (kb: kilobases).
doi:10.1371/journal.pone.0088411.g004

H4K16ac-carrying chromatosome arrays at equal H1 input amounts simply reflected subtle differences in H1 incorporation. The sensitivity of ISWI towards minor differences in H1 saturation detected in the remodelling assay was not apparent in the ATPase activity of the enzyme (data not shown).

In summary, linker histone H1 reduced the ATPase activity of ISWI by two-fold irrespective of the acetylation status of H4K16. However, the strong dependency of ISWI remodelling on slight variation of linker histone input during reconstitution together with the inherent difficulties of working with the sticky H1 protein limited our ability to interpret the tendency of H4K16ac to ameliorate the inhibition of remodelling of chromatosome arrays.

Discussion

ISWI regulation by H4K16ac

It is firmly established that the H4 tail plays a crucial role in the nucleosome sliding mechanism of ISWI [5,6]. A recent study provided mechanistic insights by identifying a peptide motif in the N-terminus of ISWI (AutoN) that resembles the basic patch of histone H4 [54]. This motif was suggested to interact with the ATPase domain and autoinhibit ISWI in absence of a nucleosome substrate. Yet, the study proposed also subsequent steps of ISWI catalysis to be promoted by the H4 tail, and these might involve other motifs than the basic patch.

To date, it is still unclear how modifications of the H4 tail affect nucleosome remodelling. Most previous studies suggested that – at the level of single nucleosomes – acetylation of H4K16 within the basic patch inhibits ISWI activity, but the extent and nature of the effect remained controversial [23,30,37–39,54,57]. We reassessed the effect of H4K16ac on ISWI activity in the context of defined, folded nucleosome and chromatosome arrays that resemble the physiological remodelling substrate. In our quantitative biochemical analyses, the acetylation neither inhibited ISWI nor ACF activity.

In contrast to the prevalent interpretation of earlier reports [23,37,54], we found the maximal ATP turnover by ISWI undisturbed by H4K16ac in the context of chromatin arrays. Small effects of the acetylation observed upon stimulation of DNA-bound ISWI with H4 peptides were well within the experimental variability of our carefully controlled assays and therefore should not be interpreted any further.

Not only the ATPase, but also the remodelling activity of ISWI on nucleosome arrays was not inhibited by H4K16ac. Differential labelling of unmodified and acetylated arrays allowed us to analyse remodelling of both substrates in the same reaction. Therefore, the assay was very sensitive to H4K16ac-dependent variations in remodelling progress, and ISWI activity was easily quantifiable. Tuning the assay conditions by varying the enzyme or substrate concentrations permitted to distinguish effects of the acetylation on different steps of ISWI catalysis. Due to the competitive substrate conditions, relative affinities of ISWI to the two array types could be isolated. Whereas H4K16ac did not influence steps of ISWI remodelling subsequent to nucleosome binding, our results indicated preferred binding to the acetylated fibre. This preference could simply reflect a higher affinity of ISWI for nucleosomes carrying H4K16ac. Alternatively, H4 tail availability and access of ISWI to the nucleosome substrate might be facilitated by H4K16ac-promoted unfolding of the fibre [30–32,39,46]. Other scenarios are also possible. For example, H4K16 acetylation may facilitate dimerization of ISWI [18]. In any case, the observed difference in remodelling velocity was modest (1.5-fold) and absent when ISWI was part of the physiologically relevant ACF complex.

Regulation of ISWI by the linker histone H1

ISWI can remodel chromatosomes in the context of arrays, although with reduced efficiency in comparison to nucleosomes [43]. Here, we confirmed this finding and additionally report a two-fold reduction in ISWI ATPase activity in presence of the linker histone. This reduction was independent of H4K16 acetylation.

The nature of the inhibitory effect of H1 on ISWI activity remains to be determined. It is conceivable that a combination of mechanisms is in play. For example, H1 might directly hinder nucleosome sliding by blocking the entry or exit of DNA [58–60]. Association of H1 with the nucleosome is furthermore expected to interfere with productive ISWI interaction via the ISWI SANT-SLIDE domain, which is required for efficient nucleosome sliding

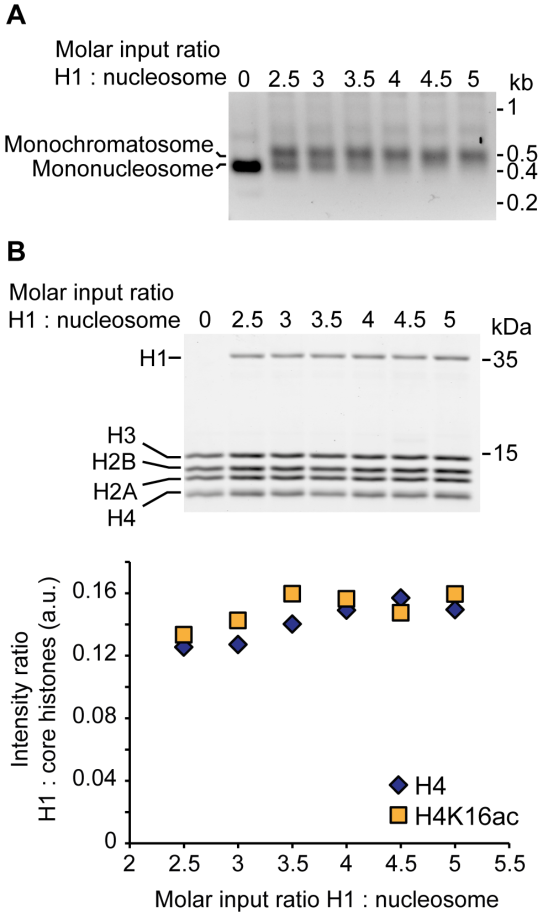

Figure 5. Reconstitution of chromatosome arrays. (A) AvaI digests of chromatosome arrays carrying H4K16ac. Chromatosome arrays were reconstituted with increasing amounts of H1, purified by $MgCl_2$ precipitation and digested to monomers with AvaI. Mononucleosomes were separated from chromatosomes on native agarose gels and visualized by ethidium bromide stain. Faint additional bands may contain coprecipitating competitor DNA or multimers arising from incomplete AvaI digest. (kb: kilobases). (B) Analysis of the relative ratio of H1 to core histones in chromatosome arrays. Top: Chromatosome arrays from the H1 titration shown in A were loaded onto SDS gels and the protein content visualized by Coomassie stain. The gel of the acetylated chromatosome arrays is depicted. Bottom: Quantification of the relative ratio of H1 to core histones. The theoretically expected ratio of 0.24 for a 1:1 stoichiometry of H1 to octamers was not reached, presumably because the Coomassie staining did not linearly correlate with the molecular weight of the proteins [79]. (kDa: kilodaltons; a.u.: arbitrary units).

doi:10.1371/journal.pone.0088411.g005

[5,6]. Moreover, H1 binding effectively reduces the accessible length of linker DNA, which might lead to decreased ISWI activity, as ISWI as well as ACF activity depends on the linker length [16,61–65]. Finally, the high degree of array compaction induced by H1 incorporation [31,47] might hinder ISWI access and chromatosome repositioning. The latter effect may be partially antagonized by the chromatin unfolding effect of H4K16ac [31], resulting in enhanced remodelling of acetylated chromatosome arrays. Although an effect of H4K16ac was not apparent in the ATPase assay, it remains possible that H4K16ac facilitates remodelling of chromatosome arrays.

We were surprised about the pronounced dependency of ISWI remodelling velocity on small variations in the amount of linker histone during array reconstitution and suspect that excess H1 readily occupies secondary binding sites in fibres [66–68], thereby affecting ISWI remodelling. Unfortunately, we cannot exclude subtle differences in H1 stoichiometry between acetylated and unmodified chromatosome arrays, which hampered analysing the effect of the H4K16 acetylation on ISWI remodelling.

Investigating remodelling on chromatin fibres with physiological nucleosome spacing and linker histone content allowed us to shed light on the effect of H4K16 acetylation on ISWI catalysis. Our study highlights the usefulness of the *in vitro* system for the dissection of the function of histone modifications. A technical challenge that needs to be tackled is to generate histones with combinatorial histone marks, as they are emerging to be of key importance in regulating chromatin processes [69,70].

In vivo implications

ISWI activity *in vivo* has been suggested to promote chromatin compaction [13,41,71], whereas H4K16ac seems to be involved in the establishment and maintenance of decondensed regions of chromatin [34–36]. Common models postulate that H4K16ac contributes to chromatin decompaction, amongst others, by inhibiting ISWI [1,38]. Notably, this mechanism was proposed to play a role in dosage compensation in *Drosophila*. Our findings do not support the simplest of such models, as we did not observe reduced activity of ISWI in presence of the acetylation. However, *in vivo* the local context of the chromatin fibre is expected to influence ISWI activity at regions enriched in H4K16ac. This includes associated factors, histone variants and modifications, as well as the concentration of remodelling complexes, their subunit stoichiometry and modification state.

Materials and Methods

Expression and purification of remodelling enzymes

ISWI. *D. melanogaster* ISWI harbouring an N-terminal His_6-TEV tag was bacterially expressed (BL21(DE3)) and purified as described [72]. In brief, a nickel affinity purification was performed by FPLC using a HisTrap column (GE healthcare) in 50 mM Tris-Cl pH 7.4, 300 mM NaCl and 20–400 mM imidazole. TEV-cleavage was followed by another nickel affinity chromatography step to remove uncleaved protein and His-tagged TEV protease. The flow-through was applied to a Mono S column (GE Healthcare) in 15 mM Tris-Cl pH 8, 1 mM β-mercaptoethanol and 100–2000 mM NaCl. For the final gel filtration, a Superdex 200 column (GE healthcare) in 50 mM Hepes-KOH pH 7.6, 0.2 mM EDTA, 200 mM KOAc, 10 mM β-mercaptoethanol was used. Enzyme concentration was determined by absorption measurement at 280 nm (extinction coefficient: 119950 cm^{-1} M^{-1}). The pPROEX-HTb-based expression plasmid was a kind gift from C. Mueller (EMBL, Heidelberg).

ACF. *D. melanogaster* ACF complex was purified from Sf21 cells co-expressing flag-ISWI and Acf1-flag from baculovirus constructs. The baculovirus stocks were kind gifts from C. Wu [73] and J. Kadonaga [74], respectively. Virus-infected Sf21 cells were harvested, resuspended in 100 mM Tris-Cl pH 7.8, 500 mM KOAc, 10% glycerol supplemented with protease inhibitors, and lysed by ultrasonication (Branson). Flag affinity purification was performed using M2 agarose beads (Sigma). Contaminations as well as excess flag-ISWI were removed by Mono Q ion exchange chromatography (12 mM Tris-Cl pH 8, 1 M urea, 1 mM DTT, and 240–880 mM NaCl) followed by Superose 6 gel filtration (100 mM Tris-Cl pH 7.8, 500 mM KOAc, 1.5 mM $Mg(OAc)_2$, 1 M urea, 10% glycerol, 10 mM DTT, 0.2% CHAPSO) (both columns GE Healthcare). Fractions containing monomeric ACF

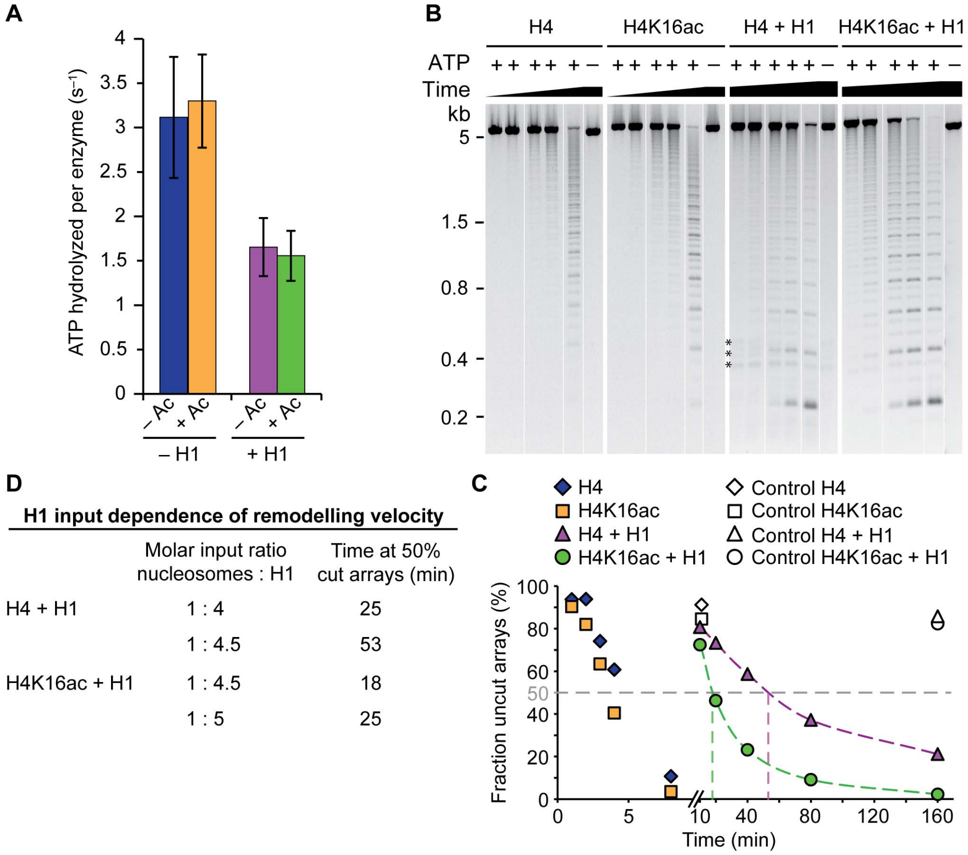

H1 input dependence of remodelling velocity

	Molar input ratio nucleosomes : H1	Time at 50% cut arrays (min)
H4 + H1	1 : 4	25
	1 : 4.5	53
H4K16ac + H1	1 : 4.5	18
	1 : 5	25

Figure 6. H1 inhibits ISWI activity. (A) Steady-state ATPase assay. Saturating concentrations (600 nM) of unmodified (– Ac) or acetylated (+ Ac) chromatosome arrays (+ H1) were employed to stimulate ISWI (100 nM) in presence of saturating ATP (1 mM). ATP hydrolysis rates for nucleosome arrays (– H1) were taken from Figure 2. Error bars represent standard deviations (– H1: n = 5; + H1 n = 6). (B) Exemplary remodelling assay using nucleosome and chromatosome arrays (200 nM) as substrates for ISWI (50 nM) at 100 μM ATP. The chromatosome arrays had been reconstituted with a 1:4.5 molar ratio of nucleosomes to H1. The assay was performed as in Figure 3 except that the arrays lacked a fluorescent label and all array types were tested in separate reactions. The DNA was visualized by ethidium bromide stain. All samples of a reaction were loaded onto one gel and empty lanes were spliced out. ATP was omitted from control reactions (–). The most prominent DNA bands comprise multiples of 197 bp reflecting the distance between two AluI sites within the array (Figure 1A). Faint interspersed bands arose from a single AluI cut; they harbour one of the ends of the array DNA and therefore deviate in length from the internal cleavage products. Asterisks mark DNA bands originating from contaminating competitor DNA. (kb: kilobases). (C) Quantification of the experiment depicted in B. Analysis was done as in Figure 3C. (D) Summary of the remodelling activity of ISWI on chromatosome arrays reconstituted with different input amounts of H1 (see B and Figure S4).
doi:10.1371/journal.pone.0088411.g006

were pooled, concentrated (Microcon-30 kDa Centrifugal Filters; Millipore) and flash frozen in liquid nitrogen. Concentration of the complex was determined by measuring absorption at 280 nm (extinction coefficient: 244220 cm^{-1} M^{-1}).

Reconstitution of nucleosome and chromatosome arrays

DNA preparation. The array DNA, comprising 25 consecutive repeats of a 197 bp Widom-601 nucleosome positioning sequence derivative, was excised with HincII and EcoRI from a pUC18-based plasmid (a kind gift from D. Rhodes, NTU, Singapore). The vector backbone was fragmented further to pieces that served as competitor DNA in the reconstitution reactions by either DraI or combinations of DraI with AseI and DdeI (all from NEB). For the assembly of chromatosome arrays, the vector backbone was cleaved with all three enzymes, yielding fragments not exceeding 445 bp, because in presence of H1 longer histone-bound competitor DNA fragments tended to co-precipitate with the arrays in the $MgCl_2$ precipitation step. After restriction enzyme digest, the DNA was purified by phenol/chloroform/isoamyl alcohol extraction. For the fluorescent labelling, array DNA was purified from the vector backbone fragments (generated with DraI and DdeI) by PEG6000 (5.5–6%) precipitation. The EcoRI end of the array DNA was labelled with either dUTP-DY-682 or dUTP-DY-776 (Dyomics) using Klenow-exo^{-} polymerase (NEB). Unincorporated nucleotides as well as proteins were removed by phenol/chloroform/isoamyl alcohol extraction and purification over gel filtration-columns (Micro Bio-Spin P-30 Gel Column; Bio-Rad).

Generation of acetylated histone H4. *X. laevis* histone H4 quantitatively acetylated at lysine 16 (K16) was prepared as described previously [32] (see also Figure S1). Quantitative acetylation of K16 was controlled by tandem mass spectrometry analysis of histone H4 incorporated into arrays. The proteins of the arrays were loaded on an 18% SDS gel and stained with Coomassie. The H4 band was excised, chemically acetylated with deuterated acetic anhydride and digested into peptides using trypsin as described previously [75]. Tryptic peptides were injected in an Ultimate HPLC system (LC Packings Dionex). Samples were desalted on-line in a C18 microcolumn (300 μm i.d. ×5 mm, packed with C18 PepMap™, 5 μm, 100 Å; LC Packings) and peptides were separated with a gradient from 5 to 60% acetonitrile in 0.1% formic acid over 40 min at 300 nl/min on a C18 analytical column (75 μm i.d. ×15 cm, packed in-house with Reprosil Pur C18 AQ 2.4 μm; Doctor Maisch). The effluent from the HPLC was directly electrosprayed into a linear trap quadrupole-Orbitrap mass spectrometer (Thermo Fisher Scientific). The MS instrument was programmed to acquire survey full-scan MS spectra (m/z 718–730) in the Orbitrap with resolution R = 15,000 at m/z 400 (after accumulation to a "target value" of 500,000 in the linear ion trap) followed by the isolation to a target value of 10,000 and fragmentation by collision-induced dissociation of the masses corresponding to the second isotope of the one, two and three times acetylated H4 4–17 peptide (724.95, 723.44, 721.92 m/z). Typical MS conditions were spray voltage, 1.5 kV; no sheath and auxiliary gas flow; heated capillary temperature, 200°C; normalized collision-induced dissociation energy 35%; activation q = 0.25; and activation time = 30 ms.

Octamer assembly. Histone octamers were reconstituted from bacterially expressed histones H2A, H2B, H3 and H4 that was acetylated (see above) or unmodified. Reconstitution was done as described [76] with the following modifications. Lyophilized histones were resolved in 20 mM Tris-Cl pH 7.5, 7 M guanidinium-HCl, 10 mM DTT. Dissolved histones were mixed and extensively dialysed against 10 mM Tris-Cl pH 7.5, 2 M NaCl, 1 mM EDTA pH 8, 5 mM β-mercaptoethanol. Assembled octamers were purified by gel filtration in the same buffer (Superdex 200), and stoichiometric incorporation of the histones was controlled by SDS-PAGE and Coomassie stain. The octamers were concentrated (Amicon Ultra-4 Centrifugal Filter Units 30 kDa; Millipore), flash frozen in liquid nitrogen, and stored at -80°C. Concentrations of the octamer preparations were determined by absorption measurement at 280 nm (extinction coefficient: 44700 cm^{-1} M^{-1}). All histones comprised the *D. melanogaster* amino acid sequence, except for histone H4 that harboured the *X. laevis* sequence. *X. laevis* and *D. melanogaster* histone H4 vary in only one amino acid at position 1. This amino acid was shown not to be essential for ISWI activity in a previous study [23]. Furthermore, both *D. melanogaster* and *X. laevis* nucleosomes stimulate ISWI ATP hydrolysis [20,23].

Linker histone H1. Native linker histone was purified from 0–12 h after egg laying *D. melanogaster* embryos as previously decribed [77] with the following modifications. The H1-containing supernatant of the second ammonium sulphate precipitation was subjected to phenyl sepharose chromatography (column volume: 20 ml; Phenyl Sepharose 6 Fast Flow; GE Healthcare). The pooled H1-containing fractions were subjected to extensive dialysis against 25 mM Hepes-KOH pH 7.6, 100 mM KCl, 0.1 mM EDTA, 10% glycerol, 5 mM β-mercaptoethanol. For the final cation exchange step, a Mono S column was used. H1-containing fractions were pooled, concentrated (Amicon Ultra-4 Centrifugal Filter Units 10 kDa; Millipore), and glycerol was added to 50% for storage at −20°C. H1 concentration was determined by Coomassie staining of SDS gels taking BSA as a reference. Band intensities were quantified using the Odyssey Infrared Imaging System (LI-COR). The yield from 60 g of embryos was ~1 mg of H1.

Array reconstitution. Nucleosome as well as chromatosome arrays were reconstituted by salt gradient dialysis over approximately 24 h at 4°C [44]. The final buffer contained 10 mM Tris-Cl pH 7.6, 50 mM NaCl, 1 mM EDTA pH 8, 0.01% NP-40, 1 mM DTT. pUC18 vector backbone fragments served as low affinity competitors for histones in the reconstitution reactions. The mass ratio of array to competitor DNA was 2:1. To determine the histone octamer concentrations needed to saturate the arrays, titrations were performed. Since the mass of a histone octamer (~108 kDa) is comparable to the mass of 197 bp of DNA (~122 kDa), the indicated mass ratios of array DNA to histone octamers are similar to the respective molar ratios of Widom-601 nucleosome positioning sequences to octamers. The assembled arrays were purified by $MgCl_2$ precipitation [53] with a final magnesium concentration of 3.5 to 4.4 mM for the nucleosome and 3.25 mM for the chromatosome arrays.

Quality control of the arrays. Saturation of the arrays with histone octamers and linker histone was controlled essentially as described previously [43]. Array preparations (amounts corresponding to approximately 150–200 ng array DNA) were loaded onto native 0.7% agarose gels in 0.2x TB buffer before and after $MgCl_2$ precipitation, and the DNA was visualised by staining with ethidium bromide. Purified arrays (65 fmol according to measurements of the DNA content at 260 nm) were digested into monomers with AvaI (15 U; NEB) in 10 mM Hepes-NaOH pH 7.6, 50 mM KCl, 1.5 mM $MgCl_2$, 0.5 mM EGTA pH 8 for 75 min at 26°C (15 μl final volume). The reactions were analysed on 1.1% native agarose gels as above. To probe for accessibility of the AluI site, the arrays (82 fmol) were incubated for 1 h at 26°C with AluI (10 U; NEB) in 25 mM Hepes-KOH pH 7.6, 50 mM NaCl, 1 mM $MgCl_2$, 0.1 mM EDTA, 10% glycerol, 1 mM DTT (20 μl final volume). The digest was stopped by addition of EDTA (20–40 mM) and SDS (0.3–1%), followed by Proteinase K treatment (Genaxxon). The array DNA fragments were purified by ethanol precipitation and resolved on ethidium bromide-containing agarose gels. Stoichiometric incorporation of the histone octamers and H1 were controlled by separating the protein content of the purified arrays on SDS gels (15–18%) and staining with Coomassie. The relative protein ratios were determined by quantifying the intensities of the protein bands using the Odyssey Infrared Imaging System (LI-COR). To achieve saturating levels of H1 in the reconstitution reactions, an excess of H1 relative to nucleosomes had to be added. This is presumably due to several factors including presence of the competitor DNA, loss of H1 on plastic surfaces and inaccuracies in protein concentration determination [78].

Enzyme assays

Unless indicated otherwise, all assays were performed at 26°C in a buffer containing 25 mM Hepes-KOH pH 7.6, 50 mM NaCl, 1 mM $MgCl_2$, 0.1 mM EDTA, 0.2 g/l BSA, 10% glycerol and 1 mM DTT or 10 mM β-mercaptoethanol and in presence of an ATP regenerating system consisting of phosphoenolpyruvate (2–6 mM), a pyruvate kinase-lactate dehydrogenase mixture (15.5 U/ml; Sigma) and NADH (0.5 mM). For remodelling and sliding assays, NADH was omitted from the regenerating system. ATP was always added in a stoichiometric complex with Mg^{2+}. Concentrations of nucleosome and chromatosome arrays were determined by quantifying the DNA content via absorption measurement at 260 nm. Indicated molar concentrations refer to individual nucleosomes.

Steady-state ATPase assay. ATP hydrolysis was measured by a coupled ATPase assay as described [72] with the indicated concentrations and buffer conditions. In the array-stimulated ATPase assay, a 4-fold lower ATP concentration yielded comparable rates within 75% regardless of array type, indicating saturation with ATP. Unmodified and acetylated *D. melanogaster* H4 N-terminal peptides comprising amino acids 1–24 were purchased from Peptide Specialty Laboratories (counter ion: bicarbonate; H4 (and H4K16ac) peptide: TGRGKGGKGLGKGGAK(ac)RHRKVLRD, scrambled peptide: KLRRGGKacGDVKTGKLGGRKAGRGH (ac: acetylation)). The lyophilized peptides were dissolved in 10 mM Hepes-KOH pH 7.6, and relative peptide concentration was controlled by absorption measurement at 214 and 220 nm. Peptide-stimulated ISWI ATPase activity was followed in 25 mM Hepes-KOH pH 7.6, 100 mM KOAc, 1.5 mM $Mg(OAc)_2$, 0.1 mM EDTA, 0.2 g/l BSA, 10% glycerol, 1 mM DTT.

Remodelling assay. To follow remodelling, arrays were incubated with ATP and ISWI or ACF at the indicated concentrations along with 0.5 U/µl AluI (NEB) [43,52]. After terminating the reaction by addition of EDTA (20–40 mM) and SDS (0.33–0.4%), the samples were deproteinized. The DNA was purified by ethanol precipitation and resolved on a 0.9% agarose gel. Fluorescently labelled DNA was visualized using the Odyssey Infrared Imaging System (LI-COR), and band intensities were quantified with the Odyssey software. Unlabelled DNA was quantified after ethidium bromide staining by densitometry (AIDA; raytest). To assure that AluI was not limiting, 4–5-fold lower concentrations were tested, yielding results that deviated by less than 2-fold regardless of the reaction conditions. Saturation with ISWI was controlled by using a 3.3-fold lower enzyme concentration. Under these conditions, remodelling was slightly faster (1.6-fold), which is in full agreement with previous observations of ISWI remodelling slowing down with increasing enzyme concentrations [52] and confirmed saturation.

Sliding assay. The sliding assay was performed as described [52,55] with the indicated concentrations. Longer AvaI digests with higher enzyme concentrations yielded comparable results.

Supporting Information

Figure S1 **Synthesis of histone H4 site-specifically acetylated at lysine 16.** (A) Scheme of the semi-synthetic method applied for generation of the acetylated H4 [32]. A truncated H4 harbouring amino acids (aa) 20–102 with lysine 20 mutated to cysteine (C_{20}) was bacterially expressed and purified. Using native chemical ligation, this H4 derivative was N-terminally fused to a chemically synthesized peptide comprising aa 1–19 of H4 carrying an acetylation (Ac) on lysine 16 (K_{16}). Next, C_{20} was converted into a lysine analogue (K_S) by S-alkylation. (B) Structure of lysine (K) and the lysine analogue (K_S). Except for the thioether in the side chain of the lysine analogue at position 20, the synthesized acetylated H4 bore the canonical aa sequence. (C) Full survey spectrum of the unmodified (top: H4) and the site-specifically acetylated (bottom: H4K16ac) peptide 4–17 of histone H4. The analysis was performed on histones that were incorporated into nucleosome arrays. The protein content of the arrays was separated on an SDS gel, stained with Coomassie, and the histone H4 band was excised. Prior to trypsin digestion, the non-acetylated lysines were chemically acetylated with deuterated acetic anhydride (Ac_3). Acetylation prevented trypsin from cutting after lysine, and therefore longer peptides were generated. (M: molecule; m/z: mass-to-charge ratio; m: monoisotopic mass value; Δm: difference between the expected and the measured masses; R: resolution of the mass spectrometry measurement). (D) Determination of the acetylated lysine in the monoacetylated peptide H4K16ac. To determine which of the four lysine residues (K5, K8, K12 or K16) within the 4–17 peptide was acetylated, the b- and y-ions were analysed. For the y_5-ion comprising K16 a peak corresponding to the naturally acetylated ion (+Ac) was detected, whereas no peak corresponding to the chemically acetylated peptide ($+Ac_3$) was observed (inset I). Furthermore, for the b_9-ion comprising the other three lysine residues of the analysed peptide (K5, K8 and K12) only a peak corresponding to the three-times chemically acetylated ion ($+3xAc_3$) was detected. No ions carrying one natural acetylation along with two chemically introduced ones were present ($+1xAc +2xAc_3$). This result proves that the single natural acetylation in the H4K16ac peptide observed in panel C was indeed located on K16.
(TIF)

Figure S2 **Quality controls of the histone octamers and nucleosome arrays.** (A) Example of a Coomassie-stained SDS gel to control relative histone stoichiometry on purified saturated nucleosome arrays. (B) Native agarose gels of the nucleosome arrays from Figure 1B before and after $MgCl_2$ precipitation. Samples of the reconstitution reactions directly after assembly (i), the pellet fraction after $MgCl_2$ precipitation (p), and the corresponding supernatant (SN) were loaded. The gels were stained with ethidium bromide after the run. The nucleosome arrays ran well above the 5 kb DNA marker band, where free array DNA would be expected. A homogenous population of fully saturated arrays was indicated by one sharp band. Excess histone octamers present in the reconstitution reaction bound to the competitor DNA resulting in a band shift. After $MgCl_2$ precipitation only the nucleosome arrays were retained in the pellet, no contaminating competitor DNA was present. Only fully saturated arrays precipitated quantitatively with $MgCl_2$. (C) AluI digests of the purified nucleosome arrays from B. The purified DNA was loaded onto agarose gels and stained with ethidium bromide. In fully saturated arrays (histone octamer to DNA ratio of 1.4:1) all AluI sites were protected by a nucleosome and the array DNA was not cut by the enzyme. Contrary, unoccupied Widom-601 sites in non-saturated arrays exposed an AluI site and got cut, giving rise to a ladder of DNA fragments. (kb: kilobases).
(TIF)

Figure S3 **ISWI ATPase activity in presence of nucleosome and chromatosome arrays.** Result of an exemplary steady-state ATPase assay. The assay was performed as in Figure 2A and 6A employing different concentrations of nucleosome and chromatosome arrays. Reactions were performed in duplicates or triplicates. Data were fit to single exponential functions (dashed lines; Kaleidagraph). Note that no affinities were retrievable, as ISWI at 100 nM was not subsaturating. Nevertheless, nucleosome array concentrations needed for enzyme saturation could be extracted.
(TIF)

Figure S4 **Remodelling of chromatosome arrays reconstituted with different H1 input amounts.** Remodelling of unmodified and acetylated chromatosome arrays assembled with different molar ratios of nucleosomes to H1 (indicated in brackets) was performed and analysed as in Figure 6B, C. Control reactions did not contain ATP.
(TIF)

Acknowledgments

We are grateful to H. Schiessel and R. Schram (Leiden University, Netherlands) for stimulating discussions. We thank A. Allahverdi (Nanyang Technological University, Singapore) for discussions and preparing *X. laevis* histone H4; A. Imhof (LMU, Munich, Germany) for support in the mass spectrometry analysis; C. Haas (LMU, Munich, Germany) for assistance in protein purification; J. Ludwigsen, N. Hepp and S. Vollmer (LMU, Munich, Germany) for providing recombinant proteins and *D. melanogaster* embryo extract.

Author Contributions

Conceived and designed the experiments: HK FMP PBB. Performed the experiments: HK IF. Analyzed the data: HK FMP IF PBB. Contributed reagents/materials/analysis tools: RY CFL LN. Wrote the paper: HK FMP PBB.

References

1. Clapier CR, Cairns BR (2009) The biology of chromatin remodeling complexes. Annu Rev Biochem 78: 273–304.
2. Flaus A, Martin DM, Barton GJ, Owen-Hughes T (2006) Identification of multiple distinct Snf2 subfamilies with conserved structural motifs. Nucleic Acids Res 34: 2887–2905.
3. Becker PB, Workman JL (2013) Nucleosome remodeling and epigenetics. Cold Spring Harb Perspect Biol 5.
4. Yadon AN, Tsukiyama T (2011) SnapShot: Chromatin remodeling: ISWI. Cell 144: 453–453 e451.
5. Mueller-Planitz F, Klinker H, Becker PB (2013) Nucleosome sliding mechanisms: new twists in a looped history. Nat Struct Mol Biol 20: 1026–1032.
6. Narlikar GJ, Sundaramoorthy R, Owen-Hughes T (2013) Mechanisms and functions of ATP-dependent chromatin-remodeling enzymes. Cell 154: 490–503.
7. Corona DF, Langst G, Clapier CR, Bonte EJ, Ferrari S, et al. (1999) ISWI is an ATP-dependent nucleosome remodeling factor. Mol Cell 3: 239–245.
8. Gelbart ME, Rechsteiner T, Richmond TJ, Tsukiyama T (2001) Interactions of Isw2 chromatin remodeling complex with nucleosomal arrays: analyses using recombinant yeast histones and immobilized templates. Mol Cell Biol 21: 2098–2106.
9. He X, Fan HY, Narlikar GJ, Kingston RE (2006) Human ACF1 alters the remodeling strategy of SNF2h. J Biol Chem 281: 28636–28647.
10. Ito T, Bulger M, Pazin MJ, Kobayashi R, Kadonaga JT (1997) ACF, an ISWI-containing and ATP-utilizing chromatin assembly and remodeling factor. Cell 90: 145–155.
11. Torigoe SE, Urwin DL, Ishii H, Smith DE, Kadonaga JT (2011) Identification of a rapidly formed nonnucleosomal histone-DNA intermediate that is converted into chromatin by ACF. Mol Cell 43: 638–648.
12. Varga-Weisz PD, Wilm M, Bonte E, Dumas K, Mann M, et al. (1997) Chromatin-remodelling factor CHRAC contains the ATPases ISWI and topoisomerase II. Nature 388: 598–602.
13. Corona DF, Tamkun JW (2004) Multiple roles for ISWI in transcription, chromosome organization and DNA replication. Biochim Biophys Acta 1677: 113–119.
14. Erdel F, Rippe K (2011) Chromatin remodelling in mammalian cells by ISWI-type complexes–where, when and why? FEBS J 278: 3608–3618.
15. Zofall M, Persinger J, Kassabov SR, Bartholomew B (2006) Chromatin remodeling by ISW2 and SWI/SNF requires DNA translocation inside the nucleosome. Nat Struct Mol Biol 13: 339–346.
16. Dang W, Kagalwala MN, Bartholomew B (2006) Regulation of ISW2 by concerted action of histone H4 tail and extranucleosomal DNA. Mol Cell Biol 26: 7388–7396.
17. Schwanbeck R, Xiao H, Wu C (2004) Spatial contacts and nucleosome step movements induced by the NURF chromatin remodeling complex. J Biol Chem 279: 39933–39941.
18. Racki LR, Yang JG, Naber N, Partensky PD, Acevedo A, et al. (2009) The chromatin remodeller ACF acts as a dimeric motor to space nucleosomes. Nature 462: 1016–1021.
19. Luger K, Mader AW, Richmond RK, Sargent DF, Richmond TJ (1997) Crystal structure of the nucleosome core particle at 2.8 A resolution. Nature 389: 251–260.
20. Clapier CR, Langst G, Corona DF, Becker PB, Nightingale KP (2001) Critical role for the histone H4 N terminus in nucleosome remodeling by ISWI. Mol Cell Biol 21: 875–883.
21. Hamiche A, Kang JG, Dennis C, Xiao H, Wu C (2001) Histone tails modulate nucleosome mobility and regulate ATP-dependent nucleosome sliding by NURF. Proc Natl Acad Sci U S A 98: 14316–14321.
22. Eberharter A, Ferrari S, Langst G, Straub T, Imhof A, et al. (2001) Acf1, the largest subunit of CHRAC, regulates ISWI-induced nucleosome remodelling. EMBO J 20: 3781–3788.
23. Clapier CR, Nightingale KP, Becker PB (2002) A critical epitope for substrate recognition by the nucleosome remodeling ATPase ISWI. Nucleic Acids Res 30: 649–655.
24. Fazzio TG, Gelbart ME, Tsukiyama T (2005) Two distinct mechanisms of chromatin interaction by the Isw2 chromatin remodeling complex in vivo. Mol Cell Biol 25: 9165–9174.
25. Pepenella S, Murphy KJ, Hayes JJ (2013) Intra- and inter-nucleosome interactions of the core histone tail domains in higher-order chromatin structure. Chromosoma.
26. Gordon F, Luger K, Hansen JC (2005) The core histone N-terminal tail domains function independently and additively during salt-dependent oligomerization of nucleosomal arrays. J Biol Chem 280: 33701–33706.
27. Dorigo B, Schalch T, Bystricky K, Richmond TJ (2003) Chromatin fiber folding: requirement for the histone H4 N-terminal tail. J Mol Biol 327: 85–96.
28. Kan PY, Caterino TL, Hayes JJ (2009) The H4 tail domain participates in intra- and internucleosome interactions with protein and DNA during folding and oligomerization of nucleosome arrays. Mol Cell Biol 29: 538–546.
29. Wang X, Hayes JJ (2008) Acetylation mimics within individual core histone tail domains indicate distinct roles in regulating the stability of higher-order chromatin structure. Mol Cell Biol 28: 227–236.
30. Shogren-Knaak M, Ishii H, Sun JM, Pazin MJ, Davie JR, et al. (2006) Histone H4-K16 acetylation controls chromatin structure and protein interactions. Science 311: 844–847.
31. Robinson PJ, An W, Routh A, Martino F, Chapman L, et al. (2008) 30 nm chromatin fibre decompaction requires both H4-K16 acetylation and linker histone eviction. J Mol Biol 381: 816–825.
32. Allahverdi A, Yang R, Korolev N, Fan Y, Davey CA, et al. (2011) The effects of histone H4 tail acetylations on cation-induced chromatin folding and self-association. Nucleic Acids Res 39: 1680–1691.
33. McBryant SJ, Lu X, Hansen JC (2010) Multifunctionality of the linker histones: an emerging role for protein-protein interactions. Cell Res 20: 519–528.
34. Bell O, Schwaiger M, Oakeley EJ, Lienert F, Beisel C, et al. (2010) Accessibility of the Drosophila genome discriminates PcG repression, H4K16 acetylation and replication timing. Nat Struct Mol Biol 17: 894–900.
35. Shia WJ, Pattenden SG, Workman JL (2006) Histone H4 lysine 16 acetylation breaks the genome's silence. Genome Biol 7: 217.
36. Conrad T, Akhtar A (2011) Dosage compensation in Drosophila melanogaster: epigenetic fine-tuning of chromosome-wide transcription. Nat Rev Genet 13: 123–134.
37. Ferreira H, Flaus A, Owen-Hughes T (2007) Histone modifications influence the action of Snf2 family remodelling enzymes by different mechanisms. J Mol Biol 374: 563–579.
38. Corona DF, Clapier CR, Becker PB, Tamkun JW (2002) Modulation of ISWI function by site-specific histone acetylation. EMBO Rep 3: 242–247.
39. Nightingale KP, Baumann M, Eberharter A, Mamais A, Becker PB, et al. (2007) Acetylation increases access of remodelling complexes to their nucleosome targets to enhance initiation of V(D)J recombination. Nucleic Acids Res 35: 6311–6321.
40. Deuring R, Fanti L, Armstrong JA, Sarte M, Papoulas O, et al. (2000) The ISWI chromatin-remodeling protein is required for gene expression and the maintenance of higher order chromatin structure in vivo. Mol Cell 5: 355–365.
41. Corona DF, Siriaco G, Armstrong JA, Snarskaya N, McClymont SA, et al. (2007) ISWI regulates higher-order chromatin structure and histone H1 assembly in vivo. PLoS Biol 5: e232.
42. Lusser A, Urwin DL, Kadonaga JT (2005) Distinct activities of CHD1 and ACF in ATP-dependent chromatin assembly. Nat Struct Mol Biol 12: 160–166.
43. Maier VK, Chioda M, Rhodes D, Becker PB (2008) ACF catalyses chromatosome movements in chromatin fibres. EMBO J 27: 817–826.
44. Huynh VA, Robinson PJ, Rhodes D (2005) A method for the in vitro reconstitution of a defined "30 nm" chromatin fibre containing stoichiometric amounts of the linker histone. J Mol Biol 345: 957–968.
45. Becker PB, Wu C (1992) Cell-free system for assembly of transcriptionally repressed chromatin from Drosophila embryos. Mol Cell Biol 12: 2241–2249.
46. Oppikofer M, Kueng S, Martino F, Soeroes S, Hancock SM, et al. (2011) A dual role of H4K16 acetylation in the establishment of yeast silent chromatin. EMBO J 30: 2610–2621.
47. Routh A, Sandin S, Rhodes D (2008) Nucleosome repeat length and linker histone stoichiometry determine chromatin fiber structure. Proc Natl Acad Sci U S A 105: 8872–8877.
48. Ner SS, Travers AA (1994) HMG-D, the Drosophila melanogaster homologue of HMG 1 protein, is associated with early embryonic chromatin in the absence of histone H1. EMBO J 13: 1817–1822.
49. Lu X, Simon MD, Chodaparambil JV, Hansen JC, Shokat KM, et al. (2008) The effect of H3K79 dimethylation and H4K20 trimethylation on nucleosome and chromatin structure. Nat Struct Mol Biol 15: 1122–1124.
50. Simon MD, Chu F, Racki LR, de la Cruz CC, Burlingame AL, et al. (2007) The site-specific installation of methyl-lysine analogs into recombinant histones. Cell 128: 1003–1012.
51. Lowary PT, Widom J (1998) New DNA sequence rules for high affinity binding to histone octamer and sequence-directed nucleosome positioning. J Mol Biol 276: 19–42.
52. Mueller-Planitz F, Klinker H, Ludwigsen J, Becker PB (2013) The ATPase domain of ISWI is an autonomous nucleosome remodeling machine. Nat Struct Mol Biol 20: 82–89.
53. Schwarz PM, Hansen JC (1994) Formation and stability of higher order chromatin structures. Contributions of the histone octamer. J Biol Chem 269: 16284–16289.
54. Clapier CR, Cairns BR (2012) Regulation of ISWI involves inhibitory modules antagonized by nucleosomal epitopes. Nature 492: 280–284.
55. Ludwigsen J, Klinker H, Mueller-Planitz F (2013) No need for a power stroke in ISWI-mediated nucleosome sliding. EMBO Rep.
56. van Holde KE (1989) Chromatin. New York: Springer.
57. Georgel PT, Tsukiyama T, Wu C (1997) Role of histone tails in nucleosome remodeling by Drosophila NURF. EMBO J 16: 4717–4726.
58. Bednar J, Horowitz RA, Grigoryev SA, Carruthers LM, Hansen JC, et al. (1998) Nucleosomes, linker DNA, and linker histone form a unique structural motif that directs the higher-order folding and compaction of chromatin. Proc Natl Acad Sci U S A 95: 14173–14178.
59. Pennings S, Meersseman G, Bradbury EM (1994) Linker histones H1 and H5 prevent the mobility of positioned nucleosomes. Proc Natl Acad Sci U S A 91: 10275–10279.

60. Ura K, Hayes JJ, Wolffe AP (1995) A positive role for nucleosome mobility in the transcriptional activity of chromatin templates: restriction by linker histones. EMBO J 14: 3752–3765.
61. Yang JG, Madrid TS, Sevastopoulos E, Narlikar GJ (2006) The chromatin-remodeling enzyme ACF is an ATP-dependent DNA length sensor that regulates nucleosome spacing. Nat Struct Mol Biol 13: 1078–1083.
62. Zofall M, Persinger J, Bartholomew B (2004) Functional role of extranucleosomal DNA and the entry site of the nucleosome in chromatin remodeling by ISW2. Mol Cell Biol 24: 10047–10057.
63. Kagalwala MN, Glaus BJ, Dang W, Zofall M, Bartholomew B (2004) Topography of the ISW2-nucleosome complex: insights into nucleosome spacing and chromatin remodeling. EMBO J 23: 2092–2104.
64. Yamada K, Frouws TD, Angst B, Fitzgerald DJ, DeLuca C, et al. (2011) Structure and mechanism of the chromatin remodelling factor ISW1a. Nature 472: 448–453.
65. Stockdale C, Flaus A, Ferreira H, Owen-Hughes T (2006) Analysis of nucleosome repositioning by yeast ISWI and Chd1 chromatin remodeling complexes. J Biol Chem 281: 16279–16288.
66. Nelson PP, Albright SC, Wiseman JM, Garrard WT (1979) Reassociation of histone H1 with nucleosomes. J Biol Chem 254: 11751–11760.
67. Nightingale KP, Pruss D, Wolffe AP (1996) A single high affinity binding site for histone H1 in a nucleosome containing the Xenopus borealis 5 S ribosomal RNA gene. J Biol Chem 271: 7090–7094.
68. Rodriguez-Campos A, Shimamura A, Worcel A (1989) Assembly and properties of chromatin containing histone H1. J Mol Biol 209: 135–150.
69. Rando OJ (2012) Combinatorial complexity in chromatin structure and function: revisiting the histone code. Curr Opin Genet Dev 22: 148–155.
70. Ruthenburg AJ, Li H, Patel DJ, Allis CD (2007) Multivalent engagement of chromatin modifications by linked binding modules. Nat Rev Mol Cell Biol 8: 983–994.
71. Fyodorov DV, Blower MD, Karpen GH, Kadonaga JT (2004) Acf1 confers unique activities to ACF/CHRAC and promotes the formation rather than disruption of chromatin in vivo. Genes Dev 18: 170–183.
72. Forne I, Ludwigsen J, Imhof A, Becker PB, Mueller-Planitz F (2012) Probing the conformation of the ISWI ATPase domain with genetically encoded photoreactive crosslinkers and mass spectrometry. Mol Cell Proteomics 11: M111 012088.
73. Hamiche A, Sandaltzopoulos R, Gdula DA, Wu C (1999) ATP-dependent histone octamer sliding mediated by the chromatin remodeling complex NURF. Cell 97: 833–842.
74. Ito T, Levenstein ME, Fyodorov DV, Kutach AK, Kobayashi R, et al. (1999) ACF consists of two subunits, Acf1 and ISWI, that function cooperatively in the ATP-dependent catalysis of chromatin assembly. Genes Dev 13: 1529–1539.
75. Villar-Garea A, Israel L, Imhof A (2008) Analysis of histone modifications by mass spectrometry. Curr Protoc Protein Sci Chapter 14: Unit 14 10.
76. Luger K, Rechsteiner TJ, Flaus AJ, Waye MM, Richmond TJ (1997) Characterization of nucleosome core particles containing histone proteins made in bacteria. J Mol Biol 272: 301–311.
77. Croston GE, Kerrigan LA, Lira LM, Marshak DR, Kadonaga JT (1991) Sequence-specific antirepression of histone H1-mediated inhibition of basal RNA polymerase II transcription. Science 251: 643–649.
78. Routh A, Rhodes D (2009) In vitro reconstitution of nucleosome arrays with a stoichiometric content of histone octamer and linker histone (PROT42).
79. Tal M, Silberstein A, Nusser E (1985) Why does Coomassie Brilliant Blue R interact differently with different proteins? A partial answer. J Biol Chem 260: 9976–9980.

Supplementary material

“ISWI Remodelling of Physiological Chromatin Fibres Acetylated at Lysine 16 of Histone H4”

Klinker et al., PLoS ONE, 2014

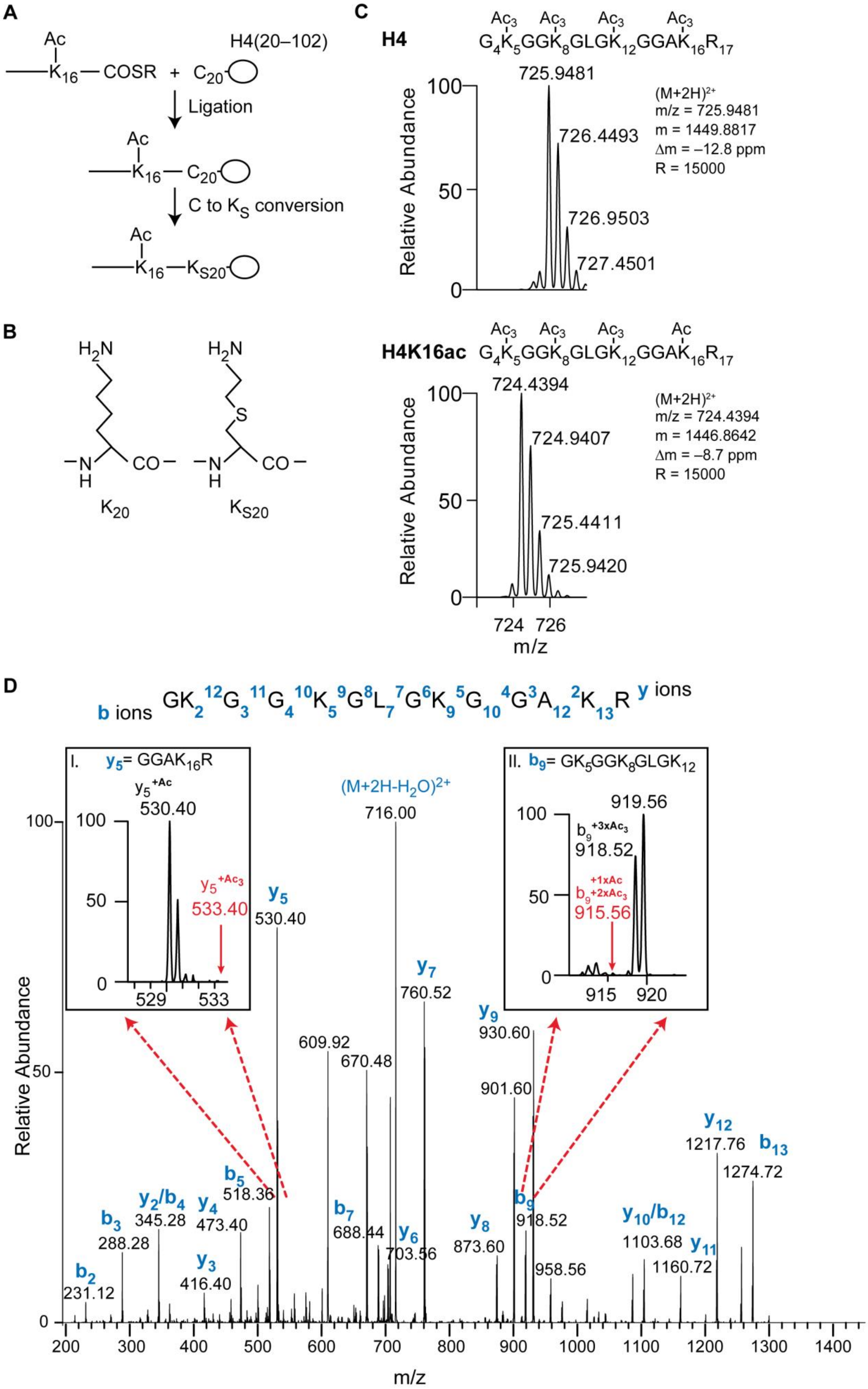
A
Ac
K16
COSR
+
H4(20–102)
C20
Ligation
Ac
K16
C20
C to KS conversion
Ac
K16
KS20
B
H2N
N
H
CO
K20
H2N
S
N
H
CO
KS20
C
H4
Ac3 Ac3 Ac3 Ac3
G4K5GGK8GLGK12GGAK16R17
Relative Abundance
100
50
0
725.9481
726.4493
726.9503
727.4501
(M+2H)2+
m/z = 725.9481
m = 1449.8817
Δm = –12.8 ppm
R = 15000
H4K16ac
Ac3 Ac3 Ac3 Ac
G4K5GGK8GLGK12GGAK16R17
724.4394
724.9407
725.4411
725.9420
(M+2H)2+
m/z = 724.4394
m = 1446.8642
Δm = –8.7 ppm
R = 15000
724
726
m/z
D
b ions
GK2 12 G3 11 G4 10 K5 9 G 8 L7 7 G 6 K9 5 G10 4 G 3 A12 2 K13 R
y ions
I. y5= GGAK16R
y5+Ac
530.40
y5+Ac3
533.40
529
533
II. b9= GK5GGK8GLGK12
919.56
b9+3xAc3
918.52
+1xAc
b9+2xAc3
915.56
915
920
(M+2H-H2O)2+
716.00
y5
530.40
y7
760.52
609.92
670.48
y9
930.60
901.60
y12
1217.76
b13
1274.72
b5
518.36
b7
688.44
y6
703.56
y8
873.60
b9
918.52
y10/b12
1103.68
y11
1160.72
958.56
b2
231.12
b3
288.28
y2/b4
345.28
y4
473.40
y3
416.40
Relative Abundance
100
50
0
200
300
400
500
600
700
800
900
1000
1100
1200
1300
1400
m/z

Figure S1: Synthesis of histone H4 site-specifically acetylated at lysine 16. (A) Scheme of the semi-synthetic method applied for generation of the acetylated H4 [32]. A truncated H4 harbouring amino acids (aa) 20–102 with lysine 20 mutated to cysteine (C_{20}) was bacterially expressed and purified. Using native chemical ligation, this H4 derivative was N-terminally fused to a chemically synthesized peptide comprising aa 1–19 of H4 carrying an acetylation (Ac) on lysine 16 (K_{16}). Next, C_{20} was converted into a lysine analogue (K_S) by S-alkylation. (B) Structure of lysine (K) and the lysine analogue (K_S). Except for the thioether in the side chain of the lysine analogue at position 20, the synthesized acetylated H4 bore the canonical aa sequence. (C) Full survey spectrum of the unmodified (top: H4) and the site-specifically acetylated (bottom: H4K16ac) peptide 4–17 of histone H4. The analysis was performed on histones that were incorporated into nucleosome arrays. The protein content of the arrays was separated on an SDS gel, stained with Coomassie, and the histone H4 band was excised. Prior to trypsin digestion, the non-acetylated lysines were chemically acetylated with deuterated acetic anhydride (Ac_3). Acetylation prevented trypsin from cutting after lysine, and therefore longer peptides were generated. (M: molecule; m/z: mass-to-charge ratio; m: monoisotopic mass value; Δm: difference between the expected and the measured masses; R: resolution of the mass spectrometry measurement). (D) Determination of the acetylated lysine in the monoacetylated peptide H4K16ac. To determine which of the four lysine residues (K5, K8, K12 or K16) within the 4–17 peptide was acetylated, the b- and y-ions were analysed. For the y_5-ion comprising K16 a peak corresponding to the naturally acetylated ion (+Ac) was detected, whereas no peak corresponding to the chemically acetylated peptide ($+Ac_3$) was observed (inset I). Furthermore, for the b_9-ion comprising the other three lysine residues of the analysed peptide (K5, K8 and K12) only a peak corresponding to the three-times chemically acetylated ion ($+3xAc_3$) was detected. No ions carrying one natural acetylation along with two chemically introduced ones were present (+1xAc $+2xAc_3$). This result proves that the single natural acetylation in the H4K16ac peptide observed in panel C was indeed located on K16.

doi:10.1371/journal.pone.0088411.s001

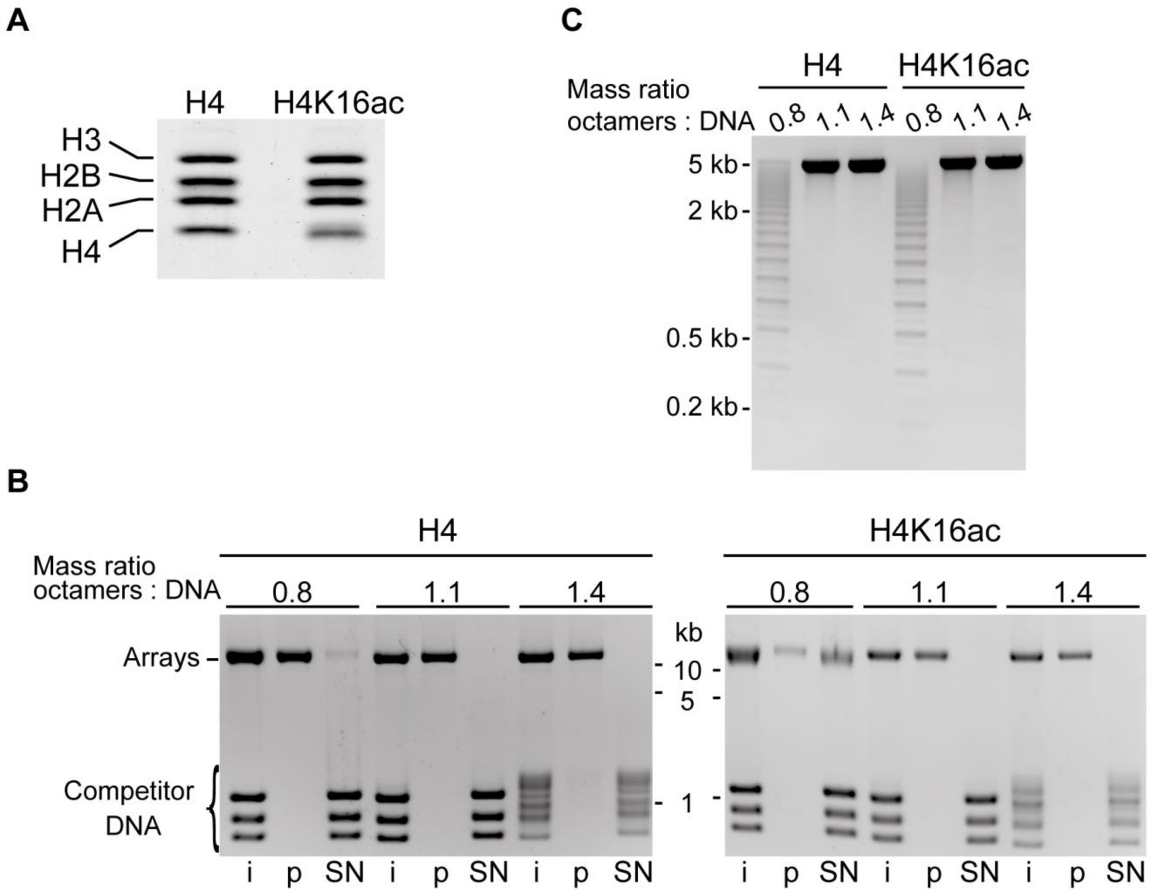
A
H4
H4K16ac
H3
H2B
H2A
H4
C
H4
H4K16ac
Mass ratio
octamers : DNA
0.8
1.1
1.4
0.8
1.1
1.4
5 kb
2 kb
0.5 kb
0.2 kb
B
H4
H4K16ac
Mass ratio
octamers : DNA
0.8
1.1
1.4
0.8
1.1
1.4
Arrays
Competitor DNA
kb
10
5
1
i
p
SN
i
p
SN
i
p
SN
i
p
SN
i
p
SN
i
p
SN

Figure S2: Quality controls of the histone octamers and nucleosome arrays. (A) Example of a Coomassie-stained SDS gel to control relative histone stoichiometry on purified saturated nucleosome arrays. (B) Native agarose gels of the nucleosome arrays from Figure 1B before and after $MgCl_2$ precipitation. Samples of the reconstitution reactions directly after assembly (i), the pellet fraction after $MgCl_2$ precipitation (p), and the corresponding supernatant (SN) were loaded. The gels were stained with ethidium bromide after the run. The nucleosome arrays ran well above the 5 kb DNA marker band, where free array DNA would be expected. A homogenous population of fully saturated arrays was indicated by one sharp band. Excess histone octamers present in the reconstitution reaction bound to the competitor DNA resulting in a band shift. After $MgCl_2$ precipitation only the nucleosome arrays were retained in the pellet, no contaminating competitor DNA was present. Only fully saturated arrays precipitated quantitatively with $MgCl_2$. (C) AluI digests of the purified nucleosome arrays from B. The purified DNA was loaded onto agarose gels and stained with ethidium bromide. In fully saturated arrays (histone octamer to DNA ratio of 1.4:1) all AluI sites were protected by a nucleosome and the array DNA was not cut by the enzyme. Contrary, unoccupied Widom-601 sites in non-saturated arrays exposed an AluI site and got cut, giving rise to a ladder of DNA fragments. (kb: kilobases).

doi:10.1371/journal.pone.0088411.s002

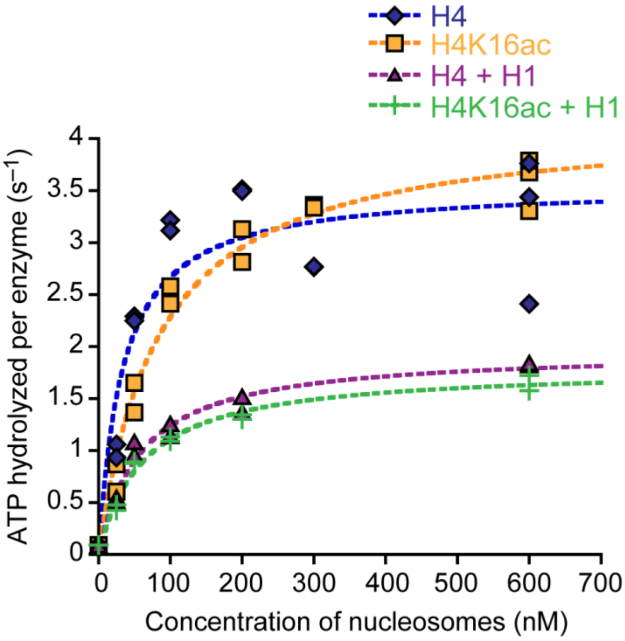

Figure S3: ISWI ATPase activity in presence of nucleosome and chromatosome arrays. Result of an exemplary steady-state ATPase assay. The assay was performed as in Figure 2A and 6A employing different concentrations of nucleosome and chromatosome arrays. Reactions were performed in duplicates or triplicates. Data were fit to single exponential functions (dashed lines; Kaleidagraph). Note that no affinities were retrievable, as ISWI at 100 nM was not subsaturating. Nevertheless, nucleosome array concentrations needed for enzyme saturation could be extracted.

doi:10.1371/journal.pone.0088411.s003

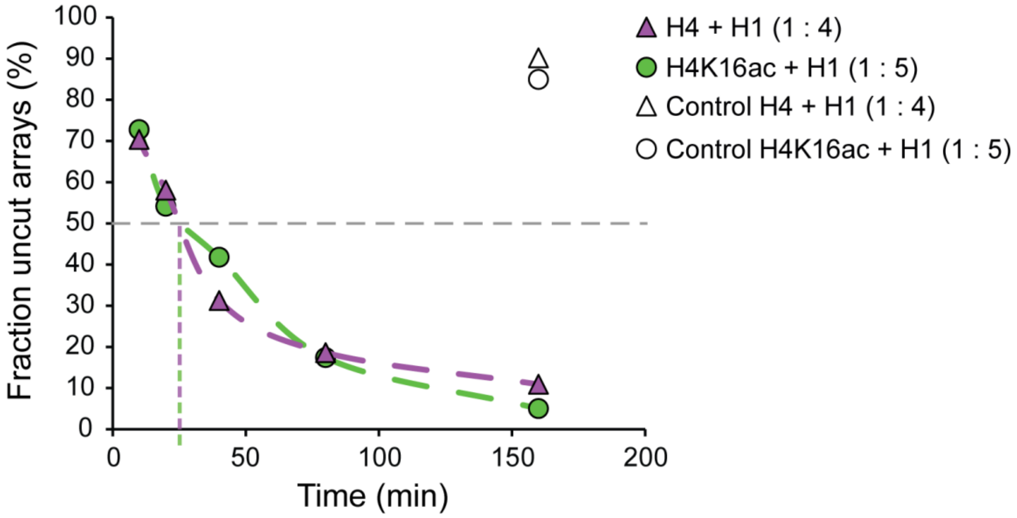

Figure S4: Remodelling of chromatosome arrays reconstituted with different H1 input amounts. Remodelling of unmodified and acetylated chromatosome arrays assembled with different molar ratios of nucleosomes to H1 (indicated in brackets) was performed and analysed as in Figure 6B, C. Control reactions did not contain ATP.

doi:10.1371/journal.pone.0088411.s004

2.5 Rapid purification of recombinant histones

Henrike Klinker[1,2], Caroline Haas[3,4], Peter B. Becker[1,2] and Felix Mueller-Planitz[1]

[1]Adolf Butenandt Institute, [2]Center for Integrated Protein Science Munich,
[3]Department of Biochemistry and [4]Gene Center,
Ludwig-Maximilians-Universität München, Munich, Germany

Important note: The manuscript presented in the following is currently under revision.

Declaration of contributions to "Rapid purification of recombinant histones"

The method described in this manuscript was initially developed by F. Mueller-Planitz. C. Haas and I applied the protocol to purify the canonical Drosophila histones and advanced the method together with F. Mueller-Planitz and his co-workers. C. Haas and I performed all experiments contained in the manuscript in close collaboration. I prepared the figures and wrote the first draft of the manuscript including the figure legends. Together with F. Mueller-Planitz, C. Haas, and P.B. Becker I developed the enclosed version of the manuscript.

Abstract

The development of methods to assemble nucleosomes from recombinant histones decades ago has transformed chromatin research. Nevertheless, nucleosome reconstitution remains time consuming to this day, not least because the four individual histones must be purified first. Here, we present a streamlined purification protocol of recombinant histones from bacteria. We termed this method “rapid histone purification” (RHP) as it circumvents isolation of inclusion bodies and thereby cuts out the most time-consuming step of traditional purification protocols. Instead of inclusion body isolation, whole cell extracts are prepared under strongly denaturing conditions that directly solubilize inclusion bodies. By ion exchange chromatography, the histones are purified from the extracts. The protocol has been successfully applied to all four canonical *Drosophila* and human histones. The quality of histone octamers reconstituted from these histones and from histones that were purified from isolated inclusion bodies was indistinguishable. We expect that the RHP protocol can be readily applied to the purification of canonical histones from other species as well as the numerous histone variants.

Introduction

The development of a method to reconstitute nucleosomes from recombinant histone proteins and DNA constituted a milestone in chromatin research[1-3]. Current research still heavily depends on the availability of sufficient quantities of pure and homogenous nucleosomes that can, for example, be used as substrates for histone modifying enzymes, to characterize the interactions of nucleosome binding factors, to generate nucleosome arrays for physicochemical analysis, or to explore the function of the many naturally occurring histone variants.

Recombinant histones are commonly expressed in bacteria where they typically partition into inclusion bodies[4]. Therefore, standard protocols begin with the preparation of inclusion bodies, which are isolated from the insoluble fraction of whole cell extracts in a series of washing steps[1-3]. During each washing step, the insoluble fraction is resuspended in buffer and then pelleted again by centrifugation. To stringently remove impurities, detergent is added to the buffer during the first washing steps. Subsequent washes serve to dilute the detergent. Next, the histones are solubilised and extracted from the inclusion bodies under denaturing conditions by addition of DMSO followed by incubation in a buffer containing 7 M guanidine hydrochloride. Further purification of the histones is achieved by gel filtration and cation exchange chromatography in a urea-based buffer. A final dialysis against water is required to remove salt and urea (Fig. 1A).

The purification of recombinant histones, however, is time-consuming and often rate-limiting for many applications. Several short-cuts to the original purification method were suggested to speed up the procedure. For example, the gel filtration and a lyophilisation step preceding the cation exchange chromatography have been successfully omitted[5-9] (Fig. 1A). Nevertheless, the purification of the inclusion bodies through the series of long centrifugation and laborious resuspension procedures remained the bottle-neck of the purification procedure. Even worse, we observed that extensive washing of the inclusion bodies can lead to loss of material for some histones.

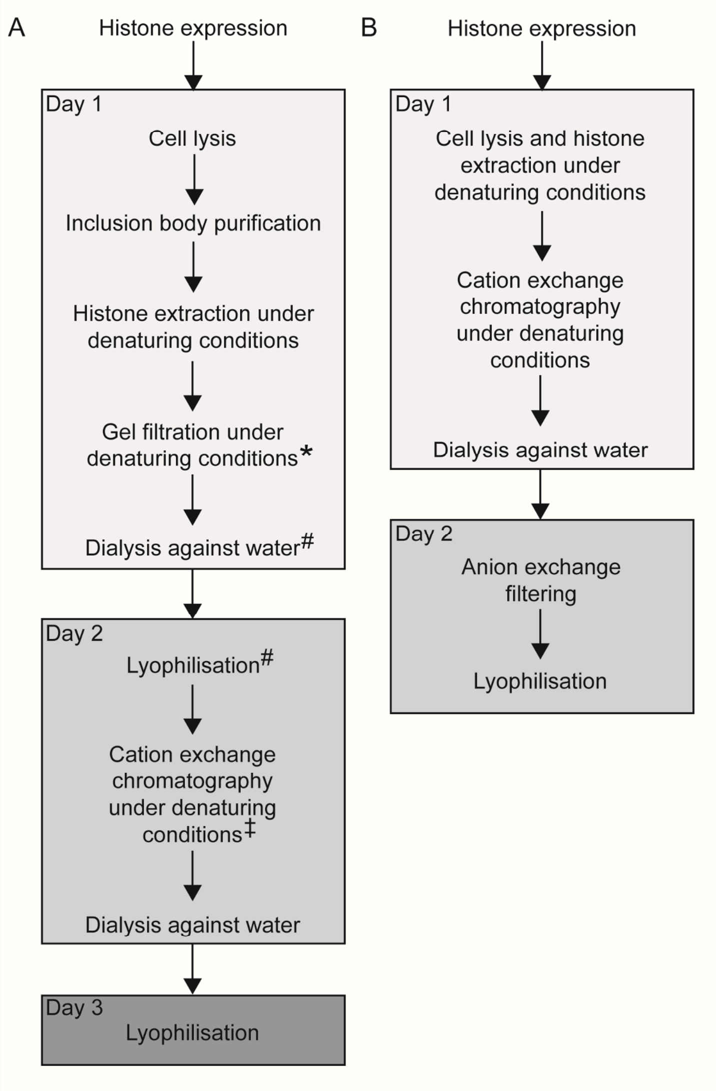
A
Histone expression
Day 1
Cell lysis
Inclusion body purification
Histone extraction under denaturing conditions
Gel filtration under denaturing conditions*
Dialysis against water#
Day 2
Lyophilisation#
Cation exchange chromatography under denaturing conditions‡
Dialysis against water
Day 3
Lyophilisation
B
Histone expression
Day 1
Cell lysis and histone extraction under denaturing conditions
Cation exchange chromatography under denaturing conditions
Dialysis against water
Day 2
Anion exchange filtering
Lyophilisation

Figure 1: Histone purification strategies. Schematic depiction of the workflow of (**A**) the conventional histone purification method according to Luger and coworkers[2,3] and (**B**) our RHP protocol. For further details see the main text. Footnotes indicate variations and simplifications of the initial protocol.

* The gel filtration step was successfully omitted in simplified purification schemes[5,7-9].

# These steps can be replaced by dilution into or dialysis against SAU 200 buffer[5-9].

‡ To remove possible DNA contaminations, it was suggested to filter the sample through an anion exchange resin prior to applying it to the cation exchange chromatography[7-9].

Here, we introduce a simplified and robust protocol, termed RHP, for the purification of histones expressed in bacteria that circumvents the laborious isolation of the inclusion bodies (Fig. 1B). The method uses denaturing conditions already during cell lysis to extract the histones. Therefore, this strategy is also applicable to histone derivatives that do not fully partition into inclusion bodies. Similar to standard methods, the histones are purified by cation exchange chromatography. If DNA contaminations have to be avoided, we recommend filtering the solution through an anion exchange resin. The RHP method requires considerably less hands-on working time than previous methods. Histones purified according to the RHP method readily incorporated into histone octamers, and these octamers were indistinguishable in purity from octamers that were reconstituted from more traditional histone preparations[5].

Materials and Methods

The protein content of samples taken throughout the purification procedure was analyzed on 15 or 18% SDS gels by Coomassie staining. The gels were scanned with the Odyssey Infrared Imaging System (LI-COR).

Histone expression

Drosophila histones H3 and H4 were expressed from pET3c-based constructs[10]. Codon-optimized genes for *Drosophila* H2A and H2B were synthesized and subcloned into pET15b (pFMP128 and pFMP129, respectively; Table S1; Eurofins MWG). BL21(DE3) cells were transformed with the expression plasmids and grown at 37°C to a density of OD_{600} 0.6–0.8 in LB supplemented with Ampicillin (100 mg/l) in shaking cultures (2 l for H3 and 4 l for all other histones). Histone expression was induced by addition of 1 mM IPTG. After 2 h, the cells were harvested by centrifugation at 4°C and stored at -80°C.

Histone expression was verified by removing 1 ml of the culture directly before induction and before harvesting. Cells in these samples were pelleted, resuspended in sample buffer (150 µl per OD_{600}; 9 M urea, 1% SDS, 25 mM Tris-Cl pH 6.8, 1 mM EDTA, 0.02% Bromophenol Blue, 100 mM DTT) and heated (15 min at 65°C). It is recommended to strongly vortex the whole cell extract to shear genomic DNA. The protein contents of equivalent amounts of the extracts were analyzed on SDS gels.

Cell lysis and histone extraction

The bacteria pellet was resuspended in SAU buffer (40 mM NaOAc pH 5.2, ≥6 M urea, 1 mM EDTA pH 8, 5 mM β-Mercaptoethanol, 10 mM lysine) supplemented with 200 mM NaCl (SAU 200) and protease inhibitors (1 mM PMSF, 1 mg/l Aprotinin, 1 mg/l Leupeptin, 0.7 mg/l Pepstatin). We typically resuspend the cell pellet of up to 6 l cultures in a final volume of 35 ml. Defined buffer conditions are most conveniently achieved by adding 10x SA buffer (400 mM NaOAc pH 5.2, 10 mM EDTA pH 8, 100 mM lysine, 50 mM β-Mercaptoethanol), NaCl to a final concentration of 200 mM and protease inhibitors directly to the cell pellet. Once the cells are properly resuspended, urea powder is added to a concentration of 6 M and the suspension is filled up to the final volume with water.

All steps during lysis and purification were performed at 4°C. Cells were lyzed by three passes through a French Press (1,500 psi; Thermo Spectronic) and sonication on ice (at least 2 min effective sonication time with an amplitude of 30% with pulses of 15 sec followed by 30 sec pauses; Branson Ultrasonics). If urea is added as powder as described above, we recommend to perform sonication prior to the French Press and to use longer sonication times (up to 20 min with occasional mixing) to ensure that all urea is fully dissolved.

The extract was cleared by centrifugation for 20–30 min at ~41,000 g (SS-34 rotor, Sorvall RC 6 Plus; Thermo Scientific) and filtration. For the histone preparations shown in this paper, conventional 0.45 µM syringe filters were used. These filters easily clogged, in contrast to syringe filters containing a glass-fiber prefilter (HPF Millex, Millipore) that were successfully employed in later preparations.

Cation exchange and dialysis

The pre-cleared cell extract was loaded onto a HiTrap SP HP column (5 ml; GE Healthcare) pre-equilibrated in SAU 200 buffer. The column was washed with 200 mM NaCl for several column volumes (CV). A gradient from 200 to 600 mM NaCl over 5–10 CV was applied to elute bound protein. Pooled histone-containing fractions were dialyzed against cold water over night (3 times ≥3 l) in dialysis tubing with a molecular weight cut-off of 6000-8000 Da (Spectra/Por).

Anion exchange

The dialysate was centrifuged to remove precipitates, supplemented with 15 mM Tris-Cl pH 8, and filtered using conventional syringe filters (0.45 µm). The sample was passed through a HiTrap Q HP column (1 ml; GE Healthcare) that was pre-equilibrated in 15 mM Tris-Cl pH 8. The flow-through of the column was collected and the histone concentration was determined by absorption measurement at 280 nm (see Table 1 for the extinction coefficients). Yields typically ranged between 2 and 15 mg per liter expression culture. Aliquots of the purified histone were flash frozen in liquid nitrogen. The purity of the proteins was assessed by SDS-PAGE. To regenerate the resin and to control whether a fraction of the histones had bound to the resin, a gradient up to 2 M NaCl was applied. The elution fractions contained little or no protein.

Purification of histones from inclusion bodies

Preparation of recombinant histones from purified inclusion bodies was done essentially as described[5]. In short, the histones were expressed in BL21(DE3) cells that were lysed in 50 mM Tris-Cl pH 7.5, 100 mM NaCl, 1 mM EDTA pH 8, 5 mM β-Mercaptoethanol supplemented with protease inhibitors by sonication and French Press as described above. Inclusion bodies were purified by a succession of four washing steps using lysis buffer that was supplemented with Triton X-100 (1%) during the first two washes. Histones were extracted from inclusion bodies by homogenization in DMSO and unfolding buffer (7 M guanidine hydrochloride, 20 mM Tris-Cl pH 7.5, 10 mM DTT). After dialysis against SAU 200 buffer, cation exchange chromatography and subsequent dialysis against water was performed as described above.

Octamer assembly

Histone octamers were assembled with ~1 mg of each *Drosophila* histone according to Luger and coworkers[2,3]. Histones were lyophilized (Alpha 1-2, Christ; RZ 2.5, vacuubrand) and solubilized in unfolding buffer as described in the Results and Discussion section (see step 5.2). To analyze histone stoichiometry by SDS-PAGE, the samples were diluted in water (1:10) prior to loading to reduce the concentration of guanidine hydrochloride, which can negatively affect the gel run. Dialysis into refolding buffer (3 times 2 l; 10 mM Tris-Cl pH 7.5, 2 M NaCl, 1 mM EDTA, 5 mM β-Mercaptoethanol) was performed in dialysis tubing with a molecular weight cut-off of 6000–8000 Da. Precipitates were removed by centrifugation and the sample was loaded onto a size exclusion chromatography column (Superdex 200 HiLoad 16/60, 120 ml; GE Healthcare) pre-equilibrated in refolding buffer. Elution fractions were analyzed by SDS-PAGE. Octamer-containing fractions were pooled according to purity and histone stoichiometry. After concentration to 2–3 mg/ml in centrifugal filters (Amicon Ultra-4 or Microcon, 30 kDa MWCO; Millipore), the octamers were stored as described in the Results and Discussion section.

Results and discussion

Here we present the RHP method for the purification of recombinant histones from bacteria. With this method, we purified the four core histones from *Drosophila melanogaster*. Human histones, the *Drosophila* histone variant H2Av as well as several histone H4 mutants including tail-deleted H4 can be purified using the same protocol (Jens Michaelis, personal communication, and data not shown). For clarity, the important steps of the RHP protocol are listed as bullet points. Further details are given in the Materials and Methods section.

1. Histone expression

Some histones express poorly in bacteria. Species bias of codon usage of the recombinant gene or toxicity of the gene product are two potential causes of poor expression. *Drosophila* H2A and H2B, for example, showed low and variable expression levels, whereas H3 and H4 always expressed robustly from the same vector (pET3c). To circumvent codon bias and toxicity, we codon-optimized the genes for H2A and H2B (Table S1) and cloned them into a vector that provides a more stringent control over the expression through co-expression of the *lac* repressor (pET15b). H2A and H2B were robustly expressed from these optimized expression plasmids in standard BL21(DE3) *E. coli* cells. Histone expression comprised the following steps:

1.1 Transformation of BL21(DE3) *E. coli* with the respective expression plasmid.
Depending on the expression plasmid and the source of the histones, bacterial strains expressing rare tRNAs or strains that restrict leaky expression may improve the yield.

1.2 Growth of up to 6 l of culture to OD_{600} = 0.6–0.8.

1.3 Induction of histone expression by addition of 1 mM IPTG for 2 h at 37°C.
We recommend verifying the expression by SDS-PAGE before proceeding with the protocol (see Materials and Methods). Overexpression must be clearly visible in whole cell extracts.

1.4 Harvesting of the cells by centrifugation.
After centrifugation, it is recommended to resuspend the cells in small volumes of cold water, transfer the cells to a 50 ml conical tube and pellet the cells a second time.

1.5 Storage of the bacteria pellets at -80°C until further use.

2. Cell lysis and histone extraction

Histones expressed in bacteria are typically insoluble and form inclusion bodies. To extract both the soluble and insoluble fraction, whole cell extracts were prepared under denaturing conditions in presence of ≥6 M urea. Addition of free lysine to the lysis buffer served to prevent carbamylation of the histone proteins that might occur upon reaction with natural degradation products of urea[11]. Nevertheless, exposure of the histone proteins to the urea-containing buffer (SAU buffer) should be kept to a minimum. Also note that the urea solution should always be prepared freshly and never be warmed up. Cell lysis and histone extraction required the following steps:

2.1 Resuspension of the bacteria pellet in sodium-acetate-urea (SAU) buffer containing 200 mM NaCl (SAU 200).

Care should be taken that the final urea concentration during cell lysis and extraction is between 6–7.5 M to assure efficient protein denaturation and histone extraction without exceeding the solubility of urea. A defined final urea concentration is most conveniently achieved by resuspending the cell pellet in an appropriate volume of 10x SA buffer and adding urea powder directly to the suspension. Water is added and the suspension is mixed to dissolve the urea.

2.2 Cell lysis by French Press and sonication.

The order of the lysis steps is optional. However, we recommend to sonicate the sample before employing the French Press. This order of events has the advantage that urea has additional time to dissolve during sonication so that it does not clog the French Press. Note that the French Press step may be left out completely, as it only marginally enhanced extraction (data not shown).

To check the efficiency of the cell lysis and histone extraction, equivalent amounts of the pellet and supernatant fractions obtained after centrifugation (see step 2.3) were removed and proteins resolved by SDS-PAGE. Figure 2 shows exemplary results for histone H2B; similar results were obtained for the other three core histones. The majority of H2B was detected in the soluble extract, suggesting that cell lysis and histone extraction were efficient under the chosen conditions. Nevertheless, should a major fraction of the histone be found in the pellet, the extraction procedure should be repeated. For efficient extraction, ensure that the urea concentration in the cell suspension exceeds 6 M.

2.3 Removal of cell debris by centrifugation.

It is critical to remove most insoluble particles from the cell extract as they easily clog filters and chromatography media in the following steps. We routinely perform two rounds of centrifugation to achieve acceptable results. A loose, viscous pellet may form. We therefore recommend recovering the soluble fraction by careful pipetting instead of decanting.

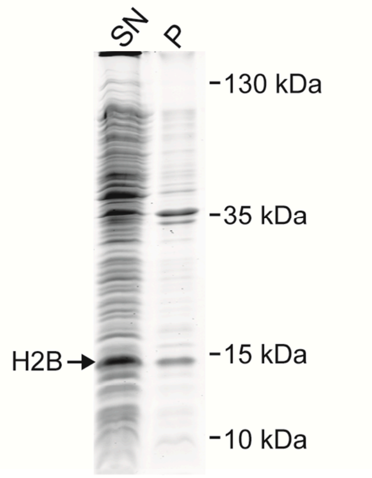

Figure 2: Histone extraction. Whole cell extracts were prepared from bacteria expressing *Drosophila* H2B by French Press and sonication. Cell debris and residual insoluble material were pelleted by centrifugation. Efficiency of the histone extraction was analyzed on Coomassie-stained SDS gels by loading equivalent amounts of the supernatant containing the solubilized histones (SN) and the corresponding pellet fraction (P). Most H2B was present in the supernatant.

3. Cation exchange and dialysis

The histones were purified from the cell extract by cation exchange chromatography under denaturing conditions. As the histones carry a net positive charge at the pH of the buffer (pH 5.2), they bound to the cation exchange resin at low salt concentrations, in contrast to the majority of bacterial proteins (Fig. 3A). The histones were then eluted by a salt gradient.

3.1 Filtering of the sample.
Filtering of the supernatant from step 2.3 prior to the cation exchange is necessary to remove residual particulate material that can block the chromatography column. As conventional syringe filters easily clogged, we strongly recommend using syringe filters that contain a glass-fiber prefilter instead (HPF Millex; Millipore).

3.2 Loading of the filtered sample onto a HiTrap SP HP column (5 ml; GE Healthcare) pre-equilibrated in SAU 200 buffer.

3.3 Washing of the column with a minimum of 5 column volumes of SAU 200 buffer.

3.4 Elution of the histones by applying a gradient from 200 to 600 mM NaCl over 5 to 10 column volumes.
All histones eluted in a broad peak centered around 430 ± 50 mM NaCl.

3.5 Analysis of the protein content of the elution fractions by SDS-PAGE (Fig. 3B).

3.6 Pooling of the fractions according to histone abundance and purity.
As yields typically are not limiting, we suggest to pool according to purity.

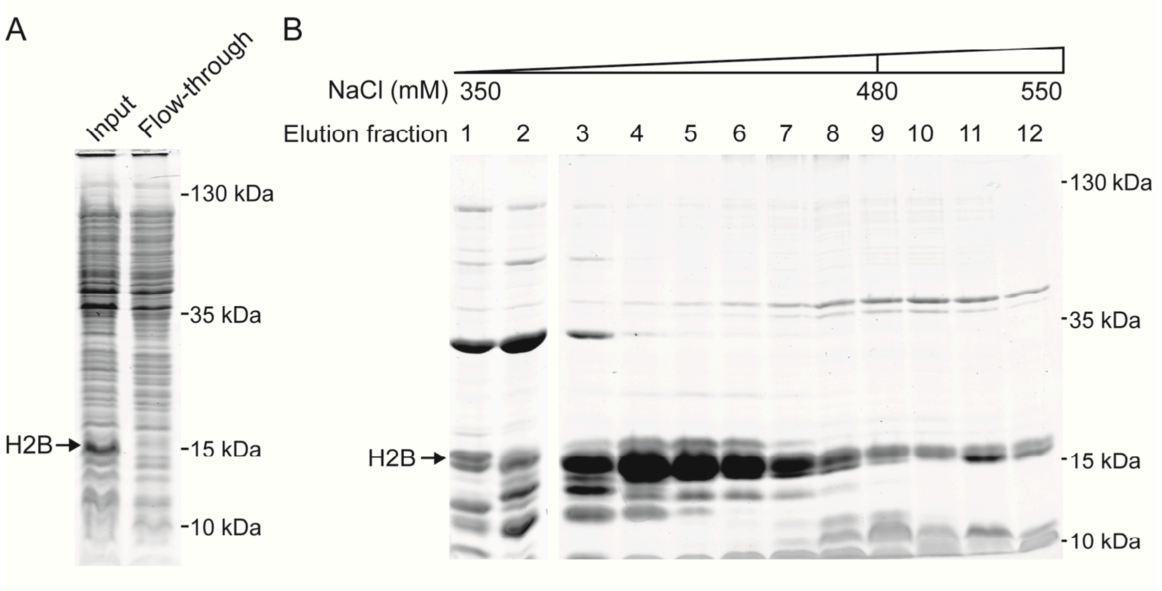

Figure 3: Histone purification by cation exchange chromatography. The whole cell extract from Figure 2 containing solubilized *Drosophila* H2B (SN) was filtered and applied to cation exchange chromatography under denaturing conditions. (**A**) Equivalent amounts of the filtered whole cell extract (Input) and the flow-through fraction of the cation exchange column were analyzed by SDS-PAGE. Most H2B bound to the chromatography resin. (**B**) H2B was eluted by a NaCl gradient as indicated. Fractions 4–8 were pooled and processed further as described in the main text.

3.7 Dialysis of the pooled histone fractions against water.

The pooled histone-containing fractions were extensively dialyzed against water to remove salts and urea.

4. Anion exchange and storage of purified histones

By virtue of their positive charge, histones strongly bind to nucleic acids. Therefore, *E. coli*-derived nucleic acids may co-purify with histones. A contamination with nucleic acids can affect the concentration measurements of the purified histones (see below) or interfere with downstream applications. We therefore filtered the samples over an anion exchange column. The negatively charged nucleic acids are expected to bind to the positively charged resin along with some contaminating proteins, whereas histones pass through the resin unimpededly.

4.1 Addition of Tris-Cl pH 8 to the dialysate to a final concentration of 15 mM.

A buffered solution with a defined pH is necessary for robust binding of contaminations to the resin.

4.2 Centrifugation and filtering of the sample to remove particles.

Conventional syringe filters were used to filter the dialysate.

4.3 Passing of the filtered sample over a HiTrap Q HP column and collection of the flow-through.

As expected, the histones were found in the flow-through of the anion exchange column (Fig. 4A).

4.4 Determination of the concentration.

The concentration is most conveniently measured by absorption of UV light. The extinction coefficients of *Drosophila* histones at 280 nm are listed in Table 1.

Table 1: Extinction coefficients of *Drosophila* histones at 280 nm.

	Molecular weight (Da)*	**ε_{280} (cm^{-1} M^{-1})#**
H2A	13,232	4,470
H2B	13,565	7,450
H3	15,257	4,470
H4	11,250	5,960
Octamer	106,608	44,700

* Molecular weights do not include the initial methionine.

The extinction coefficients were calculated using the ProtParam tool with water as solvent (Swiss Institute of Bioinformatics; http://web.expasy.org/protparam/)[12].

4.5 Storage of the purified histones at –80°C until further use.
Storage in aliquots that contain 0.5 to 2 mg is useful for most downstream applications.

In a variation of the protocol, the anion exchange filtration step is performed prior to the cation exchange chromatography (step 3)[7-9], further simplifying the protocol. To this end, a HiTrap Q HP column is attached on top of the HiTrap SP HP column. The cell extract from step 3.1 is then passed over the two columns. Before eluting the histones with the salt gradient, the Q HP column is detached from the FPLC system. Note that this version of the protocol, though simpler, filters out fewer impurities.

5. Reconstitution of histone octamers

All four canonical *Drosophila* core histones were purified according to the method outlined in steps 1–4 (Fig. 4A). Next, we assembled histone octamers with these histone preparations essentially as described[2,3]. Briefly, the four histones were lyophilized, dissolved in denaturing buffer and mixed. Dialysis was used to dilute the denaturant, allowing the histones to refold. Furthermore, the dialysis buffer contained 2 M NaCl, conditions that facilitate stable formation of histone octamers. Fully assembled histone octamers were separated from

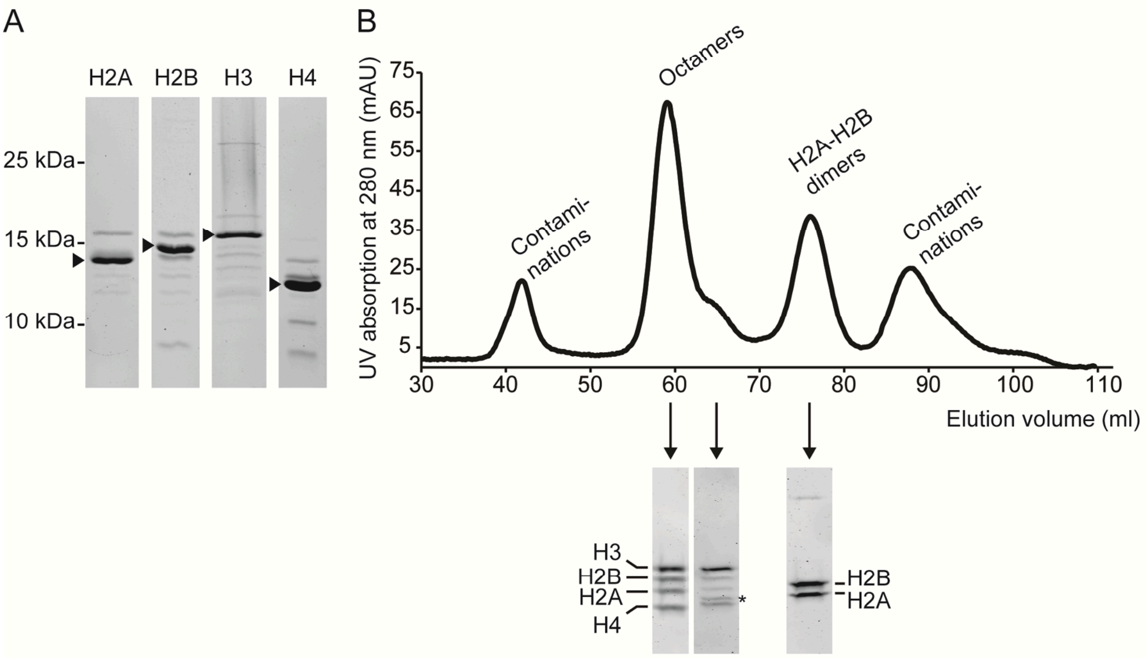

Figure 4: Histone octamer assembly. (**A**) The four canonical *Drosophila* histones were purified according to the RHP method and analyzed by SDS-PAGE. Arrowheads indicate the respective histones. (**B**) The histones from A were assembled into octamers. The elution profile of the size exclusion chromatography column is depicted (upper panel). The protein content of selected elution fractions was analysed by SDS-PAGE (lower panel and Figure S1). Octamers eluted with a tailing shoulder, which contained a contaminating protein (asterisk).

excess histones and contaminating bacterial proteins by size exclusion chromatography.

5.1 Lyophilisation of each histone.

5.2 Dissolving of the lyophilized histones in guanidine hydrochloride-containing unfolding buffer to a concentration of 2–4 mg/ml.

The histone suspensions were gently mixed at room temperature for 30 min. Note that histones should not remain in the unfolding buffer for an extended period of time (>3 h)[2,3].

5.3 Determination of the concentration of the histones by UV absorption as described in step 4.4.

5.4 Mixing of the histones.

We recommend mixing the histones for the assembly with a 1.2-fold excess of H2A and H2B over H3 and H4. Adding H2A and H2B in excess prevents the formation of free H3-H4 tetramers or histone hexamers, which are difficult to separate from histone octamers in the subsequent size exclusion chromatography step. Contrary, H2A-H2B dimers can be separated easily from the octamers (see step 5.7 and Fig. 4B).

In addition to determining the concentration by UV absorption, we suggest analyzing the individual histone samples and the histone mix by SDS-PAGE and Coomassie-staining to judge the stoichiometry of the mix. If the ratios of the histones are found unbalanced, the mix can be adjusted accordingly by addition of the underrepresented proteins before dialysis (see step 5.5).

5.5 Dialysis into refolding buffer.

5.6 Removal of precipitates by centrifugation and filtration.

5.7 Size exclusion chromatography (Superdex 200).

Typically, four major peaks eluted from the column. SDS-PAGE analysis showed that the second and third peak contained the histone octamers and H2A–H2B dimers, respectively (Fig. 4B and S1). The other peaks consisted of aggregates and low molecular weight impurities. Fractions containing pure octamers with the proper stoichiometry were pooled and stored as described in step 5.8.

We noticed that the octamers eluted in a peak with a shoulder tailing towards later elution volumes. SDS-PAGE analysis revealed a contaminating band in these side fractions of the octamer peak (Fig. 4B). This contamination presumably originated from a protein co-purifying with H4. We detected the contamination in H4 preparations irrespective of the purification method (data not shown). Additionally, late-eluting octamers are known to be contaminated by H3-H4 tetramers and histone hexamers, especially if H2A and H2B are limiting. It is therefore advisable to narrowly pool the peak.

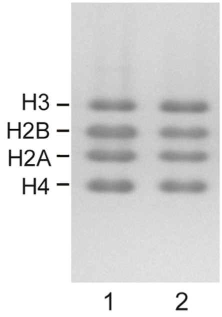

Figure 5: Quality control of the histone octamers. Stoichiometry and purity of the octamers assembled from the histones purified according to the RHP method outlined in the main text were analyzed by SDS-PAGE (lane 1). An octamer preparation assembled from histones purified by a method based on the standard purification protocol[5] was loaded in parallel (lane 2).

5.8 Storage of the octamers.

The pooled fractions were concentrated, aliquots were shock-frozen in liquid N_2 and stored at –80°C. Alternatively, the octamer sample can be stored at –20°C after addition of glycerol to a final concentration of 50% (v/v).

Comparison of octamer quality and conclusions

The RHP protocol above describes a straightforward way to purify histones, and histones purified by this method readily incorporated into octamers. Octamers assembled from histones purified by RHP or conventional inclusion body purification-based methods[5] were indistinguishable in purity and stoichiometry as judged by SDS-PAGE and Coomassie staining (Fig. 5).

In summary, the RHP method offers a rapid and robust procedure to purify recombinant histones expressed in bacteria. RHP does not require laborious preparation of inclusion bodies and thus substantially reduces the required handling time. So far, the protocol was successfully applied to prepare canonical *Drosophila* histones (this study), human histones (Jens Michaelis, personal communication), the *Drosophila* histone variant H2Av and various H4 mutants (data not shown). We expect that it will be useful also for the preparation of histones and histone variants from other organisms.

Acknowledgements

We thank Verena K. Maier for histones and octamers that were purified from inclusion bodies and members of the Mueller-Planitz laboratory for helping to establish the protocol. CH gratefully acknowledges financial support by Roland Beckmann (through DFG SFB 594).

References

1. Luger, K., Rechsteiner, T.J., Flaus, A.J., Waye, M.M. & Richmond, T.J. Characterization of nucleosome core particles containing histone proteins made in bacteria. *J Mol Biol* **272**, 301-11 (1997).
2. Luger, K., Rechsteiner, T.J. & Richmond, T.J. Expression and purification of recombinant histones and nucleosome reconstitution. *Methods Mol Biol* **119**, 1-16 (1999).
3. Luger, K., Rechsteiner, T.J. & Richmond, T.J. Preparation of nucleosome core particle from recombinant histones. *Methods Enzymol* **304**, 3-19 (1999).
4. Dyer, P.N. et al. Reconstitution of nucleosome core particles from recombinant histones and DNA. *Methods Enzymol* **375**, 23-44 (2004).
5. Clapier, C.R., Langst, G., Corona, D.F., Becker, P.B. & Nightingale, K.P. Critical role for the histone H4 N terminus in nucleosome remodeling by ISWI. *Mol Cell Biol* **21**, 875-83 (2001).
6. Gordon, F., Luger, K. & Hansen, J.C. The core histone N-terminal tail domains function independently and additively during salt-dependent oligomerization of nucleosomal arrays. *J Biol Chem* **280**, 33701-6 (2005).
7. Vary, J.C., Jr., Fazzio, T.G. & Tsukiyama, T. Assembly of yeast chromatin using ISWI complexes. *Methods Enzymol* **375**, 88-102 (2004).
8. Wittmeyer, J., Saha, A. & Cairns, B. DNA translocation and nucleosome remodeling assays by the RSC chromatin remodeling complex. *Methods Enzymol* **377**, 322-43 (2004).
9. Gelbart, M.E., Rechsteiner, T., Richmond, T.J. & Tsukiyama, T. Interactions of Isw2 chromatin remodeling complex with nucleosomal arrays: analyses using recombinant yeast histones and immobilized templates. *Mol Cell Biol* **21**, 2098-106 (2001).
10. Morales, V. et al. Functional integration of the histone acetyltransferase MOF into the dosage compensation complex. *EMBO J* **23**, 2258-68 (2004).
11. Stark, G.R., Stein, W.H. & Moore, S. Reactions of the Cyanate Present in Aqueous Urea with Amino Acids and Proteins. *The Journal of Biological Chemistry* **235**, 3177-3182 (1960).
12. Artimo, P. et al. ExPASy: SIB bioinformatics resource portal. *Nucleic Acids Res* **40**, W597-603 (2012).

Supplementary material

“Rapid purificarion of recombinant histones”

Klinker et al. in revision

Supplementary Table 1: DNA sequences of codon-optimized *Drosophila* H2A and H2B genes.

H2A	ATGTCCGGCCGTGGGAAAGGCGGTAAAGTCAAGGGTAAGGCGAAGAGTCGCAGCAACCGCGCAGGTCTGCAATTTCCGGTGGGTCGCATTCATCGCCTGCTGCGTAAAGGTAACTACGCTGAACGCGTAGGCGCGGGCGCGCCTGTATATCTGGCTGCAGTCATGGAGTATCTGGCAGCCGAGGTTTTAGAACTGGCGGGCAACGCGGCTCGTGATAACAAAAAAACTCGTATCATCCCACGCCACCTGCAGCTGGCGATTCGCAATGACGAAGAATTAAATAAATTGCTGTCGGGCGTGACGATTGCCCAGGGCGGCGTTCTGCCGAATATCCAGGCCGTGTTGCTGCCGAAAAAAACCGAAAAAAAAGCCTAA
H2B	ATGCCACCGAAAACCTCCGGTAAAGCGGCCAAAAAAGCCGGCAAAGCCCAAAAGAACATCACGAAAACCGATAAGAAGAAGAAACGCAAACGCAAAGAGTCCTATGCGATTTACATCTATAAGGTGCTGAAACAGGTACATCCGGATACTGGcATTAGCAGTAAAGCCATGAGCATCATGAATAGCTTCGTGAATGACATCTTTGAACGCATTGCTGCAGAAGCGAGTCGTTTGGCTCACTACAACAAACGGTCGACCATTACCTCTCGTGAGATTCAGACTGCAGTTCGTCTGTTACTGCCTGGTGAACTCGCGAAACATGCGGTTTCAGAAGGCACAAAAGCAGTCACCAAATATACGTCGTCTAAATAA

Supplementary Figure:

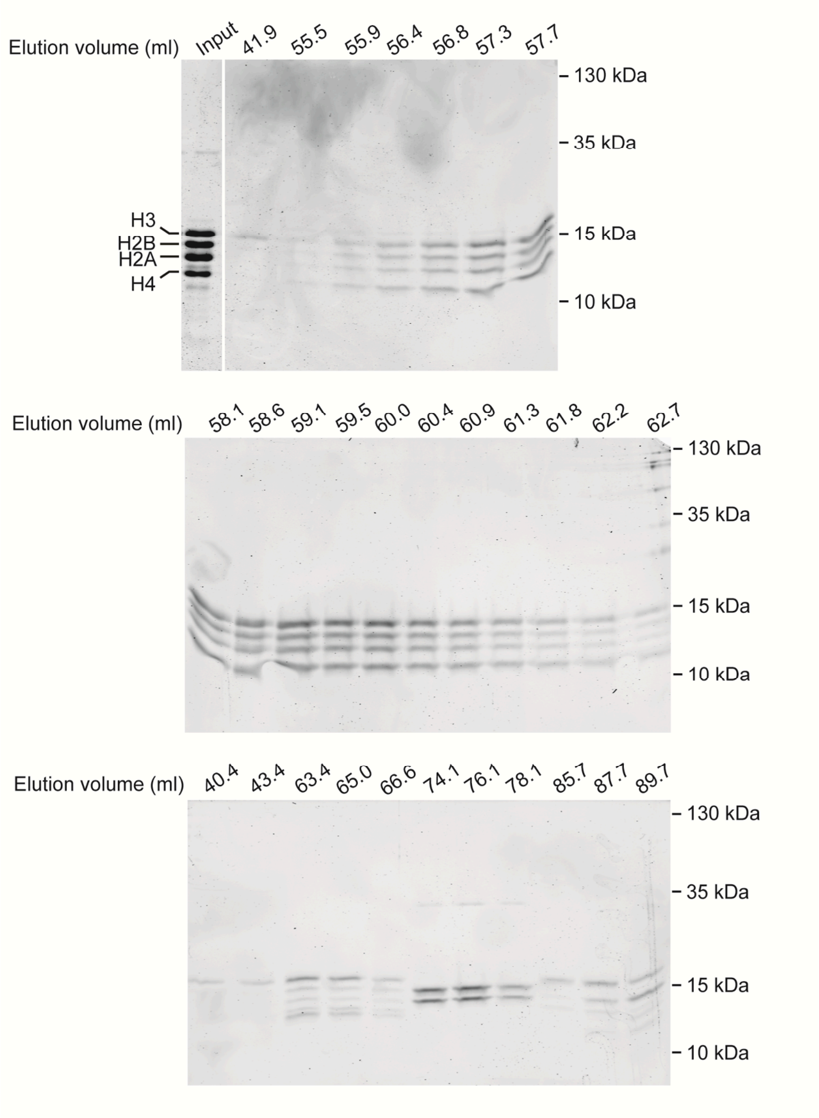
Elution volume (ml)
Input
41.9
55.5
55.9
56.4
56.8
57.3
57.7
130 kDa
35 kDa
15 kDa
10 kDa
H3
H2B
H2A
H4
Elution volume (ml)
58.1
58.6
59.1
59.5
60.0
60.4
60.9
61.3
61.8
62.2
62.7
130 kDa
35 kDa
15 kDa
10 kDa
Elution volume (ml)
40.4
43.4
63.4
65.0
66.6
74.1
76.1
78.1
85.7
87.7
89.7
130 kDa
35 kDa
15 kDa
10 kDa

Figure S1: Purification of histone octamers by size exclusion chromatography. Analysis of the gel filtration elution fractions from the octamer purification shown in Figure 4B. Selected elution fractions were analyzed by SDS-PAGE, the corresponding elution volumes are indicated.

3 Discussion

3.1 The molecular mechanism of ISWI-mediated nucleosome sliding

Recent findings by us and others considerably advanced our understanding of the nucleosome sliding mechanism of ISWI (see also chapter 2.2). Contrary to wide-spread expectations but in accordance with observations for the related chromatin remodeling factor Chd1 (Hauk et al., 2010), we could demonstrate that the HSS domain of ISWI is dispensable for a basic nucleosome sliding reaction (see chapter 2.1). The HSS domain facilitates but is not essential for nucleosome sliding. Therefore, prominent models of the ISWI nucleosome sliding mechanism postulating a pivotal role of the HSS domain have to be revisited. Instead, we propose that ATP-dependent translocation of the ATPase domain of ISWI at SHL2 is sufficient to catalyze nucleosome repositioning. How the translocation activity mechanistically translates into nucleosome sliding remains to be determined. Conceivably, ISWI binding or activity breaks key nucleosomal contacts creating a window of opportunity for the reorganization of the structure and possibly position of the nucleosome (see Figure 7 in chapter 2.1). Notably, recent results from single molecule experiments revealed nucleosome sliding to occur in single base pair steps (see below) (Deindl et al., 2013). This observation is consistent with a helicase-like translocation activity of the histone-tethered ISWI ATPase domain pumping DNA base pair-wise towards the nucleosome exit site. A concerted large-scale rearrangement of the nucleosome, on the contrary, seems to be incompatible with the finding. In conclusion, the ISWI ATPase domain – most likely by its translocation activity – turns out to be the driving force of sliding, although the mechanism by which the individual base pairs are further propagated from the site of translocation to the nucleosome exit site is not yet clear.

As the ATPase domains of all chromatin remodeling enzymes are homologous, it is conceivable that the basic nucleosome remodeling reaction described above is shared by all remodeling factors. To achieve the variety of different remodeling outcomes observed *in vitro* and *in vivo*, a plethora of accessory domains and subunits evolved to regulate, modulate, and optimize catalysis (see chapter 2.2). The HSS domain, for example, increases not only the affinity – and thereby likely the sliding processivity – but also the specificity of ISWI to the nucleosome and may help to properly position the ATPase domain at SHL2 (see chapter 2.1). Furthermore, the domain might be fundamentally involved in the nucleosome spacing activity of ISWI, for instance by functioning as a protein ruler (see chapter 1.3.3). Additionally, the C-terminus of ISWI harboring the HSS domain serves as interaction surface for non-catalytic complex subunits. In *Drosophila* ISWI, for example, a domain directly C-terminal to the HSS domain mediates the interaction with Acf1, whereas the SANT and/or SLIDE domains of the yeast ISWI homologs are required for association of their specific complex subunits (Eberharter et al., 2004; Hota et al., 2013; Pinskaya et al., 2009). Thus, the C-terminus is expected to be essential for proper chromatin remodeling *in vivo* where ISWI does not act as a single entity but in the context of various remodeling complexes.

Besides these “passive” functions of the HSS domain in nucleosome sliding by ISWI, the domain may also assume more “active” roles in catalysis. In our analysis, the ISWI mutant lacking the HSS domain remodeled nucleosomes about one order of magnitude more slowly than the wild-type enzyme under saturating conditions (see chapter 2.1). This defect may result from a missing “active” contribution of the HSS domain to the sliding reaction, for example the pushing of extranucleosomal DNA into the nucleosome, an activity that was even proposed to be the major driving force of sliding in prominent models (see chapters 1.3.2 and 2.2). Thereby, an ATP hydrolysis-triggered conformational change between the ATPase and HSS domain was suggested to serve as a kind of “power stroke” creating a DNA loop on the surface of the nucleosome by mechanically pushing in extranucleosomal DNA (see Figure 5 of chapter 2.3). Although our work with the HSS-depleted mutant had demonstrated that the HSS domain was not essential for sliding, enhancement of the reaction by active co-operation of the domains resulting in a power stroke remained possible. However, our study employing ISWI mutants harboring flexible linkers between the ATPase and HSS domain to interrupt possible direct, force-transducing co-operation provided compelling evidence against the power stroke model, as the mutants behaved like the wild-type enzyme in ATPase, remodeling, and sliding assays (see chapter 2.3). Notably, a study on Chd1 conducted in parallel in the Bowman laboratory using even longer flexible linker insertions came to the same conclusion, lending further credence to our findings (Nodelman and Bowman, 2013). As the presence of the flexibly connected HSS domain rescued full remodeling activity in comparison to the HSS-depleted ISWI mutant, we propose that the HSS domain serves as an anchor assisting in positioning the ATPase domain at SHL2, thereby promoting productive engagement of ISWI with the nucleosome. In addition, binding of the HSS domain may facilitate sliding in a more active manner by weakening nucleosomal contacts close to the DNA entry site. Nevertheless, direct communication between the ATPase and HSS domain of ISWI is not supported by our findings.

Further exciting insight into how the HSS domain may contribute to nucleosome sliding was derived from recent findings of the Bartholomew, Zhuang, and Cairns laboratories (Clapier and Cairns, 2012; Deindl et al., 2013; Hota et al., 2013). Performing single molecule experiments, Deindl et al. carefully dissected a nucleosome sliding reaction by ISWI-type complexes and revealed remarkable details (see also chapter 2.2) (Deindl et al., 2013). In short, they demonstrated that during ISWI remodeling initially 7 bp of DNA exit the nucleosome in single base pair steps before 3 bp enter from the opposite side. In a subsequent step, 3 bp exit followed by the entry of 3 bp. Consequently, during sliding the nucleosomal DNA continuously lacks up to 7 bp in comparison to the canonical nucleosome structure, resulting in considerable distortion. Given that the ISWI ATPase domain responsible for pumping the DNA towards the exit site by translocation is located at SHL2, the deficit in base pairs is presumably not evenly distributed over the nucleosome but restricted to the topological domain delimitated by the binding of the ISWI ATPase module at SHL2 and the HSS domain at the entry site (see Figure 4b in chapter 2.2). Therefore, the DNA in this region accumulates a strain in the cause of sliding when base pairs exit the nucleosome. Only when the strain is sufficiently strong, extranucleosomal DNA ratchets in at the entry site, partially relieving it and allowing the ATPase domain to continue translocating. The HSS domain seems to be importantly involved in regulating this succession of events as suggested by Hota et al. (Hota et al., 2013). In this study, mutation of the SLIDE domain that weakened its interaction with the extranucleosomal DNA impaired the entry of DNA more pronouncedly than its exit in the context of the CHRAC-like yeast ISW2 complex. Moreover, the SLIDE domain assisted in determining sliding directionality as its mutation caused an increase in back tracking of the DNA at early stages of sliding. Notably, positioning of the ATPase domain at SHL2 was not affected by the mutations introduced into the SLIDE domain. Therefore, the authors concluded that the HSS domain not only serves as an anchor to put into place the ATPase domain but also critically contributes to sliding in a more active manner. However, details of the mechanism remain to be determined. Presumably, the interaction of the HSS domain with the nucleosome at the entry site is important for the buildup of the strain that is generated by the translocation activity of the ATPase domain at SHL2. Accumulation of a certain amount of strain may trigger a temporal detaching of the HSS domain allowing DNA to ratchet in. Efficient, unidirectional sliding apparently depends on the proper generation and timely release of the strain and thus may rely on the HSS domain. Of note, studies on the chromatin remodeling enzyme Chd1 proposed that no specific contacts between the HSS domain and the extranucleosomal DNA are required for nucleosome sliding. Substitution of the HSS domain with sequence-specific DNA binding domains yielded fully functional enzymes with undisturbed sliding activity on substrate nucleosomes harboring the DNA consensus sequence within a certain distance from the entry site (McKnight et al., 2011). Taken together, besides stabilizing and positioning ISWI on the nucleosome the HSS domain probably assists nucleosome sliding by gripping on the extranucleosomal DNA and regulating its entry into the nucleosome.

An additional role of the HSS domain in ISWI catalysis was indicated by Clapier and Cairns (Clapier and Cairns, 2012). They suggested the domain to be critically involved in regulating ISWI activity as its binding to extranucleosomal DNA induced a conformational change relieving an intrinsic autoinhibition mediated by the so-called NegC domain – also referred to as “bridge” by us and others –, located directly C-terminal to the ATPase module (see chapter 2.2). Release of the NegC-mediated inhibition was proposed to be essential for the efficient coupling of ATP hydrolysis to nucleosome sliding. Therefore, persistent autoinhibition by NegC in the absence of the HSS domain may contribute to the reduced nucleosome sliding activity we observed with the HSS-depleted ISWI mutant (see chapter

2.1). However, how the HSS and NegC region communicate is currently unclear. Notably, the insertion of flexible linkers between both regions did not affect ISWI activity and thus NegC release (see chapter 2.3). In summary, the HSS domain seems to regulate, facilitate, and optimize nucleosome sliding employing a variety of mechanisms, whereas the remodeling reaction as such is mainly driven by the activity of the ATPase domain at SHL2.

3.2 Regulation of ISWI by the histone H4 tail

The sensitivity of ISWI and its complexes to the histone H4 tail protruding from the nucleosome at SHL2 was established in a series of *in vitro* studies (see chapter 1.3.3). However, the underlying mechanism as well as the extent of the H4 tail-dependency of ISWI remained largely elusive and controversial (e.g. (Clapier and Cairns, 2012; Clapier et al., 2001; Dang et al., 2006; Fazzio et al., 2005; Ferreira et al., 2007)). We quantified the remodeling activity of ISWI in the context of folded nucleosome arrays and compared wild-type to H4 tail-deleted substrates (see chapter 2.1). Under saturating conditions, ISWI remodeling was reduced about six-fold in absence of the H4 tail. This finding indicated that also in the context of folded chromatin fibers where the H4 tail is expected to be engaged in inter-nucleosomal interactions (see chapter 1.1.3) epitopes of the H4 tail involved in enhancing ISWI remodeling were available for the enzyme. Notably, both full-length ISWI and the HSS-deficient mutant reacted to depletion of the H4 tail, demonstrating that the N-terminus or the ATPase domain of ISWI comprised an H4-sensing epitope. Given the localization of the ATPase domain at SHL2, direct association of the tail with the ATPase domain seems likely. As we conducted the remodeling assay under saturating enzyme conditions, a step of ISWI catalysis subsequent to enzyme binding must be affected by the H4 tail. Consistently, footprinting studies showed that the H4 tail promoted productive engagement of ISWI with the nucleosome at SHL2 in the context of yeast ISW2, whereas the overall affinity to nucleosomes was independent from the H4 tail (Dang et al., 2006). However, whether the H4 tail mainly provides a grip for ISWI stabilizing the ATPase at SHL2 during translocation and assuring processivity (Gangaraju et al., 2009) or fulfills more refined functions remains an open question.

A recent publication by Clapier and Cairns (see above) provided some insight into the mechanism of the H4 tail-dependency of ISWI and postulated a critical role of the tail in regulating enzyme activity and substrate specificity (Clapier and Cairns, 2012). The Cairns laboratory discovered a region in the N-terminus of ISWI – “AutoN” – that contains a peptide motif resembling the basic patch of the H4 tail. As mutation of this motif rendered ISWI largely independent of the H4 tail in ATPase assays and a translocation assay and furthermore increased sliding of H4 tail-depleted or basic patch-mutated nucleosomes, the authors concluded that AutoN autoinhibited ISWI activity in the absence of a nucleosomal substrate. Presumably, interaction of AutoN with the ATPase domain stabilized the enzyme in a conformation incompatible with ATP hydrolysis. Upon binding to the nucleosome, the basic patch of the H4 tail competed for binding with AutoN and released the autoinhibition (see also chapter 2.2). However, the H4 tail was apparently also critically involved in later steps of catalysis like efficient coupling of ATP hydrolysis to sliding as H4 tail-depleted nucleosomes were remodeled much less efficiently than wild-type nucleosomes even when AutoN was mutated. While lysine 12 of histone H4 was proposed to partially mediate this additional H4 tail-dependency of ISWI, the molecular details and whether further epitopes of the tail were involved remained unclear. Notably, also in the sliding mechanism employed by Chd1 the H4 tail apparently fulfills diverse functions (Hauk et al., 2010). Taken together, the H4 tail obviously governs several key steps of ISWI catalysis we are just starting to understand.

3.2.1 The regulatory potential of H4K16ac

H4 tail modifications are likely candidates for regulating and targeting ISWI activity *in vivo*, and especially H4K16ac was postulated to play a crucial role by negatively affecting ISWI remodeling (see chapter 1.3.3). Unexpectedly, in our analyses we did not observe inhibition of the remodeling activities of ISWI and ACF by H4K16ac (Clapier and Cairns, 2012; Clapier et al., 2002; Corona et al., 2002; Ferreira et al., 2007; Shogren-Knaak et al., 2006). Under saturating conditions, the ATPase as well as remodeling activity of ISWI was indistinguishable on acetylated and unmodified chromatin fibers. Even when stimulating DNA-bound ISWI with H4 tail peptides in an experimental setting closely resembling published results (Clapier and Cairns, 2012; Clapier et al., 2002) we did not detect a striking inhibitory effect of the acetylation. We observed, however, a moderate preference of ISWI – but not ACF – for the acetylated nucleosome fibers at the level of substrate choice. The underlying principle is unclear, and different scenarios are conceivable. For instance, the acetylation may increase the accessibility of H4 tail or further nucleosomal epitopes involved in binding ISWI and stabilizing it on the nucleosome. Tight inter-nucleosomal interactions may occlude these epitopes in the absence of acetylation (see chapter 1.1.3). Analogously, in chromatin fibers containing the linker histone H1 H4K16ac may have a decompacting effect resulting in better accessibility of the individual chromatosomes for ISWI. This increased accessibility may explain the faster remodeling of acetylated chromatin fibers we observed. Nevertheless, technical issues complicated the interpretation of our findings in case of the H1-containing fibers and need to be overcome before the results can be analyzed with confidence. Taken together, we could clearly demonstrate that H4K16ac does not inhibit ISWI or ACF activity in a pure *in vitro* system of chromatin fibers. Therefore, the previously observed negative regulatory effect of the modification is apparently less robust and universally relevant than widely assumed. Instead, it seems to be context-dependent and even cancelled and counteracted at the level of folded chromatin fibers, the currently most accurate *in vitro* correlate of *in vivo* chromatin structures (see chapter 1.1.3). Although contrary to prominent models, these conclusions are in accordance with further studies reporting an only very subtle (Clapier and Cairns, 2012; Clapier et al., 2002; Corona et al., 2002; Ferreira et al., 2007) or even no (Clapier and Cairns, 2012; Georgel et al., 1997; Nightingale et al., 2007) impact of H4K16 acetylation or mutation to glutamine or alanine on the activity of ISWI complexes in different experimental settings. Thus, long-held concepts of the role of H4K16ac for regulating ISWI have to be reconsidered and carefully reassessed taking the local chromatin context into account. Moreover, our study underlines the importance of employing folded chromatin fibers instead of mononucleosomes to investigate chromatin-based processes to assure capturing physiologically relevant effects.

3.2.2 Implications for the *in vivo* role of ISWI in chromatin organization

In the light of our finding of H4K16ac not reducing ISWI activity, prominent models of how ISWI complexes and the acetylation interplay in establishing higher order chromatin structures *in vivo* have to be reconsidered. According to a simple model, ISWI complexes globally establish and maintain chromatin compaction. H4K16ac, on the contrary, decondenses chromatin by a mechanism including inhibition of the nucleosome sliding activity of ISWI, rendering the male X chromosome of *Drosophila* especially sensitive to ISWI loss (see chapter 1.3.4). This scenario is not supported by our observation of H4K16ac rather enhancing than reducing ISWI activity. However, the chromatin compaction capabilities of ISWI complexes apparently do not solely depend on their nucleosome sliding and spacing activities, as nucleosome positions were largely retained upon ISWI depletion, whereas chromatin higher order structure was dramatically deranged (Sala et al., 2011). Likely, also a failure in properly incorporating the linker histone H1 into chromatin contributed to the chromatin decondensation observed in ISWI-depleted flies. Whether ISWI complexes are directly engaged in linker histone deposition as implied by *in vitro* studies, and whether H4K16ac interferes with this activity remain open questions. Recent evidence suggests that in case of the chromatin remodeling factor Chd1 nucleosome assembly and sliding are distinct activities (Torigoe et al., 2013). Thus, it is conceivable that also the different remodeling capabilities of ISWI – chromatosome assembly and sliding – vary mechanistically and are differentially regulated. Whereas H4K16ac did not negatively affect sliding in the context of chromatin fibers, assembly may be impaired. In summary, much remains to be learnt about the complex interplay of ISWI, H4K16ac, and the linker histone in the formation of higher order chromatin structures. While *in vitro* studies are well suited to test different, isolated aspects and components of this interplay, it has to be appreciated that the situation *in vivo* is probably much more sophisticated. Plenty of additional factors, modifications, and enzymatic activities are locally and globally contributing to fine-tuning chromatin organization in a context-dependent manner.

3.3 Future goals

Although much progress has been made in biochemically characterizing the ISWI enzyme, its molecular mechanism and regulation, many open questions remain. A pressing goal on the way to understanding the mechanistic details of a nucleosome sliding reaction is to carefully characterize the interaction of ISWI and the nucleosome at different steps of the catalytic cycle. Thereby, how the HSS domain contributes to the sliding reaction and how it cooperates with the ATPase domain may finally be revealed. Also the role of the HSS domain in guiding sliding directionality and nucleosome spacing remains to be elucidated. Furthermore, determining ISWI conformational states in conjunction with nucleosomal substrates and ATP analogs will advance our knowledge on the regulation of the enzymatic activity by nucleosomal as well as intrinsic features including AutoN and NegC. Of special interest is the nature of the interaction of ISWI with the H4 tail and the role different tail epitopes play during catalysis. How and at which step H4K16ac may affect catalysis could be clarified that way. Besides characterizing details of the ISWI sliding reaction, also expanding the analysis to further chromatin remodeling factors will be of interest to uncover common principles and individual differences. Thereby, an in-depth understanding of the distinct properties and functions of the numerous accessory domains and subunits will be gained, a key step towards unraveling the complexity of chromatin remodeling complexes.

Another exciting aspect of chromatin remodeling concerns the structural plasticity of the nucleosome during a sliding reaction. So far, it is unknown how the nucleosome accommodates the permanent deficit of DNA imposed by the activity of ISWI (see chapter 3.1). Changes in the structure of not only the nucleosomal DNA but also the octamer are likely. Maybe also an altered path of the DNA on the octamer surface is adopted. Investigating these conformational states of the nucleosome will importantly contribute to the emerging view of the nucleosome as variable, flexible particle instead of a rigid entity. On a related note, characterizing the mechanism by which the base pairs mobilized by the translocation activity of ISWI at SHL2 are transported towards the exit site constitutes another major challenge.

To further explore the regulatory potential of histone modifications for ISWI activity, the role of H4K16ac in the context of H1-containing chromatin fibers should be investigated in more detail. Moreover, also the capability of other histone modifications to modulate ISWI remodeling should be analysed. Acetylation of histone H4 at lysine 12, for example, was reported earlier to reduce ISWI activity (Clapier and Cairns, 2012; Clapier et al., 2002). Therefore, testing the influence of this modification in the context of chromatin fibers would certainly be interesting. Moreover, combinations of histone PTMs may synergistically affect ISWI function, and single, individual marks may be of minor relevance. As already mentioned in chapter 1.2.3, recently a positive allosteric effect of H4K16ac on the binding affinity of BPTF, the human homolog of Nurf301, to nucleosomes carrying a trimethylation on lysine 4 of histone H3 was described. Similar synergistic effects at the level of factor binding or later catalytic steps may exist in the context of other ISWI complexes. Acf1, for instance, also harbors PHD fingers and a bromodomain that might recognize combinatorial histone marks. A special focus should furthermore be put on exploring the interplay of H4K16ac and highly abundant histone marks like methylation of histone H4 at lysine 20 (C. Feller and P.B. Becker, personal communication). In fact, given its frequency the methylated rather than the unmodified state may represent the default nucleosome configuration *in vivo* in flies. This observation should be taken into account also in *in vitro* studies. In conclusion, regulation of ISWI complexes by histone modifications remains an attractive concept that deserves further exploration. These studies will profit from the increasing availability of large quantities of post-translationally modified histones. The rapid histone purification method we developed (see chapter 2.4) will further stream-line histone production and promote *in vitro* studies.

Performing restriction enzyme accessibility-based remodeling assays with ISWI and ACF, we noted remodeling factor-dependent differences in the distribution of DNA fragment sizes (see Figure 3 in chapter 2.4). We speculate that these differences may reflect distinct ways of how ISWI and ACF encounter the chromatin fibers, for example by initially remodeling central or outer nucleosomes of an array. To investigate this biologically potentially relevant aspect of chromatin remodeling further, we are currently collaborating with the Schiessel laboratory (Universiteit Leiden, Netherlands) to set up a mathematical model capturing the DNA digestion kinetics. Thereby, we hope to learn which mechanism is underlying the observed differences.

As discussed in chapter 1.1.3, the compaction capabilities of chromatin fibers depend on the NRL. It is therefore conceivable that the extent of the chromatin decondensing effect of H4K16ac varies with NRL. Probing this hypothesis by analytical ultracentrifugation remains a future challenge. Should H4K16ac-driven decondensation indeed depend on the NRL, analyzing ISWI remodeling activity on acetylated and unmodified chromatin fibers with variable NRL and therefore compaction state would be an important next step. These studies would help us understand the role of nucleosome accessibility for ISWI activity. In general, further improvement and characterization of the chromatin *in vitro* systems is desirable to be able to represent the *in vivo* situation even more accurately than currently possible. These refinements should include stable incorporation of the linker histone. Furthermore, strategies and conditions allowing to closely mimic the fractal structures chromatin presumably adapts *in vivo* should be explored, such as employing high concentrations of chromatin and salts to promote inter-fiber interactions and fiber oligomerization (see chapter 1.1.3).

References

Aasland, R., Stewart, A.F., and Gibson, T. (1996). The SANT domain: a putative DNA-binding domain in the SWI-SNF and ADA complexes, the transcriptional co-repressor N-CoR and TFIIIB. Trends in biochemical sciences *21*, 87-88.

Akhtar, A., and Becker, P.B. (2000). Activation of transcription through histone H4 acetylation by MOF, an acetyltransferase essential for dosage compensation in Drosophila. Molecular cell *5*, 367-375.

Allahverdi, A., Yang, R., Korolev, N., Fan, Y., Davey, C.A., Liu, C.F., and Nordenskiöld, L. (2011). The effects of histone H4 tail acetylations on cation-induced chromatin folding and self-association. Nucleic acids research *39*, 1680-1691.

Allan, J., Harborne, N., Rau, D.C., and Gould, H. (1982). Participation of core histone "tails" in the stabilization of the chromatin solenoid. The Journal of cell biology *93*, 285-297.

Allan, J., Hartman, P.G., Crane-Robinson, C., and Aviles, F.X. (1980). The structure of histone H1 and its location in chromatin. Nature *288*, 675-679.

Allan, J., Mitchell, T., Harborne, N., Bohm, L., and Crane-Robinson, C. (1986). Roles of H1 domains in determining higher order chromatin structure and H1 location. Journal of molecular biology *187*, 591-601.

Allfrey, V.G., Faulkner, R., and Mirsky, A.E. (1964). Acetylation and Methylation of Histones and Their Possible Role in the Regulation of Rna Synthesis. Proceedings of the National Academy of Sciences of the United States of America *51*, 786-794.

Andrews, A.J., and Luger, K. (2011). Nucleosome structure(s) and stability: variations on a theme. Annual review of biophysics *40*, 99-117.

Badenhorst, P., Voas, M., Rebay, I., and Wu, C. (2002). Biological functions of the ISWI chromatin remodeling complex NURF. Genes & development *16*, 3186-3198.

Bannister, A.J., and Kouzarides, T. (2011). Regulation of chromatin by histone modifications. Cell research *21*, 381-395.

Barth, T.K., and Imhof, A. (2010). Fast signals and slow marks: the dynamics of histone modifications. Trends in biochemical sciences *35*, 618-626.

Becker, P.B., and Workman, J.L. (2013). Nucleosome remodeling and epigenetics. Cold Spring Harbor perspectives in biology *5*.

Bednar, J., Horowitz, R.A., Grigoryev, S.A., Carruthers, L.M., Hansen, J.C., Koster, A.J., and Woodcock, C.L. (1998). Nucleosomes, linker DNA, and linker histone form a unique structural motif that directs the higher-order folding and compaction of chromatin. Proceedings of the National Academy of Sciences of the United States of America *95*, 14173-14178.

Bell, O., Schwaiger, M., Oakeley, E.J., Lienert, F., Beisel, C., Stadler, M.B., and Schübeler, D. (2010). Accessibility of the Drosophila genome discriminates PcG repression, H4K16 acetylation and replication timing. Nature structural & molecular biology *17*, 894-900.

Berdasco, M., and Esteller, M. (2013). Genetic syndromes caused by mutations in epigenetic genes. Human genetics *132*, 359-383.

Bergmann, J.H., and Spector, D.L. (2014). Long non-coding RNAs: modulators of nuclear structure and function. Current opinion in cell biology *26C*, 10-18.

Blank, T.A., and Becker, P.B. (1995). Electrostatic mechanism of nucleosome spacing. Journal of molecular biology *252*, 305-313.

Bönisch, C., and Hake, S.B. (2012). Histone H2A variants in nucleosomes and chromatin: more or less stable? Nucleic acids research *40*, 10719-10741.

Bouazoune, K., and Brehm, A. (2006). ATP-dependent chromatin remodeling complexes in Drosophila. Chromosome research : an international journal on the molecular, supramolecular and evolutionary aspects of chromosome biology *14*, 433-449.

Boulikas, T., Wiseman, J.M., and Garrard, W.T. (1980). Points of contact between histone H1 and the histone octamer. Proceedings of the National Academy of Sciences of the United States of America *77*, 127-131.

Bowman, G.D. (2010). Mechanisms of ATP-dependent nucleosome sliding. Current opinion in structural biology *20*, 73-81.

Braunschweig, U., Hogan, G.J., Pagie, L., and van Steensel, B. (2009). Histone H1 binding is inhibited by histone variant H3.3. The EMBO journal *28*, 3635-3645.

Brown, D.T., Izard, T., and Misteli, T. (2006). Mapping the interaction surface of linker histone H1(0) with the nucleosome of native chromatin in vivo. Nature structural & molecular biology *13*, 250-255.

Buning, R., and van Noort, J. (2010). Single-pair FRET experiments on nucleosome conformational dynamics. Biochimie *92*, 1729-1740.

Calestagne-Morelli, A., and Ausio, J. (2006). Long-range histone acetylation: biological significance, structural implications, and mechanisms. Biochemistry and cell biology = Biochimie et biologie cellulaire *84*, 518-527.

Caron, F., and Thomas, J.O. (1981). Exchange of histone H1 between segments of chromatin. Journal of molecular biology *146*, 513-537.

Carruthers, L.M., Bednar, J., Woodcock, C.L., and Hansen, J.C. (1998). Linker histones stabilize the intrinsic salt-dependent folding of nucleosomal arrays: mechanistic ramifications for higher-order chromatin folding. Biochemistry *37*, 14776-14787.

Carruthers, L.M., and Hansen, J.C. (2000). The core histone N termini function independently of linker histones during chromatin condensation. The Journal of biological chemistry *275*, 37285-37290.

Caterino, T.L., Fang, H., and Hayes, J.J. (2011). Nucleosome linker DNA contacts and induces specific folding of the intrinsically disordered H1 carboxyl-terminal domain. Molecular and cellular biology *31*, 2341-2348.

Caterino, T.L., and Hayes, J.J. (2011). Structure of the H1 C-terminal domain and function in chromatin condensation. Biochemistry and cell biology = Biochimie et biologie cellulaire *89*, 35-44.

Catez, F., Ueda, T., and Bustin, M. (2006). Determinants of histone H1 mobility and chromatin binding in living cells. Nature structural & molecular biology *13*, 305-310.

Chatterjee, C., and Muir, T.W. (2010). Chemical approaches for studying histone modifications. The Journal of biological chemistry *285*, 11045-11050.

Chioda, M., Vengadasalam, S., Kremmer, E., Eberharter, A., and Becker, P.B. (2010). Developmental role for ACF1-containing nucleosome remodellers in chromatin organisation. Development *137*, 3513-3522.

Chodaparambil, J.V., Barbera, A.J., Lu, X., Kaye, K.M., Hansen, J.C., and Luger, K. (2007). A charged and contoured surface on the nucleosome regulates chromatin compaction. Nature structural & molecular biology *14*, 1105-1107.

Clapier, C.R., and Cairns, B.R. (2009). The biology of chromatin remodeling complexes. Annual review of biochemistry *78*, 273-304.

Clapier, C.R., and Cairns, B.R. (2012). Regulation of ISWI involves inhibitory modules antagonized by nucleosomal epitopes. Nature *492*, 280-284.

Clapier, C.R., Längst, G., Corona, D.F., Becker, P.B., and Nightingale, K.P. (2001). Critical role for the histone H4 N terminus in nucleosome remodeling by ISWI. Molecular and cellular biology *21*, 875-883.

Clapier, C.R., Nightingale, K.P., and Becker, P.B. (2002). A critical epitope for substrate recognition by the nucleosome remodeling ATPase ISWI. Nucleic acids research *30*, 649-655.

Clark, D.J., and Kimura, T. (1990). Electrostatic mechanism of chromatin folding. Journal of molecular biology *211*, 883-896.

Clausell, J., Happel, N., Hale, T.K., Doenecke, D., and Beato, M. (2009). Histone H1 subtypes differentially modulate chromatin condensation without preventing ATP-dependent remodeling by SWI/SNF or NURF. PloS one *4*, e0007243.

Conrad, T., and Akhtar, A. (2011). Dosage compensation in Drosophila melanogaster: epigenetic fine-tuning of chromosome-wide transcription. Nature reviews Genetics *13*, 123-134.

Corona, D.F., Clapier, C.R., Becker, P.B., and Tamkun, J.W. (2002). Modulation of ISWI function by site-specific histone acetylation. EMBO reports *3*, 242-247.

Corona, D.F., Eberharter, A., Budde, A., Deuring, R., Ferrari, S., Varga-Weisz, P., Wilm, M., Tamkun, J., and Becker, P.B. (2000). Two histone fold proteins, CHRAC-14 and CHRAC-16, are developmentally regulated subunits of chromatin accessibility complex (CHRAC). The EMBO journal *19*, 3049-3059.

Corona, D.F., Längst, G., Clapier, C.R., Bonte, E.J., Ferrari, S., Tamkun, J.W., and Becker, P.B. (1999). ISWI is an ATP-dependent nucleosome remodeling factor. Molecular cell *3*, 239-245.

Corona, D.F., Siriaco, G., Armstrong, J.A., Snarskaya, N., McClymont, S.A., Scott, M.P., and Tamkun, J.W. (2007). ISWI regulates higher-order chromatin structure and histone H1 assembly in vivo. PLoS biology *5*, e232.

Correll, S.J., Schubert, M.H., and Grigoryev, S.A. (2012). Short nucleosome repeats impose rotational modulations on chromatin fibre folding. The EMBO journal *31*, 2416-2426.

Daban, J.R., and Bermudez, A. (1998). Interdigitated solenoid model for compact chromatin fibers. Biochemistry *37*, 4299-4304.

Dang, W., Kagalwala, M.N., and Bartholomew, B. (2006). Regulation of ISW2 by concerted action of histone H4 tail and extranucleosomal DNA. Molecular and cellular biology *26*, 7388-7396.

Davey, C.A., Sargent, D.F., Luger, K., Maeder, A.W., and Richmond, T.J. (2002). Solvent mediated interactions in the structure of the nucleosome core particle at 1.9 a resolution. Journal of molecular biology *319*, 1097-1113.

Deindl, S., Hwang, W.L., Hota, S.K., Blosser, T.R., Prasad, P., Bartholomew, B., and Zhuang, X. (2013). ISWI remodelers slide nucleosomes with coordinated multi-base-pair entry steps and single-base-pair exit steps. Cell *152*, 442-452.

Deuring, R., Fanti, L., Armstrong, J.A., Sarte, M., Papoulas, O., Prestel, M., Daubresse, G., Verardo, M., Moseley, S.L., Berloco, M.*, et al.* (2000). The ISWI chromatin-remodeling protein is required for gene expression and the maintenance of higher order chromatin structure in vivo. Molecular cell *5*, 355-365.

Diesinger, P.M., and Heermann, D.W. (2009). Depletion effects massively change chromatin properties and influence genome folding. Biophysical journal *97*, 2146-2153.

Dorigo, B., Schalch, T., Bystricky, K., and Richmond, T.J. (2003). Chromatin fiber folding: requirement for the histone H4 N-terminal tail. Journal of molecular biology *327*, 85-96.

Dorigo, B., Schalch, T., Kulangara, A., Duda, S., Schroeder, R.R., and Richmond, T.J. (2004). Nucleosome arrays reveal the two-start organization of the chromatin fiber. Science *306*, 1571-1573.

Du, J., Zhou, Y., Su, X., Yu, J.J., Khan, S., Jiang, H., Kim, J., Woo, J., Kim, J.H., Choi, B.H., *et al.* (2011). Sirt5 is a NAD-dependent protein lysine demalonylase and desuccinylase. Science *334*, 806-809.

Dürr, H., Flaus, A., Owen-Hughes, T., and Hopfner, K.P. (2006). Snf2 family ATPases and DExx box helicases: differences and unifying concepts from high-resolution crystal structures. Nucleic acids research *34*, 4160-4167.

Eberharter, A., and Becker, P.B. (2002). Histone acetylation: a switch between repressive and permissive chromatin. Second in review series on chromatin dynamics. EMBO reports *3*, 224-229.

Eberharter, A., Ferrari, S., Längst, G., Straub, T., Imhof, A., Varga-Weisz, P., Wilm, M., and Becker, P.B. (2001). Acf1, the largest subunit of CHRAC, regulates ISWI-induced nucleosome remodelling. The EMBO journal *20*, 3781-3788.

Eberharter, A., Vetter, I., Ferreira, R., and Becker, P.B. (2004). ACF1 improves the effectiveness of nucleosome mobilization by ISWI through PHD-histone contacts. The EMBO journal *23*, 4029-4039.

Emelyanov, A.V., Vershilova, E., Ignatyeva, M.A., Pokrovsky, D.K., Lu, X., Konev, A.Y., and Fyodorov, D.V. (2012). Identification and characterization of ToRC, a novel ISWI-containing ATP-dependent chromatin assembly complex. Genes & development *26*, 603-614.

Evertts, A.G., Zee, B.M., Dimaggio, P.A., Gonzales-Cope, M., Coller, H.A., and Garcia, B.A. (2013). Quantitative dynamics of the link between cellular metabolism and histone acetylation. The Journal of biological chemistry *288*, 12142-12151.

Fan, J.Y., Rangasamy, D., Luger, K., and Tremethick, D.J. (2004). H2A.Z alters the nucleosome surface to promote HP1alpha-mediated chromatin fiber folding. Molecular cell *16*, 655-661.

Fan, Y., Nikitina, T., Morin-Kensicki, E.M., Zhao, J., Magnuson, T.R., Woodcock, C.L., and Skoultchi, A.I. (2003). H1 linker histones are essential for mouse development and affect nucleosome spacing in vivo. Molecular and cellular biology *23*, 4559-4572.

Fan, Y., Nikitina, T., Zhao, J., Fleury, T.J., Bhattacharyya, R., Bouhassira, E.E., Stein, A., Woodcock, C.L., and Skoultchi, A.I. (2005). Histone H1 depletion in mammals alters global chromatin structure but causes specific changes in gene regulation. Cell *123*, 1199-1212.

Fazzio, T.G., Gelbart, M.E., and Tsukiyama, T. (2005). Two distinct mechanisms of chromatin interaction by the Isw2 chromatin remodeling complex in vivo. Molecular and cellular biology *25*, 9165-9174.

Ferreira, H., Flaus, A., and Owen-Hughes, T. (2007). Histone modifications influence the action of Snf2 family remodelling enzymes by different mechanisms. Journal of molecular biology *374*, 563-579.

Finch, J.T., and Klug, A. (1976). Solenoidal model for superstructure in chromatin. Proceedings of the National Academy of Sciences of the United States of America *73*, 1897-1901.

Flaus, A., Martin, D.M., Barton, G.J., and Owen-Hughes, T. (2006). Identification of multiple distinct Snf2 subfamilies with conserved structural motifs. Nucleic acids research *34*, 2887-2905.

Fletcher, T.M., and Hansen, J.C. (1995). Core histone tail domains mediate oligonucleosome folding and nucleosomal DNA organization through distinct molecular mechanisms. The Journal of biological chemistry *270*, 25359-25362.

Fussner, E., Ching, R.W., and Bazett-Jones, D.P. (2011). Living without 30nm chromatin fibers. Trends in biochemical sciences *36*, 1-6.

Fussner, E., Strauss, M., Djuric, U., Li, R., Ahmed, K., Hart, M., Ellis, J., and Bazett-Jones, D.P. (2012). Open and closed domains in the mouse genome are configured as 10-nm chromatin fibres. EMBO reports *13*, 992-996.

Fyodorov, D.V., Blower, M.D., Karpen, G.H., and Kadonaga, J.T. (2004). Acf1 confers unique activities to ACF/CHRAC and promotes the formation rather than disruption of chromatin in vivo. Genes & development *18*, 170-183.

Gangaraju, V.K., and Bartholomew, B. (2007a). Dependency of ISW1a chromatin remodeling on extranucleosomal DNA. Molecular and cellular biology *27*, 3217-3225.

Gangaraju, V.K., and Bartholomew, B. (2007b). Mechanisms of ATP dependent chromatin remodeling. Mutation research *618*, 3-17.

Gangaraju, V.K., Prasad, P., Srour, A., Kagalwala, M.N., and Bartholomew, B. (2009). Conformational changes associated with template commitment in ATP-dependent chromatin remodeling by ISW2. Molecular cell *35*, 58-69.

Garcia-Ramirez, M., Dong, F., and Ausio, J. (1992). Role of the histone "tails" in the folding of oligonucleosomes depleted of histone H1. The Journal of biological chemistry *267*, 19587-19595.

Garcia-Ramirez, M., Rocchini, C., and Ausio, J. (1995). Modulation of chromatin folding by histone acetylation. The Journal of biological chemistry *270*, 17923-17928.

Gelbart, M.E., Larschan, E., Peng, S., Park, P.J., and Kuroda, M.I. (2009). Drosophila MSL complex globally acetylates H4K16 on the male X chromosome for dosage compensation. Nature structural & molecular biology *16*, 825-832.

Georgel, P.T., Tsukiyama, T., and Wu, C. (1997). Role of histone tails in nucleosome remodeling by Drosophila NURF. The EMBO journal *16*, 4717-4726.

Gordon, F., Luger, K., and Hansen, J.C. (2005). The core histone N-terminal tail domains function independently and additively during salt-dependent oligomerization of nucleosomal arrays. The Journal of biological chemistry *280*, 33701-33706.

Goytisolo, F.A., Gerchman, S.E., Yu, X., Rees, C., Graziano, V., Ramakrishnan, V., and Thomas, J.O. (1996). Identification of two DNA-binding sites on the globular domain of histone H5. The EMBO journal *15*, 3421-3429.

Grigoryev, S.A. (2012). Nucleosome spacing and chromatin higher-order folding. Nucleus *3*, 493-499.

Grigoryev, S.A., Arya, G., Correll, S., Woodcock, C.L., and Schlick, T. (2009). Evidence for heteromorphic chromatin fibers from analysis of nucleosome interactions. Proceedings of the National Academy of Sciences of the United States of America *106*, 13317-13322.

Grigoryev, S.A., and Woodcock, C.L. (2012). Chromatin organization - the 30 nm fiber. Experimental cell research *318*, 1448-1455.

Grüne, T., Brzeski, J., Eberharter, A., Clapier, C.R., Corona, D.F., Becker, P.B., and Müller, C.W. (2003). Crystal structure and functional analysis of a nucleosome recognition module of the remodeling factor ISWI. Molecular cell *12*, 449-460.

Gunjan, A., Alexander, B.T., Sittman, D.B., and Brown, D.T. (1999). Effects of H1 histone variant overexpression on chromatin structure. The Journal of biological chemistry *274*, 37950-37956.

Hall, M.A., Shundrovsky, A., Bai, L., Fulbright, R.M., Lis, J.T., and Wang, M.D. (2009). High-resolution dynamic mapping of histone-DNA interactions in a nucleosome. Nature structural & molecular biology *16*, 124-129.

Hamiche, A., Kang, J.G., Dennis, C., Xiao, H., and Wu, C. (2001). Histone tails modulate nucleosome mobility and regulate ATP-dependent nucleosome sliding by NURF. Proceedings of the National Academy of Sciences of the United States of America *98*, 14316-14321.

Hamiche, A., Sandaltzopoulos, R., Gdula, D.A., and Wu, C. (1999). ATP-dependent histone octamer sliding mediated by the chromatin remodeling complex NURF. Cell *97*, 833-842.

Hamiche, A., Schultz, P., Ramakrishnan, V., Oudet, P., and Prunell, A. (1996). Linker histone-dependent DNA structure in linear mononucleosomes. Journal of molecular biology *257*, 30-42.

Hanai, K., Furuhashi, H., Yamamoto, T., Akasaka, K., and Hirose, S. (2008). RSF governs silent chromatin formation via histone H2Av replacement. PLoS genetics *4*, e1000011.

Hansen, J.C. (2002). Conformational dynamics of the chromatin fiber in solution: determinants, mechanisms, and functions. Annual review of biophysics and biomolecular structure *31*, 361-392.

Hansen, J.C. (2012). Human mitotic chromosome structure: what happened to the 30-nm fibre? The EMBO journal *31*, 1621-1623.

Hartlepp, K.F., Fernandez-Tornero, C., Eberharter, A., Grüne, T., Müller, C.W., and Becker, P.B. (2005). The histone fold subunits of Drosophila CHRAC facilitate nucleosome sliding through dynamic DNA interactions. Molecular and cellular biology *25*, 9886-9896.

Hauk, G., McKnight, J.N., Nodelman, I.M., and Bowman, G.D. (2010). The chromodomains of the Chd1 chromatin remodeler regulate DNA access to the ATPase motor. Molecular cell *39*, 711-723.

He, X., Fan, H.Y., Narlikar, G.J., and Kingston, R.E. (2006). Human ACF1 alters the remodeling strategy of SNF2h. The Journal of biological chemistry *281*, 28636-28647.

Hebbes, T.R., Clayton, A.L., Thorne, A.W., and Crane-Robinson, C. (1994). Core histone hyperacetylation co-maps with generalized DNase I sensitivity in the chicken beta-globin chromosomal domain. The EMBO journal *13*, 1823-1830.

Heise, F., Chung, H.R., Weber, J.M., Xu, Z., Klein-Hitpass, L., Steinmetz, L.M., Vingron, M., and Ehrenhofer-Murray, A.E. (2012). Genome-wide H4 K16 acetylation by SAS-I is deposited independently of transcription and histone exchange. Nucleic acids research *40*, 65-74.

Hendzel, M.J., Lever, M.A., Crawford, E., and Th'ng, J.P. (2004). The C-terminal domain is the primary determinant of histone H1 binding to chromatin in vivo. The Journal of biological chemistry *279*, 20028-20034.

Henikoff, S., Furuyama, T., and Ahmad, K. (2004). Histone variants, nucleosome assembly and epigenetic inheritance. Trends in genetics : TIG *20*, 320-326.

Hilfiker, A., Hilfiker-Kleiner, D., Pannuti, A., and Lucchesi, J.C. (1997). mof, a putative acetyl transferase gene related to the Tip60 and MOZ human genes and to the SAS genes of yeast, is required for dosage compensation in Drosophila. The EMBO journal *16*, 2054-2060.

Hizume, K., Yoshimura, S.H., and Takeyasu, K. (2005). Linker histone H1 per se can induce three-dimensional folding of chromatin fiber. Biochemistry *44*, 12978-12989.

Hochheimer, A., Zhou, S., Zheng, S., Holmes, M.C., and Tjian, R. (2002). TRF2 associates with DREF and directs promoter-selective gene expression in Drosophila. Nature *420*, 439-445.

Hon, G.C., Hawkins, R.D., and Ren, B. (2009). Predictive chromatin signatures in the mammalian genome. Human molecular genetics *18*, R195-201.

Horikoshi, N., Kumar, P., Sharma, G.G., Chen, M., Hunt, C.R., Westover, K., Chowdhury, S., and Pandita, T.K. (2013). Genome-wide distribution of histone H4 Lysine 16 acetylation sites and their relationship to gene expression. Genome integrity *4*, 3.

Horowitz-Scherer, R.A., and Woodcock, C.L. (2006). Organization of interphase chromatin. Chromosoma *115*, 1-14.

Hota, S.K., Bhardwaj, S.K., Deindl, S., Lin, Y.C., Zhuang, X., and Bartholomew, B. (2013). Nucleosome mobilization by ISW2 requires the concerted action of the ATPase and SLIDE domains. Nature structural & molecular biology *20*, 222-229.

Huynh, V.A., Robinson, P.J., and Rhodes, D. (2005). A method for the in vitro reconstitution of a defined "30 nm" chromatin fibre containing stoichiometric amounts of the linker histone. Journal of molecular biology *345*, 957-968.

Ito, T., Bulger, M., Pazin, M.J., Kobayashi, R., and Kadonaga, J.T. (1997). ACF, an ISWI-containing and ATP-utilizing chromatin assembly and remodeling factor. Cell *90*, 145-155.

Ito, T., Levenstein, M.E., Fyodorov, D.V., Kutach, A.K., Kobayashi, R., and Kadonaga, J.T. (1999). ACF consists of two subunits, Acf1 and ISWI, that function cooperatively in the ATP-dependent catalysis of chromatin assembly. Genes & development *13*, 1529-1539.

Izzo, A., Kamieniarz-Gdula, K., Ramirez, F., Noureen, N., Kind, J., Manke, T., van Steensel, B., and Schneider, R. (2013). The genomic landscape of the somatic linker histone subtypes H1.1 to H1.5 in human cells. Cell reports *3*, 2142-2154.

Izzo, A., Kamieniarz, K., and Schneider, R. (2008). The histone H1 family: specific members, specific functions? Biological chemistry *389*, 333-343.

Joti, Y., Hikima, T., Nishino, Y., Kamada, F., Hihara, S., Takata, H., Ishikawa, T., and Maeshima, K. (2012). Chromosomes without a 30-nm chromatin fiber. Nucleus *3*, 404-410.

Jung, H.R., Sidoli, S., Haldbo, S., Sprenger, R.R., Schwammle, V., Pasini, D., Helin, K., and Jensen, O.N. (2013). Precision mapping of coexisting modifications in histone H3 tails from embryonic stem cells by ETD-MS/MS. Analytical chemistry *85*, 8232-8239.

Kagalwala, M.N., Glaus, B.J., Dang, W., Zofall, M., and Bartholomew, B. (2004). Topography of the ISW2-nucleosome complex: insights into nucleosome spacing and chromatin remodeling. The EMBO journal *23*, 2092-2104.

Kalashnikova, A.A., Porter-Goff, M.E., Muthurajan, U.M., Luger, K., and Hansen, J.C. (2013a). The role of the nucleosome acidic patch in modulating higher order chromatin structure. Journal of the Royal Society, Interface / the Royal Society *10*, 20121022.

Kalashnikova, A.A., Winkler, D.D., McBryant, S.J., Henderson, R.K., Herman, J.A., DeLuca, J.G., Luger, K., Prenni, J.E., and Hansen, J.C. (2013b). Linker histone H1.0 interacts with an extensive network of proteins found in the nucleolus. Nucleic acids research *41*, 4026-4035.

Kan, P.Y., Caterino, T.L., and Hayes, J.J. (2009). The H4 tail domain participates in intra- and internucleosome interactions with protein and DNA during folding and oligomerization of nucleosome arrays. Molecular and cellular biology *29*, 538-546.

Kapoor-Vazirani, P., Kagey, J.D., and Vertino, P.M. (2011). SUV420H2-mediated H4K20 trimethylation enforces RNA polymerase II promoter-proximal pausing by blocking hMOF-dependent H4K16 acetylation. Molecular and cellular biology *31*, 1594-1609.

Korolev, N., Allahverdi, A., Yang, Y., Fan, Y., Lyubartsev, A.P., and Nordenskiöld, L. (2010). Electrostatic origin of salt-induced nucleosome array compaction. Biophysical journal *99*, 1896-1905.

Kouzarides, T. (2007). Chromatin modifications and their function. Cell *128*, 693-705.

Kowalski, A., and Palyga, J. (2012). Linker histone subtypes and their allelic variants. Cell biology international *36*, 981-996.

Kruithof, M., Chien, F.T., Routh, A., Logie, C., Rhodes, D., and van Noort, J. (2009). Single-molecule force spectroscopy reveals a highly compliant helical folding for the 30-nm chromatin fiber. Nature structural & molecular biology *16*, 534-540.

Kukimoto, I., Elderkin, S., Grimaldi, M., Oelgeschlager, T., and Varga-Weisz, P.D. (2004). The histone-fold protein complex CHRAC-15/17 enhances nucleosome sliding and assembly mediated by ACF. Molecular cell *13*, 265-277.

Kurdistani, S.K., Tavazoie, S., and Grunstein, M. (2004). Mapping global histone acetylation patterns to gene expression. Cell *117*, 721-733.

Kurumizaka, H., Horikoshi, N., Tachiwana, H., and Kagawa, W. (2013). Current progress on structural studies of nucleosomes containing histone H3 variants. Current opinion in structural biology *23*, 109-115.

Kwon, S.Y., Xiao, H., Glover, B.P., Tjian, R., Wu, C., and Badenhorst, P. (2008). The nucleosome remodeling factor (NURF) regulates genes involved in Drosophila innate immunity. Developmental biology *316*, 538-547.

Längst, G., Bonte, E.J., Corona, D.F., and Becker, P.B. (1999). Nucleosome movement by CHRAC and ISWI without disruption or trans-displacement of the histone octamer. Cell *97*, 843-852.

Lantermann, A.B., Straub, T., Stralfors, A., Yuan, G.C., Ekwall, K., and Korber, P. (2010). Schizosaccharomyces pombe genome-wide nucleosome mapping reveals positioning mechanisms distinct from those of Saccharomyces cerevisiae. Nature structural & molecular biology *17*, 251-257.

Laybourn, P.J., and Kadonaga, J.T. (1991). Role of nucleosomal cores and histone H1 in regulation of transcription by RNA polymerase II. Science *254*, 238-245.

Leroy, G., Dimaggio, P.A., Chan, E.Y., Zee, B.M., Blanco, M.A., Bryant, B., Flaniken, I.Z., Liu, S., Kang, Y., Trojer, P.*, et al.* (2013). A quantitative atlas of histone modification signatures from human cancer cells. Epigenetics & chromatin *6*, 20.

Li, F., Allahverdi, A., Yang, R., Lua, G.B., Zhang, X., Cao, Y., Korolev, N., Nordenskiöld, L., and Liu, C.F. (2011). A direct method for site-specific protein acetylation. Angewandte Chemie *50*, 9611-9614.

Li, G., Levitus, M., Bustamante, C., and Widom, J. (2005). Rapid spontaneous accessibility of nucleosomal DNA. Nature structural & molecular biology *12*, 46-53.

Liu, C.L., Kaplan, T., Kim, M., Buratowski, S., Schreiber, S.L., Friedman, N., and Rando, O.J. (2005). Single-nucleosome mapping of histone modifications in S. cerevisiae. PLoS biology *3*, e328.

Lowary, P.T., and Widom, J. (1998). New DNA sequence rules for high affinity binding to histone octamer and sequence-directed nucleosome positioning. Journal of molecular biology *276*, 19-42.

Lu, X., and Hansen, J.C. (2004). Identification of specific functional subdomains within the linker histone H10 C-terminal domain. The Journal of biological chemistry *279*, 8701-8707.

Lu, X., Wontakal, S.N., Emelyanov, A.V., Morcillo, P., Konev, A.Y., Fyodorov, D.V., and Skoultchi, A.I. (2009). Linker histone H1 is essential for Drosophila development, the establishment of pericentric heterochromatin, and a normal polytene chromosome structure. Genes & development *23*, 452-465.

Lu, X., Wontakal, S.N., Kavi, H., Kim, B.J., Guzzardo, P.M., Emelyanov, A.V., Xu, N., Hannon, G.J., Zavadil, J., Fyodorov, D.V.*, et al.* (2013). Drosophila H1 regulates the genetic activity of heterochromatin by recruitment of Su(var)3-9. Science *340*, 78-81.

Luger, K., Dechassa, M.L., and Tremethick, D.J. (2012). New insights into nucleosome and chromatin structure: an ordered state or a disordered affair? Nature reviews Molecular cell biology *13*, 436-447.

Luger, K., and Hansen, J.C. (2005). Nucleosome and chromatin fiber dynamics. Current opinion in structural biology *15*, 188-196.

Luger, K., Mader, A.W., Richmond, R.K., Sargent, D.F., and Richmond, T.J. (1997). Crystal structure of the nucleosome core particle at 2.8 A resolution. Nature *389*, 251-260.

Luger, K., Rechsteiner, T.J., and Richmond, T.J. (1999). Expression and purification of recombinant histones and nucleosome reconstitution. Methods in molecular biology *119*, 1-16.

Lusser, A., and Kadonaga, J.T. (2004). Strategies for the reconstitution of chromatin. Nature methods *1*, 19-26.

Lusser, A., Urwin, D.L., and Kadonaga, J.T. (2005). Distinct activities of CHD1 and ACF in ATP-dependent chromatin assembly. Nature structural & molecular biology *12*, 160-166.

Maeshima, K., Hihara, S., and Eltsov, M. (2010). Chromatin structure: does the 30-nm fibre exist in vivo? Current opinion in cell biology *22*, 291-297.

Maier, V.K., Chioda, M., Rhodes, D., and Becker, P.B. (2008). ACF catalyses chromatosome movements in chromatin fibres. The EMBO journal *27*, 817-826.

Maresca, T.J., Freedman, B.S., and Heald, R. (2005). Histone H1 is essential for mitotic chromosome architecture and segregation in Xenopus laevis egg extracts. The Journal of cell biology *169*, 859-869.

McBryant, S.J., Adams, V.H., and Hansen, J.C. (2006). Chromatin architectural proteins. Chromosome research : an international journal on the molecular, supramolecular and evolutionary aspects of chromosome biology *14*, 39-51.

McBryant, S.J., Lu, X., and Hansen, J.C. (2010). Multifunctionality of the linker histones: an emerging role for protein-protein interactions. Cell research *20*, 519-528.

McKnight, J.N., Jenkins, K.R., Nodelman, I.M., Escobar, T., and Bowman, G.D. (2011). Extranucleosomal DNA binding directs nucleosome sliding by Chd1. Molecular and cellular biology *31*, 4746-4759.

Meyer, S., Becker, N.B., Syed, S.H., Goutte-Gattat, D., Shukla, M.S., Hayes, J.J., Angelov, D., Bednar, J., Dimitrov, S., and Everaers, R. (2011). From crystal and NMR structures, footprints and cryo-electron-micrographs to large and soft structures: nanoscale modeling of the nucleosomal stem. Nucleic acids research *39*, 9139-9154.

Millan-Arino, L., Islam, A.B., Izquierdo-Bouldstridge, A., Mayor, R., Terme, J.M., Luque, N., Sancho, M., Lopez-Bigas, N., and Jordan, A. (2014). Mapping of six somatic linker histone H1 variants in human breast cancer cells uncovers specific features of H1.2. Nucleic acids research.

Miyagi, A., Ando, T., and Lyubchenko, Y.L. (2011). Dynamics of nucleosomes assessed with time-lapse high-speed atomic force microscopy. Biochemistry *50*, 7901-7908.

Mizzen, C.A., and Allis, C.D. (1998). Linking histone acetylation to transcriptional regulation. Cellular and molecular life sciences : CMLS *54*, 6-20.

Moore, S.C., and Ausio, J. (1997). Major role of the histones H3-H4 in the folding of the chromatin fiber. Biochemical and biophysical research communications *230*, 136-139.

Narlikar, G.J., Sundaramoorthy, R., and Owen-Hughes, T. (2013). Mechanisms and functions of ATP-dependent chromatin-remodeling enzymes. Cell *154*, 490-503.

Nightingale, K.P., Baumann, M., Eberharter, A., Mamais, A., Becker, P.B., and Boyes, J. (2007). Acetylation increases access of remodelling complexes to their nucleosome targets to enhance initiation of V(D)J recombination. Nucleic acids research *35*, 6311-6321.

Nishino, Y., Eltsov, M., Joti, Y., Ito, K., Takata, H., Takahashi, Y., Hihara, S., Frangakis, A.S., Imamoto, N., Ishikawa, T.*, et al.* (2012). Human mitotic chromosomes consist predominantly of irregularly folded nucleosome fibres without a 30-nm chromatin structure. The EMBO journal *31*, 1644-1653.

Nodelman, I.M., and Bowman, G.D. (2013). Nucleosome sliding by Chd1 does not require rigid coupling between DNA-binding and ATPase domains. EMBO reports *14*, 1098-1103.

Noll, M., and Kornberg, R.D. (1977). Action of micrococcal nuclease on chromatin and the location of histone H1. Journal of molecular biology *109*, 393-404.

O'Neill, T.E., Meersseman, G., Pennings, S., and Bradbury, E.M. (1995). Deposition of histone H1 onto reconstituted nucleosome arrays inhibits both initiation and elongation of transcripts by T7 RNA polymerase. Nucleic acids research *23*, 1075-1082.

Oberg, C., and Belikov, S. (2012). The N-terminal domain determines the affinity and specificity of H1 binding to chromatin. Biochemical and biophysical research communications *420*, 321-324.

Offermann, C.A. (1936). Branched chromosomes as symmetrical duplications. Journal of Genetics *32*, 103-116.

Oppikofer, M., Kueng, S., and Gasser, S.M. (2013). SIR-nucleosome interactions: structure-function relationships in yeast silent chromatin. Gene *527*, 10-25.

Orrego, M., Ponte, I., Roque, A., Buschati, N., Mora, X., and Suau, P. (2007). Differential affinity of mammalian histone H1 somatic subtypes for DNA and chromatin. BMC biology *5*, 22.

Patel, D.J., and Wang, Z. (2013). Readout of epigenetic modifications. Annual review of biochemistry *82*, 81-118.

Pennings, S., Meersseman, G., and Bradbury, E.M. (1994). Linker histones H1 and H5 prevent the mobility of positioned nucleosomes. Proceedings of the National Academy of Sciences of the United States of America *91*, 10275-10279.

Pepenella, S., Murphy, K.J., and Hayes, J.J. (2013). Intra- and inter-nucleosome interactions of the core histone tail domains in higher-order chromatin structure. Chromosoma.

Perez-Montero, S., Carbonell, A., Moran, T., Vaquero, A., and Azorin, F. (2013). The embryonic linker histone H1 variant of Drosophila, dBigH1, regulates zygotic genome activation. Developmental cell *26*, 578-590.

Perisic, O., Collepardo-Guevara, R., and Schlick, T. (2010). Modeling studies of chromatin fiber structure as a function of DNA linker length. Journal of molecular biology *403*, 777-802.

Phanstiel, D., Brumbaugh, J., Berggren, W.T., Conard, K., Feng, X., Levenstein, M.E., McAlister, G.C., Thomson, J.A., and Coon, J.J. (2008). Mass spectrometry identifies and quantifies 74 unique histone H4 isoforms in differentiating human embryonic stem cells. Proceedings of the National Academy of Sciences of the United States of America *105*, 4093-4098.

Pinskaya, M., Nair, A., Clynes, D., Morillon, A., and Mellor, J. (2009). Nucleosome remodeling and transcriptional repression are distinct functions of Isw1 in Saccharomyces cerevisiae. Molecular and cellular biology *29*, 2419-2430.

Poirier, M.G., Bussiek, M., Langowski, J., and Widom, J. (2008). Spontaneous access to DNA target sites in folded chromatin fibers. Journal of molecular biology *379*, 772-786.

Poot, R.A., Dellaire, G., Hulsmann, B.B., Grimaldi, M.A., Corona, D.F., Becker, P.B., Bickmore, W.A., and Varga-Weisz, P.D. (2000). HuCHRAC, a human ISWI chromatin remodelling complex contains hACF1 and two novel histone-fold proteins. The EMBO journal *19*, 3377-3387.

Protacio, R.U., Li, G., Lowary, P.T., and Widom, J. (2000). Effects of histone tail domains on the rate of transcriptional elongation through a nucleosome. Molecular and cellular biology *20*, 8866-8878.

Rando, O.J. (2012). Combinatorial complexity in chromatin structure and function: revisiting the histone code. Current opinion in genetics & development *22*, 148-155.

Richmond, T.J., and Davey, C.A. (2003). The structure of DNA in the nucleosome core. Nature *423*, 145-150.

Robinson, P.J., An, W., Routh, A., Martino, F., Chapman, L., Roeder, R.G., and Rhodes, D. (2008). 30 nm chromatin fibre decompaction requires both H4-K16 acetylation and linker histone eviction. Journal of molecular biology *381*, 816-825.

Robinson, P.J., Fairall, L., Huynh, V.A., and Rhodes, D. (2006). EM measurements define the dimensions of the "30-nm" chromatin fiber: evidence for a compact, interdigitated structure. Proceedings of the National Academy of Sciences of the United States of America *103*, 6506-6511.

Robinson, P.J., and Rhodes, D. (2006). Structure of the '30 nm' chromatin fibre: a key role for the linker histone. Current opinion in structural biology *16*, 336-343.

Rodriguez-Campos, A., Shimamura, A., and Worcel, A. (1989). Assembly and properties of chromatin containing histone H1. Journal of molecular biology *209*, 135-150.

Roth, S.Y., Denu, J.M., and Allis, C.D. (2001). Histone acetyltransferases. Annual review of biochemistry *70*, 81-120.

Routh, A., Sandin, S., and Rhodes, D. (2008). Nucleosome repeat length and linker histone stoichiometry determine chromatin fiber structure. Proceedings of the National Academy of Sciences of the United States of America *105*, 8872-8877.

Ruthenburg, A.J., Li, H., Milne, T.A., Dewell, S., McGinty, R.K., Yuen, M., Ueberheide, B., Dou, Y., Muir, T.W., Patel, D.J.*, et al.* (2011). Recognition of a mononucleosomal histone modification pattern by BPTF via multivalent interactions. Cell *145*, 692-706.

Ruthenburg, A.J., Li, H., Patel, D.J., and Allis, C.D. (2007). Multivalent engagement of chromatin modifications by linked binding modules. Nature reviews Molecular cell biology *8*, 983-994.

Ryan, D.P., Sundaramoorthy, R., Martin, D., Singh, V., and Owen-Hughes, T. (2011). The DNA-binding domain of the Chd1 chromatin-remodelling enzyme contains SANT and SLIDE domains. The EMBO journal *30*, 2596-2609.

Sala, A., Toto, M., Pinello, L., Gabriele, A., Di Benedetto, V., Ingrassia, A.M., Lo Bosco, G., Di Gesu, V., Giancarlo, R., and Corona, D.F. (2011). Genome-wide characterization of chromatin binding and nucleosome spacing activity of the nucleosome remodelling ATPase ISWI. The EMBO journal *30*, 1766-1777.

Sandaltzopoulos, R., Blank, T., and Becker, P.B. (1994). Transcriptional repression by nucleosomes but not H1 in reconstituted preblastoderm Drosophila chromatin. The EMBO journal *13*, 373-379.

Schalch, T., Duda, S., Sargent, D.F., and Richmond, T.J. (2005). X-ray structure of a tetranucleosome and its implications for the chromatin fibre. Nature *436*, 138-141.

Schlick, T., Hayes, J., and Grigoryev, S. (2012). Toward convergence of experimental studies and theoretical modeling of the chromatin fiber. The Journal of biological chemistry *287*, 5183-5191.

Schlick, T., and Perisic, O. (2009). Mesoscale simulations of two nucleosome-repeat length oligonucleosomes. Physical chemistry chemical physics : PCCP *11*, 10729-10737.

Schwaiger, M., Stadler, M.B., Bell, O., Kohler, H., Oakeley, E.J., and Schübeler, D. (2009). Chromatin state marks cell-type- and gender-specific replication of the Drosophila genome. Genes & development *23*, 589-601.

Schwarz, P.M., Felthauser, A., Fletcher, T.M., and Hansen, J.C. (1996). Reversible oligonucleosome self-association: dependence on divalent cations and core histone tail domains. Biochemistry *35*, 4009-4015.

Shahbazian, M.D., and Grunstein, M. (2007). Functions of site-specific histone acetylation and deacetylation. Annual review of biochemistry *76*, 75-100.

Sharma, A., Jenkins, K.R., Heroux, A., and Bowman, G.D. (2011). Crystal structure of the chromodomain helicase DNA-binding protein 1 (Chd1) DNA-binding domain in complex with DNA. The Journal of biological chemistry *286*, 42099-42104.

Shogren-Knaak, M., Ishii, H., Sun, J.M., Pazin, M.J., Davie, J.R., and Peterson, C.L. (2006). Histone H4-K16 acetylation controls chromatin structure and protein interactions. Science *311*, 844-847.

Simpson, R.T. (1978). Structure of the chromatosome, a chromatin particle containing 160 base pairs of DNA and all the histones. Biochemistry *17*, 5524-5531.

Sims, R.J., 3rd, Mandal, S.S., and Reinberg, D. (2004). Recent highlights of RNA-polymerase-II-mediated transcription. Current opinion in cell biology *16*, 263-271.

Sinha, D., and Shogren-Knaak, M.A. (2010). Role of direct interactions between the histone H4 Tail and the H2A core in long range nucleosome contacts. The Journal of biological chemistry *285*, 16572-16581.

Siriaco, G., Deuring, R., Chioda, M., Becker, P.B., and Tamkun, J.W. (2009). Drosophila ISWI regulates the association of histone H1 with interphase chromosomes in vivo. Genetics *182*, 661-669.

Smith, C.M., Gafken, P.R., Zhang, Z., Gottschling, D.E., Smith, J.B., and Smith, D.L. (2003). Mass spectrometric quantification of acetylation at specific lysines within the amino-terminal tail of histone H4. Analytical biochemistry *316*, 23-33.

Smith, Z.D., and Meissner, A. (2013). DNA methylation: roles in mammalian development. Nature reviews Genetics *14*, 204-220.

Spadafora, C., Bellard, M., Compton, J.L., and Chambon, P. (1976). The DNA repeat lengths in chromatins from sea urchin sperm and gastrule cells are markedly different. FEBS letters *69*, 281-285.

Stein, A., and Bina, M. (1984). A model chromatin assembly system. Factors affecting nucleosome spacing. Journal of molecular biology *178*, 341-363.

Stockdale, C., Flaus, A., Ferreira, H., and Owen-Hughes, T. (2006). Analysis of nucleosome repositioning by yeast ISWI and Chd1 chromatin remodeling complexes. The Journal of biological chemistry *281*, 16279-16288.

Struhl, K. (1998). Histone acetylation and transcriptional regulatory mechanisms. Genes & development *12*, 599-606.

Struhl, K., and Segal, E. (2013). Determinants of nucleosome positioning. Nature structural & molecular biology *20*, 267-273.

Sun, J., Zhang, Q., and Schlick, T. (2005). Electrostatic mechanism of nucleosomal array folding revealed by computer simulation. Proceedings of the National Academy of Sciences of the United States of America *102*, 8180-8185.

Sun, J.M., Ali, Z., Lurz, R., and Ruiz-Carrillo, A. (1990). Replacement of histone H1 by H5 in vivo does not change the nucleosome repeat length of chromatin but increases its stability. The EMBO journal *9*, 1651-1658.

Syed, S.H., Goutte-Gattat, D., Becker, N., Meyer, S., Shukla, M.S., Hayes, J.J., Everaers, R., Angelov, D., Bednar, J., and Dimitrov, S. (2010). Single-base resolution mapping of H1-nucleosome interactions and 3D organization of the nucleosome. Proceedings of the National Academy of Sciences of the United States of America *107*, 9620-9625.

Szenker, E., Boyarchuk, E., and Almouzni, G. (2014). Properties and Functions of Histone Variants. In Fundamentals of Chromatin, J.L. Workman, and S.M. Abmayr, eds. (Springer).

Szerlong, H.J., and Hansen, J.C. (2011). Nucleosome distribution and linker DNA: connecting nuclear function to dynamic chromatin structure. Biochemistry and cell biology = Biochimie et biologie cellulaire *89*, 24-34.

Talasz, H., Sapojnikova, N., Helliger, W., Lindner, H., and Puschendorf, B. (1998). In vitro binding of H1 histone subtypes to nucleosomal organized mouse mammary tumor virus long terminal repeat promotor. The Journal of biological chemistry *273*, 32236-32243.

Talbert, P.B., and Henikoff, S. (2010). Histone variants--ancient wrap artists of the epigenome. Nature reviews Molecular cell biology *11*, 264-275.

Tan, M., Luo, H., Lee, S., Jin, F., Yang, J.S., Montellier, E., Buchou, T., Cheng, Z., Rousseaux, S., Rajagopal, N.*, et al.* (2011). Identification of 67 histone marks and histone lysine crotonylation as a new type of histone modification. Cell *146*, 1016-1028.

Tan, S., and Davey, C.A. (2011). Nucleosome structural studies. Current opinion in structural biology *21*, 128-136.

Taylor, G., Eskeland, R., Hekimoglu-Balkan, B., Pradeepa, M., and Bickmore, W.A. (2013). H4K16 acetylation marks active genes and enhancers of embryonic stem cells, but does not alter chromatin compaction. Genome research.

Tessarz, P., Santos-Rosa, H., Robson, S.C., Sylvestersen, K.B., Nelson, C.J., Nielsen, M.L., and Kouzarides, T. (2014). Glutamine methylation in histone H2A is an RNA-polymerase-I-dedicated modification. Nature *505*, 564-568.

Thoma, F., Koller, T., and Klug, A. (1979). Involvement of histone H1 in the organization of the nucleosome and of the salt-dependent superstructures of chromatin. The Journal of cell biology *83*, 403-427.

Tims, H.S., Gurunathan, K., Levitus, M., and Widom, J. (2011). Dynamics of nucleosome invasion by DNA binding proteins. Journal of molecular biology *411*, 430-448.

Torigoe, S.E., Patel, A., Khuong, M.T., Bowman, G.D., and Kadonaga, J.T. (2013). ATP-dependent chromatin assembly is functionally distinct from chromatin remodeling. eLife *2*, e00863.

Torigoe, S.E., Urwin, D.L., Ishii, H., Smith, D.E., and Kadonaga, J.T. (2011). Identification of a rapidly formed nonnucleosomal histone-DNA intermediate that is converted into chromatin by ACF. Molecular cell *43*, 638-648.

Tremethick, D.J., and Frommer, M. (1992). Partial purification, from Xenopus laevis oocytes, of an ATP-dependent activity required for nucleosome spacing in vitro. The Journal of biological chemistry *267*, 15041-15048.

Tropberger, P., and Schneider, R. (2013). Scratching the (lateral) surface of chromatin regulation by histone modifications. Nature structural & molecular biology *20*, 657-661.

Tse, C., and Hansen, J.C. (1997). Hybrid trypsinized nucleosomal arrays: identification of multiple functional roles of the H2A/H2B and H3/H4 N-termini in chromatin fiber compaction. Biochemistry *36*, 11381-11388.

Tse, C., Sera, T., Wolffe, A.P., and Hansen, J.C. (1998). Disruption of higher-order folding by core histone acetylation dramatically enhances transcription of nucleosomal arrays by RNA polymerase III. Molecular and cellular biology *18*, 4629-4638.

Tsukiyama, T., and Wu, C. (1995). Purification and properties of an ATP-dependent nucleosome remodeling factor. Cell *83*, 1011-1020.

Turner, B.M. (1991). Histone acetylation and control of gene expression. Journal of cell science *99 (Pt 1)*, 13-20.

Valouev, A., Johnson, S.M., Boyd, S.D., Smith, C.L., Fire, A.Z., and Sidow, A. (2011). Determinants of nucleosome organization in primary human cells. Nature *474*, 516-520.

van Holde, K.E. (1989). Chromatin (New York: Springer).

Vaquero, A., Sternglanz, R., and Reinberg, D. (2007). NAD+-dependent deacetylation of H4 lysine 16 by class III HDACs. Oncogene *26*, 5505-5520.

Varga-Weisz, P.D., Wilm, M., Bonte, E., Dumas, K., Mann, M., and Becker, P.B. (1997). Chromatin-remodelling factor CHRAC contains the ATPases ISWI and topoisomerase II. Nature *388*, 598-602.

Vogler, C., Huber, C., Waldmann, T., Ettig, R., Braun, L., Izzo, A., Daujat, S., Chassignet, I., Lopez-Contreras, A.J., Fernandez-Capetillo, O.*, et al.* (2010). Histone H2A C-terminus regulates chromatin dynamics, remodeling, and histone H1 binding. PLoS genetics *6*, e1001234.

Vyas, P., and Brown, D.T. (2012). N- and C-terminal domains determine differential nucleosomal binding geometry and affinity of linker histone isotypes H1(0) and H1c. The Journal of biological chemistry *287*, 11778-11787.

Whitehouse, I., Stockdale, C., Flaus, A., Szczelkun, M.D., and Owen-Hughes, T. (2003). Evidence for DNA translocation by the ISWI chromatin-remodeling enzyme. Molecular and cellular biology *23*, 1935-1945.

Widom, J. (1986). Physicochemical studies of the folding of the 100 A nucleosome filament into the 300 A filament. Cation dependence. Journal of molecular biology *190*, 411-424.

Widom, J. (1992). A relationship between the helical twist of DNA and the ordered positioning of nucleosomes in all eukaryotic cells. Proceedings of the National Academy of Sciences of the United States of America *89*, 1095-1099.

Wiren, M., Silverstein, R.A., Sinha, I., Walfridsson, J., Lee, H.M., Laurenson, P., Pillus, L., Robyr, D., Grunstein, M., and Ekwall, K. (2005). Genomewide analysis of nucleosome density histone acetylation and HDAC function in fission yeast. The EMBO journal *24*, 2906-2918.

Wolffe, A.P., and Hayes, J.J. (1999). Chromatin disruption and modification. Nucleic acids research *27*, 711-720.

Wong, H., Victor, J.M., and Mozziconacci, J. (2007). An all-atom model of the chromatin fiber containing linker histones reveals a versatile structure tuned by the nucleosomal repeat length. PloS one *2*, e877.

Woodcock, C.L. (1994). Chromatin fibers observed in situ in frozen hydrated sections. Native fiber diameter is not correlated with nucleosome repeat length. The Journal of cell biology *125*, 11-19.

Woodcock, C.L., Frado, L.L., and Rattner, J.B. (1984). The higher-order structure of chromatin: evidence for a helical ribbon arrangement. The Journal of cell biology *99*, 42-52.

Woodcock, C.L., Skoultchi, A.I., and Fan, Y. (2006). Role of linker histone in chromatin structure and function: H1 stoichiometry and nucleosome repeat length. Chromosome research : an international journal on the molecular, supramolecular and evolutionary aspects of chromosome biology *14*, 17-25.

Worcel, A., Strogatz, S., and Riley, D. (1981). Structure of chromatin and the linking number of DNA. Proceedings of the National Academy of Sciences of the United States of America *78*, 1461-1465.

Wu, C., Bassett, A., and Travers, A. (2007). A variable topology for the 30-nm chromatin fibre. EMBO reports *8*, 1129-1134.

Wysocka, J., Swigut, T., Xiao, H., Milne, T.A., Kwon, S.Y., Landry, J., Kauer, M., Tackett, A.J., Chait, B.T., Badenhorst, P.*, et al.* (2006). A PHD finger of NURF couples histone H3 lysine 4 trimethylation with chromatin remodelling. Nature *442*, 86-90.

Xiao, H., Sandaltzopoulos, R., Wang, H.M., Hamiche, A., Ranallo, R., Lee, K.M., Fu, D., and Wu, C. (2001). Dual functions of largest NURF subunit NURF301 in nucleosome sliding and transcription factor interactions. Molecular cell *8*, 531-543.

Yadon, A.N., and Tsukiyama, T. (2011). SnapShot: Chromatin remodeling: ISWI. Cell *144*, 453-453 e451.

Yamada, K., Frouws, T.D., Angst, B., Fitzgerald, D.J., DeLuca, C., Schimmele, K., Sargent, D.F., and Richmond, T.J. (2011). Structure and mechanism of the chromatin remodelling factor ISW1a. Nature *472*, 448-453.

Yang, J.G., Madrid, T.S., Sevastopoulos, E., and Narlikar, G.J. (2006). The chromatin-remodeling enzyme ACF is an ATP-dependent DNA length sensor that regulates nucleosome spacing. Nature structural & molecular biology *13*, 1078-1083.

Yang, X.J., and Seto, E. (2008). Lysine acetylation: codified crosstalk with other posttranslational modifications. Molecular cell *31*, 449-461.

Yun, M., Wu, J., Workman, J.L., and Li, B. (2011). Readers of histone modifications. Cell research *21*, 564-578.

Zheng, Y., Thomas, P.M., and Kelleher, N.L. (2013). Measurement of acetylation turnover at distinct lysines in human histones identifies long-lived acetylation sites. Nature communications *4*, 2203.

Zhou, B.R., Feng, H., Kato, H., Dai, L., Yang, Y., Zhou, Y., and Bai, Y. (2013). Structural insights into the histone H1-nucleosome complex. Proceedings of the National Academy of Sciences of the United States of America *110*, 19390-19395.

Zhou, J., Fan, J.Y., Rangasamy, D., and Tremethick, D.J. (2007). The nucleosome surface regulates chromatin compaction and couples it with transcriptional repression. Nature structural & molecular biology *14*, 1070-1076.

Zhou, Y., and Grummt, I. (2005). The PHD finger/bromodomain of NoRC interacts with acetylated histone H4K16 and is sufficient for rDNA silencing. Current biology : CB *15*, 1434-1438.

Zhou, Y.B., Gerchman, S.E., Ramakrishnan, V., Travers, A., and Muyldermans, S. (1998). Position and orientation of the globular domain of linker histone H5 on the nucleosome. Nature *395*, 402-405.

Zippo, A., Serafini, R., Rocchigiani, M., Pennacchini, S., Krepelova, A., and Oliviero, S. (2009). Histone crosstalk between H3S10ph and H4K16ac generates a histone code that mediates transcription elongation. Cell *138*, 1122-1136.

Zlatanova, J., Bishop, T.C., Victor, J.M., Jackson, V., and van Holde, K. (2009). The nucleosome family: dynamic and growing. Structure *17*, 160-171.

Zofall, M., Persinger, J., and Bartholomew, B. (2004). Functional role of extranucleosomal DNA and the entry site of the nucleosome in chromatin remodeling by ISW2. Molecular and cellular biology *24*, 10047-10057.

Declaration of contributions

Declaration of contributions to “The ATPase domain of ISWI is an autonomous nucleosome remodeling machine”

This study was conceived by F. Mueller-Planitz. I contributed the mono- and polynucleosome-sliding experiments (Figure 5a, c) and the restriction enzyme accessibility experiment shown in Figure 5d. Furthermore, I performed all the restriction enzyme accessibility experiments employing wt-H4 arrays and some of the experiments employing g-H4 arrays that are summarized in Figure 6 and Figure S7. I prepared Figure 5 and the corresponding figure legend and materials and methods sections. Together with J. Ludwigsen, I prepared Figure 6 including figure legend and the respective materials and methods sections. I assisted in developing and revising the manuscript that was mostly written by F. Mueller-Planitz and P.B. Becker and edited it at all stages of the publication process.

Declaration of contributions to “Nucleosome sliding mechanisms: new twists in a looped history”

This review was conceived and developed by F. Mueller-Planitz, P.B. Becker and me. I designed and prepared Figures 1, 3, 4, and 5 and all figure legends. I assisted in finalizing the text, edited and helped revising the manuscript. In addition, I wrote drafts for the short summaries of the key references.

Declaration of contributions to “No need for a power stroke in ISWI-mediated nucleosome sliding”

This study was conceived by J. Ludwigsen and F. Mueller-Planitz. I performed the nucleosome sliding experiment shown in Figure 4, edited and helped revising the manuscript.

Declaration of contributions to “ISWI Remodelling of Physiological Chromatin Fibres Acetylated at Lysine 16 of Histone H4”

This study was conceived by P.B. Becker and me. I performed all experiments except for the mass spectrometry analysis that was done by I. Forné (Figure S1C, D). He also wrote the corresponding materials and methods section and revised the figure legend. The acetylated and unmodified histones H4 were provided by R. Yang, C.-F. Liu, and L. Nordenskiöld. I conceived and wrote the first draft of the manuscript and developed the final version together with P.B. Becker and F. Mueller-Planitz. I prepared all figures and figure legends.

Declaration of contributions to "Rapid purification of recombinant histones"

The method described in this manuscript was initially developed by F. Mueller-Planitz. C. Haas and I applied the protocol to purify the canonical *Drosophila* histones and advanced the method together with F. Mueller-Planitz and his co-workers. C. Haas and I performed all experiments contained in the manuscript in close collaboration. I prepared the figures and wrote the first draft of the manuscript including the figure legends. Together with F. Mueller-Planitz, C. Haas, and P.B. Becker I developed the enclosed version of the manuscript.

(Prof. Dr. Peter Becker)

(Henrike Klinker)

Abbreviations

aa	Amino acids
ACF	ATP-utilizing chromatin assembly and remodeling factor
ATP	Adenosine triphosphate
AutoN	N-terminal autoinhibitory region
bp	Base pairs
BPTF	Bromodomain PHD finger transcription factor
Chd1	Chromodomain helicase DNA binding protein 1
CHRAC	Chromatin accessibility complex
Chromodomain	Chromatin organization modifier domain
CoA	Coenzyme A
CtBP	C-terminal binding domain
DCC	Dosage compensation complex
DNA	Desoxyribonucleic acid
EM	Electron microscopy
FRAP	Fluorescence recovery after photobleaching
g-H4	Globular histone H4 (histone H4 lacking the N-terminal tail)
H4K16	Lysine 16 of histone H4
H4K16ac	Histone H4 acetylated at lysine 16
HAT	Histone acetyltransferase
HDAC	Histone deacetylase
HEK293	Human embryonic kidney cells 293
HP1	Heterochromatin protein 1
ISW2	Imitation switch (complex in *Saccharomyces cerevisiae*)
ISWI	Imitation switch (enzyme in *Drosophila melanogaster*)
MOF	Males absent on the first
NAP1	Nucleosome assembly protein 1
NoRC	Nucleolar remodeling complex
NRL	Nucleosomal repeat length
NuRD	Nucleosome remodeling and histone deacetylation
NURF	Nucleosome remodeling factor
PHD finger	Plant homeobox finger
PolII	RNA polymerase II
PRC1	Polycomb repressive complex 1
PTM	Post-translational modification

RNA	Ribonucleic acid
RSF	Remodeling and spacing factor
SANT	SWI3, ADA2, N-CoR, TFIIIB
SAXS	Small angle X-ray scattering
Set	Su(var)3-9, Enhancer of Zeste, Trithorax
SHL	Superhelix location
SIR/Sir	Silent information regulator
SLIDE	SANT-like ISWI domain
Snf2	Sucrose non-fermenting 2
Snf2H	Sucrose non-fermenting 2 homolog
ToRC	Toutatis-containing chromatin remodeling complex
wt-H4	Wild-type H4

Curriculum Vitae

Personal information

Name	Henrike Klinker
Date of birth	24. August 1983
Place of birth	Frankenberg (Eder)
Nationality	German

Education

Jan. 2009 – present	PhD thesis in the laboratory of Prof. Dr. Peter B. Becker Adolf-Butenandt-Institute, Department of Molecular Biology, Ludwig-Maximilians-Universität München, Munich, Germany Project: *ATP-dependent nucleosome sliding by ISWI – molecular mechanism and regulation*
Nov. 2010 – Oct. 2013	Member of the International Graduate Program *Protein Dynamics in Health and Disease* of the Elite Network of Bavaria
Jan. 2008 – Nov. 2008	Diploma thesis in the laboratory of Prof. Dr. Alexander Brehm Institute of Molecular Biology and Tumor Research, Philipps-University, Marburg, Germany Project: *Structural and Functional Analysis of the Drosophila Protein MEP-1*
Oct. 2005 – Dec. 2008	Diploma studies in Biomedical Science (Humanbiologie) Philipps-University, Marburg, Germany
April 2004 – Sept. 2008	Scholarship of the German National Academic Foundation (Studienstiftung des deutschen Volkes)
Oct. 2003 – Sept. 2005	Pre-Diploma studies in Biomedical Science (Humanbiologie) Philipps-University, Marburg, Germany
June 2003	Final secondary school examinations (Abitur)

Publications

Klinker H, Mueller-Planitz F, Yang R, Forné I, Liu CF, Nordenskiöld L, Becker PB (2014)
ISWI Remodelling of Physiological Chromatin Fibres Acetylated at Lysine 16 of Histone H4.
PLoS ONE 9(2), e88411.

Ludwigsen J, **Klinker H**, Mueller-Planitz F (2013)
No need for a power stroke in ISWI-mediated nucleosome sliding.
EMBO reports 14, 1092-1097.

Mueller-Planitz F, **Klinker H**, Becker PB (2013)
Nucleosome sliding mechanisms: new twists in a looped history.
Nature Structural & Molecular Biology 20, 1026-1032.

Mueller-Planitz F, **Klinker H**, Ludwigsen J, Becker PB (2013)
The ATPase domain of ISWI is an autonomous nucleosome remodeling machine.
Nature Structural & Molecular Biology 20, 82-89.

Kunert N, Wagner E, Murawska M, **Klinker H**, Kremmer E, Brehm A (2009)
dMec: a novel Mi-2 chromatin remodelling complex involved in transcriptional repression.
The EMBO Journal 28, 533–544.

Acknowledgements

Last but not least I would like to thank some people that supported, helped, and encouraged me during the past years and without whom this thesis would not have been possible.

First of all, I want to thank Peter Becker for giving me the opportunity to join his lab as a PhD student. I am deeply grateful for his continuous support, his patience and valuable input, his confidence and a door that was always open.

Special thanks go to Felix Mueller-Planitz for innumerable fruitful discussions, for introducing me to the world of enzyme kinetics, and for being a patient and supportive mentor, teacher, and collaborator throughout the time of my PhD.

In addition, I want to acknowledge the further members of my thesis advisory committee Philipp Korber and Gernot Längst who took the time to discuss my project and gave precious advice.

I want to express my gratitude to my collaboration partners Renliang Yang, Chuan-Fa Liu and Lars Nordenskiöld for providing acetylated and unmodified histone H4 and Helmut Schiessel and Raoul Schram for ongoing modeling efforts and stimulating discussions.

I furthermore want to thank all former and present members of the Becker lab and the whole Molecular Biology Unit that at all times created an extraordinarily stimulating and pleasant working atmosphere, were always ready to help with advice, helping hands, or reagents, and turned retreats, happy hours, and after-work-events into unforgettable memories. I am especially grateful to all my “labroommates” making every day lab life so enjoyable.

I want to thank…

… Verena Maier for giving me a good start in the lab and sharing her expertise in chromatin assembly.

… my longtime desk neighbor Raffaella Villa for being much more than a colleague.

… Johanna Ludwigsen for being a fabulous collaboration partner in lab and cake projects.

… Caroline Haas for a summer spent together in the cold room.

… Nadine Harrer for persuing the establishment of the rapid histone purification method and invaluable advice in personal projects.

… Natascha Steffen for always lending me an ear and being a tolerant and humorous bench neighbor.

… the 7th floor crowd, especially Teresa Barth, Silvia Dambacher, Edith Mentele, Miriam Pusch, Dennis Sadic, Viola Sansoni, Irene Vetter, Simone Vollmer, and Gabriele Wagner,

for always having an extra chair in the kitchen for me, for numerous fun lunch breaks and other events.

… the Wednesday club for feeding me and all the great evenings we spent together.

Moreover, I am grateful to the Elite Network of Bavaria for supporting me in the context of the International Graduate Program *Protein Dynamics in Health and Disease*. In this regard I also want to thank Kai Hell and all members of the program for all the great experiences we shared and for being a source of inspiration.

Schließlich möchte ich mich noch bei meiner Familie, meinen Freunden und Rainer für die Unterstützung, das Verständnis und die Liebe bedanken, die sie mir nicht nur in den letzten Jahren und vor allem auch in schwierigen Zeiten entgegengebracht haben. Ohne euch...